TECHNISCHE UNIVERSITÄT MÜNCHEN
Integrative Research Center Campus Straubing für Biotechnologie und Nachhaltigkeit

Material Utilization of Algal Carbohydrates: Focus on Analytical Methods and Enzymatic Processing

José Guillermo Ortiz Tena

Vollständiger Abdruck der von der promotionsführenden Einrichtung Campus Straubing für Biotechnologie und Nachhaltigkeit der Technischen Universität München zur Erlangung des akademischen Grades eines

Doktors der Naturwissenschaften (Dr. rer. nat.)

genehmigten Dissertation.

Vorsitzender: Prof. Dr. Matthias Gaderer
Prüfer der Dissertation: 1. Prof. Dr. Volker Sieber
2. Prof. Dr. Thomas Brück

Die Dissertation wurde am 12.07.2019 bei der Technischen Universität München eingereicht und von der promotionsführenden Einrichtung Campus Straubing für Biotechnologie und Nachhaltigkeit am 28.10.2019 angenommen.

Preface

Scientific reporting involves a structured presentation of ideas and findings using an appropriate writing style and language. The sequence of topics that are brought to paper are determining for a precise transmission of ideas to the reader. Scientific research, however, is a dynamic process in which decisions are, very often, made "on the way". Normally, this should not represent an obstacle for presenting results concisely with a defined path. Yet sometimes, the matter of study is wide, so a splitting in sub-topics provides an amenable discourse to the reader.

This is exactly the case for the present Thesis, which bears the Title "*Material utilization of algal carbohydrates: Focus on analytical methods and enzymatic processing"*. The first sentence is certainly rather general and may be ambiguous, especially because the term *algae* denote a very broad group of aquatic organisms. The historical classification of such organisms is based on the *size* of the algae in micro-, for unicellular organisms, and macroalgae, for multicellular, seaweed species. The study of these two very different types of algae is thus facilitated by a separated approach in terms of methodology and discussion. Consequently, the present work is structured in two parts, as it deals with valorization strategies for both categories.

After a brief introduction on the general utilization of diverse types of biomass as renewable resource and the concept of bio refinery, this work explores the challenges and opportunities for the material utilization of *microalgae* in Part A, expanding on carbohydrates. As the sub-title denotes, special focus is paid on detection procedures. The development and transfer of analytical methods aim to set the basis for subsequent enzymatic utilization of the carbohydrates towards value added products, as this represents a significant and still underutilized share of algal biomass. Some results presented in the first part were published in peer-reviewed scientific journals, especially those concerning the transfer, development, and application of analytical methods for microalgal **monomeric** sugars. Analytical method development for **oligomeric** sugars and their utilization for **enzymatic saccharification** of microalgal polysaccharides are addressed next.

In part B, a similar analysis is provided for carbohydrates from *macroalgae*. The literature review is partly presented as a book chapter that was published in collaboration with expert scientists in the field of macroalgae production. Herein, interesting opportunities for the *enzymatic conversion* of sulfated seaweed polysaccharides were identified. Therefore, a proper analytical assay for such a biotechnological processing was designed and validated. With the published procedure, the development of relevant sulfate-active enzymes for improving the properties of macroalgal polysaccharides will be facilitated.

The author is confident that this work can help for future research in the field of micro- and macro-algal biomass utilization as renewable resource for expanding applications.

Summary

The establishment of a bio economy plays a key role for alleviating global pollution and climate change. In this frame, renewable feedstocks hold an enormous potential for numerous fields. Algae represent a promising option as raw material, as they capture CO_2 and can be cultured under controlled conditions. However, the technology portfolio for their utilization is, to date, very limited and needs to be expanded. As carbohydrates can represent a significant share of algal biomass, novel analysis procedures (or at least adaptations of existing methods) as well as sustainable processing will certainly facilitate its utilization in relevant fields.

Algae can be divided into micro and macroalgae. This work contributes to the evaluation of the potential for the comprehensive utilization of carbohydrates from both types. In the field of microalgae, special focus is laid on the transfer of a previously developed UHPLC-MS analytical method for bacterial exopolysaccharides towards microalgal carbohydrates. The so-called HT-PMP method, which is based on pre-column sugar derivatization with 1-phenyl-3-methyl-5-pyrazolone (PMP), can detect neutral sugars, amino and substituted sugars. Thus, the vast variety of microalgal monosaccharides can be easily explored, allowing a more accurate valuation for biomass utilization than with conventional methods.

This was demonstrated by three aspects. First, the carbohydrate distribution in the model microalga *C. vulgaris* was determined for the first time. With the PMP-method previously unnoticed sugars were detected, such as sulphated and methylated monosaccharides. For this, a fragmentation procedure was carried out to obtain different biomass fractions (e.g., lipid, protein, cell wall) which were subsequently analyzed. Secondly, the sugar profile of different *S. obtusiusculus* microalgal biomasses was examined using the adapted method. These biomasses were obtained using different growth conditions (e.g., varying nutrients and microelements). Thus, a carbohydrate enriched biomass (containing mainly mannose, galactose and glucose) could be obtained, which was used further by research colleagues in fermentative processes. Thirdly, based on the results obtained with the PMP-method, different commercial hydrolases were selected and tested for saccharification of lipid-extracted *Scenedesmus* biomass. Additionally, the same PMP derivatization reaction used for monosaccharide determination was employed within a newly designed workflow to detect oligosaccharides from the obtained hydrolysates. This allowed identifying missing activities for a complete enzymatic saccharification.

For macroalgae, promising biotechnological approaches were assessed to increase the added value of important established carbohydrate-based algal products. Concretely, this work focuses on the utilization of carrageenan from the seaweed *Kappaphycus*. In this context, the enzymatic conversion of this sulfated hydrocolloid using sulfatases was identified as possible approach for biomass valorization. Nevertheless, high-throughput analytical tools for functional-based screening of sulfatases from unexplored (meta-) genomic sources (e.g., marine environments) are still unavailable. Therefore, a microplate sulfatase assay based on a two-step enzymatic cascade was developed, optimized and validated. The involved enzymes were carefully selected to overcome the energetically unfavorable incorporation of free sulfate into ATP. This reaction generates adenosine-phosphosulfate as well as inorganic pyrophosphate as co-product, which ultimately is converted into a colorimetric signal that is linear with the concentration of sulfate between 10 and 250 µM. With this method, the wildtype activity landscape of an alkyl and an aryl sulfatase expressed in *E. coli* could be confirmed. This opens the opportunity to the biotechnological development of e.g., carrageenan sulfatases in terms of screening, engineering and characterization.

Acknowledgments

First, I would like to thank my doctoral advisor Prof. Volker Sieber for his valuable supervision not only during the three and half years of practical work, but also for the support in the writing process. His door was always open for critical and constructive discussions even in busy times. Under his guidance I could have a balanced mixture between guided instruction and creative progress. I am very grateful for having the opportunity to do applied research with enzymes at the TU Munich in his chair.

In the same line, I would like to express a very special gratitude to my supervisors Dr. Doris Schieder and Dr. Broder Rühmann. Both contributed with their very best in every meeting, discussion, proofread, and advise. I learnt a lot from you and I really enjoyed working together, thank you for your commitment, your time and experience.

Special thanks to Prof. Thomas Brück, which accompanied me since my Master Studies in *Industrial Biotechnology*. The topics covered in his valuable lectures *New Enzymes* helped me in the development of the sulfatase assay. Besides, I appreciate having the chance to work the ABV project team directed by him. Thank you to the project members which I had direct collaboration with. To Prof. Weuster-Botz (TUM-BVT), PD Sabine Mundt (Univ. Greifswald), Nadine Igl (NATECO2) and all their teams.

To my colleagues of the chair, especially to Petra, Anja, Meggi, and Korby for their technical support. For the moral support huge thanks to Marius, Daniel, Hendrik, and Dominik. Without you guys, this adventure would have been a bit dull. From coworkers to true friends.

Thanks to my fiancée Franzi, which I knew in the last days of practical work. Thank you for caring of me in the hard days of writing. To Beate and Hermann, thank you for taking me in your lovely family.

Working far from home is not always easy and certainly impossible without the support of your family. I was always encouraged by my father Guillermo Ortiz (┼) and my brother Francisco Ortiz to follow this journey. I will always be in debt with you both. Finally, this Doctoral Thesis has a very special dedication to my mother Cristina Tena (┼). You fought, did everything, and gave everything from you for me to pursue my dreams until your last days. I miss you, and I still feel your love. Gracias mama.

Table of Contents

Preface 2
Summary 3
Acknowledgments 4
Introduction 7
A. Microalgae 9
A1. Literature review 10
  A1.1. Microalgal biomass 10
  A1.2. Microalgal carbohydrates 13
  A1.3. Analytical methods for microalgal carbohydrates 15
  A1.4. Enzymatic hydrolysis of algal carbohydrates 18
A2. Scope of the work 21
A3. Materials and Methods 22
  A3.1. Equipment 22
  A3.2. Software and databases 23
  A3.3. Enzymes and reagents 24
  A3.4. Special consumables 26
  A3.5. Microalgal biomass 27
  A3.6. Monosaccharide analysis 28
  A3.7. Oligosaccharide analysis 29
  A3.8. Protein analysis 29
  A3.9. Enzymatic hydrolysis 30
A4. Results 32
  A4.1. Revealing the diversity of algal monosaccharides: Fast carbohydrate fingerprinting of microalgae using crude biomass and showcasing sugar distribution in *Chlorella vulgaris* by biomass fractionation 32
  A4.2. A one-stage cultivation process for lipid- and carbohydrate-rich biomass of *Scenedesmus obtusiusculus* based on artificial and natural water sources 53
  A4.3. Enzymatic saccharification of carbohydrate-rich algal biomass 62
A5. Discussion 73
  A5.1. PMP carbohydrate analysis for algal biomass: advantages, limitations and application in biomass development 73
  A5.2. Enzymatic hydrolysis of microalgal carbohydrates 79
A6. Conclusions and Perspectives 81

B. Macroalgae 82
B1. Literature review 83
B1.1. Macroalgal biomass 83
B1.2. Carrageenan and More: Biorefinery Approaches with Special Reference to the Processing of *Kappaphycus* 85
B1.3. Biotechnological processing of hydrocolloids 97
B2. Scope of the work 99
B3. Materials and Methods 100
B3.1. Cloning 100
B3.2. Heterologous enzyme production 100
B3.3. Synthesis of PISA1 substrate 2-heptyl-sulfate 102
B3.4. Sulfate analysis of carrageenan TFA hydrolysates 102
B4. Results 104
B4.1. Colorimetric determination of sulfate *via* an enzyme cascade for high-throughput detection of sulfatase activity 104
B5. Discussion 121
B5.1. Enzymatic sulfatase assay: analysis of advantages, limitations and optimization potential 121
B5.2. Assay application on hydrolysates from sulfated polysaccharides 124
B6. Conclusions and Perspectives 126
References 127
Appendix 135
Abbreviations 146
List of Figures 149
List of Tables 151
Curriculum Vitae 153
List of Publications 154

Introduction

Since the industrial revolution one and a half centuries ago, the carbon-based production systems for energy and commodities have had an incommensurable impact on the ecological balance of Planet Earth. Today, nearly the complete scientific community agrees that the resulting emissions are responsible for the observable global temperature increase, causing climate change and ocean acidification. This scenario, together with the accompanying pollution of air, water, and land, loss of biodiversity as well as over-population, jeopardizes the very existence of humankind. Thus, a profound transformation in the manufacturing chains is urgent to avoid a collapse of the current society.

Before the oil era, people relied on natural feedstock such as wood, grass, crops, and landfill to satisfy their needs. This changed rapidly with the discovery of accessible carbon and petroleum deposits as well as its cheap extraction and processing. As the available technologies at that time did not allow an effective utilization of renewable resources, an enormous rise in carbon and oil exploitation occurred, bringing the global consequences that we experience today. The recent advances in key areas such as nano-, and biotechnology have triggered a re-thinking in the utilization of renewables, such as biomass, for the production of energy and commodities (Tuck et al., 2012).

The term *biomass* designates the bulk organic material forming living organisms, which includes animals, plants, fungi, and bacteria. The primary energy source for biomass formation is provided by the Sun, which is mainly converted into organic matter by marine or terrestrial photosynthetic organisms. Nowadays, the most commonly used biomass types in bulk terms are land-type and comprise food crops, hydrocarbon-rich plants, waste (e.g., straw, peels), weed and wild grasses, and woody biomass (Abbasi & Abbasi, 2010). The most important valorization routes of this feedstock currently include: energy generation by gasification, pyrolysis (Huber et al., 2006), or by hydrothermal liquefaction (Toor et al., 2011), fermentative production of bioethanol (Manochio et al., 2017) and, to a lower extent, of polymers (Zhu et al., 2016).

The utilization potential of biomass is determined by its chemical composition, which varies primarily according to its origin and growth conditions. Most of the produced land biomass is composed by the carbohydrates cellulose and hemicellulose, and the attached lignin (Ragauskas et al., 2006). Some types of plants may contain higher amounts of protein (e.g., soybean) or lipids (e.g., palm tree), but their volume is negligible compared to the above-mentioned components. Lignin, the polyphenolic compound involved in the structural support of terrestrial plants, represents a challenge for biomass processing. Pretreatments for improving its digestibility, such as thermal, mechanical, acid, alkaline, or oxidative, are often unavoidable and can be unfavorable for the economy of scale of biomass processing (Hendriks & Zeeman, 2009).

To increase the economics of biomass, the concept of *biorefinery* has been introduced over the last years. This term denote “an integral unit that can accept different biological feedstocks and convert them into a range of useful products including chemicals, energy and materials” (Clark et al., 2006). This implicates that all the components of the biomass are converted into added-value products, which is specially promising for substituting oil as raw material. Different platform chemicals have been identified as potential substances that can be produced from biomass carbohydrates, such as ethanol, furans, glycerol and derivatives, hydrocarbons, organic acids, and sugar alcohols (Bozell & Petersen, 2010). The development of new bio-technologies, such as enzyme and metabolic engineering will enlarge even more the portfolio in the coming years (J. W. Lee et al., 2012).

Recently, biomass utilization from aquatic environments has raised the attention of the research community and various industrial players. This is a very attractive idea, as more than 70% of the Earth’s surface is covered with water. Besides, the generation of marine biomass does not compete with agricultural production and their lack of lignin may simplify its processing at larger scale. Presently, marine biomass in the form of fishing residues is mainly used as low-cost fertilizers or dumped back to the sea. The most important sources of marine biomass and its currently established products include: residues from fish vertebrates to extract unsaturated lipids, invertebrates (such as crabs) as source of chitin, microalgae for pigments (e.g., astaxanthin) and macroalgae for hydrocolloids (e.g., agars and carrageenan) (Kerton et al., 2013).

Algal biomass represent an especially interesting raw material for the production of energy and commodities (Lieve M. L. Laurens et al., 2017). The conceivable *algal biorefinery* present several advantages and poses important challenges, which will be discussed throughout this text. In this regard, new concepts and strategies are needed for the valorization of algal biomass in new fields beyond current applications. In this work, special focus is placed on the carbohydrate share of the algae, providing discussions, methods and processing strategies for a seemly material utilization of algal mono-, oligo-, and polysaccharides.

A. Microalgae

A1. Literature review

A1.1. Microalgal biomass

Microalgae comprise a broad group of eukaryotic and unicellular organisms that utilize light as energy source to synthesize organic macromolecules (lipids, proteins, and carbohydrates) from CO_2, nitrogen, sulfur, phosphor, and trace elements, such as iron (Figure 1). From an evolutionary perspective, microalgae originated after a primary endosymbiosis event of a cyanobacterium with photosynthetic plastids around 1.6 billion years ago (Yoon et al., 2004). Since then, microalgae have populated nearly every aquatic ecosystem: from ponds, lakes and rivers, through seas and oceans, and even alpine and polar regions (Lyon & Mock, 2014). Microalgal metabolism can be photoautotroph (light-based) and photo-heterotroph (based on light and organic matter), and they are able to grow in saline, fresh, or brackish water. The diversity of microalgae is enormous: between 350,000 and 1 million different species have been estimated, yet only a small fraction has been characterized (Y. K. Lee, 2016). Microalgae are ecologically very important, as they produce half of the atmospheric oxygen (Barsanti & Gualtieri, 2014) and constitute the basis of marine food chains (Long et al., 2011).

As shown in Figure 1, microalgae have been identified as promising feedstock for the production of feed and food ingredients (Milledge, 2011), biofuels (Wijffels & Barbosa, 2010), and chemicals (Foley et al., 2011). The culture of microalgae offers significant advantages over that of terrestrial crops: they present 10 to 100-fold higher biomass yields per unit area, can be cultivated in non-arable lands using any type of water (including wastewater), and are able to utilize CO_2 to reduce industrial emissions and alleviate global warming (Correa et al., 2017; Schenk et al., 2008). The lack of lignin and the possibility to influence the biomass composition by different culture strategies (e.g., nutrient starvation), allow an easier and more flexible processing than other renewables (C. Schulze, Reinhardt, et al., 2016). Most importantly, microalgae do not stand in direct competition with food production systems, avoiding the "*food vs fuel*" debate. The commercial cultivation of microalgal biomass still faces various challenges for an economic and profitable production. High energetic costs for biomass harvesting, for example, are caused by the very high water demand for culturing algae, which makes their separation and drying costly (Brennan & Owende, 2010; Greenwell et al., 2009). To increase the economy of scale of microalgal production, the technological portfolio still needs to be completed, adapted and expanded. This includes technical infrastructure for large-scale production, biomass processing technologies, analytical procedures, as well as molecular biology protocols (Ziolkowska & Simon, 2014). Modern high-throughput (HT) omics and genome editing methods, such as CRISPR-CAS, will enable an accelerated exploration of the microalgal metabolic potential in the near future (Brodie et al., 2017).

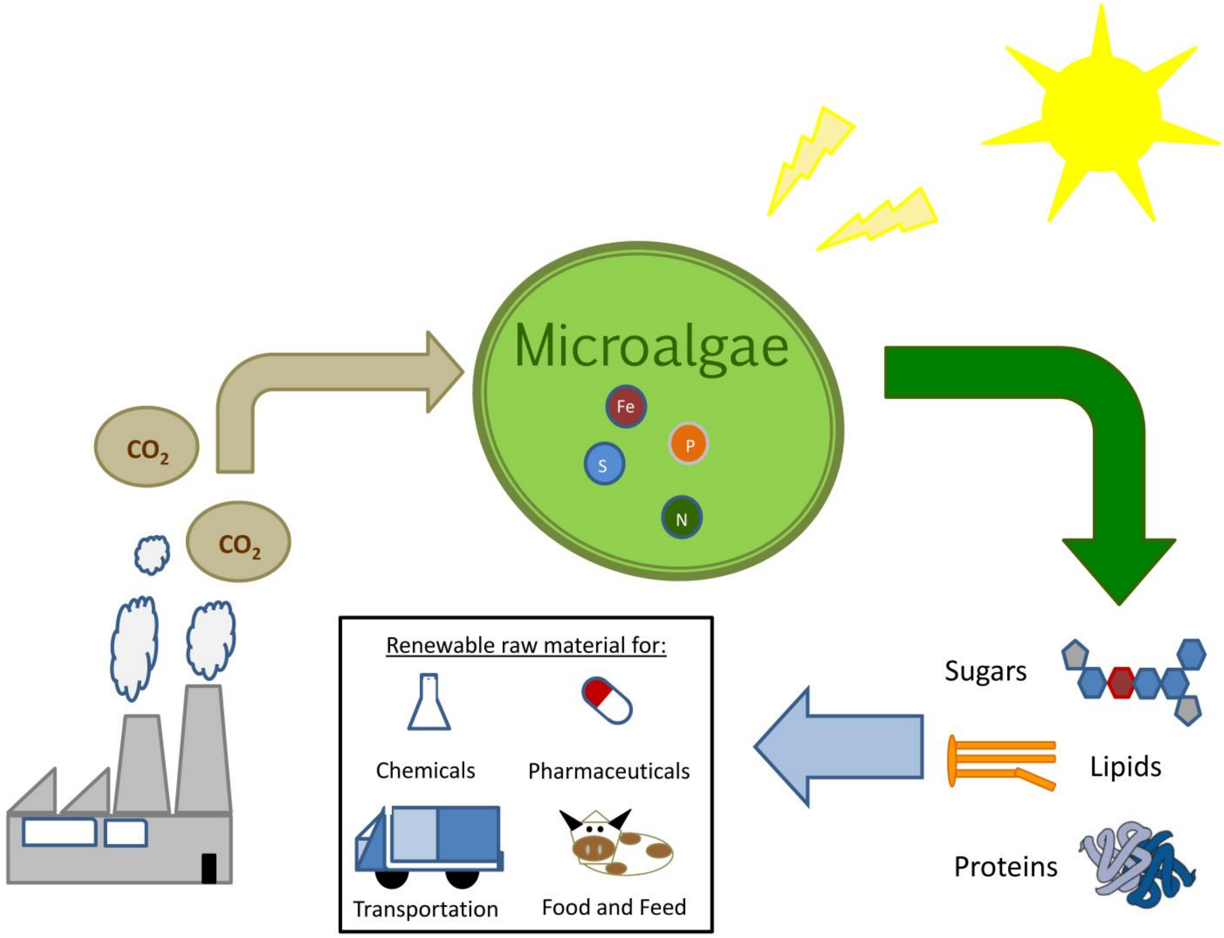

Figure 1 Schematic representation of a microalga as renewable feedstock

The culture of microalgae is carried out in so called photo-bioreactors. In these devices, the conditions needed for their growth (e.g., light intensity, temperature, pH, CO_2) are provided. Such reactors can be designed according to the desired scale, productivity and purpose (e.g., for biomass or metabolite production). The first step in process development involves the growth of microalgae at lab-scale (up to 5 L) in illuminated and bubbled shaking flasks (Y. K. Lee, 2016). At this stage, different strains are usually screened to produce specific components of commercial interest, such as metabolites or proteins. Furthermore, a screening step can also be performed to determine the best growing conditions for a particularly desired biomass composition. In the next phase, microalgae are grown at larger scale (up to 20 L) under much more controlled conditions using several types of reactors. The most common reactor types include bubble column, airlift, flat panel, horizontal tubular, and stirred tank bioreactor (Singh & Sharma, 2012). As they provide a closed system in a regulated environment, these devices are more suitable for producing high-value products for use in pharmaceutical or cosmetic sectors than open systems (Pulz, 2001). Besides, they permit culture of single species with lower risk of bacterial or fungal contamination. High biomass productions can be achieved at lower costs with open systems at larger scale (e.g., raceway ponds), in areas in which proper climatic conditions are given (Brennan & Owende, 2010).

From a chemical perspective, microalgal biomass is mainly composed by organic macromolecules (lipids, proteins and carbohydrates), with the different components varying broadly according to species and growth conditions (Foley et al., 2011). Typically, the lipid fraction (10 – 60% DW) is employed in the production of biofuels by transesterification with short-chain alcohols (Chisti, 2007) or by hydrogenation of fatty acids into linear hydrocarbons (Lestari et al., 2009). To obtain these lipids from the biomass, diverse extraction strategies have been applied. These methods include solvent extraction, microwave- or ultrasound-assisted extraction, hydrothermal liquefaction, osmotic shock, enzymatic disruption, electroporation, and supercritical carbon dioxide extraction. Details on each procedure can be found in a comprehensive summary (Ghasemi Naghdi et al., 2016). The defatted protein fraction, which accounts for 10 – 50% DW, is generally employed for food, animal feed or as fertilizer, depending on the amino acid composition (Becker, 2007). Some species, such as *Spirulina platensis*, have been identified as high protein microalga, producing up to 600 g protein per kg biomass with optimal, nutrient replete growth conditions. Today, this microalga is commercially available as protein-rich food supplement as powder, tablets and capsules (Griffiths et al., 2016). The proportion of essential amino acids in proteins of some microalgal species is comparable to those of animal products, especially of methionine, and a number of promising biological activities have been identified (Lupatini et al., 2017). Other species, such as *Porphyridium* sp., are important producers of phycobiliproteins. This type of proteins can be found in mature commercialized products, such as fluorescent marker in clinical areas, colorant for textiles, and as pharmaceutical agents (Sekar & Chandramohan, 2008). Lastly, the carbohydrate fraction of the biomass, which may be found as mono- or polysaccharides, has been primarily employed for producing biofuels by biological (aerobic or anaerobic fermentation) or thermochemical conversion (Markou et al., 2012). For this, polysaccharides must be hydrolyzed to monomeric sugars by chemical or enzymatic methods, (Gerken et al., 2013; L. M. L. Laurens et al., 2015). Although the carbohydrate content of some species can reach up to 40% DW (e.g., *Chlorella*) and various potential applications have been devised, this share has remained underutilized (Lieve M. L. Laurens et al., 2017).

To improve the economic viability of algae production, comprehensive and integrative concepts for biomass utilization are needed (Scott et al., 2010). The conception of new products and intermediates for niche industries (e.g., chemical sector), that increase their adding value is essential in this process. Thus, the concept of microalgal bio refinery has been introduced in the last years. The central idea of this concept is the comprehensive utilization of all biomass components towards a maximum valorization. In this frame, several potential products have been identified from microalgal biomass including surfactants, fuel additives, poly-acids, and nutraceuticals (Lieve M. L. Laurens et al., 2017). The implementation of such a bio refinery requires the standardization and adaptation of the technology portfolio not only for biomass generation and processing, but also for biomass characterization (ABO, 2017). Addressing this aspect, the present work analyzes the most important challenges for the material utilization and analytical characterization of microalgal carbohydrates.

A1.2. Microalgal carbohydrates

The photosynthetic biomass production on Planet Earth is estimated at 170 billion metric tons p.a. From the resulting production of organic matter, 75% can be assigned to carbohydrates existing as mono- or polymers (Hu et al., 2012). Therefore, poly-, oligo-, and monosaccharides are the most abundant biogenic resource present in nature. The chemical diversity of carbohydrates surpasses that of lipids and proteins. In microalgae, they can either serve as short-term energy storage (e.g., starch or chrysolaminarin) or fulfill structural purposes forming the protective cell wall. Both starch and chrysolaminarin consist of repeating glucose units. While starch exists as amylose units of $\alpha(1\rightarrow4)$ glycosidic bonds and branched amylopectin of $\alpha(1\rightarrow6)$ glycosidic bonds, chrysolaminarin is a linear polymer of $\beta(1\rightarrow3)$ and $\beta(1\rightarrow6)$ linked units. The industrial applications of starch are broad and range from food, textile, papermaking, and pharmaceutical products. On the other hand, the carbohydrates present in the microalgal cell walls are highly variable depending on the strain and the developmental stage of the organism. This opens the opportunity for steering the abundance of specific sugar components without compromising cell growth (Pauly & Keegstra, 2008). The most common constituents of the cell wall include cellulose, xyloglucans, heteromannans, heteroxylans, pectic polysaccharides, and β-glucans (Pettolino et al., 2012). As the material utilization of carbohydrates from lignocellulosic land biomass (crops, wood, grass) has now been conducted for various years, the technologic portfolio for its analysis and processing is well-established. Conversely, the technologies available for marine biomass including microalgae are still in development. Therefore, the characterization of microalgal carbohydrates, especially from the cell wall is challenging.

The first investigations on carbohydrates from microalgae were conducted with the model microalga *Chlorella*. Starch and hemicellulose fractions were obtained after alkali extraction of the biomass followed by differential centrifugation. After acid hydrolysis (2 N H_2SO_4, 100°C), glucose, galactose, arabinose, mannose, xylose, rhamnose, and glucosamine were identified in these fractions by paper chromatography (Northcote et al., 1958; Olaitan & Northcote, 1962). Further improvements in instrumental and preparative chromatography allowed a more precise determination of algal carbohydrates: alkali-soluble and insoluble wall fractions were obtained from *C. pyrenoidosa* by ion-exchange chromatography and gel filtration (R. C. White & Barber, 1972). The monomeric composition of the extracted polysaccharides determined by GC (as alditol acetates after TFA hydrolysis) revealed monosaccharides other than neutral sugars, such as uronic acids (4.1% – 24% DW) and glucosamine (6.3% – 15% DW) (Blumreisinger et al., 1983).

Due to the high variability in the sugar composition, a taxonomic marker based on cell wall carbohydrates was proposed for microalgae (Takeda, 1988a, 1993; Takeda & Hirokawa, 1978). After extracting an alkali-soluble "hemicellulose" fraction and an insoluble "rigid wall" fraction, various microalgal species were classified according to following parameters: a.) The monomeric composition of fractions, b.) Ruthenium red stainability for pectin (uronic acid residues) determination, and c.) Anisotropy. According to this classification, nearly 20 *Chlorella* species were assigned as shown in Figure 2.

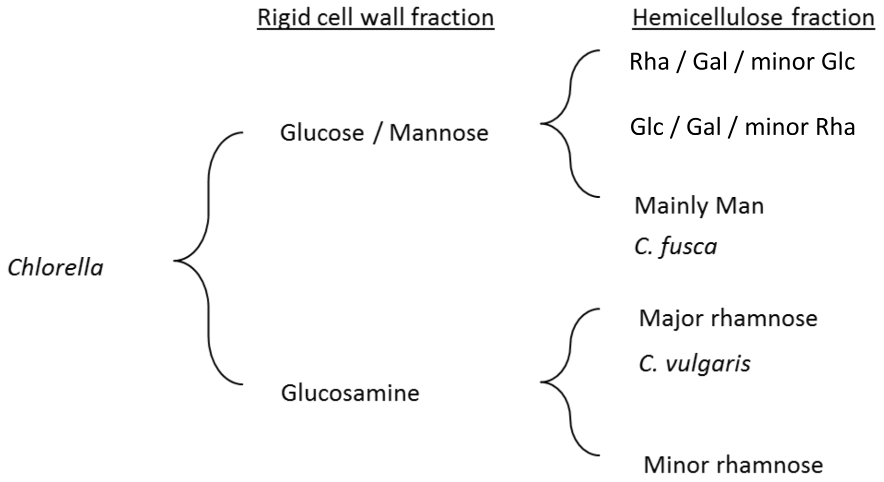
Rigid cell wall fraction
Hemicellulose fraction
Chlorella
Glucose / Mannose
Glucosamine
Rha / Gal / minor Glc
Glc / Gal / minor Rha
Mainly Man
C. fusca
Major rhamnose
C. vulgaris
Minor rhamnose

Figure 2 Summary of classification criteria for the microalga *Chlorella* proposed by Takeda (Takeda, 1988a, 1988b, 1993)

Subsequent efforts were targeted towards a more accurate identification of the sugar polymeric compounds from microalgae using different analysis methods. For example, polysaccharides containing amino sugars and a slight degree of crystallinity were found in the cell wall of *Chlorella* using a fluorescence-tagged lectin for the binding motif GlcNAc-β-(1-4)-GlcNAc-β-(1-4)-GlcNAc (Kapaun & Reisser, 1995). Specially substituted sugars were further identified using X-ray diffraction and infrared spectroscopy after partial hydrolysis (Figure 3), such as 3-*O*-methylated D-galactose, L-rhamnose, and 2-*O*-methyl-L-rhamnose (Ogawa et al., 1994, 1997).

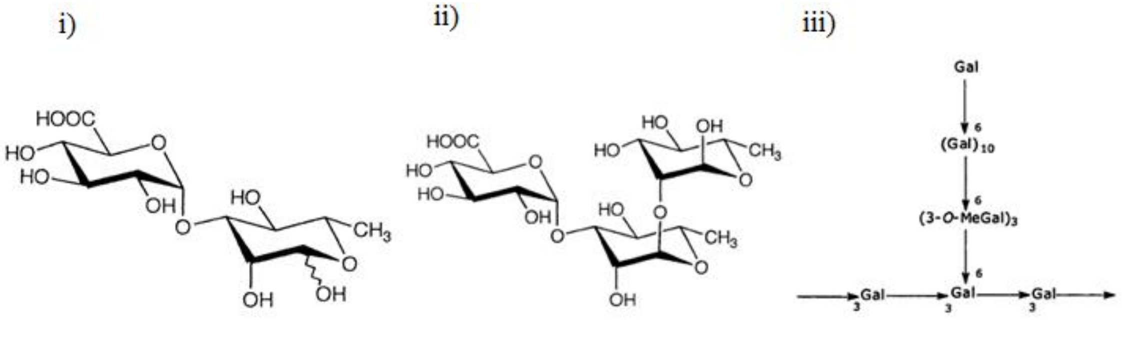
i)
ii)
iii)
HOOC
HO
OH
O
CH3
Gal
(Gal)10
(3-O-MeGal)3
6
3

Figure 3 Chemical structure of the carbohydrates found in *Chlorella* by Ogawa, (Ogawa et al., 1994, 1997)
i) 3-*O*-α-D-glucopyranuronosyl-L-rhamnopyranose, ii) α-D-glucopyranuronosyl-(1→3)-α-L-rhamnopyranosyl-(1→2)-α-L-rhamnopyranose and iii) a branched (partially methylated) β-D-galactan

Some algal poly- and oligosaccharides from *Chlorella*, such as arabinogalactans, galactans, glucans, and phosphoglucans have been reported to present immunoactivity. For example, the structure of a purified arabinomannan from *C. vulgaris* was elucidated (Pieper et al., 2012). These carbohydrates are often obtained after laborious purification procedures including ethanol precipitation, gel filtration and anion exchange chromatography (Suárez et al., 2010; Suárez et al., 2005). The extraction procedure itself plays a key role for the yield and quality of the polysaccharides. Very commonly, alkali extraction is applied for recovering microalgal polysaccharides. Alternative procedures, such as with a mildly acidic solution of sodium chlorite, have proven to yield higher polysaccharide amounts than the treatment with alkaline solutions (Sui et al., 2012).

In contrast to *Chlorella*, the cell walls of 11 species of *Scenedesmus*, another commercially relevant microalgal strain, resulted to be highly homogeneous, containing only mannose, galactose and glucose (Takeda, 1996). Beside *Chlorella* and *Scenedesmus*, *Nannochloropsis* is broadly used for biofuel and biorefinery applications (Lieve M. L. Laurens et al., 2017). For this microalga, a much simpler cell wall composition was found containing glucose from cellulose as major sugar component (98%). Also minor amounts of fucose, galactose, galactosamine, and rhamnose were detected (Scholz et al., 2014).

Some species of microalgae and cyanobacteria excrete carbohydrates in their extracellular environment, so called exopolysaccharides (EPS), as defense response or to produce biofilms to provide favorable growth conditions (Delattre et al., 2016). This type of carbohydrates is also associated to various biological activities and different cosmetic and pharmaceutical applications have been devised (De Jesus Raposo et al., 2013). To date, microalgal EPSs have been limited to lab-scale production, playing a modest role in the frame of a large-scale microalgal biomass refinery. For this reason, the work presented here will focus on the material utilization of storage and cell wall carbohydrates.

A1.3. Analytical methods for microalgal carbohydrates

As mentioned above, most of the carbohydrate analytical methods available to date have been developed and optimized for analyzing terrestrial biomass. In this material, only a limited amount of monomeric neutral sugars are present in polysaccharide structures, especially xylose, glucose, and arabinose. Accordingly, the analytical methods applied for lignocellulosic biomass are specialized in detecting these neutral monosaccharides. Traditionally, such methods have been also used for characterizing carbohydrates from microalgae, even when this biomass displays a higher variability. However, an incomplete or inaccurate carbohydrate determination resulting from unsuitable methods commonly hampers a correct calculation of product yields, e.g., in fermentative ethanol production processes from algal biomass (L. M. L. Laurens et al., 2015). For this reason, the need for new methods, or at least adaptations of existing ones, has been identified for the study of microalgal carbohydrates (Templeton et al., 2012). Thereupon, robust and reliable carbohydrate analytical procedures are essential for the successful development of microalgal biomass and the corresponding processing strategies.

To date, different carbohydrate analytical methods are available, and they are employed depending on the intended biomass usage. While some applications require a general analysis of total carbohydrates indistinctly of the monosaccharide type (e.g., to estimate biomass composition), others demand a more or less precise determination of the monomeric composition (e.g., to design fermentation strategies) or even the exact elucidation of oligomeric or polymer structures (e.g., to identify bioactive compounds) (C. Schulze et al., 2017). As explained below, analytical methods having a higher carbohydrate resolution (e.g., exact determination of substituents or side chains) are more complex, as special instrumentation is required and sample processing requires more time.

Total carbohydrate analysis: Photometric methods are the simplest and fastest analytical procedures available. These are usually called total carbohydrate methods, as they are employed for rapid estimations of the overall sugar content in biomass. Such methods are very convenient for a rapid monitoring of, for example, carbohydrate formation as a function of varying growth parameters. A well-established procedure of this type is the phenol sulfuric acid method. The underlying principle relies in the one-step biomass hydrolysis and subsequent colorimetric reaction of the released furan aldehyde groups with phenol (Nielsen, 2010). Its use for algal biomass is rather limited, as interference with pigments may cause over or under quantification. Further, highly variable absorbance responses are observed from different monomeric sugars and the method is insensitive to specific algal monosaccharides, such as amino sugars. An alternative spectrophotometric method based on the derivatization of aldoses with 3-methyl-2-benzothiazolinone hydrazone (MBTH) displays a better sensitivity towards algal-specific monosaccharides without interference from hydrolysate components (Van Wychen et al., 2017). Consequently, this method has been adopted by the US National Renewable Energy Laboratory (NREL) as a standard laboratory analytical procedure for total carbohydrate determination in microalgal biomass. A critical step for a correct carbohydrate determination is the chemical hydrolysis applied to release the monosaccharides from polymeric structures. Often, the relevant parameters, such as acid type and concentration, temperature, and hydrolysis time must be adjusted to ensure a complete release of monomeric sugars with the lowest degree of degradation possible. To avoid this hydrolysis step, non-invasive techniques using Fourier-Transform infrared spectroscopy (FT-IR) can be applied for algal biomass (Mayers et al., 2013).

Monomeric sugar analysis: For analyzing the monomeric sugar *composition* after biomass hydrolysis, chromatographic techniques that separate the monosaccharides for analysis must be applied. This is a particularly challenging task for microalgae, given the broad monosaccharide diversity which includes neutral sugars, uronic acids, amino, methylated, and sulfated sugars. For a first qualitative estimation, thin layer chromatography (TLC) offers a simple and inexpensive alternative even for microalgal strains presenting complex carbohydrate mixtures (C. Schulze et al., 2017). This procedure does not require any special instrumentation equipment, but the quantification is limited. Quantitative monosaccharide detection using instrumental procedures enable a more detailed study of microalgal carbohydrates. The most widely used methods include high performance liquid chromatography (HPLC) and gas chromatography (GC). Both methods can be coupled to mass spectroscopy (MS) to analyze unknown or coeluting peaks. A comparative study of chromatographic methods for analyzing a mixture of 13 typical microalgal monosaccharides revealed that traditional HPLC configurations used for lignocellulosic biomass are unsuitable, as poor peak resolution is observed and co-elution may occur (Templeton et al., 2012). In contrast, GC offers important advantages, such as a higher peak resolution, low limit of detection (LOD), and identification of unknown or co eluting peaks *via* coupled MS. As GC is restricted to volatile compounds, monomeric sugars must be derivatized first, most commonly as alditol acetates or silanes. Besides, disturbing salts must be eventually removed. This reaction is cumbersome for some carbohydrates present in microalgae (e.g., uronic acids) so this alternative may not always be suitable for analyzing microalgal sugars. Furthermore, additional salt precipitation with ethanol and evaporation steps (e.g., for H_2SO_4) are usually needed to generate a volatile sample and allow MS detection, which further increases the sample preparation time (McConnell & Antoniewicz, 2016). High performance anion exchange chromatography (HPAEC) coupled with pulsed amperometric detection (PAD) has shown to be a very robust method for separating complex monosaccharide mixtures with very good resolution, and detection of amino sugars and uronic acids is also possible. Still, the use of strong ionic eluents (such as NaOH) makes its use for MS difficult, limiting the method resolution. Besides, issues concerning reproducibility and baseline stability have been observed (Templeton et al. 2012). In some cases, pre-column derivatization of monosaccharides can be advantageous, as it may allow UV detection and quantification using active compounds and at the same time, their ionization behavior is enhanced for MS analysis. 1-phenyl-3-methyl-5-pyrazolone (PMP) for example, has been employed for the study of monosaccharides using coupled MS. This UHPLC-MS method has been successfully applied in high-throughput (HT) mode for analyzing bacterial EPS (Rühmann et al., 2014) as well as polysaccharide fractions of *Dunaliella* sp., in which also uronic acids and amino sugars can be detected (Dai et al., 2010). Thus, this method seems a promising alternative for analyzing microalgal carbohydrates with a good compromise between simplicity, fastness, and analytical resolution. A schematic representation of the resolution and complexity of the discussed carbohydrate analytical methods is shown in Figure 4.

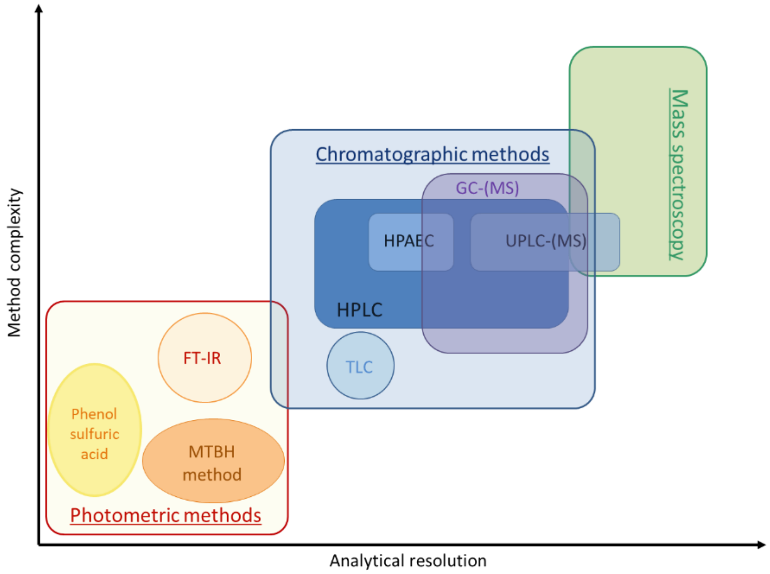

Figure 4 Analytical methods for studying microalgal carbohydrates: simplicity and resolution

Oligomeric sugar analysis: When a more precise elucidation of the oligo- or polysaccharide structure is needed, more complex analytical strategies are required. Methylation analysis, for example, is usually performed to identify the linkage of saccharide chains (Pettolino et al., 2012).

Such procedures are especially important for establishing the chemical structure of bioactive carbohydrates. The method is based on the hydrolysis of previously methylated polysaccharides, subsequent reduction with deuterated compounds, acetylation, and GC-MS analysis.

Further analytical methods can be complementarily used for identifying the anomeric configuration of glycosidic bonds as well as possible substituents. Nuclear magnetic resonance (NMR) spectroscopy, for example, enables the identification of important substituent groups such as sulfate or carboxylic acids, as previously demonstrated with polysaccharides from *Phorphyridium* sp. (Geresh et al., 2009). In general, NMR methods require special equipment, are very sensitive to impurities, and involve intensive data interpretation. Therefore, its application demands a larger sample processing, as high sample purity is required. That is why this method is reserved to very special applications.

The analysis of the carbohydrate distribution within the cells is also of importance when designing culture strategies. For this, monosaccharides from starch and structural carbohydrates must be discerned. Due to their high specificity, enzymes play a key role in the targeted hydrolysis of specific polysaccharide fractions, which can be then analyzed by the methods mentioned above. Amylases and certain glucosidases for example, selectively break down the glyosidic bonds from starch leaving other types of polysaccharides intact. Therefore, they are usually employed for starch determination in biological samples and biomasses, and even some commercial kits are available (B. Fernandes et al., 2012). In addition to these analytical applications, the use of enzymes for the material utilization of microalgae is of great advantage, as addressed in the next section.

A1.4. Enzymatic hydrolysis of algal carbohydrates

Enzymes (i.e., “biocatalysts”) catalyze the reactions needed for the growth and metabolism of all living organisms. Their potential for converting specific substrate molecules into useful products has been identified in numerous fields, such as biotechnology, chemical industry, cleaning products, food and oil processing, medicine and pharma, textile and leather manufacturing, etc. (Porter et al., 2016). The use of enzymes offers significant advantages over chemical catalysts, such as high substrate selectivity, optimization potential with molecular biology tools, reduction of hazardous compounds (e.g., strong acids), and process flexibility. However, enzymes are prone to denaturation or product inhibition and are still a considerable cost factor, which may limit their application in industrial processes (Faber, 2017).

The production of high fructose corn syrup by starch hydrolysis with the enzyme α-amylase, glucoamylase, and glucose isomerase in the early 1970s is one of the first developed enzymatic processes for biomass carbohydrates (J. S. White, 2014). Ever since, the discovery of new enzymatic activities has permitted the production of, e.g., fermentation media from distinct types of biomass for a broader range of applications. Different hydrolases, for instance, have been developed for improving the filterability of fruit juices (P. Fernandes, 2010). Furthermore, a considerable number of commodity chemicals can be enzymatically produced from the hydrolysis products of biomass, such as alkanes, alkenes, aromatic hydrocarbons, alcohols, etc. (Straathof, 2014). For generating the corresponding precursors from the hydrolysis of biomass, various enzymes are commercially available (Sweeney & Xu, 2012). Although most of these biocatalysts have been developed for lignocellulosic feedstock, current HT analysis technologies are allowing a rapid biomass-tailored process development, and microalgal biomass is not an exception.

One of the earliest investigations on the enzymatic hydrolysis of algal polysaccharides aimed to determine the constitution of the cell wall by producing spheroplasts from *Chlorella* using a mixture of cellulase, hemicellulase and pectinase (Atkinson Jr et al., 1972). In further studies, β-1,4-mannanase and β-D-fucosidase were identified as responsible for the cell wall lytic activity during cell division in *C. fusca* (Loos & Meindl, 1985). Also, the saccharification and liquefaction of starch from *Clamydomonas* microalgal biomass for bioethanol production was described by separate hydrolysis and fermentation (SHF) using commercial amylases (Choi et al., 2010). Similarly, microalgal cells were hydrolyzed with commercial cellulases, yielding around 65% reducing sugar to total sugar (glucose, mannose, and galactose) under optimal pH and temperature (Razif Harun & Danquah, 2011). Cellulases can also be applied to break the algal cell wall and so significantly increase the lipid extraction efficiency from microalgal biomass (Fu et al., 2010). A similar approach was described to enhance the lipid recovery from *Nannochloropsis* after cell wall disruption (Zuorro et al., 2016). Due to the complexity of algal carbohydrates however, saccharification of microalgal biomass using cellulases and amylases commonly results significantly in lower hydrolysis yields than chemical treatments (Mirsiaghi & Reardon, 2015). Therefore, specialized enzymes and enzymes mixtures for microalgal biomass are needed. Optimal commercial enzyme combinations may be developed for maximizing sugar yield, e.g., for fermentative applications. Studies evaluating the use of microalgal biomass for the fermentative production of bioethanol coincide in the need for more efficient, biomass-tailored saccharification processes to increase the efficiency of biofuel conversion and render this process more rentable (Chen et al., 2013; R. Harun et al., 2014). In most published studies, only cellulose and starch are considered for the processing of microalgal biomass, excluding the rest of the cell wall. This may probably be one reason for the reported incomplete saccharification.

The search for suitable enzymes for degrading the complex cell wall is a challenging task. Significant differences can be found in the wall structure among microalgal species. Besides, microalgae are dynamic organisms, so that the growth phase and the culturing conditions, such as nutrient supply or light intensity affect the carbohydrate composition. This makes an appropriate enzyme selection even more difficult. In a recent study, clear distinction was made between starch carbohydrates (which accumulated under nitrogen starvation) and cell wall polysaccharides from *C. vulgaris* (Kim et al., 2014). Starch was degraded by treatment with amylase (pH 4.8, 50°C), whereas different hydrolytic enzymes were tested on the cell wall. Cellulase, amylase, xylanase, β-glucosidase, chitinase, lysozyme, and sulfatase displayed sugar conversion yields lower than 15%. Only pectinase from *Aspergillus* yielded a 79% sugar conversion after a bead-milling pretreatment step. A very effective, two-step approach for discovering cell wall active enzymes was based in the ability of different enzymes for inhibiting growth of microalgae in agar plates (primary screen). Secondly, the effectiveness of the enzymes for breaking the cell wall was confirmed by cell permeability analysis using a fluorescent DNA stain and flow cytometry (Gerken et al., 2013). Of the 20 commercial enzymes tested on *Chlorella*, chitinase, lysozyme and pectinase were most effective in the primary screen. Chitosanase, β-glucuronidase, endoglucanase, sulfatase, and trypsin also caused growth inhibition. After the secondary screen, lysozyme and combinations with sulfatase, phospholipase, lyticase and chitinase were active on the cell wall. Another promising alternative for the saccharification of the cell wall is the controlled autolysis of the polysaccharides by inducing the expression of lytic enzymes (Demuez et al., 2015). However, unless this technology becomes available in a large scale, the development of biomass-specific exogenous enzymes will still be an essential part in process design for a microalgal biorefinery.

A2. Scope of the work

The general goal of this work was to develop complementary tools for the existing technology portfolio for the analysis, hydrolysis, and bioconversion of microalgal carbohydrates. The developed methods and protocols intend to provide a reliable approach for utilizing microalgae as renewable feedstock. Although the potential of this source of biomass has been identify long time ago, its development has remained stagnant in the last years due to a slow and inaccurate characterization of its components. The lack of adequate analysis procedures as well as culture and processing strategies in this field often bottlenecks a maximized valorization of microalgae beyond the established raw materials and products. The detection and utilization of uncommon saccharides attached to the cell wall of many microalgae, for example, could increase the added value of the carbohydrates in algal biomass beyond starch.

The first step for achieving this goal is the development and transfer of analytical procedures that covers the broad spectrum of microalgal monosaccharides (e.g., glucose, mannose, rhamnose, and substituted sugars) for a proper biomass characterization. The previously developed HT-PMP carbohydrate detection method for microbial exopolysaccharides was identified as promising candidate for this requisite (Rühmann et al., 2014). As algal biomass can substantially differ in composition from terrestrial biomass, the detection capabilities of this method offer significant advantages over existing procedures. The essential PMP derivatization step demands a comprehensive adaptation and validation for crude and processed algal biomass.

To further elucidate the distribution of valuable sugar components within the cell, a proper biomass fractionation approach must be designed. A distinction between energy storage and structural carbohydrates must be possible with this procedure. Thus, culture strategies and even future genome editing techniques could be, for example, targeted towards modulating the production of the one or the other type of carbohydrate within the cell. Moreover, different microalgal growth modes (e.g., nutrient de-, or repletion) often influences the carbohydrate composition. Thus, once the analysis method was adapted and validated, it was used on differently cultured microalgae to demonstrate its applicability in designing and optimizing the composition of microalgal biomass.

Finally, commercially available enzyme cocktails were selected for the saccharification of microalgal biomass to obtain reducing monomeric sugars. The released sugars can be then used for the fermentative production of bioethanol or other value-added products. As these enzyme mixtures are not specifically designed for the hydrolysis of microalgal biomass, significant amounts of oligosaccharides were expected in the supernatants. The qualitative determination of these short-chained sugars allows a much more effective selection of complementary hydrolytic activities for a complete saccharification. In this regard, an extension of the HT-PMP carbohydrate method using LC-MS to analyze oligosaccharides was evaluated to set the basis for optimizing the enzymatic hydrolysis.

In summary, a comprehensive approach for the material utilization of microalgal carbohydrates is presented, which includes its analysis, targeted production and saccharification. Although the procedures presented here focused on model microalgal organisms, they can be translated to any cultured photosynthetic species.

A3. Materials and Methods

The laboratory and analytical equipment employed throughout this work is reported in Table 1. The computer software (if license was needed, this was provided by the TUM) is listed in Table 2. A list of enzyme and reagents can be found in Table 3. Special consumables for the analytical methods, such as chromatographic columns and microtiter plates, are enumerated in Table 4.

A3.1. Equipment

Table 1: Overview of lab equipment used

Equipment name	Manufacturer / Model
Agarose gel electrophoresis apparatus	Bio-Rad (München), Mini-Sub Cell GT System
Autoclave	Thermo Scientific (Ulm) Varioklav 135S
Bacterial colony picker	Hudson (Springfield, NJ) RapidPick® CP-7200
Centrifuge	Thermo Scientific (Ulm) Sorvall RC-6 Plus
Clean bench	Thermo Scientific (Ulm) MSC-Advantage
Drying oven	Thermo Scientific (Ulm) Function line T12
Electroporator	Bio-Rad (München), MicroPulser^{TM}
Elementary analysis system	EuroEA, HEKAtech GmbH (Wegberg)
FPLC	GE Healthcare Europe (Freiburg), ÄKTA purifier
FPLC-Controller	GE Healthcare Europe (Freiburg), UPC-900
FPLC-Pump module	GE Healthcare Europe (Freiburg), P-900
FPLC-Sample pump	GE Healthcare Europe (Freiburg), UP-960
Freezer -20°C	Liebherr-Hausgeräte (Ochsenhausen)
Freezer -80°C	Thermo Scientific (Ulm) Forma 906 -86°C ULT
Gel documentation system	Intas Science Imaging (Göttingen), Gel iX Imager
Heating block	VLM (Bielefeld), EC model series Tmix (Jena) Jenaanalytik
High pressure cell disrupter	Constant Systems (Daventry, GB), Basic Z Model
Incubator	Binder (Tuttlingen) KBF 240 E5.1/C Infors HT (Bottmingen-CH) Minitron
Lyophilizer	Martin Christ (Osterode), Alpha 2-4 LD plus
Lyophilizer High-vacuum pump	Vacuubrand (Olching), RC 6
Magnetic stirrer	Thermo Scientific (Ulm) Variomag Telesystem
Microplate shaker	Edmund Bühler (Hechingen) TiMix 5 contron and TH 15
Multichannel pipette	Eppendorf AG (Hamburg) Research pro 8x 1200 µL
Nanophotometer	Implen (München), P-330
pH-meter and electrode	Mettler-Toledo (Giessen) Five Easy^{TM} and InLab® Expert Pro
Pipettes	BRAND (Wertheim) Transferpetten

Equipment name	Manufacturer / Model
Rotor	Thermo Scientific (Ulm) SS-34, SH-3000, F9-4x 1000y
Scale	Sartorius (Göttingen) TE1502 and TE6101
SDS-electrophoresis chamber	Bio-Rad (München), Mini-PROTEAN®-Tetra Cell
SDS-Power supply unit	Bio-Rad (München), PowerPac^{TM} Basic
Shaker	Thermo Scientific (Ulm) MaxQ 2000
Special clamping device	K. Rühmann (Goltoft) In-house development
Spectrophotometer	Thermo Scientific (Ulm) Varioskan Flash and Multiskan
Table centrifuge	Thermo Scientific (Ulm) Heraeus Fresco 21
Thermo cycler	Bio-Rad (München) MyCycler^{TM}
UHPLC	Dionex (Idstein) Ultimate 3000RS
UHPLC-Autosampler	Dionex (Idstein) WPS 3000TRS
UHPLC-Column compartment	Dionex (Idstein) TCC 3000RS
UHPLC-Degasser	Dionex (Idstein) SRD 3400
UHPLC-Diode array detector	Dionex (Idstein) DAD 3000RS
MS-High capacity ion trap	Bruker Daltonics (Bremen) HCT
UHPLC-Pump module	Dionex (Idstein) HPG 3400RS
Ultrapure water system	ELGA LabWater (Celle) PURELAB classic
Ultrasonic cell disruptor	Hielscher (Teltow), UIS250L
Ultrasonic sonotrode	Hielscher (Teltow), LS24d10, VialTweeter
UV-Cabinet	CAMAG (Berlin), UV INSPECTION 022.9070
Vortexer	Scientific Industries (Bohemia) Vortex Genie 2
Water bath	Huber (Offenburg) CC1

A3.2. Software and databases

Table 2: Overview of electronic media employed

Product	Manufacturer	Application
Algaebase	National University of Ireland	Algae taxonomy database
Basic Local Alignment Search Tool (BLAST)	National Center for Biotechnology Information	Protein sequence alignment
Braunschweig Enzyme Database (BRENDA)	Technische Universität Braunschweig	Enzyme research
ChemBio Draw Ultra 14.0	Cambridge Soft	Drawing of chemical structures
Chromeleon	Dionex	Data analysis UHPLC
Clone Manager 8	Scientific & Educational Software	*In silico* DNA sequence analysis
DataAnalysis	Bruker	Data analysis MS

Product	**Manufacturer**	**Application**
EndNote X7	Clarivate Analytics	Literature citing managing
GENtle	Universität Köln	*In silico* DNA sequence analysis
HyStar	Bruker	UPLHC-MS System control
LibraryEditor	Bruker	MS-Spectra database
ProtParam tool	ETH Zürich	Analysis of protein parameters
QuantAnalysis	Bruker	Quantification of MS-data
ScanIt	Thermo Scientific	MTP-reader control software
SigmaPlot 11.0	Systat Software	Data visualization
Statgraphics Centurion XVII	Statpoint Technologies	Data analysis for DoE
UNICORN	GE Healthcare Life Sciences	FPLC System control
Web of Knowledge	Thomson Reuters	Literature research

A3.3. Enzymes and reagents

Table 3: Overview of the enzymes and reagents used

Name	**Manufacturer**	**Catalog number**
1-Phenyl-3-methyl-5-pyrazolone	Sigma-Aldrich	M70800
2-Heptanol	Sigma-Aldrich	H3003
Acetic acid	Sigma-Aldrich	338826
Acetone	Carl-Roth	7328
Acetonitrile LC-MS grade	VWR	83040.320
Acetyl xylan esterase from *Orpinomyces* sp. (1,000 U)	Megazyme	E-AXEAO
Adenosin-5´-triphosphate	Carl-Roth	K056
Adenosin-5'-phosphat, bi-Na-salt	Alfa Aesar	J61643
Ammonium solution 32%	Carl-Roth	P093.1
Anhydrotetracycline	IBA	2-0401-001
Bovine serum albumin	Sigma-Aldrich	A2153
B-Per^{TM}	Merck	78248
Bugbuster® protein extraction reagent	Thermo-Scientific	70584-4
Calcium chloride	Carl-Roth	5239.1
Carbenicillin	AppliChem	A1491
Cobalt chloride	Alfa Aesar	A16346
Copper chloride	Alfa Aesar	A16346
DA-64	Wako Chemicals	043-22351

Name	Manufacturer	Catalog number
Dioxane	Sigma-Aldrich	296309
DMF	Carl-Roth	T921.1
DMSO	Carl-Roth	AE02.1
DNase	AppliChem	A3778.0500
Ethanol absolute	VWR	20821.321
Galactomannan	Megazyme	P-GALML
Glucose oxidase	Sigma-Aldrich	G2133
Glucomannan	Megazyme	P-GLCML
GoTaq DNA-polymerase	PROMEGA	M3001
Guanosin-5´-triphosphate	Carl-Roth	HN53.1
HEPES	Carl-Roth	HN78.3
Horseradish peroxidase	Sigma-Aldrich	P6782
IPTG	Carl-Roth	CN08.3
Iota-carrageenan (analytical grade)	Carl-Roth	3675.1
Iota-carrageenan (technical grade)	Marcel carrageenan	SMIII033-13 Aquagel GU8435
Iron chloride tetrahydrate	Carl-Roth	P742.1
Isopropanol	Carl-Roth	7343.1
Kappa-carrageenan (analytical grade)	Carl-Roth	3059.1
Kappa-carrageenan (technical grade)	Marcel carrageenan	SMIII033-13 Aquagel GU8450
Lambda-carrageenan	Marcel carrageenan	SMIII033-13 Aquavis GU8123
Lysozyme	Carl-Roth	8259.2
Magnesium chloride hexahydrate	Sigma-Aldrich	31413
Methanol LC-MS	VWR	83638.320
MOPS	Carl-Roth	6979.4
Nickel chloride hexahydrate	AppliChem	A3917
Pectin GENU® type LM-12 CG low ester standardized with sucrose	CP Kelco	0002004 B.GR03496
Peptone from casein	Carl-Roth	8952.5
Phenol red	Alfa Aesar	B21710
Phosphoenolpyruvate	Sigma-Aldrich	860077
Phusion high-fidelity DNA-Polymerase	New England Biolabs	M0530
p-nitrophenol	Sigma-Aldrich	425753
Potassium 4-nitrophenyl sulfate	Sigma-Aldrich	N3877
Potassium phosphate dibasic	Carl-Roth	P749.3

Name	Manufacturer	Catalog number
Potassium phosphate monobasic	Merck	1.04873.1000
Potassium sulfate	Merck	221368
Pullulan standard	Sigma-Aldrich	53168
Pyruvate oxidase	Sigma-Aldrich	P4591
Rohament® CL	AB Enzymes	9012-54-8
Rohapect® B1L	AB Enzymes	9032-75-1 / 9012-54-8 / 37288-54-3
Rohapect® UF	AB Enzymes	9032-75-1
Rubidium chloride	Alfa Aesar	12892
Sodium, metallic	VWR	8222840250
Sodium-azide	Sigma-Aldrich	71290
Sulfur trioxide triethylamine complex	Sigma-Aldrich	84739
Thiamine pyrophosphate	Sigma-Aldrich	C8754
Trifluoroacetic acid	Sigma-Aldrich	T6508
TRIS	Carl-Roth	AE15.2
TRIS-HCl	Carl-Roth	9090.3
Xylan	Carl-Roth	7500.1
Zinc chloride	Merck	1.08816.0250
Zink sulfate	Merck	1.08883.1000

A3.4. Special consumables

Table 4: Overview of the special consumables employed

Material name	Manufacturer	Catalog number
96-well deep well plate 2.0 mL (DWP)	Greiner Bio-One	780271
96-well microtiter plate F-Bottom (MTP)	Greiner Bio-One	655101
96-well deep well plate U-Bottom, Riplate	Ritter	43001-0020
96-well silicon cap mat	Whatmann	7704-0105
96-well PCR-plate	Brand	781350
Aluminum sealing film	Axygen	PCR-AS-200
Breathable sealing film	Axygen	BF-400-S
Filter plate 0.2 µm Supor	Pall Corporation	PN 8019
Pipette tips PHS 5-300 µL	Brand	732150
Glass tubes borosilicate, 15 mL	VWR	212-7442

Material name	Manufacturer	Catalog number
Syringe filters, PTFE 0.2 µm	VWR	514-0068
Column UPLC NUCLEODUR C18 Gravity, 1.8 µm, 100 mm, ID: 2 mm	Macherey-Nagel	SN E16110239 LOT 37205011
Column YMC-Triart Diol HILIC, , 1.9 µm, 100 mm x 2.0 mm ID	YMC Europe	TDH12SP9-1002PT LOT 11115
HisTrap FastFlow 5 mL	GE Healthcare Europe	17-5255-01
HisTrap Desalting HiPrep 26/10	GE Healthcare Europe	17508701
GeneJET^{TM} Plasmid Miniprep	Thermo Fischer Scientific	K0502
Strep-Tactin® Sepharose® Column Gravity flow	IBA Life Sciences	2-1202-001
Nucleospin® Gel and PCR Clean-up Kit	Macherey-Nagel	740609.250
Roti®-Nanoquant Kit for protein determination (Bradford)	Carl-Roth	K880.1-3

A3.5. Microalgal biomass

Dry biomass from the strains listed in Table 5 was externally obtained and employed for the transfer, evaluation, and validation of the PMP UHPLC-MS method for microalgal carbohydrates. Biomass from *C. vulgaris* was obtained commercially, the cultivation method is not available. All other microalgae were cultivated under no nutrient limitation and without light stress for 14 days at 25°C. The culture media were prepared as reported before (EPSAG, 2018).

Table 5: Overview of the microalgal strains for PMP UHPLC-MS method transfer, evaluation, and validation. N.A. not available.

Strain	Producer	Culture medium
Chlorella vulgaris	Algomed (Klötze, Germany)	N.A. (commercial product)
Phaeodactylum tricornutum	Institut für Pharmazie, EMAU Greifswald	SWES
Nannochloropsis salina	Institut für Pharmazie, EMAU Greifswald	SWES
Phorphyridium purpureum	Institut für Pharmazie, EMAU Greifswald	f/2 supplemented with trace elements
Dunalliela salina	Institut für Pharmazie, EMAU Greifswald	DUN supplemented
Scenedesmus ovalternus	Institut für Pharmazie, EMAU Greifswald	BG-11

The Ernst-Moritz-Arndt-Universität (EMAU) in Greifswald (Germany) performed a comprehensive strain screening to find promising microalgae with a balanced composition in the context of a biorefinery. Thus, the microalga *Scenedesmus obtusiusculus* A189 was selected for experiments concerning enzymatic hydrolysis of algal carbohydrates. Different biomasses of this specie were produced by the EMAU and employed in this work. Some of them were cultured using optimized media for carbohydrate production, while others were lipid-extracted by the industrial partner NATECO2. The different biomasses, their treatments and applications in this work are detailed in Table 6.

Table 6: Overview of the biomasses from *S. obtusiusculus* A189 addressed throughout this work

Denomination	Medium optimization	Lipid-extracted	Application (section)
ABV1-3	Yes	No	Culture optimization (section A4.2)
ABV6-13	Yes	Yes	Enzymatic saccharification (section A4.3)

On the other hand, the biomass from the strains listed in Table 7 was cultured by the author at the Algal Biotechnology Laboratory of the University of Queensland (Australia). A 1000 mL pre-culture in nutrient replete conditions was grown for 5 days from the strain collection. After that, the pre-culture was split under sterile conditions into 150 mL triplicates. Each triplicate was then cultured using different conditions for further 14 days. The biomass was collected by centrifugation (5,000 x g) and lyophilized for analysis. The resulting biomass was analyzed by Sinzinger (2016) using the transferred PMP UHPLC-MS method.

Table 7: Overview of microalgal strains cultured at The University of Queensland for method characterization

Strain	Culture medium	Triplicate culture conditions
Chaetoceros muelleri	f/2 supplemented with trace elements	Nitrogen replete (~80 mg L^{-1} NO_3) Nitrogen deplete
Tetraselmis sp.	f/2 supplemented with trace elements	Nitrogen replete (~160 mg L^{-1} NO_3) Nitrogen deplete
Isochrysis galbana	f/2 supplemented with trace elements	Nitrogen replete (~160 mg L^{-1} NO_3) Nitrogen deplete
Phaeodactylum tricornutum.	f/2 supplemented with trace elements	Nitrogen deplete: white, red and green light
Spirulina sp.	Spirulina medium modified	Nitrogen replete (~160 mg L^{-1} NO_3) Nitrogen deplete

A3.6. Monosaccharide analysis by PMP UHPLC-MS

6 mg algal biomass was mixed with 6 mL 2 M TFA in borosilicate glass tubes. The resulting suspension was incubated at 121°C in a heating block either for 90 min (referred as TFA standard hydrolysis) or a variable time for the optimization experiments. After cooling in a water bath, the mixture was neutralized with a 3.2% (v/v) ammonium solution (pH 8 ± 0.05) inside of an ice bath. 25 µL of the neutralized hydrolysate were transferred into a 96-well PCR plate and 75 µL of PMP derivatization mix (0.2 M methanolic-PMP-solution: 1.6% v/v NH_4OH solution, 2:1) were added.

After mixing and centrifuging (2,000 x g, 20 min, 20°C), the plate was incubated at 70°C for 100 min in a PCR cycler. A 20 µL aliquot of the derivatized samples was mixed with 130 µL of a 0.5 M diluted (1:26) acetic acid solution. The mixture was transferred to a Supor filter plate and centrifuged (2,500 x g, 5 min, 20°C) into a MTP. The plate was then sealed with a silicon mat and the samples were analyzed by the HT-PMP method, as previously described (Rühmann et al., 2014).

A3.7. Oligosaccharide analysis

Samples containing oligosaccharides ($1 – 3\ \mathrm{g\ L^{–1}}$) obtained from enzymatic or chemical hydrolysates were brought to pH 8 ± 0.05 with a 3.2% (v/v) ammonium solution. A 25 µL aliquot was derivatized with 75 µL derivatization mix (0.2 M methanolic-PMP-solution: 1.6% v/v NH_4OH solution 2:1) in 1.5 mL test tubes in a water bath using the conditions described above. 0.5 M acetic acid (25 µL), acetonitrile (525 µL) and ddH_2O (125 µL) were added. The samples were filtered with PTFE syringe filters and analyzed by LC-MS as follows. The mobile phase A consisted of a 5 mM ammonium acetate buffer pH 5.6 + 15% acetonitrile (w/w); the mobile phase B was 100% acetonitrile. The column (YMC-Triart Diol, Table 4) was tempered to 7°C and the chromatographic flow was set to $0.3\ \mathrm{mL\ min^{–1}}$ with the following gradient: start of mobile phase A at 15% for 3 min, following increase to 35% over 4 min for peak elution and immediate returning to the initial conditions over the last 5 min for regeneration (UHPLC equipment, Table 1).

The samples were qualitatively analyzed by MS as extracted ion chromatogram (EIC) of eluted peaks and mass fragmentation using the following parameters. The ion-trap was operated in the ultra-scan mode (26,000 *m/z*/s) from 500 to 3,000 *m/z*. The ion charge control (ICC) target was set to 200,000 with a maximum accumulation time of 50 ms and four averages. The ion source parameters were set as follows: capillary voltage 4,000 V, dry temperature 325°C, nebulizer pressure 40 psi and dry gas flow $6.0\ \mathrm{L\ min^{–1}}$. Auto-MS-mode with the smart target mass of 1,000 *m/z* and MS/MS fragmentation amplitude of 0.5 V was used. The qualification was performed by analyzing the EIC of the *m/z* value corresponding to the protonated molecules as well as the resulting fragments (MS^2).

For the monosaccharides analysis of the supernatants obtained from the enzymatic hydrolysis, 3 mL were mixed with 3 mL of TFA (4 M) into a borosilicate glass tube. The mixture was incubated at 121°C in a heating block for varying times and the monosaccharide content was determined as presented in section A3.6.

A3.8. Protein analysis

The protein content of algal biomass was performed by elementary analysis. Microalgal biomass was weighted (1 – 3 mg) and introduced in the commercial cartridges of the system. The samples were gasified in the system and the nitrogen content in mass percentage was obtained. A N-to-protein conversion factor of 5.03 was employed, as reported before for *Scenedesmus* microalgae (Templeton & Laurens, 2015).

A3.9. Enzymatic hydrolysis

Saccharification of algal biomass: Biomass suspensions (5% w/v) were prepared in ammonium acetate buffer 100 mM (pH value depending on the enzyme used, Table 8) in Erlenmeyer flasks and supplemented with sodium azide (0.04% w/v) for 48 h. Before adding the enzymes, the biomass was preheated for 1 h at their optimal temperature.

Table 8. Overview of the commercially available hydrolases for the saccharification of algal biomass. c_p: protein concentration, T_{opt}: optimal temperature

Enzyme name	Provider	Declared activity	T_{opt} (°C)	pH_{opt}	c_P (g L^{-1})
Rohament® CL	AB Enzymes	Cellulase	60	4.5	33
Rohapect® B1L	AB Enzymes	Pectinase Cellulase Mannanase	30	3.9	17
Rohapect® UF	AB Enzymes	Pectinase Arabanase	50	3.2	6.5

The concentration of protein in the commercial enzyme mixtures was determined using the Bradford method with a commercial kit, which is reported in Table 4. Depending on this result, the corresponding volume of enzyme was added to the biomass suspension, according to the formula:

$$V_{enzyme}(\mu L) = \frac{m_B * c_E}{c_P} * 10^6$$

(Equation 1)

Where m_B is the amount of weighted biomass in g, c_E the desired enzyme concentration in the hydrolysis treatment (1, 2 and 4% w/w in $g_{Protein}\ g_{Biomass}{}^{-1}$), and c_P the concentration of protein in the enzyme solution in g L^{-1} (Table 8). The resulting suspension was shaken at 200 rpm in an incubator at the optimum temperature; samples were taken by transferring 500 µL suspension in a 1.5 mL tube and centrifuging at 8000 x g. Finally, 50 µL of the supernatant were incubated at 90°C for 10 min to inactivate the hydrolases and stored at –20°C until analysis. Biomass and enzyme blanks were also performed and the monosaccharide content resulting from the enzymes was corrected, where applicable. After 48 h, the liquid phase was separated from the solid phase by centrifugation (SS-34 rotor, 48,808 x g). The residual biomass was lyophilized at –40°C for further 48 h. The mono-, and oligosaccharides present in both fractions was analyzed using the HT-PMP method described in sections A3.6 and A3.7, correspondingly.

Saccharification of standard polymers: A volume of 1.5 mL standard polysaccharide suspensions of each pectin, xylan, (5% w/v), and galactomannan (0.5% w/v) was prepared using acetate buffer 50 mM pH 4.0. Rohapect® B1L and Rohapect® UF (Table 8) were added to the suspension to a final concentration $c_p = 1.0\%$ w/w in $g_{protein}\, g_{polymer}{}^{-1}$. The samples were incubated at 40°C for 24 h. After 5 min incubation at 95°C to denature enzymes, the samples were centrifuged for 30 min (21,000 x g). 1 mL supernatant was taken and neutralized with 40 µL 3.2% v/v NH_4OH. The pH was measured with strips. To all samples, 1 mL isopropanol was added. Samples were then vortexed and centrifuged for 30 min (21,000 x g). Proper dilutions of each sample were measured with the PMP method (Rühmann et al., 2014). The influence of isopropanol on the derivatization reaction of the method was tested on the monosaccharide standards for quantification.

Acetyl xylan esterase reaction of enzymatic hydrolysate: The hydrolysate obtained from the enzymatic treatment (Rohapect® UF, 4% $w_{protein}/w_{biomass}$) of the carbohydrate-rich and defatted *S. obtusiusculus* biomass ABV10 was treated with a commercial esterase (200 U mg^{-1}). The hydrolysate was diluted (1:5) in sodium phosphate buffer (pH 6.7, 100 mM) containing 1 mg mL^{-1} bovine serum albumin (BSA), and 15 U esterase were added. The mixture was incubated for 3 h at 40°C and then at 95°C for 5 min to denature the enzyme. A substrate and an enzyme blank were also incubated.

A4. Results

A4.1. Revealing the diversity of algal monosaccharides: Fast carbohydrate fingerprinting of microalgae using crude biomass and showcasing sugar distribution in *Chlorella vulgaris* by biomass fractionation

Based on the previously developed HT screening platform for bacterial exopolysaccharides by Rühmann et al. (2014), this publication describes the transfer of the method for sugar determination in microalgal biomass. The procedure was applied to investigate the carbohydrate distribution in the model microalga *C. vulgaris*. The first step of the method transfer consisted in hydrolyzing the algal polysaccharides directly from crude or previously processed (e.g., lipid-extracted) biomass using TFA. The released monosaccharides were then derivatized with PMP under the previously optimized reaction conditions for microplate format. The resulting sugar derivatives could be then easily separated in RP-modus in only 12 min running time. Further, they presented UV absorbance for its detection and, most importantly, were ionizable for MS-analysis. These advantages allow the user a simplified detection and elucidation of uncommon algal sugars via mass fragmentation.

After a brief discussion of the existing chromatographic methods for the separation and quantification of the variety of monosaccharides found in microalgae, the results of the carbohydrate analysis of crude biomass from six different strains are presented. In addition to the commonly found neutral sugars (e.g., glucose, mannose, galactose) various substituted monosaccharides could be detected in the microalgae, such as deoxy-, methyl-, amino-, and sulfated sugars, uronic acids and combinations thereof. This feature outperforms conventional analytical methods, as most of them are optimized for the detection of carbohydrates from terrestrial sources. To ensure that the quantification in the algal hydrolysates is reliable, the percentage recovery of a known solution of monosaccharides was determined by spiking each hydrolysate. Very good results (90% – 105% recovery of eight sugars) were obtained for five out of six strains.

Besides, to demonstrate the potential of this method for the study of the carbohydrate distribution in microalgae, a lab-scale biomass fractionation process was designed and applied to the model microalga *C. vulgaris*. The process yielded a high monosaccharide recovery of 82%. Ultimately, the sugar amounts present as storage starch, structural polysaccharides, glycolipids and glycoproteins were determined, showing a carbohydrate profile of *C. vulgaris* for the first time in the literature. The impact of specific potential interfering compounds on the quantification (e.g., amino acids and lipids) was evaluated by spiking the corresponding enriched fractions, for which good recoveries between 90% and 110% were obtained.

The author designed and conducted all the experiments and wrote the manuscript under the supervision of his co-authors, which contributed to content, quality, and language of the article.

In addition to the published article, the results of a design of experiments are presented separately. These was performed to investigate the TFA standard hydrolysis on *C. vulgaris* in more detail.

Revealing the diversity of algal monosaccharides: Fast carbohydrate fingerprinting of microalgae using crude biomass and showcasing sugar distribution in *Chlorella vulgaris* by biomass fractionation

José G. Ortiz-Tena, Broder Rühmann, Doris Schieder, and Volker Sieber

Algal Research
2016

Reproduced with permission, license number: 4186050814724
DOI: 10.1016/j.algal.2016.05.008

Algal Research 17 (2016) 227–235

Contents lists available at ScienceDirect

Algal Research

journal homepage: www.elsevier.com/locate/algal

Revealing the diversity of algal monosaccharides: Fast carbohydrate fingerprinting of microalgae using crude biomass and showcasing sugar distribution in *Chlorella vulgaris* by biomass fractionation

Jose G. Ortiz-Tena, Broder Rühmann, Doris Schieder, Volker Sieber *

Chair of Chemistry of Biogenic Resources, Technische Universität München, Straubing, Germany

ARTICLE INFO

Article history:
Received 22 October 2015
Received in revised form 22 April 2016
Accepted 9 May 2016
Available online xxxx

Keywords:
Algal carbohydrates
1-Phenyl-3-methyl-5-pyrazolone
Automatable carbohydrate analysis
Ultra high performance liquid chromatography
Mass spectroscopy analysis

ABSTRACT

The quantitative and qualitative analysis of carbohydrates from algae is essential for the optimal utilization of algal biomass. A previously established high throughput method for the identification of complex carbohydrates was applied to microalgae. It is based on the selective derivatization of monosaccharides by 1-phenyl-3-methyl-5-pyrazolone (PMP), UHPLC separation and MS analysis of the derivatives. The crude biomass of six different representative microalgae was analyzed and the monosaccharide composition after trifluoroacetic acid (TFA) hydrolysis is reported here. In addition to the usually found neutral sugars, uronic acids, and amino sugars, with this method methylated and phosphorylated or sulfated monosaccharides were also identified. The PMP derivatization enabled a monosaccharide recovery in the hydrolysates between 90% and 105% in five strains. Furthermore, a fractionation process with an overall recovery of 82% was applied to the microalga *Chlorella vulgaris* to investigate the carbohydrate distribution in the cell. The relative amounts of starch, soluble sugars, carbohydrates associated with glycoproteins and glycolipids, as well as the structural polysaccharides were determined. Due to its advantages, this method can help in strain screening and designing of proper strategies for maximal biomass development, formation of rare sugars as well as general utilization in the emerging field of algal biorefinery.

© 2016 Elsevier B.V. All rights reserved.

1. Introduction

In the search of renewable energy and fuel production systems apart from edible sources, micro and macro algae have been increasingly investigated in the last decades. Their use as sustainable raw material is not limited to the production of biofuels, but also for fine chemicals, human nutrition and animal feed. Thus, the concept of algal biorefinery has risen in which all their components can be converted into value-added products [1]. To achieve this, the starting algal biomass must be precisely characterized so that suitable processing strategies can be applied. Since the composition of algal biomass varies according to the specific strain used, different culture strategies and growth phases, fast and reliable determination methods for algal proteins, lipids and carbohydrates are needed to accelerate the screening for new strains, as well as to optimize the production conditions [2,3]. In the recent past, efforts have been focused towards the assessment of existing analytical procedures for terrestrial plant biomass upon their applicability to algae. So the need for analytical improvement has been identified especially regarding carbohydrate analysis focused on algal-specific monosaccharides, such as uronic acids, amino sugars and sulfated sugars [4]. A precise determination of the monosaccharide composition of crude algae is decisive for the comprehensive utilization of algal biomass in the concept of biorefinery, especially when designing strategies for fermentations on algal hydrolysates. Carbohydrates from algae can be found in different forms depending on the biological task they fulfill, such as storage (starch), structural (cell wall, e.g., cellulose) or signaling (glycolipids or glycoproteins) [5], and the identification of their origin provides valuable information for developing adequate processing strategies, e.g., using hydrolytic enzymes [6,7]. Different chromatographic approaches have been extensively assessed and optimized for resolving the broad palette of microalgal monosaccharides. Conventional high performance liquid chromatography (HPLC) coupled to refractive index detection (RID) or charged aerosol detection (CAD) displays a poor separation on complex monosaccharide mixtures. Gas chromatography (GC) with flame ionization detector (FID) preceded by trimethyl silylation (TMS) or alditol acetate derivatization yields very good chromatographic resolution, is highly sensitive and also compatible with mass spectrometry (MS). However, the quantification of uronic acids and amino sugars is challenging, and the sample preparation is time consuming [8]. High performance anion exchange chromatography (HPAEC) combined with pulsed amperometric detection (PAD) is a very robust method for carbohydrate analysis without the need for sugar derivatization, and configurations have been developed for resolving up to 13 different sugars present in algae. Still, the use of strong ionic eluents impedes the direct application of MS for identifying the

---

* Corresponding author.
E-mail address: Sieber@tum.de (V. Sieber).

http://dx.doi.org/10.1016/j.algal.2016.05.008
2211-9264/© 2016 Elsevier B.V. All rights reserved.

commonly occurring unknown carbohydrates in algal hydrolysates [8]. A comparative overview of relevant existing methods for the analysis of complex carbohydrate mixtures (as those found in algal biomass) is presented in Table 1.

It is evident that standardized, fast and reliable analytical methods for algal carbohydrates are necessary. Addressing this need, we present a procedure for fast fingerprinting of monosaccharides from crude and processed algal biomass. It is based on a previously described method for the fast chromatographic analysis of carbohydrates after TFA-hydrolysis and derivatization with 1-phenyl-3-methyl-5-pyrazolone (PMP) in 96-well format [10]. Often, the derivatization of compounds for the analysis of large sets of samples is undesirable, since sample preparation is time consuming. However, the parallelized derivatization procedure enables a very fast sample processing and can potentially be used for automated platforms and higher throughput, as demonstrated previously for the screening of bacterial exopolysaccharides [11]. During the selective chemical derivatization of aldoses, two PMP molecules react by condensation with the aldehyde group of the saccharides, yielding the corresponding *bis*-PMP derivative [12]. This allows their separation by reverse phase UHPLC. At the same time, the sugars are provided with UV-absorbance, and become ionizable in positive mode for MS analysis. Thus, their identification and quantification via UV- and MS-detection is possible in similar ranges. This is a relevant feature for complex saccharide mixtures, such as biomass hydrolysates, in which potentially interfering compounds (e.g., amino acids, lipids, pigments or degradation products) are present. The two detection systems provide a cross-verification of each compound found, and co-eluting or unknown compounds can be easily identified. Although the procedure has been validated for the quantification of 18 different derivatized mono- and disaccharides in pure solution [10], the effect of potentially interfering aldehyde compounds present in algal hydrolysates (such as acetaldehyde or retinal [13]) needs to be considered. While a similar sugar quantification procedure has been employed for the compositional determination of carbohydrates from *Dunaliella salina*, the conditions were not optimized for a rapid analysis in 96-well format and were MS incompatible [9]. The remarkably short LC running time (12 min), low limit of detection (LOD), and the possibility of MS determination of unknown or co-eluting peaks as well as derivatization and sample processing in microtiter plates (Table 1) renders the optimized method a highly reliable candidate for rapid fingerprinting of algal carbohydrates. This was demonstrated by analyzing six different representative algae species. The application of this method to algal biomass was validated by spiking the algal hydrolysates and calculating the sugar recoveries. Plus, a lab-scale fractionation process was developed and applied to one of the most commonly investigated microalga, *Chlorella vulgaris*. The monosaccharide composition of the process fractions was analyzed to get an insight on the composition and distribution of the carbohydrates in the cell.

2. Materials and methods

2.1. Chemicals and algal strains

All chemicals were, unless otherwise stated, purchased in analytical grade from Sigma Aldrich (Germany), Merck KGaA (Germany) and Carl Roth GmbH (Germany). Substituted monosaccharide standards were purchased from Carbosynth Ltd. (United Kingdom). Lyophilized whole cells from *C. vulgaris* were purchased from Algomed (Klötze, Germany). All other algal strains were cultivated, lyophilized and kindly provided by Dr. Sabine Mundt (Institut für Pharmazie, University Greifswald). A standard cultivation procedure was applied under no nutrient limitation and without light stress conditions for 14 d at 25 °C. Following culture media were employed: SWES for *N. salina* and *Phaeodactylum tricornutum*, f/2 supplemented with trace elements for *Porphyridium purpureum*, DUN supplemented for *D. salina* and standard BG-11 for *Scenedesmus ovalternus*, as described previously [14].

2.2. Hydrolysis of algal biomass

Analytical chemical hydrolysis was performed by adding 6 mL of 2 M TFA to 6 mg of algal biomass (process fraction or whole lyophilized algae) into 15 mL glass tubes. The tubes were incubated in a heating block (VLM GmbH, EC-Model) for 90 min at 121 °C (referred as standard hydrolysis). After cooling to room temperature, the hydrolysates were

Table 1

Published chromatographic methods for the quantification of complex monosaccharide mixtures.

	HPLC-CAD [8]	GC-FID [8]	HPAEC-PAD [8]	HPLC-UV [9]	HPLC-UV-MS [10]
Column type; phase	Prevail ES carbohydrate; normal phase	DB-225MS	PA-1	ZORBAX Eclipse XDB-C18; reverse phase	Gravity C18; reverse phase
Column temperature (°C)	30	70 to 240 in gradient, 8 °C min^{-1}	37.5	30	50
Eluents	A: water B: ACN gradient elution	Carrier gas: helium	A: 20 mM NaOH B: 100 mM NaOH/150 mM sodium acetate gradient elution	0.1 M phosphate buffer pH 6.7 and ACN 83:17 (v/v %) isocratic elution	A: 5 mM ammonium acetate buffer pH 5.6 with 15% ACN (w/w %) B: 100% ACN gradient elution
Flow rate (mL min^{-1})	1.0	12.8 total flow (split 1:10)	NP	1	0.6
Monosacharide tagging	None	Alditol acetate-derivatization	None	PMP-derivatization	PMP-derivatization
LC running time (min)	60	35	65 (35 + 30 column regeneration)	55	12
Determination neutral sugars	Yes	Yes	Yes	Yes	Yes
Determination amino sugars	Limited	Limited	Yes	Yes	Yes
Determination uronic acids	Limited	Limited	Yes	Yes	Yes
Limit of detection (mg mL^{-1})	NP	0.5 (neutral sugars) – 3.5 (amino sugars)	6.3–40	0.7–2.0[a]	UV: 0.6–2.0 MS: 0.5–2.9
MS compatibility	No	Yes	No	No	Yes
Monosaccharide recovery (%)	NP	93.0–98.1[b]	90.4–106.2[b]	95.2–103.2[c]	UV: 94.6–101.6[b] MS: 90.6–98.8[b]

Abbreviations: CAD: charged aerosol detection, FID: flame ionization detector, PAD: pulsed amperometric detection, NP: not presented, ACN: acetonitrile, PMP: 1-Phenyl-3-methyl-5-pyrazolone.

[a] Values are published in nmol and were converted to mg mL^{-1} under described assay conditions.

[b] Recovery reported as calibration verification standard without matrix.

[c] Recovery reported from spiked samples with algal hydrolysate matrix.

brought to pH ~ 8 by adding an aqueous solution of 3.2% NH_4OH, since slightly alkaline conditions are required for the subsequent derivatization of monosaccharides, as reported before [12].

2.3. HT-PMP derivatization of algal hydrolysates

The derivatization of the hydrolysates was performed in a 96 well format as described before [10]. In short, a 25 μL aliquot of the neutralized hydrolysate was transferred to a 96-well-PCR plate (781,350, Brand) and 75 μL of derivatization reagent (0.1 M methanolic-PMP-solution: 0.4% NH_4OH solution 2:1) were added. After incubation (100 min, 70 °C) in a PCR-cycler (BioradMy-cycler, USA), a 20 μL aliquot was mixed with 130 μL of 19.23 mM acetic acid. The samples were then filtered through a 96-well plate (0.2 μm Supor, Pall Corporation) by centrifugation at 2500*g* for 5 min into a microtiter plate. The plate was then sealed with a silicon cap mat (Whatmann 7704-0105, USA).

2.4. UHPLC ESI-MS analysis of derivatized algal monosaccharides

The chromatographic analysis of the derivatized sugars was conducted as validated before [10]. Shortly, a mobile phase A consisting of 5 mM ammonium acetate buffer (pH 5.6) with 15% (w/w) acetonitrile and a mobile phase B containing pure acetonitrile were used. The column (Gravity C18, 100 mm length, 2 mm i.d.; 1.8 μm particle size, Macherey-Nagel) was tempered to 50 °C. The flow rate was set to 0.6 mL min^{-1}. The following gradient was programmed: start of mobile phase B at 1%, with an increase to 5% over 5 min, hold for 2 min, followed by an increase to 18% over 1 min. The gradient was further increased to 40% over 0.3 min, held for 2 min and returned within 0.2 min to starting conditions for 1.5 min. The first 3 min of chromatographic flow were refused by a switch valve behind the UV-detector (245 nm). Before entering ESI-MS, the flow was split 1:20 (Accurate-Post-Column-Splitter, Dionex). The temperature of the autosampler was set to 20 °C and an injection volume of 10 μL was used. All calibration standards were prepared with the neutralized TFA-hydrolysis matrix to compensate its influence on the derivatization process. Data was collected and analyzed with Bruker Hystar, QuantAnalysis, Data Analysis and Dionex Chromeleon software. Detailed mass spectroscopy parameters can be found in previous publication [10].

2.5. Spiking of algal hydrolysates for validation

A concentrated spiking solution containing all monosaccharide standards was prepared and diluted 1:50 (20 μL) into the algal hydrolysates (980 μL) prior to derivatization with PMP. The monosaccharide spiked concentration was chosen according to average expected concentration values in the samples as follows: Glucose, 200 mg L^{-1}; galactose, 100 mg L^{-1}; mannose, ribose, rhamnose and xylose 20 mg L^{-1}; glucosamine and glucuronic acid, 10 mg L^{-1}. The volume of the hydrolysates was not increased higher than 2% in order to avoid dilution of the samples. Similar to the monosaccharide standards, the spiking solution was quantified in the TFA-neutralization matrix.

2.6. Processing of Chlorella vulgaris

50 g L^{-1} algal suspension was disrupted (step A) using a high pressure cell disrupter (Basic Z Model, Constant systems) at 2.4 kbar, 5 °C and three passes. After centrifuging (12,000*g*), the pellet was lyophilized (0.12 mbar, fraction A*s*) and the liquid supernatant (fraction A*l*) was stored at −20 °C until use. The dry and disrupted cells were then extracted by a modified Sohxlet procedure [4] (step B), but using 400 mL of chloroform:methanol (2:1 v/v) at 80 °C for 48 h. The organic solvents were removed from the extract by rotary vacuum evaporation and the remaining solids (fraction B*l*) were stored at −20 °C until use. The extracted phase was dried in a desiccator under vacuum and lyophilized (fraction B*s*). Then, a 50 g L^{-1} suspension of this fraction was treated with a commercial amylase (0.5% $w_{protein}/w_B$, Distillase CS, Genencor) for 24 h at 60 °C in ammonium acetate buffer, pH 4.5, preheating the biomass at 80 °C prior to treatment (step C). After centrifuging at 12,000*g*, the supernatant was stored at −20 °C (fraction C*l*) and the pellet was lyophilized (fraction C*s*). This fraction was then treated with a commercial protease (0.1% v/v, Alcalase, Calbiochem) for 12 h at 60 °C, pH 7 (step D). After centrifuging at 12,000*g*, the supernatant was stored at −20 °C (fraction D*l*) and the pellet was lyophilized (fraction D*s*). In all process fractions, the carbohydrate content as mono- and polysaccharide was investigated. Corrections were made for monosaccharides present in the commercial enzymes. Data was collected in triplicate and the mean ± standard deviation of each sample was reported.

3. Results and discussion

3.1. Analysis of crude biomass

Nannochloropsis salina, *P. tricornutum*, *C. vulgaris* and *D. salina* were selected as model organisms for Eustigmatophyceae, diatom and green algae from freshwater and marine environment, respectively. Additionally, *P. purpureum* a model red alga and the increasingly utilized *S. ovalternus* were investigated. The monosaccharide profile of dry biomass was first determined, followed by the validation of the method by spiking the algal hydrolysates and calculating the sugar recovery.

3.1.1. Identification of monosaccharides from microalgal dry biomass

After treating the lyophilized algal biomass under standard TFA-hydrolysis conditions, the hydrolysates were neutralized with ammonium and derivatized with PMP, which strongly absorbs UV at 245 nm. With the HT-PMP method, up to 18 derivatized sugars can be baseline separated in a single run and quantified against a standard. Besides, co-eluting species having different *m/z* can be identified by analyzing the extracted ion chromatograms (EIC) generated by MS. So, the peaks found via UV can be cross-verified via EIC. However, due to the short LC running time (12 min), xylose and arabinose display the same retention time ($R_t = 7.3$ min), and cannot be differentiated by MS either [10]. In some species, such as *C. vulgaris*, both monosaccharides have been reported in the literature, though xylose has been more commonly reported and not all species present both [8]. For this reason, the corresponding peaks were quantified against a xylose standard. The monosaccharides found in the hydrolysates from the algal species investigated are reported in Table 2.

The sugar profiles of the microalgae are much more complex than those of lignocellulosic biomass and even of some bacterial exopolysaccharides. The type of hydrolysis plays a significant role in the digestion of polysaccharides to monosaccharides and consequently in their quantification. TFA is commonly applied for the analysis of various types of samples, such as bacterial exopolysaccharides [15], soluble plant polysaccharides and non-cellulosic cell wall fractions [16]. The hydrolysis of cellulose in crystalline form containing lignin (such as pulp and wood) is also feasible with TFA, but requires harsher conditions due to its recalcitrance [17]. The optimum hydrolysis parameters can be adjusted according to the type of biomass. In order to allow comparison among samples, the same standard hydrolysis conditions (2 M, 121 °C, 90 min) were applied through this study. Under such conditions, the monosaccharide quantification of different carbohydrate polymers using the presented method varies: while dimers can be found for some polymers (e.g., xanthan-, diutan-, gellan-gum or scleroglucan) after hydrolysis, high degradation rates occur for others (e.g., hyaluronic acid) [11]. Especially uronic acids and amino sugars are challenging to release from polysaccharides. Noticeably, no dimers were found in the algal hydrolysates under these conditions. One advantage of TFA compared to inorganic acids is the possibility of tandem MS analysis due to its volatile nature.

Table 2
Carbohydrate amounts in TFA hydrolysates of crude algal biomass from investigated strains. Monosaccharide quantification was primarily performed based on UV-absorbance, as far as no co-eluting compounds were detected by MS analysis. In this case, the quantification was carried out via EIC. Values are reported as the mean of $mg_{sugar}\ g^{-1}{}_{dry\ biomass}$ ± standard deviation, $n = 3$. ND: not detected.

Monosaccharide	*P. tricornutum*	*N. salina*	*P. Purpureum*	*C. vulgaris*	*D. salina*	*S. ovalternus*
Glucose	5.3 ± 0.2	61.8 ± 4.8	351.3 ± 28.8	225.5 ± 5.0	661.8 ± 35.4	332.4 ± 20.8
Galactose	21.6 ± 2.3	12.8 ± 2.7	70.6 ± 2.9	33.7 ± 2.4	7.4 ± 1.7	14.3 ± 3.1
Rhamnose	3.2 ± 0.6^{a}	5.3 ± 0.4	ND	9.0 ± 0.4	ND	ND
Mannose	33.5 ± 4.0^{a}	1.8 ± 0.3^{a}	ND	5.0 ± 0.4^{a}	2.7 ± 0.8^{a}	24.1 ± 1.5^{a}
Ribose	4.2 ± 0.1	4.2 ± 0.5	ND	6.3 ± 0.3	ND	3.1 ± 0.1
Glucuronic acid	11.5 ± 1.6^{a}	ND	9.3 ± 1.3^{a}	3.9 ± 0.3^{a}	ND	7.5 ± 0.7^{a}
Glucosamine	ND	ND	ND	4.8 ± 0.3^{a}	ND	ND
Xylose/arabinose	5.1 ± 0.6^{b}	4.4 ± 0.8^{b}	63.7 ± 5.4^{b}	6.2 ± 0.2	ND	ND
Fucose	4.3 ± 0.1	4.7 ± 0.5	ND	ND	ND	10.8 ± 0.6
Total	88.6 ± 8.7	94.5 ± 7.5	494.9 ± 30.2	294.6 ± 9.8	671.9 ± 34.9	392.2 ± 26.2

[a] Quantification via EIC.
[b] Value may be assigned to xylose, since no arabinose is reported in literature.

The reported glucose concentration of *P. tricornutum* and *N. salina* is considerably lower compared to the rest of the algae. These two species are not classified into the *Plantae* kingdom but belong to the *chromalveolatae* [18]. As a bioinformatic study on *P. tricornutum* suggests, several β-glucanases are present in this organism, which may be involved in an intense diel metabolism that uses chrysolaminaran, a β(1➔3), β(1➔6) glucan, as energy storage. This kind of metabolism is characterized by an accumulation during daylight and depletion in the dark [19], which may be one reason for the comparably low glucose concentration in these two species. Mannose, galactose, rhamnose and fucose were also detected and have been reported previously as constituents of structural polysaccharides [8,20,21]. Since little or no arabinose has been reported in these two algae, the values reported in Table 1 can be inferred to be xylose.

The rest of the algae, which belong to the *Plantae* kingdom, utilize starch as long-term storage polymer, so higher glucose concentrations were found accordingly. This is discussed in detail in Section 3.3 for *C. vulgaris*. For this well characterized green alga, our results are in good accordance with reported values, except for the absence of fucose and galacturonic acid [8,22], which may be either present in non-detectable trace amounts or absent due to differing culture conditions or hydrolysis procedure. Similarly, for *D. salina*, glucose, galactose and mannose were found from dry biomass hydrolysates. Rhamnose, galacturonic acid, glucuronic acid, xylose, arabinose and fucose were previously described in a purified and hydrolyzed polysaccharide fraction [9]. These monosaccharides were found in low concentrations in the isolated polysaccharide and therefore may not be present in detectable levels in the crude biomass. Regarding *S. ovalternus*, the sugar composition found reveals a typical pattern found for several *Scenedesmus* sp., in which glucose, galactose, mannose and fucose are the main sugars present. The 2:1 ratio found for Man:Gal and the presence of glucuronic acid may be evidence of the occurrence of acidic galactomannans as structural sugars [23]. Due to their ability to produce exopolysaccharides in major quantities, unicellular red algae of the genus *Porphyridium* (Rhodophyta) have been increasingly investigated in the last years. The monosaccharides found are in accordance with previously described sugar composition profiles, which include glucose, galactose, xylose and glucuronic acid as main sugars, as well as evidence of sulfated and methylated sugars [24,25]. A detailed analysis of the substituted sugars corresponding to the unknown peaks in the algae investigated is presented below.

3.1.2. Analysis of unknown peaks

A significant advantage of the presented method is the possibility of MS determination of unknown peaks, for which no standard for quantification is available. By analyzing the *m/z* of the compound, together with the elution profile and the MS^2 fragmentation pattern of the found peaks, postulates can be made about the nature of the monosaccharides that are present. Due to the derivatization reaction with PMP, chemical species result with *m/z* of 451, 481 or 511 for $[M + H]^+$ ions for tetroses, pentoses and hexoses, respectively [10,26]. Special monosaccharide substituents, such as amino, carboxyl, methyl, sulfuryl as well as deoxy-sugars such as rhamnose and fucose can be identified by their mass difference.

An overlay of the UV- and EIC-chromatograms (3 to 9 min) of the hydrolysate from *P. tricornutum* is shown in Fig. 1, black and color respectively. The peaks corresponding to the eight monosaccharides reported in Table 2, as well as two unknown peaks with *m/z* 575 and 525 $[M + H]^+$ are presented.

The first unknown peak co-elutes with mannose at a short R_t of 3.65 min, characteristic of hydrophilic compounds. Its comparably high *m/z* of 575 suggests the presence of substituents of large molecular mass. Additional information can be obtained by analyzing the MS^2 fragmentation pattern of the unknown sugar (Fig. 2A). The fragments obtained from the parent ion points to a sulfated or phosphorylated deoxy-hexose. For comparison, Fig. 2B and C shows the MS^2 fragmentation of rhamnose and 3-deoxy-glucose standard, respectively. The fragments of the unknown sugar found in the *m/z* range between 200 and 300 are very similar to those of rhamnose in contrast to 3-deoxy-glucose. Similarly, major differences were also found with the fragmentation patterns of 2- and 4-deoxy glucose (MS spectra, Fig. S1). These findings suggest that the unknown monosaccharide may be a sulfated deoxy-sugar, most probably rhamnose or fucose, since both are present in the hydrolysate as well. Most likely, this sugar is present in much higher concentration and undergoes degradation under the hydrolysis conditions employed.

The last part of the chromatogram (Fig. 1) reveals a small peak with *m/z* 525 $[M + H]^+$. A similar peak was observed in *C. vulgaris* (Fig. S2). Significant differences are observed in the fragmentation pattern of this peak with that of glucuronic acid (Fig. 3A and C), even though their *m/z* is identical. The MS^2 spectrum obtained from the unknown peak indicates the presence of a methyl substituent in the monosaccharide, also suggested by the comparison with the 3-O-methyl-glucose standard (Fig. 3B). Following the elution pattern of the hexoses (galactose after glucose after mannose), the unknown peak could be a 3-O-methyl-galactose, as previously reported for *C. vulgaris* [27]. This hypothesis should be validated using the appropriate sugar standard.

For all the algae investigated, at least one unknown peak was identified by mass spectrometry, though some of them in trace amounts. Chromatograms are available in the Supplementary Information. Based on their *m/z*, elution pattern and mass fragmentation, postulations were done in a similar manner as above. A summary is given in Table 3.

3.1.3. Method validation on TFA hydrolysates from algal biomass

The neutralized TFA-hydrolysis matrix influences the carbohydrate derivatization and subsequent quantification, so that the monosaccharide standards used for quantification of hydrolyzed samples were prepared in this matrix. However, in order to validate the use of the method

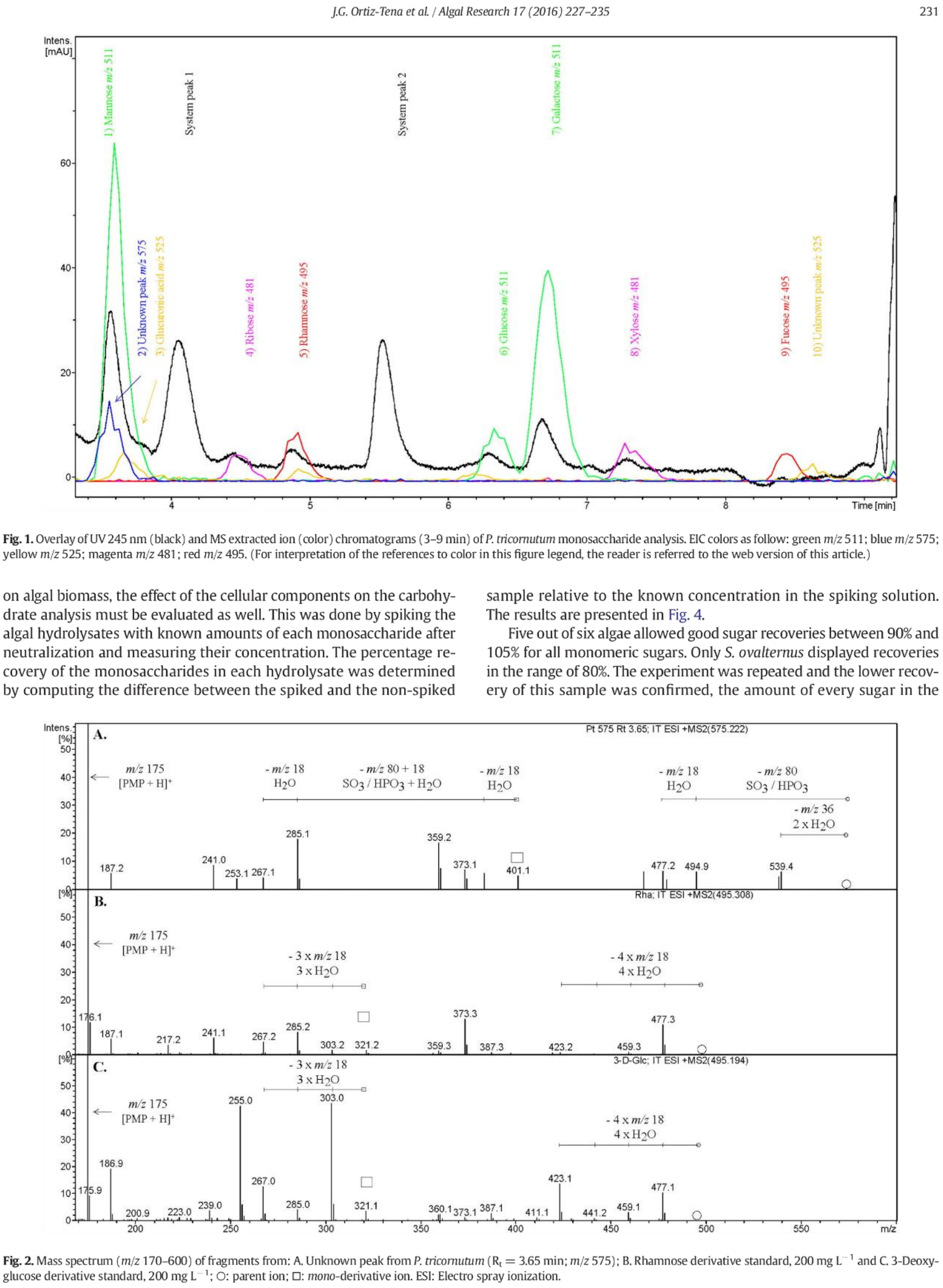

Intens. [mAU]
1) Mannose m/z 511
System peak 1
System peak 2
7) Galactose m/z 511
2) Unknown peak m/z 575
3) Glucuronic acid m/z 525
4) Ribose m/z 481
5) Rhamnose m/z 495
6) Glucose m/z 511
8) Xylose m/z 481
9) Fucose m/z 495
10) Unknown peak m/z 525
60
40
20
0
4
5
6
7
8
Time [min]

Fig. 1. Overlay of UV 245 nm (black) and MS extracted ion (color) chromatograms (3–9 min) of *P. tricornutum* monosaccharide analysis. EIC colors as follow: green *m/z* 511; blue *m/z* 575; yellow *m/z* 525; magenta *m/z* 481; red *m/z* 495. (For interpretation of the references to color in this figure legend, the reader is referred to the web version of this article.)

on algal biomass, the effect of the cellular components on the carbohydrate analysis must be evaluated as well. This was done by spiking the algal hydrolysates with known amounts of each monosaccharide after neutralization and measuring their concentration. The percentage recovery of the monosaccharides in each hydrolysate was determined by computing the difference between the spiked and the non-spiked sample relative to the known concentration in the spiking solution. The results are presented in Fig. 4.

Five out of six algae allowed good sugar recoveries between 90% and 105% for all monomeric sugars. Only *S. ovalternus* displayed recoveries in the range of 80%. The experiment was repeated and the lower recovery of this sample was confirmed, the amount of every sugar in the

Intens. [%]
A.
Pt 575 Rt 3.65; IT ESI +MS2(575.222)
m/z 175 [PMP + H]+
- m/z 18 H2O
- m/z 80 + 18 SO3 / HPO3 + H2O
- m/z 18 H2O
- m/z 18 H2O
- m/z 80 SO3 / HPO3
- m/z 36 2 x H2O
187.2
241.0
253.1
267.1
285.1
359.2
373.1
401.1
477.2
494.9
539.4
B.
Rha; IT ESI +MS2(495.308)
m/z 175 [PMP + H]+
- 3 x m/z 18 3 x H2O
- 4 x m/z 18 4 x H2O
176.1
187.1
217.2
241.1
267.2
285.2
303.2
321.2
359.3
373.3
387.3
423.2
459.3
477.3
C.
3-D-Glc; IT ESI +MS2(495.194)
- 3 x m/z 18 3 x H2O
m/z 175 [PMP + H]+
- 4 x m/z 18 4 x H2O
175.9
186.9
200.9
223.0
239.0
255.0
267.0
285.0
303.0
321.1
360.1
373.1
387.1
411.1
423.1
441.2
459.1
477.1
50
40
30
20
10
0
200
250
300
350
400
450
500
550
m/z

Fig. 2. Mass spectrum (*m/z* 170–600) of fragments from: A. Unknown peak from *P. tricornutum* (R_t = 3.65 min; *m/z* 575); B. Rhamnose derivative standard, 200 mg L^{-1} and C. 3-Deoxy-glucose derivative standard, 200 mg L^{-1}; ○: parent ion; □: *mono*-derivative ion. ESI: Electro spray ionization.

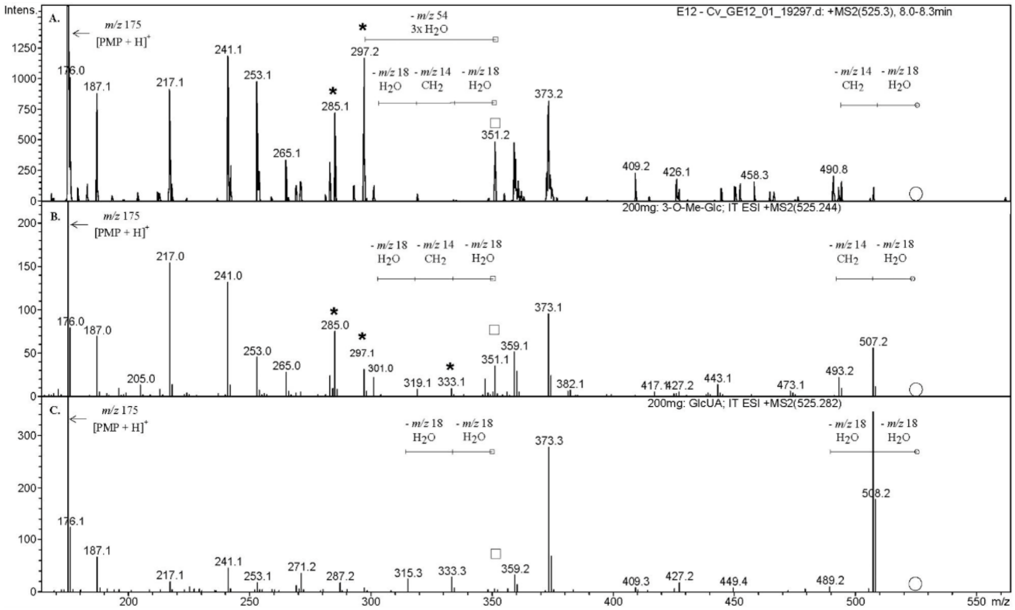

Fig. 3. Mass spectrum (*m/z* 170–550) of different compounds with *m/z* 525: A. Unknown peak from *C. vulgaris* ($R_t = 8.15$ min; *m/z* 525); B. 3-O-methyl-glucose derivative standard, 200 mg L^{-1} and C. Glucuronic acid derivative standard, 200 mg L^{-1}; ○: parent ion; □: *mono*-derivative ion. ESI: Electro spray ionization. Masses marked with * correspond to methylated fragments.

spiked samples was still below the expected values. One explanation could be that some component in the hydrolysate of this strain inhibits the derivatization of the monosaccharides with PMP. Further experiments are required to identify such compounds in the hydrolysate and delineate their effect on the derivatization reaction. A correction of this loss (between 15% and 25%) for each monosaccharide would increase the total value reported in Table 1 for this alga to 470 mg g_{BDry}^{-1}. On the other hand, the impact of specific potential interfering compounds on the carbohydrate quantification was evaluated by spiking the hydrolysates from amino acid or lipid-enriched biomass fractions of *C. vulgaris*. The fractions were obtained with the process described in section 3.2. Here, good recoveries between 90% and 110% were found (Fig. S6 and Fig. S7).

3.2. Analysis of the carbohydrate distribution in C. vulgaris

In order to examine the applicability of the method for determining the carbohydrate distribution in microalgae, a lab-scale fractionation process was applied to the well-known *C. vulgaris* (Scheme 1). A concentrated algal suspension was disrupted using a high pressure homogenizer. The solid cell lysate (A*s*) was separated from supernatant (A*l*) and further extracted with organic solvents (B*l*). The residual solid (B*s*) was dried and treated with a commercial amylase preparation (C*s*). Finally, a commercial protease was applied to concentrate the carbohydrates, in a fraction containing structural carbohydrates from the cell wall (D*s*). All fractions were analyzed for dissolved and released monosaccharides..

In total, 50 g of crude algal biomass were processed. Table 4 shows the monosaccharide mass in mg of the algal biomass after each process step. The upper part of the table contains the data from the algal biomass of the main process stream to the cell wall (structural carbohydrates) fraction D*s*. In addition, the mass fraction of each monosaccharide w_i in every process biomass fraction is reported, given by Eq. (1):

$$w_i = \frac{m_i}{m_{Total\ \ carbohydrates\ \ in\ \ process\ \ fraction}}. \qquad (1)$$

The monosaccharide yield of each process step Y_s is calculated by dividing the mass amount of each monosaccharide *i* in the corresponding process fraction *j* related to the mass amount of that sugar in the starting

Table 3
Unknown sugars found in all algal species investigated. The identity of the sugars was postulated analogously to those discussed in the text.

Peak found [*m/z*]	*P. tricornutum*	*N. salina*	*C. vulgaris*	*P. purpureum*	*D. salina*	*S. ovalternus*	Postulated sugar
	R_t [min]	R_t [min]	R_t [min]	R_t [min]	R_t [min]	R_t [min]	
451	–	–	–	5.4	5.4	5.5	Erythrose[a]
509	–	–	–	–	–	8.15	Deoxy-methyl-hexose
525	8.6	–	8.15	7.9	–	–	Methyl-hexose
538	–	–	–	8.5	–	–	Unknown amino monosaccharide
539	–	–	–	5.0	–	–	Methyl-uronic acid
575	3.65	3.65	4.2	–	–	–	Sulfated/phosphorylated deoxy-hexose

[a] Validated using a commercial standard.

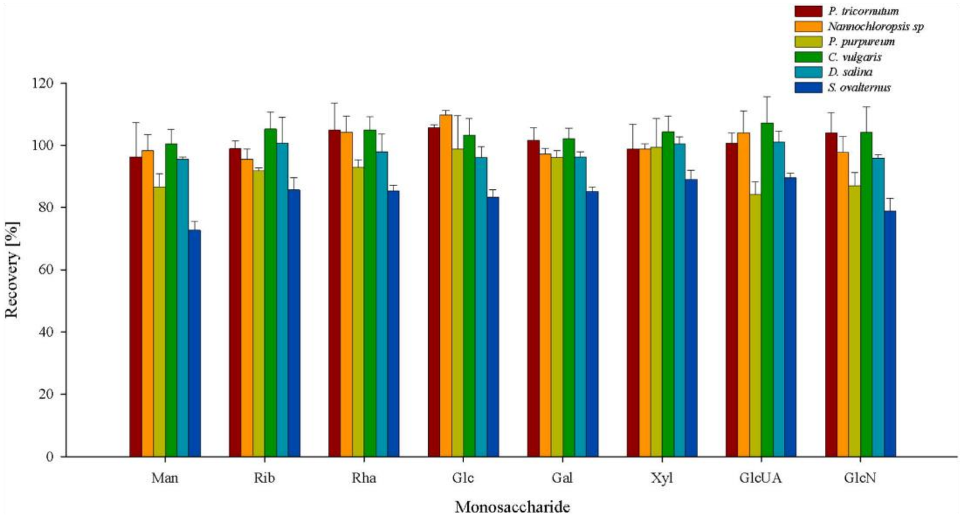

Fig. 4. Monosaccharide recovery by PMP derivatization observed after TFA-hydrolysis of microalgae calculated as explained in the text. Red: *P. tricornutum*, orange: *N. salina*, yellow: *P. purpureum*, green: *C. vulgaris*, light blue: *D. salina* and dark blue: *S. ovalternus*. ($n = 3$). Man, mannose; Rib, ribose; Rha, rhamnose; Glc, glucose; Gal, galactose; Xyl, xylose; GlcUA, glucuronic acid; GlcN, glucosamine. (For interpretation of the references to color in this figure legend, the reader is referred to the web version of this article.)

material ($j = 1$) i.e., whole cells, Eq. (2). This parameter reflects the distribution of the monosaccharide i in the overall fractionation process.

$$Y_{i,j} = \frac{m_{i,j}}{m_{i,1}} \qquad (2)$$

After disruption of the algal cells in the first step, 77% of the ribose from the starting material was detected in the hydrolysate of the cell lysate supernatant (A*l*), as expected. Ribose is found in the cell in solution as RNA and nucleotides, such as ATP and NADH. Glucose, mannose and galactose yielded 23%, 36% and 49% from the whole cells, respectively and may have been found as short-chained oligosaccharides which stayed in solution after cell lysis. In the hydrophobic fraction obtained after extraction with organic solvents (B*l*), galactose was the only monosaccharide present in detectable levels, yielding around 5% of the galactose in the original material. It is known that galactosylglycerides containing one or two galactose residues are present as the major plastid glycolipids in different species of *Chlorella* [28]. The extracted biomass was further treated with commercial hydrolytic enzymes usually applied for ethanol production from grain starch. According to the supplier, this mix contains fungal glucoamylase and alpha-amylase, so that glucose from starch storage polysaccharides is released. As expected, only glucose was found in the supernatant of this treatment (C*l*). When the supernatant was directly derivatized with PMP, around 50% of the starting glucose was measured. However, by hydrolyzing the supernatant under standard conditions with TFA, the glucose detected decreased to 43% of the starting material. This finding suggests that glucose degradation occurs due to the standard TFA-hydrolysis.

The final process step consisted in treating the algal biomass with a mix of endopeptidases, primarily subtilisin A from *B. licheniformis*. The monosaccharides associated to the algal proteins found in the supernatant (D*l*) were not higher than 5% of the starting material. Glucose, galactose, mannose, rhamnose and glucosamine were identified in the TFA hydrolysates of the fraction, whereas no sugar could be detected as monomeric form. Up to date, only glucose and galactose have been identified in isolated glycoproteins of *Chlorella* [29]. According to our results, rhamnose, mannose and glucosamine may be also present in glycoproteins, though in much lower extent. The final, carbohydrate-rich biomass D*s* fraction obtained from the fragmentation process displays a quite complex mixture of monosaccharides. Numerous studies have been performed to identify structural carbohydrates from *Chlorella*. The glucosamine detected may be part of a chitin-like polymer containing amino sugars [30] and is most probably present as *N*-acetyl glucosamine. In addition, different structures for rhamnose and galactose oligosaccharides have been proposed as constituents of isolated, acidic polysaccharides, such as α-D-glucopyranuronosyl-(1→3)-α-L-rhamnopyranosyl-(1→2)-α-L-rhamnopyranose [31,32]. Furthermore, a branched structure of an arabinomannan was elucidated from polysaccharide-rich fractions from *Chlorella*, some of them containing xylose [33]. In general, the identified monosaccharides are well in accordance

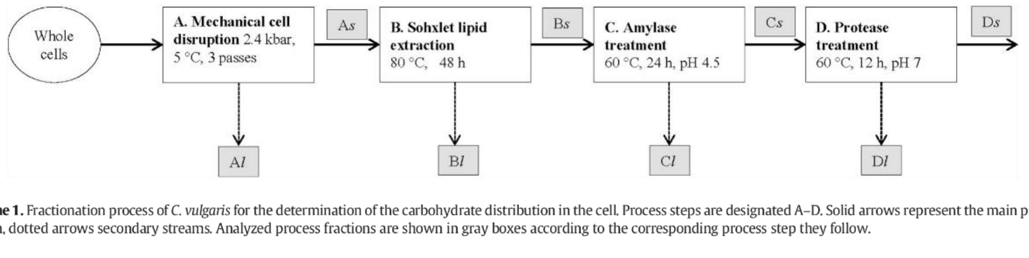
Whole cells
A. Mechanical cell disruption 2.4 kbar, 5 °C, 3 passes
As
B. Sohxlet lipid extraction 80 °C, 48 h
Bs
C. Amylase treatment 60 °C, 24 h, pH 4.5
Cs
D. Protease treatment 60 °C, 12 h, pH 7
Ds
Al
Bl
Cl
Dl

Scheme 1. Fractionation process of *C. vulgaris* for the determination of the carbohydrate distribution in the cell. Process steps are designated A–D. Solid arrows represent the main process stream, dotted arrows secondary streams. Analyzed process fractions are shown in gray boxes according to the corresponding process step they follow.

Table 4
Monosaccharides distribution analysis in *C. vulgaris* (see Scheme 1). w_i: mass fraction of monosaccharide *i* as defined in the text. $Y_{i,j}$: Yield of monosaccharide *i* in fraction *j* in relation to the whole cells as defined in the text. $n = 3$. ND: not detected.

	Whole cells			A. Cell disruption As			B. Lipid extraction Bs			C. Amylase treatment Cs			D. Protease treatment Ds		
Sugar *i*	m_i [mg]	w_i [%]	Y_i [%]	m_i [mg]	w_i [%]	$Y_{i,As}$ [%]	m_i [mg]	w_i [%]	$Y_{i,Bs}$ [%]	m_i [mg]	w_i [%]	$Y_{i,Cs}$ [%]	m_i [mg]	w_i [%]	$Y_{i,Ds}$ [%]
Glucose	11,277 ± 251	77	100	6464 ± 101	78	57	6152 ± 380	83	55	920 ± 90	47	8	143 ± 8	16	1
Galactose	1684 ± 118	11	100	737 ± 65	9	44	421 ± 28	6	25	282 ± 24	14	17	187 ± 20	21	11
Rhamnose	452 ± 22	3	100	406 ± 25	5	90	341 ± 36	5	75	320 ± 13	16	71	257 ± 28	29	57
Mannose	251 ± 18	2	100	123 ± 17	1	49	101 ± 12	1	40	99 ± 1	5	39	65 ± 2	7	26
Ribose	316 ± 14	2	100	ND	0	0	ND	0	0	ND	0	0	ND	0	0
Glucuronic acid	194 ± 17	1	100	147 ± 16	2	75	107 ± 16	1	55	95 ± 6	5	49	60 ± 3	7	31
Glucosamine	238 ± 13	2	100	162 ± 9	2	68	134 ± 18	2	56	105 ± 6	5	44	70 ± 3	8	29
Xylose/Arabinose	308 ± 8	2	100	213 ± 14	3	69	172 ± 14	2	56	132 ± 3	7	43	101 ± 7	11	33
Total	14,720 ± 488			8252 ± 20			7429 ± 645			1952 ± 93			883 ± 77		

	A*l*			B*l*			C*l*			D*l*		
	m_i [mg]	w_i [%]	$Y_{i,Al}$ [%]	m_i [mg]	w_i [%]	$Y_{i,Bl}$ [%]	m_i [mg]	w_i [%]	$Y_{i,Cl}$ [%]	m_i [mg]	w_i [%]	$Y_{i,Dl}$ [%]
Glucose	2590 ± 57	67	23	ND	0	0	4813 ± 476 5635 ± 343^a	100	43 50^a	312 ± 37	82	3
Galactose	823 ± 32	21	49	80 ± 12	100	5	ND			30 ± 3	8	2
Rhamnose	33 ± 1	1	7	ND	0	0	ND	0	0	16 ± 1	4	4
Mannose	90 ± 9	2	36	ND	0	0	ND	0	0	12 ± 1	3	5
Ribose	243 ± 19	6	77	ND	0	0	ND	0	0	ND	0	0
Glucuronic acid	11 ± 1	0	6	ND	0	0	ND	0	0	ND	0	0
Glucosamine	44 ± 2	1	18	ND	0	0	ND	0	0	12 ± 1	3	5
Xylose/Arabinose	53 ± 5	1	17	ND	0	0	ND	0	0	ND	0	0
Total	3885 ± 119			80 ± 12			4813 ± 476 5635 ± 343^a			382 ± 43		

w_i: mass fraction of monosaccharide *i* as defined in Eq. 1. $Y_{i,j}$: Yield of monosaccharide *i* in fraction *j* in relation to the whole cells as defined in Eq. 2. $n = 3$. ND: not detected.

[a] Values obtained from supernatant without TFA-hydrolysis.

with the reported monosaccharides in the literature. A detailed overview of the described carbohydrates in *Chlorella* can be found in reference [22].

To the best of our knowledge, this is the first study in which a fractionation process is applied to algae in order to determine the carbohydrate distribution in the cell. Fig. 5 summarizes the types of carbohydrates in *C. vulgaris* resulting from the different process fractions, and highlights the profile of structural polysaccharides. The overall carbohydrate recovery was 82.1%, which most probably results from unavoidable losses after each process step and from sugar degradation during TFA-hydrolysis. Starch constitutes the major part of the total carbohydrates, at least 46.5%, followed by mono- and oligosaccharides in solution released after mechanical cell disruption, 26.4%. The structural carbohydrates integrate at least 6% of the total carbohydrate content in *C. vulgaris*. This value can increase considerably if the optimal TFA-hydrolysis conditions were applied to minimize sugar degradation. Despite this fact, seven different monosaccharides were found in this fraction, revealing the complexity of the cell wall in this alga.

A recently published, comprehensive review evaluating the present and future of *C. vulgaris* showed the great potential of this alga in various application fields [34]. The results of the present study expose the need for specially tailored enzyme combinations for optimizing sugar utilization in the frame of the bio refinery concept.

4. Conclusions

In this study, a previously developed HT-PMP derivatization method for carbohydrate analysis by UHPLC and MS was applied to algal

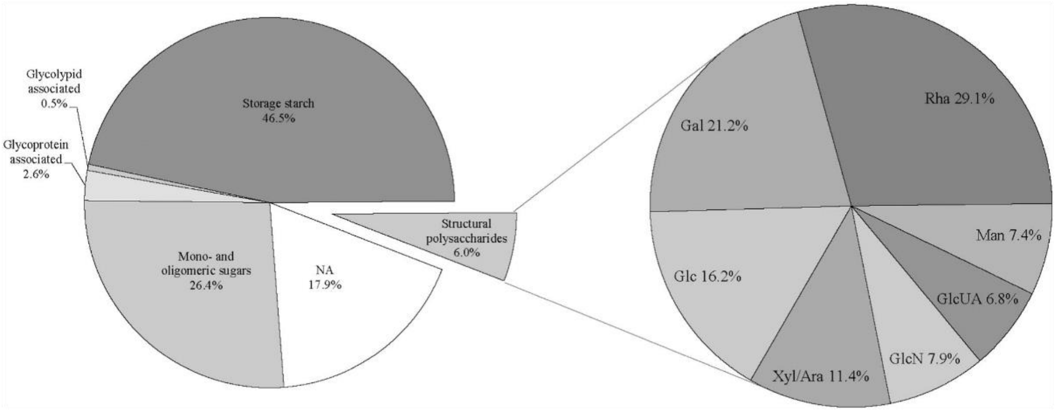

Fig. 5. Left: Carbohydrate distribution in *C. vulgaris*, NA: not assigned. Right: Monosaccharide composition of the structural cell polysaccharides after standard TFA-hydrolysis. Gal, galactose; Rha, rhamnose; Man, mannose; GlcUA, glucuronic acid; GlcN, glucosamine; Xyl, xylose; Ara, arabinose; Glc, glucose.

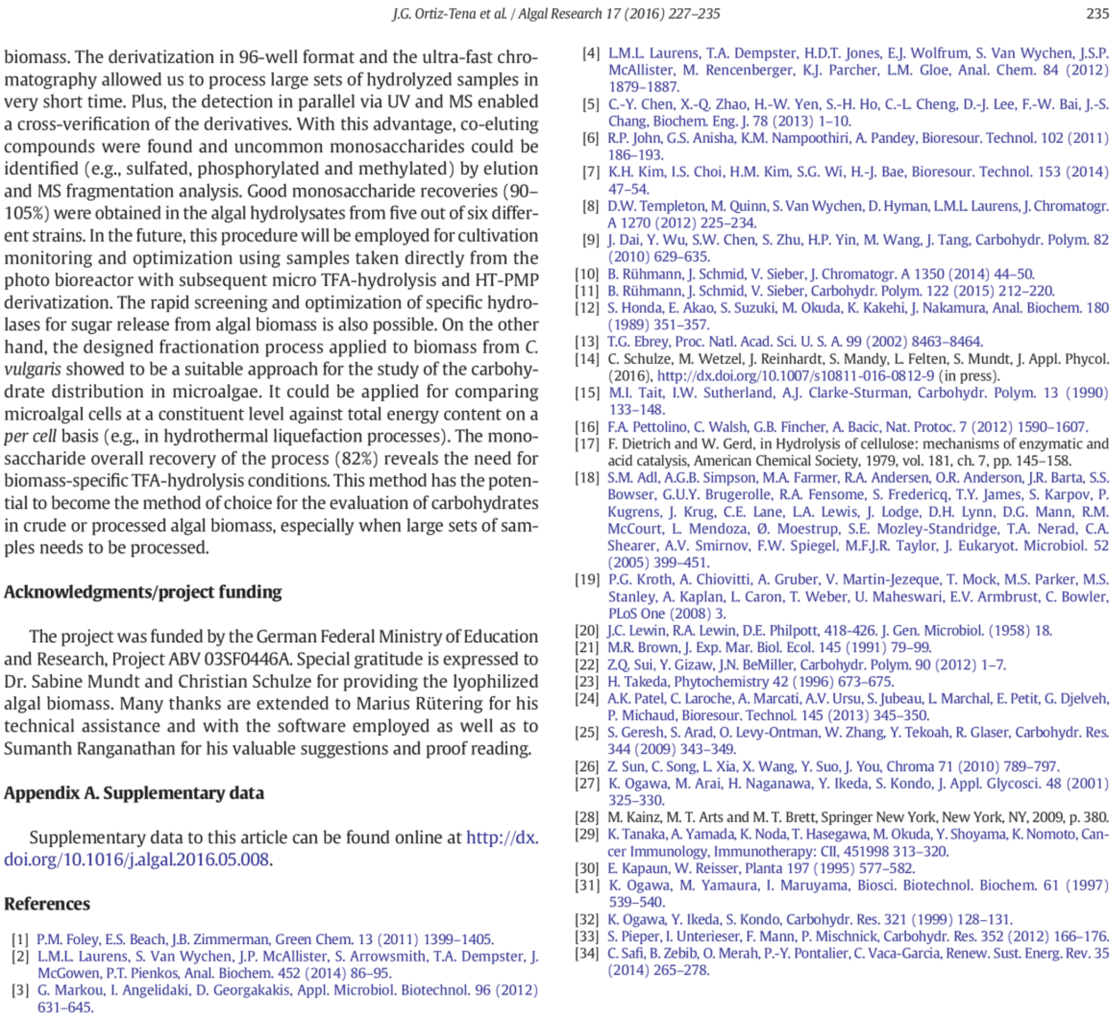

biomass. The derivatization in 96-well format and the ultra-fast chromatography allowed us to process large sets of hydrolyzed samples in very short time. Plus, the detection in parallel via UV and MS enabled a cross-verification of the derivatives. With this advantage, co-eluting compounds were found and uncommon monosaccharides could be identified (e.g., sulfated, phosphorylated and methylated) by elution and MS fragmentation analysis. Good monosaccharide recoveries (90–105%) were obtained in the algal hydrolysates from five out of six different strains. In the future, this procedure will be employed for cultivation monitoring and optimization using samples taken directly from the photo bioreactor with subsequent micro TFA-hydrolysis and HT-PMP derivatization. The rapid screening and optimization of specific hydrolases for sugar release from algal biomass is also possible. On the other hand, the designed fractionation process applied to biomass from *C. vulgaris* showed to be a suitable approach for the study of the carbohydrate distribution in microalgae. It could be applied for comparing microalgal cells at a constituent level against total energy content on a *per cell* basis (e.g., in hydrothermal liquefaction processes). The monosaccharide overall recovery of the process (82%) reveals the need for biomass-specific TFA-hydrolysis conditions. This method has the potential to become the method of choice for the evaluation of carbohydrates in crude or processed algal biomass, especially when large sets of samples needs to be processed.

Acknowledgments/project funding

The project was funded by the German Federal Ministry of Education and Research, Project ABV 03SF0446A. Special gratitude is expressed to Dr. Sabine Mundt and Christian Schulze for providing the lyophilized algal biomass. Many thanks are extended to Marius Rütering for his technical assistance and with the software employed as well as to Sumanth Ranganathan for his valuable suggestions and proof reading.

Appendix A. Supplementary data

Supplementary data to this article can be found online at http://dx.doi.org/10.1016/j.algal.2016.05.008.

References

[1] P.M. Foley, E.S. Beach, J.B. Zimmerman, Green Chem. 13 (2011) 1399–1405.
[2] L.M.L. Laurens, S. Van Wychen, J.P. McAllister, S. Arrowsmith, T.A. Dempster, J. McGowen, P.T. Pienkos, Anal. Biochem. 452 (2014) 86–95.
[3] G. Markou, I. Angelidaki, D. Georgakakis, Appl. Microbiol. Biotechnol. 96 (2012) 631–645.
[4] L.M.L. Laurens, T.A. Dempster, H.D.T. Jones, E.J. Wolfrum, S. Van Wychen, J.S.P. McAllister, M. Rencenberger, K.J. Parcher, L.M. Gloe, Anal. Chem. 84 (2012) 1879–1887.
[5] C.-Y. Chen, X.-Q. Zhao, H.-W. Yen, S.-H. Ho, C.-L. Cheng, D.-J. Lee, F.-W. Bai, J.-S. Chang, Biochem. Eng. J. 78 (2013) 1–10.
[6] R.P. John, G.S. Anisha, K.M. Nampoothiri, A. Pandey, Bioresour. Technol. 102 (2011) 186–193.
[7] K.H. Kim, I.S. Choi, H.M. Kim, S.G. Wi, H.-J. Bae, Bioresour. Technol. 153 (2014) 47–54.
[8] D.W. Templeton, M. Quinn, S. Van Wychen, D. Hyman, L.M.L. Laurens, J. Chromatogr. A 1270 (2012) 225–234.
[9] J. Dai, Y. Wu, S.W. Chen, S. Zhu, H.P. Yin, M. Wang, J. Tang, Carbohydr. Polym. 82 (2010) 629–635.
[10] B. Rühmann, J. Schmid, V. Sieber, J. Chromatogr. A 1350 (2014) 44–50.
[11] B. Rühmann, J. Schmid, V. Sieber, Carbohydr. Polym. 122 (2015) 212–220.
[12] S. Honda, E. Akao, S. Suzuki, M. Okuda, K. Kakehi, J. Nakamura, Anal. Biochem. 180 (1989) 351–357.
[13] T.G. Ebrey, Proc. Natl. Acad. Sci. U. S. A. 99 (2002) 8463–8464.
[14] C. Schulze, M. Wetzel, J. Reinhardt, S. Mandy, L. Felten, S. Mundt, J. Appl. Phycol. (2016), http://dx.doi.org/10.1007/s10811-016-0812-9 (in press).
[15] M.I. Tait, I.W. Sutherland, A.J. Clarke-Sturman, Carbohydr. Polym. 13 (1990) 133–148.
[16] F.A. Pettolino, C. Walsh, G.B. Fincher, A. Bacic, Nat. Protoc. 7 (2012) 1590–1607.
[17] F. Dietrich and W. Gerd, in Hydrolysis of cellulose: mechanisms of enzymatic and acid catalysis, American Chemical Society, 1979, vol. 181, ch. 7, pp. 145–158.
[18] S.M. Adl, A.G.B. Simpson, M.A. Farmer, R.A. Andersen, O.R. Anderson, J.R. Barta, S.S. Bowser, G.U.Y. Brugerolle, R.A. Fensome, S. Fredericq, T.Y. James, S. Karpov, P. Kugrens, J. Krug, C.E. Lane, L.A. Lewis, J. Lodge, D.H. Lynn, D.G. Mann, R.M. McCourt, L. Mendoza, Ø. Moestrup, S.E. Mozley-Standridge, T.A. Nerad, C.A. Shearer, A.V. Smirnov, F.W. Spiegel, M.F.J.R. Taylor, J. Eukaryot. Microbiol. 52 (2005) 399–451.
[19] P.G. Kroth, A. Chiovitti, A. Gruber, V. Martin-Jezeque, T. Mock, M.S. Parker, M.S. Stanley, A. Kaplan, L. Caron, T. Weber, U. Maheswari, E.V. Armbrust, C. Bowler, PLoS One (2008) 3.
[20] J.C. Lewin, R.A. Lewin, D.E. Philpott, 418-426. J. Gen. Microbiol. (1958) 18.
[21] M.R. Brown, J. Exp. Mar. Biol. Ecol. 145 (1991) 79–99.
[22] Z.Q. Sui, Y. Gizaw, J.N. BeMiller, Carbohydr. Polym. 90 (2012) 1–7.
[23] H. Takeda, Phytochemistry 42 (1996) 673–675.
[24] A.K. Patel, C. Laroche, A. Marcati, A.V. Ursu, S. Jubeau, L. Marchal, E. Petit, G. Djelveh, P. Michaud, Bioresour. Technol. 145 (2013) 345–350.
[25] S. Geresh, S. Arad, O. Levy-Ontman, W. Zhang, Y. Tekoah, R. Glaser, Carbohydr. Res. 344 (2009) 343–349.
[26] Z. Sun, C. Song, L. Xia, X. Wang, Y. Suo, J. You, Chroma 71 (2010) 789–797.
[27] K. Ogawa, M. Arai, H. Naganawa, Y. Ikeda, S. Kondo, J. Appl. Glycosci. 48 (2001) 325–330.
[28] M. Kainz, M. T. Arts and M. T. Brett, Springer New York, New York, NY, 2009, p. 380.
[29] K. Tanaka, A. Yamada, K. Noda, T. Hasegawa, M. Okuda, Y. Shoyama, K. Nomoto, Cancer Immunology, Immunotherapy: CII, 451998 313–320.
[30] E. Kapaun, W. Reisser, Planta 197 (1995) 577–582.
[31] K. Ogawa, M. Yamaura, I. Maruyama, Biosci. Biotechnol. Biochem. 61 (1997) 539–540.
[32] K. Ogawa, Y. Ikeda, S. Kondo, Carbohydr. Res. 321 (1999) 128–131.
[33] S. Pieper, I. Unterieser, F. Mann, P. Mischnick, Carbohydr. Res. 352 (2012) 166–176.
[34] C. Safi, B. Zebib, O. Merah, P.-Y. Pontalier, C. Vaca-Garcia, Renew. Sust. Energ. Rev. 35 (2014) 265–278.

Appendix: Supplementary Data

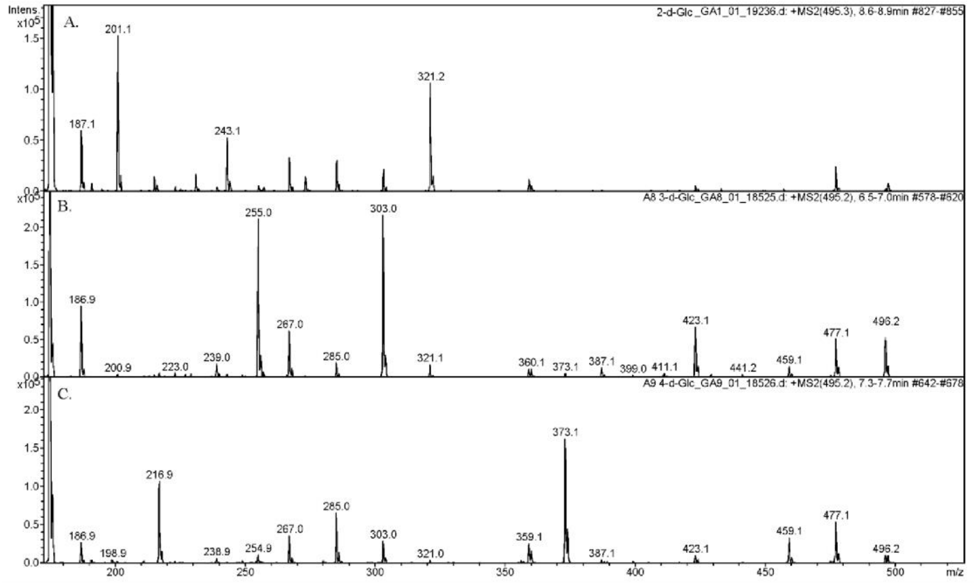

Figure S1. Mass spectrum (*m/z* 170 – 550) of different compounds with *m/z* 495: A. 2-deoxy-glucose, 200 mg L^{-1}; B. 3-deoxy-glucose 200 mg L^{-1}; C. 4-deoxy-glucose, 200 mg L^{-1}

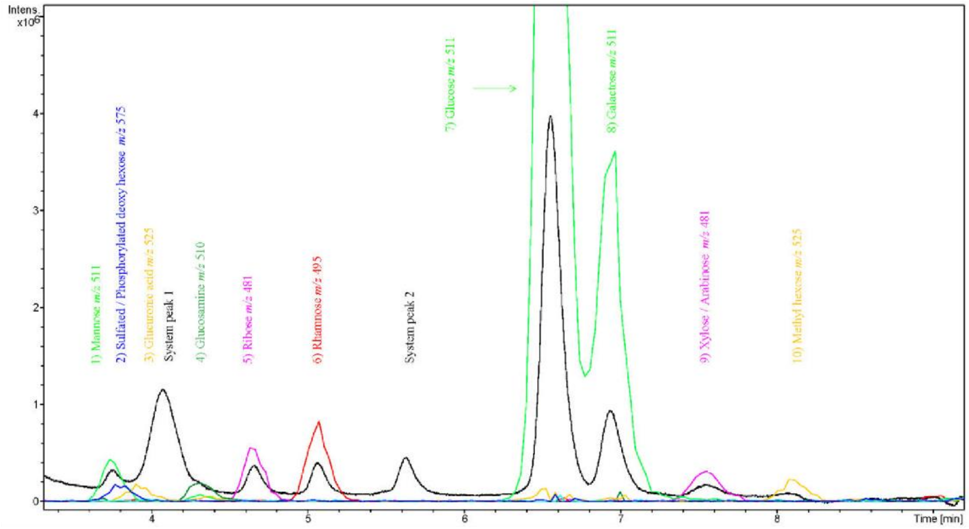

Figure S2. Overlay of UV 245 nm (black) and MS extracted ion (color) chromatograms (3-9 min) of *C. vulgaris* monosaccharide analysis. EIC colors as follow: green *m/z* 511; blue *m/z* 575; yellow *m/z* 525; dark green *m/z* 510; magenta *m/z* 481; red *m/z* 495

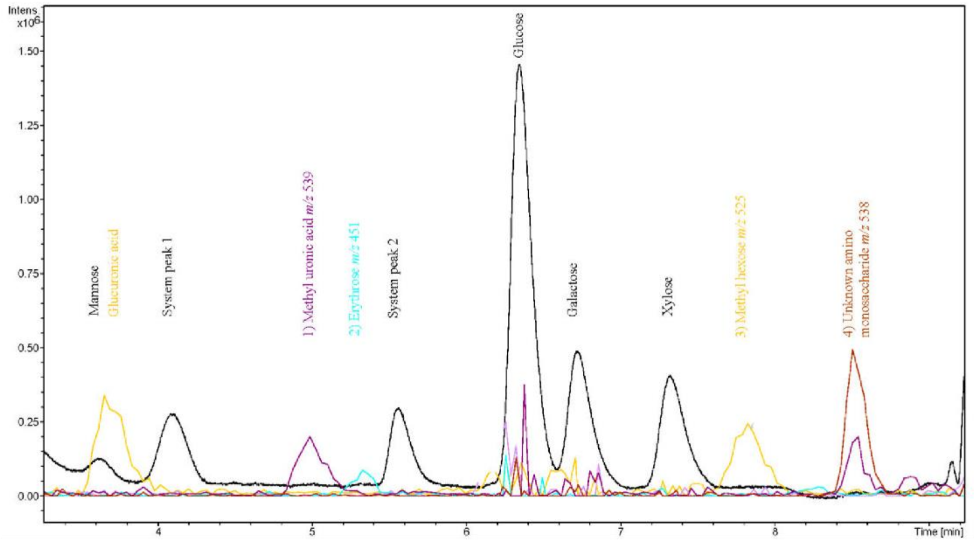

Figure S3. Overlay of UV 245 nm (black) and MS extracted ion (color) chromatograms (3-9 min) of *P. purpureum* monosaccharide analysis. EIC colors as follow: yellow *m/z* 525; violet *m/z* 539; light blue *m/z* 451; brown *m/z* 538

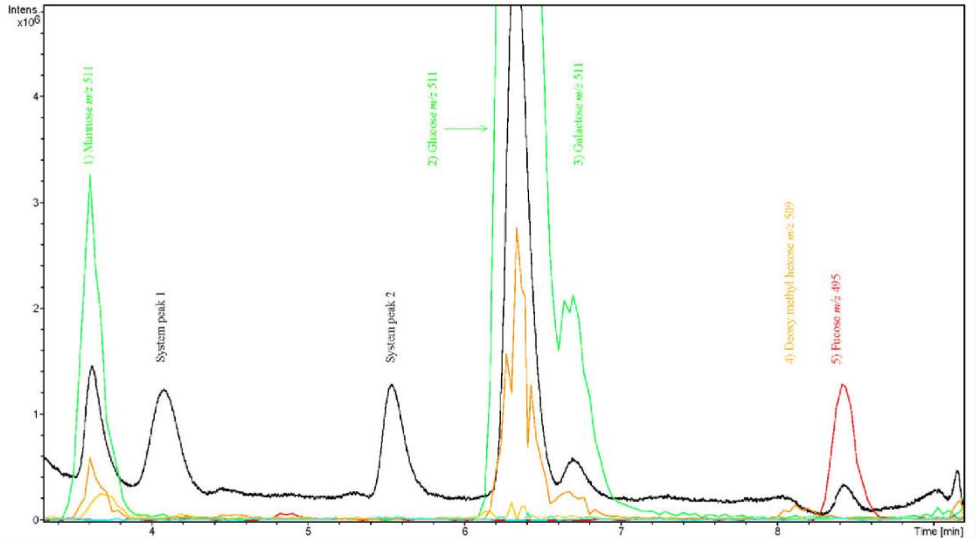

Figure S4. Overlay of UV 245 nm (black) and MS extracted ion (color) chromatograms (3-9 min) of *S. ovalternus* monosaccharide analysis. EIC colors as follow: green *m/z* 511; orange *m/z* 509; red *m/z* 595

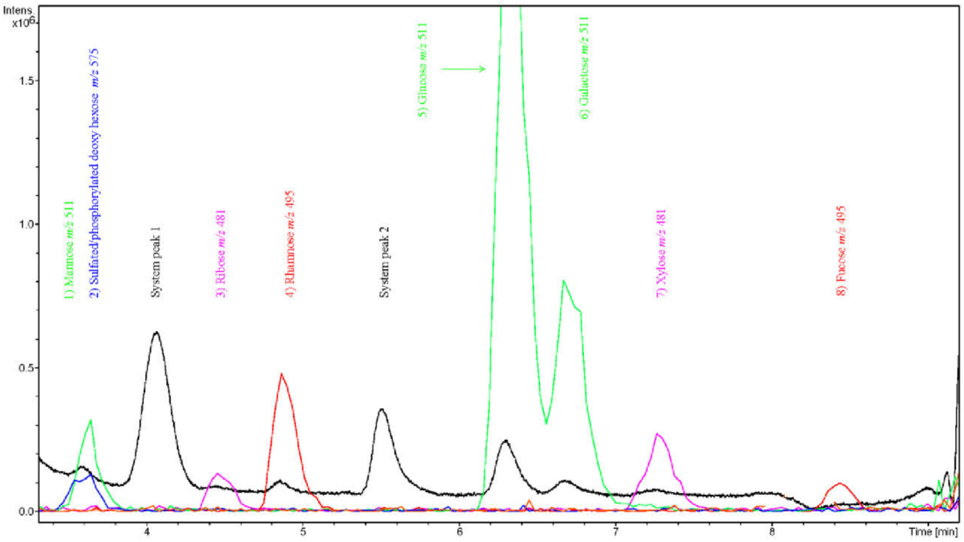

Figure S5. Overlay of UV 245 nm (black) and MS extracted ion (color) chromatograms (3-9 min) of *N. salina* monosaccharide analysis. EIC colors as follow: green *m/z* 511; blue *m/z* 575; magenta *m/z* 481; red *m/z* 495

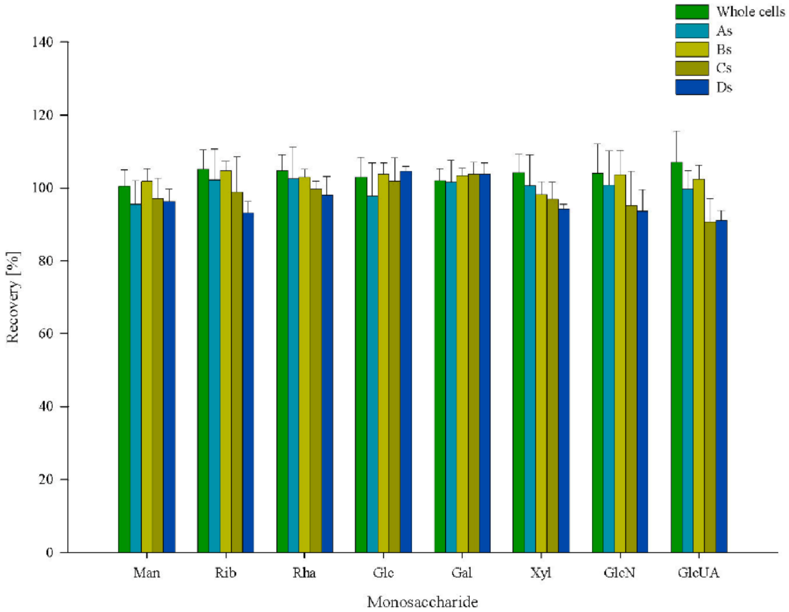

Figure S6. Monosaccharide recovery by PMP derivatization observed after TFA-hydrolysis of *C. vulgaris* solid (*s*) process fractions calculated as explained in section *3.1.3.* Process fractions as described in Scheme 1

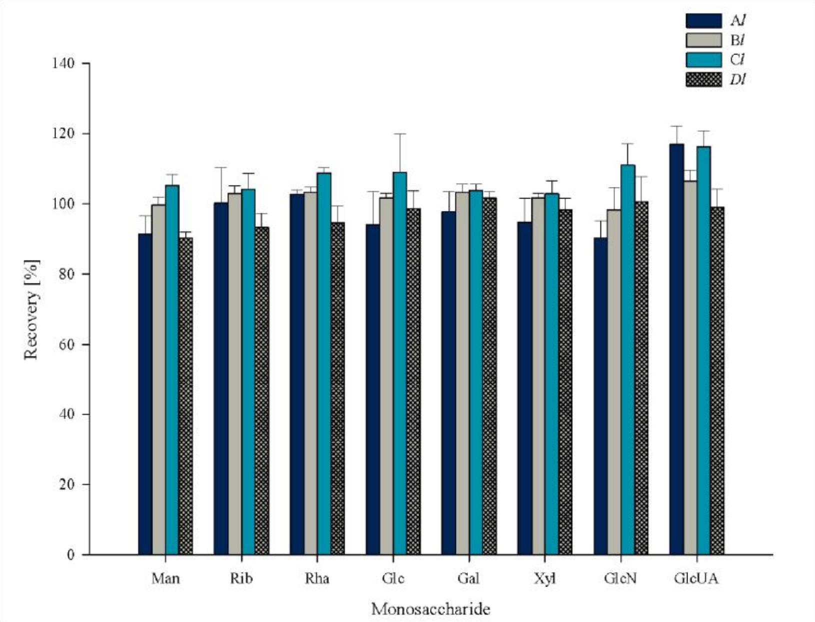

Figure S7. Monosaccharide recovery by PMP derivatization observed after TFA-hydrolysis of *C. vulgaris* liquid (*l*) process fractions calculated as explained in section *3.1.3.* Process fractions as described in Scheme 1

Design of experiments for TFA hydrolysis:

The process in which the glycolytic bonds within a polysaccharide are broken is called *hydrolysis*. In this reaction, the bond between two monosaccharides of a sugar chain is cleaved by addition of a water molecule catalyzed by acids, bases or enzymes. Simultaneously to monomer release, sugar degradation processes (e.g., de-hydration) occur during chemical hydrolysis, as temperatures above 100°C are required (Qian et al., 2005). The monomers involved play a significant role in the breakability of the glycosidic bond. Disaccharides presenting uronic acid and hexoses for example, can still be found after standard TFA hydrolysis of exopolysaccharides, which indicates incomplete hydrolysis (Rühmann, 2016). Because of these two facts (i.e., sugar degradation and incomplete hydrolysis) carbohydrate underestimation in algal biomass using TFA hydrolysis cannot be excluded, as discussed in the paper above. Therefore, the verification of the TFA standard hydrolysis (90 min, 120°C, 2 M TFA, 1 g L^{-1} biomass concentration) prior to PMP derivatization and quantification is a key aspect to ensure an accurate sugar determination.

To investigate the impact of different hydrolysis parameters on the monosaccharide yield, a design of experiments (DoE) was conducted in four experimental blocks using *C. vulgaris* biomass. Temperature (100 – 150°C), hydrolysis time (60 – 120 min), TFA (1 – 4 M), and biomass concentration (0.5 – 5 g L^{-1}) were varied in a central composite design (2^4 samples with star points). The central point (CP, 90 min, 125°C, 2.5 M TFA, 2.75 g L^{-1} biomass concentration) was analyzed nine times. Each experimental block was carried out applying the same temperature. The output parameters evaluated were concentration of released: glucose, neutral sugars excluding glucose (NS), sugar acids (UA), and amino sugars such as GlcN. The obtained results are presented in Table 9.

High concentrations of corresponding monomers in the hydrolysates are shown by a darker shading. Soft hydrolysis treatments in terms of temperature were recorded in the upper part, whereas the harsher conditions are found in the lower part of the table. Noticeable, carbohydrate dimers were found in almost all samples treated at 100°C, which indicates a partial hydrolysis of the biomass polysaccharides. As no standard was available to quantify these compounds, its occurrence was expressed summing the peak area of each disaccharide and reported in a scale + (lower third) to +++ (upper third). Within samples treated at 100°C, GlcN and UA were mostly detected at 5 g L^{-1} biomass concentration. Samples treated at 150°C showed a similar picture, as mostly those samples treated for 60 min and 5 g L^{-1} biomass concentration yielded these sugars. This can be assumed to occur because of degradation occurring at longer times than 60 min, since no dimers were detected in these samples.

The highest total monosaccharide yields were obtained at conditions close to and at the CP (light red). To verify these results, an additional set of samples to the DoE (Block 5) was examined at conditions close to the CP, but with increasing treatment time and varying TFA concentrations (blue marked samples).

Table 9 Monosaccharide yield (in mg per g dry biomass) of *C. vulgaris* after TFA hydrolysis under different conditions. Block 1-4: 2^4- Central Composite Design. The CP are marked in light red. Block 5: additional samples, marked light blue (see Text). *t*: time, *T*: temperature, *c*: concentration, B: biomass, Glc: glucose, NS: neutral sugars, GlcN: glucosamine, UA: uronic acids. Dimers are expressed as the sum of the peak area. Darker green indicates higher monosaccharide concentration.

Block	Sample	t	T	c_{TFA}	c_B	Glc	NS	GlcN	UA	Dimer	Total
Nr.	Nr.	min	°C	M	$g\,L^{-1}$	$mg\,g_B^{-1}$					$mg\,g_B^{-1}$
1	1	60	100	4	0.5	168.4	88.9	0.0	0.0	++	257.3
1	2	60	100	1	0.5	131.2	69.3	0.0	0.0	+	200.4
1	3	60	100	4	5	188.7	52.9	3.0	2.5	+	247.2
1	4	60	100	1	5	127.4	42.7	0.0	1.2	+++	171.3
1	5	90	100	2.5	2.75	208.6	55.8	3.0	0.0	+	267.4
1	6	120	100	1	0.5	255.4	90.4	0.0	0.0	++	345.7
1	7	120	100	4	0.5	197.2	85.4	0.0	0.0	0.0	282.6
1	8	120	100	1	5	205.7	56.0	1.7	1.4	+++	264.8
1	9	120	100	4	5	216.6	59.5	3.8	2.6	++	282.5
2	10	90	125	2.5	2.75	225.6	61.5	4.7	8.5	0.0	300.2
2	11	90	125	2.5	2.75	207.6	57.2	4.7	8.3	0.0	277.8
2	12	90	125	2.5	2.75	213.8	58.2	4.7	8.7	0.0	285.5
2	13	90	125	2.5	2.75	247.4	67.3	5.3	8.7	0.0	328.6
2	14	90	125	2.5	2.75	237.7	63.8	5.0	8.7	0.0	315.2
2	15	90	125	4	2.75	222.5	62.2	5.9	10.5	0.0	301.1
2	16	90	125	2.5	5	229.4	58.3	4.6	6.0	0.0	298.3
2	17	120	125	2.5	2.75	217.7	56.0	5.5	8.6	0.0	287.8
3	18	90	125	2.5	2.75	206.4	59.3	4.9	9.2	0.0	279.8
3	19	90	125	2.5	2.75	207.5	62.6	4.8	9.1	0.0	284.0
3	20	90	125	2.5	2.75	207.7	61.6	4.8	9.4	0.0	283.5
3	21	90	125	2.5	2.75	281.9	72.1	4.9	8.2	0.0	367.2
3	22	60	125	2.5	2.75	218.2	64.5	4.6	8.8	0.0	296.1
3	23	90	125	2.5	0.5	192.5	86.7	0.0	0.0	0.0	279.2
3	24	90	125	1	2.75	228.7	61.6	4.1	6.6	0.0	301.0
4	25	60	150	4	5	128.9	33.3	4.7	6.2	0.0	173.1
4	26	60	150	1	5	212.9	53.6	4.9	6.4	0.0	277.8
4	27	60	150	1	0.5	226.7	72.4	9.1	0.0	0.0	308.1
4	28	60	150	4	0.5	154.7	67.5	0.0	0.0	0.0	222.2
4	29	90	150	2.5	2.75	113.2	33.3	5.0	0.0	0.0	151.5
4	30	120	150	4	5	102.0	28.1	5.9	0.0	0.0	136.1
4	31	120	150	1	5	173.0	42.0	4.4	4.8	0.0	224.2
4	32	120	150	4	0.5	88.0	24.7	0.0	0.0	0.0	112.8
4	33	120	150	1	0.5	168.0	59.9	9.1	0.0	0.0	237.0
5	34	180	120	1.5	2	208.2	50.6	3.8	6.3	0.0	268.9
5	35	300	120	1	2	204.8	45.9	3.3	5.2	0.0	259.3
5	36	480	120	0.5	2	172.8	47.2	3.4	6.6	0.0	230.0
5	37	180	120	0.5	2	185.3	52.3	3.0	4.9	0.0	245.4
5	38	480	120	1.5	2	185.1	42.6	4.3	5.8	0.0	237.8

The obtained results give an insight into the influence of TFA hydrolysis on the monosaccharide yield of *C. vulgaris* biomass (Table 5). The input parameters evaluated were defined being as: A; time, B; temperature, C; TFA concentration, and D; biomass concentration. A basic statistical analysis of the samples at the CP (data from Table 9) is shown in Table 10.

Table 10 Comparative results of average (μ), standard deviation (SD) and coefficient of variation (CV) of the measured central point (CP, n=9) with the minimal and maximal values found. [a] excluding glucose

Output	μ CP (mg g_B^{-1})	SD CP (mg g_B^{-1})	CV CP (%)	Minimal DoE (mg g_B^{-1})	Maximal DoE (mg g_B^{-1})
Glucose	226	26	11.3%	88	282
Neutral sugars [a]	63	5	7.4%	25	90
Glucosamine	4.9	0.2	4.2%	0	9.1
Uronic acids	8.8	0.4	4.6%	0	10.5
Σ	302	30	9.9%	113	392

A coefficient of variation (CV) of ca. 10% was found for total sugar determination, which indicates good reproducibility among single samples. Using the hydrolysis conditions at the CP, 302 ± 30 mg g_B^{-1} total monosaccharides could be detected. The lowest value found within the DoE-range was 113 mg g_B^{-1} (120 min, 150°C, 4M TFA and 0.5 g_B L^{-1}, sample 32, Table 9), which is ca. one third of that found for the conditions employed at the CP. If the maximal amounts found for each measured monosaccharide are summed up, a theoretical maximum carbohydrate concentration of 392 mg g_B^{-1} can be accounted in *C. vulgaris* biomass. This value is 30% higher than that computed for the CP (302 mg g_B^{-1}). The highest concentration detected for neutral sugars was 90 mg m_B^{-1} (sample 6, Table 9), at much lower temperature of 100°C, for 120 min, 1M TFA and 0.5 g_B L^{-1}. This value is ca. 50% higher than the average found for neutral sugars at the CP (63 mg g_B^{-1}). Plus, almost twice as much glucosamine (9.1 mg g_B^{-1}) compared to the CP (4.9 mg g_B^{-1}) was found in samples 27 and 33, (both 150°C, 1 M TFA, and 0.5 g_B L^{-1}, for 60 and 120 min, respectively).

These results indicate that each of the four input parameters of the TFA hydrolysis influence the release of each monosaccharide (outputs) differently. To analyze these dependences, a multiple linear regression model was created for each output based on the data generated by the DoE. The first step of this methodology is the determination of the statistically relevant input parameters for each output variable with a standardized pareto chart (Figure 5A). In this chart, the standardized effect of each input as well as their interactions is calculated by the software used (Table 2). The length of each bar in the diagram is proportional to the value of a *t*-statistic computed for the corresponding effect. The bars with higher values than the vertical line indicate those statistically significant, so called main effects within the selected confidence interval of 95%. For glucose, this analysis revealed that the parameters B (temperature) and C (TFA concentration) along with their interaction (BC) are statistically significant. Besides, the interactions between A (time) and B (temperature) as well as the quadratic effect of the temperature (BB) play a significant role in the release of glucose. The biomass concentration (D) does not affect significantly glucose hydrolysis.

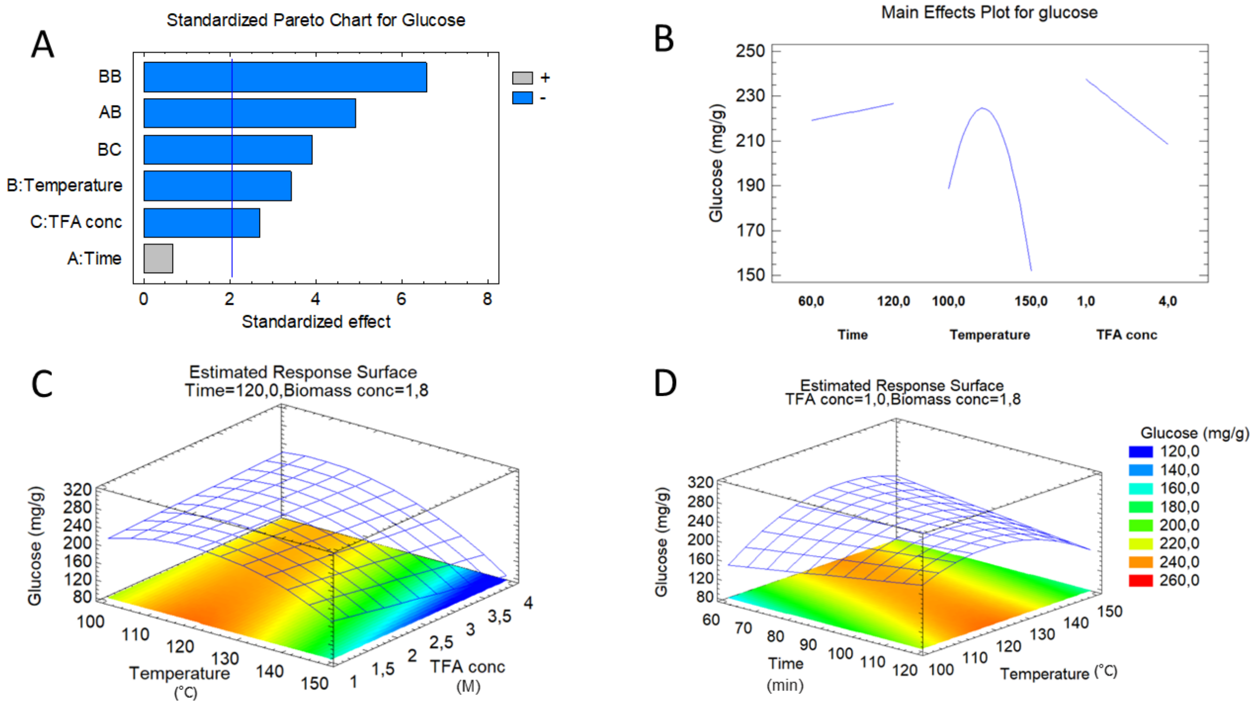

Figure 5: Multiple linear regression model for output glucose concentration in mg g_B^{-1} A. Standardized pareto diagram after excluding non-significant effects (confidence interval 95%,), B. main effects plot, C. Surface response plot for temperature (°C) and c_{TFA} (M), D. Surface response plot for time (min) and temperature (°C)

The impact of each significant parameter on the output variable can be better visualized with a main effect plot (Figure 5B). The lines indicate the estimated change in glucose yield as each factor is moved from the low to the high level selected in the DoE, with all other factors held at their optima within the investigated range. For glucose, a maximum yield was found at 119.2°C and 1.8 g L^{-1} biomass, which lies within the investigated range. The glucose release increased with longer hydrolysis times and lower TFA concentration, reaching the highest yield at the DoE boundary values (120 min and 1 M, respectively). This means that global optimum parameters for TFA and hydrolysis time may well be found beyond these set values. Additional explorative biomass treatments outside the DoE range for time and TFA concentration at optimum temperature and biomass concentration (Table 9, blue shaded samples) did not yield higher glucose concentrations. Thus, a local maximum glucose yield could be found at the DoE high boundary of parameter A (time) and low boundary for C (TFA concentration).

Once the relevant parameters were established, a fitting equation for output yield was obtained for glucose:

$$Glc = -1596.9 + 4.8 * A + 25.2 * B + 64.9 * C - 0.03 * A * B - 0.08 * B^2 - 0.59 * B * C \quad \text{(Equation 2)}$$

A 3-D representation of the model as surface response plots based on the fitting equation helps for better visualization (Figure 5C-D). As mentioned above, the highest glucose yields within the DoE range are obtained at 1 M TFA concentration (120 min, 1.8 g L^{-1} biomass). If the concentration of TFA is increased up to 4 M, lower temperature values than the optimum found can help maintain a yield around 240 mg g_B^{-1}. Furthermore, a clear temperature pattern is observed for the time span between 60 and 120 min (1 M TFA, 1.8 g L^{-1} biomass). Consequently, glucose yields of around 240 mg g_B^{-1} could be obtained by the combination short time and high temperature or long time and lower temperature.

The same multiple linear regression analysis was performed for the rest of the output variables and is reported in the Appendix section: identification of significant factors for all outputs with a pareto chart (Figure A1), main effect plots and surface response plots for the significant interactions of the yield for neutral sugars (Figure A2), uronic acids (Figure A3), and glucosamine (Figure A4). The underlying equations are also reported in Table A 1.

To simplify the statistical analysis, all non-glucose monosaccharides from *C. vulgaris* (galactose, mannose, ribose, rhamnose, arabinose/xylose) were grouped into the output parameter "neutral sugars". For these sugars, a clear optimum could be found within the selected range for temperature (113.2°C) and biomass concentration (0.56 g L^{-1}); both values being lower than those for glucose. Local maxima for TFA concentration and hydrolysis time were found, again, at the range boundaries. However, none of these two parameters resulted to be statistically significant, i.e., values outside the range may only negligibly increase sugar yield, as can be seen from the flat surface response plots for neutral sugars (Figure A2 B-C).

The maximum release of uronic acids could be achieved by a biomass concentration of 3.5 g L^{-1}, a temperature of 127°C and the highest TFA concentration of the DoE range (Figure A3). It is not clear whether the highest or the lowest DoE boundary value for parameter A (time) is best to maximize uronic acids yield. For a statistically significant release however, the hydrolysis time plays a minor role.

Finally, the optimum conditions to maximize glucosamine yields were found to be 2 g L^{-1} biomass, a relatively high temperature of 149°C, and the low boundary of TFA concentration and hydrolysis time within the DoE range (Figure A4). These two last parameters, however, should not influence significantly glucosamine release according to the corresponding pareto chart.

A summary of the optimum hydrolysis conditions found to maximize each output within the DoE range is presented in Table 11.

Table 11 Hydrolysis parameters found to maximize sugar yields of *C. vulgaris* biomass within the DoE range. Values obtained by multiple linear regression analysis of the data generated. **Underlined bold** entries indicate statistically significant parameters according to the corresponding pareto analysis. TFA: Trifluoroacetic acid

Output variable	**A time (min)**	**B temperature (°C)**	**C TFA (M)**	**D Biomass (g L^{-1})**
Glucose	120	**119.2**	**1.0**	1.8
Neutral sugars	60	**113.2**	4.0	**0.56**
Uronic acids	60	127.3	4.0	**3.5**
Glucosamine	60	**149.0**	1.0	**2.0**

These results corroborate that a single combination of parameters within the investigated range could not produce a global optimum yield of all sugars. Instead, local maxima within the DoE limits could be determined for single sugars (e.g., glucose and glucosamine), or sugar groups, (e.g., neutral sugars and uronic acids). Noticeably, the hydrolysis time (A) is not statistically significant for any of the output sugars, which means that its effect is not determining for attaining high sugar yields after TFA hydrolysis of the biomass of *C. vulgaris*. In contrast, temperature and biomass concentration play a statistically significant role for three out of four output sugar variables. Further discussions on TFA hydrolysis for carbohydrate determination by PMP derivatization in microalgal biomass based on the DoE results presented here can be found in section A5.1.

A4.2. A one-stage cultivation process for lipid- and carbohydrate-rich biomass of *Scenedesmus obtusiusculus* based on artificial and natural water sources

This paper illustrates a relevant application of the adapted carbohydrate HT-PMP analytical method presented above in the field of microalgal bio refinery. One of the important advantages of biomass from microalgae compared to other biogenic resources is the possibility to modulate its composition in the short term by designing targeted cultivation strategies. This approach provides high flexibility in the production of microalgal biomass as raw material depending on the devised application. In this work, subsequent optimization rounds were conducted for culturing *S. obtusiusculus* A189 towards maximized carbohydrate and lipid, as well as minimized protein content. Resulting from the optimization procedure, a tailored low-cost medium was obtained, enabling a cultivation procedure in a single stage for *S. obtusiusculus* with the desired composition without loss in biomass productivity.

The optimization started with the commonly employed medium for algae and cyanobacteria BG-11. In the first round, the nitrate concentration was varied and adjusted to 25% of BG-11. Further, the optimal harvesting time was determined as 14 days. Next, the influence of phosphate and iron on the biomass composition was investigated, adjusting its concentration to 100% of BG-11 for PO_4^{3-} and 10% for Fe. Once these parameters were successfully optimized, the costly BG-11 medium, which contains a generic mixture of micronutrients, was replaced by artificial sea water (ABV1 medium), Baltic Sea water (ABV2 medium) and Peene River water (ABV3 medium).

The composition of the produced biomass was first monitored in terms of total lipids, total carbohydrates and total protein using standard methods (gravimetric analysis of hexane extracts, thymol-sulfuric acid method, and ninhydrin assay, respectively). Next, the monomeric sugar composition of all generated biomasses was determined using the transferred HT-PMP method. Glucose, mannose and galactose were the main sugars identified, as previously reported for several *Scenedesmus* species. The results indicated that a significant amount of the sugars is present as energy storage, since glucose (most probably from starch) made up at least 80% of the total carbohydrate content after standard TFA hydrolysis of the biomass. Mannose and galactose, which are associated to the algal cell wall, represented about 10% and 5% of total carbohydrates, respectively. Similarly, the fatty acid composition of the cultured biomasses was determined by GC, being C16 (saturated) and C18 (both saturated and unsaturated) the primarily found compounds.

The generated composition profiles of the biomass set the basis for designing appropriate material or energetic utilization strategies. In this case, for example, the use of fermentative organisms that can metabolize mannose and galactose would be advantageous for an economic bio refinery process.

The author conducted the experiments to determine the carbohydrate composition, wrote the corresponding section 3.2.2 of the manuscript, and contributed to content and language of the article.

A one-stage cultivation process for lipid- and carbohydrate-rich biomass of *Scenedesmus obtusiusculus* based on artificial and natural water sources

Christian Schulze, Jakob Reinhardt, Martina Wurster, José G. Ortiz-Tena,
Volker Sieber, and Sabine Mundt

Bioresource Technology
2016

Reproduced with permission, license number: 4206621306380
DOI: 10.1016/j.biortech.2016.06.109

Bioresource Technology 218 (2016) 498–504

Contents lists available at ScienceDirect

Bioresource Technology

journal homepage: www.elsevier.com/locate/biortech

A one-stage cultivation process for lipid- and carbohydrate-rich biomass of *Scenedesmus obtusiusculus* based on artificial and natural water sources

Christian Schulze [a],*, Jakob Reinhardt [a], Martina Wurster [a], José Guillermo Ortiz-Tena [b], Volker Sieber [b], Sabine Mundt [a]

[a] *Ernst-Moritz-Arndt-University of Greifswald, Institute of Pharmacy, Department Pharmaceutical Biology, Friedrich-Ludwig-Jahn-Str. 17, 17491 Greifswald, Germany*
[b] *Technische Universität München, Chair of Chemistry of Biogenic Resources, Straubing Center of Science, Schulgasse 16, Straubing, Germany*

HIGHLIGHTS

- Medium nitrate, phosphate and iron were optimized for high-value algal biomass.
- Low-cost medium based on artificial sea water or natural water sources was designed.
- Lipid- and carbohydrate-rich algal biomass was obtained in a one stage cultivation process.

ARTICLE INFO

Article history:
Received 26 May 2016
Received in revised form 25 June 2016
Accepted 27 June 2016
Available online 29 June 2016

Keywords:
Scenedesmus obtusiusculus
Nitrate starvation
Lipids
Carbohydrates
Medium optimization

ABSTRACT

A one-stage cultivation process of the microalgae *Scenedesmus obtusiusculus* with medium based on natural water sources was developed to enhance lipids and carbohydrates. A medium based on artificial sea water, Baltic Sea water and river water with optimized nutrient concentrations compared to the standard BG-11 for nitrate (−75%), phosphate and iron (−90%) was used for cultivation. Although nitrate exhaustion over cultivation resulted in nitrate limitation, growth of the microalgae was not reduced. The lipid content increased from 6.0% to 19.9%, an increase in oleic and stearic acid was observed. The unsaponifiable matter of the lipid fraction was reduced from 19.5% to 11.4%. The carbohydrate yield rose from 45% to 50% and the protein content decreased from 32.4% to 15.9%. Using natural water sources with optimized nutrient concentrations could open the opportunity to modulate biomass composition and to reduce the cultivation costs.

© 2016 Elsevier Ltd. All rights reserved.

1. Introduction

In the last decades microalgae became more and more valuable for science and industry. Various approaches have been pursued in order to utilize these organisms. For example a number of high value products and applications has been developed (Borowitzka, 2013) such as dietary supplements, and nutraceuticals like astaxanthin or polyunsaturated fatty acids. In the era of rising prices of fossil resources and increasing awareness about their limitation, the potential of microalgae as source for renewable energies has gained much interest. Algae have certain advantages as resources for biofuels compared to land plants. The biomass productivity is several times higher per surface unit, they can be cultured on barren land so there is no competition with food production (Xu and Boeing, 2014) and the required resources sunlight, natural water and some nutrients are inexpensive and mostly readily available. Even though not every algal species is suitable for energy production, several microalgae have been identified as promising basis for the production of biofuels (Nascimento et al., 2013; Rodolfi et al., 2009). Some algae like *Chlorella* sp. (Francisco et al., 2010) and *Scenedesmus* sp. (Aravantinou et al., 2013) showed very high growth rates, whereas others like *Porphyridium* sp. (Song et al., 2013) and *Nannochloropsis* sp. (Rodolfi et al., 2009) were reported to be good lipid producers. A combination of both properties is rare but can be achieved by different cultivation techniques. Cabello et al. (2015) varied pH, temperature, light intensity and nitrate content of the cultivation medium to optimize the photosynthetic activity and growth of *Scenedesmus obtusiusculus*. As previously described for many algal species, nitrate starvation seems to be the most efficient method to enhance lipid productivity (Griffiths et al., 2012; Rodolfi et al., 2009). On the other hand for optimization of the carbohydrate content, which is of interest when biomass is used as feedstock

---

* Corresponding author.
E-mail address: christian.schulze@uni-greifswald.de (C. Schulze).

http://dx.doi.org/10.1016/j.biortech.2016.06.109
0960-8524/© 2016 Elsevier Ltd. All rights reserved.

(e.g., for bioethanol fermentation), different methods like nutrient starvation, light or salt stress have been described (Markou et al., 2012). Otherwise salt stress can also influence the protein synthesis in algae (Fabregas et al., 1985). Wang et al. (2013) showed that *Scenedesmus dimorphus* was able to produce either lipid-, carbohydrate- or protein-rich biomass, depending on nitrate concentration of culture medium, light intensity and cultivation time. This opens up new ways for influencing the composition of algal biomass to be utilized for different purposes. However, increasing the yield of a desired product by any stress condition often leads to a decrease in the biomass productivity, which results in a reduced space-time yield even though the relative productivity is enhanced. For an optimized space-time yield, identifying the balance between stress and growth conditions is a challenge that needs to be tackled for each individual application to obtain high content of the target product and sufficient biomass production.

For reducing the production costs of microalgal biomass, one relevant approach is to reduce the cost of cultivation media. Artificial media like the common used BG-11 are quite expensive because they are based on deionized or distilled water and all required components are added in a high chemical purity. In literature, there are some attempts described for low-cost culture media based on North Sea water (Pohl et al., 1987), artificial (Feng et al., 2011) or natural wastewater (Kim et al., 2007) or even freshly diluted human urine (Adamsson, 2000) either to reduce costs or to re-use the waste of other processes.

Very often, two-stage cultivation processes are used (Cabello et al., 2015; Ho et al., 2010; Ho et al., 2013b; Toledo-Cervantes et al., 2013; Xia et al., 2013). In the first stage, algae are grown under nutrient-repleted conditions for maximal biomass production. In the second stage, cultures are transferred into nutrient-depleted medium to accumulate lipids, carbohydrates or both. For the production of bulk chemicals or bio-fuels such strategies are not suitable because additional costs for medium exchange make the processes unprofitable. Only some authors described attempts for one-stage processes where one nutrient is exhausted during cultivation, resulting in optimized biomass composition (Ho et al., 2012; Griffiths et al., 2014; Gao et al., 2015). The observed effects were similar to the two-stage cultivation: a few days after nutrient exhaustion the biochemical composition changed from protein-rich to lipid- and carbohydrate-rich.

In most studies only one or two medium components are considered (mainly nitrate and phosphate) for optimization of algal biomass, whereas further nutrients are rarely examined (Dahmen et al., 2014). However, for a low-cost medium, every component should be optimized so that at the end of cultivation all nutrients are completely used up by the algae, saving resources and preserving the environment.

The aim of this study was to develop a one-step cultivation process for *Scenedesmus obtusiusculus* A189 that combines the advantages of the different approaches. After identification of the optimal irradiance, the main nutrients nitrate, phosphate and iron were optimized. Trace elements and other macro nutrients were replaced by artificial sea water, Peene River water or Baltic Sea water, respectively. As a result of this optimization, a low-cost medium was available for one-stage cultivation, which allowed the same biomass yield as the high-cost BG 11 medium with significantly higher amounts of valuable products as carbohydrates and lipids.

2. Material and methods

2.1. Biological material

Scenedesmus obtusiusculus A189 from the strain collection of the Pharmaceutical Biology, University of Greifswald, was isolated by Hübel in Prerow, park pond, Germany (54°26′31.7″ N, 12°36′42.2″ E) and identified in 1995. The unicellular, elliptic alga is 10–12 µm in size and belongs to Scenedesmaceae, Chlorophyceae.

2.2. Cultivation

Pre-cultures of *Scenedesmus obtusiusculus* A189 were cultivated in 400 mL BG-11 medium in ventilated Schott bottles (VWR, Germany) until an optical density, measured at 750 nm (OD_{750}), of at least 2 was reached. Then the algae were cultivated in a 500 mL Schott bottle, each with 200 mL medium. The starting OD_{750} was 0.1 (approx. 0.03 g L^{-1} dry weight, DW), the irradiance was 200 ± 5 µmol photons $m^{-2}\,s^{-1}$ (Osram LUMILUX Cool White 39 W, Germany) in a 12/12 h light/dark cycle. Cultures were ventilated with sterile filtered fresh air at a flow of approx. 1.5 vvm. The temperature was set at 25 ± 2 °C and the cultivation time was 14 d. Every second day, 0.1 mL was taken from the cultures to measure optical density to control growth. Evaporated water was refilled with sterile distilled water to 200 mL every second day. Cultures were harvested by centrifugation (Rotanta 96 R, Hettich Zentrifugen, Germany) at 5700*g* for 5 min and dried in a lyophilizer (Vaco5, Zirbus Technology, Germany).

For the nitrate (N) starvation experiments, pre-cultures were centrifuged and resuspended in BG-11 medium with N-concentrations of 100, 75, 50, 40, 35, 30, 25, 20, 15, 10, 5 and 0% of the standard concentration. Then the algae were cultivated in a 500 mL Schott Bottle, each with 200 mL of BG-11 medium, containing the different N concentrations. During cultivation, the residual nitrate concentration in medium was measured. After 14 d, cultures were harvested as described above.

For monitoring biomass production and composition after different cultivation times, A189 was cultivated in BG-11 medium with 25 % sodium nitrate. The biochemical composition of freeze-dried biomass and the residual nitrate concentration was analyzed after 3, 5, 7, 10, 12, 14, 17, 19, 21, 24 and 26 days.

For the phosphate (P) and iron (Fe) starvation experiments, pre-cultures were centrifuged and resuspended in BG-11 medium with 100, 75, 50, 25, 10 and 0% of the standard concentrations of P and Fe, respectively, and cultivated in 200 mL medium containing the P and Fe concentrations. After 14 d, cultures were harvested as described above. Three replicates were cultivated for each nutrient concentration. The N starvation experiments were carried out thrice, the other experiments twice.

After identifying the optimum concentrations of N, P and Fe, a new medium ("ABV-Medium", named after the funding project "Advanced Biomass Value") was designed. As proof of concept, the algae were cultivated in 40-L-airlift fermenters containing BG-11 as control and the ABV1-Medium (Table 1). Cultivation was performed in 37 L medium and irradiation was set to 4 × 200 ± 10 µmol photons $s^{-1}\,m^{-2}$ (continuous light) at 30 ± 1 °C. The pH was monitored and adjusted to 8.5 ± 0.1 with CO_2-enriched air (0.7% V/V); the total gas flow was 0.03 vvm. After 14 d, cultures were harvested by flow centrifugation (Heraeus Biofuge Stratos, Thermo Scientific, USA, 10,000*g*, 120 ml min^{-1}). 2 L of the culture were left in the reactor as stock and the fermenter was refilled to 37 L again resulting in a starting biomass concentration of approx. 0.1 g L^{-1} DW. The fermenter with the ABV1 medium was refilled ten times to verify whether a long-time cultivation was possible.

Scenedesmus obtusiusculus A189 was cultivated in ABV2 and ABV3 to evaluate whether natural water sources were useable as medium base. Baltic Sea water (brackish water) and Peene River water (fresh water) was collected, centrifuged at 12,000*g* to remove particles and autoclaved to prevent culture contamination.

Table 1
Composition of BG-11 (Waterbury and Stanier, 1981) and the new developed ABV-Medium (g L^{-1} unless otherwise stated).

Component	BG-11	ABV1	ABV2	ABV3
$NaNO_3$	1.5	0.375	0.375	0.375
K_2HPO_4	0.031	0.031	0.031	0.031
Ferric ammonium citrate	0.006	0.0006	0.0006	0.0006
$MgSO_4 \times 7H_2O$	0.075	0	0	0
$CaCl_2 \times 2H_2O$	0.03576	0	0	0
Citric acid	0.006	0	0	0
Na_2EDTA	0.001	0	0	0
Na_2CO_3	0.02	0	0	0
Trace Element Solution[a]	1 mL	0	0	0
Distilled Water	1 L	1 L	0	0
Artificial sea salt[b]	0	5.0	0	0
Baltic Sea water[c]	0	0	1 L	0
Peene River water[d]	0	0	0	1 L

[a] Trace element solution contains (mg L^{-1}) (Kuhl and Lorenzen, 1964): H_3BO_3 0.61; $MnSO_4 \times 4H_2O$ 2.23; $ZnSO_4 \times 7H_2O$ 2.87; $CuSO_4 \times 5H_2O$ 0.025; $(NH_4)_6Mo_7O_{24} \times 4H_2O$ 0.125.

[b] "Premium Meersalz pure"; Tropic Meeresaquaristik. www.tropic-meeresaquaristik.de.

[c] Collected in September 2015, Lubmin, Mecklenburg-Western Pomerania, Germany (54°08′24.6″ N; 13°36′41.5″ E).

[d] Collected in November 2015, near Gützkow, Mecklenburg-Western Pomerania, Germany (53°54′58.9″ N, 13°25′32.8″ E).

Cultivation and harvesting was done as described above. For each medium, three cultivation cycles were processed.

2.3. Determination of nitrate

The nitrate content in the medium was measured according to DIN 38405-9 as a modified semi-micro method. Each sample was centrifuged (4 min, 4100 g) and 100 µL of the supernatant were heated to dryness at 120 °C together with 100 µL of a sodium salicylate solution (10 g L^{-1}). The residue was resolved in 100 µL of concentrated sulfuric acid; 700 µL of potassium sodium tartrate salt solution (400 g NaOH and 60 g potassium sodium tartrate in 1 L distilled water) were added. After dilution with 700 µL distilled water, 200 µL of the yellowish solution were measured at 410 nm (Fluostar Omega, BMG Labtech, Germany) in 96-well plates (Nuncleon Delta Surface, Thermo Scientific, USA). A calibration curve was recorded with sodium nitrate and a blank was prepared with 100 µL distilled water.

2.4. Lipid, carbohydrate and protein determination

The primary metabolites were analyzed as previously described (Schulze et al., 2016): Lipids were extracted with n-hexane after cell disruption with an ultrasonic probe and the yield of the n-hexane extract was estimated gravimetrically. The total carbohydrates were measured with a modified thymol-sulfuric acid method after acid hydrolysis of the biomass in 2 N hydrochloric acid for 2 h at 100 °C. Proteins were determined with a modified ninhydrin-assay.

2.5. Carbohydrate composition

The method described by Ortiz-Tena et al. (2016) was used. After acid hydrolysis with 2 M TFA at 121 °C, the carbohydrates were derivatized with PMP (1-Phenyl-3-methyl-5-pyrazolone) in microplates, separated and analyzed by LC-MS.

2.6. Unsaponifiable matter

For determination of the unsaponifiable matter approx. 10 g of crude algal biomass cultivated in BG-11 or ABV1 medium were extracted with n-hexane in a Soxhlet-apparatus for 15 h. After evaporation of the solvent, the obtained oil was stored at −20 °C until analysis. The unsaponifiable matter of the extracted algae oil was determined with a modified method according to the European Pharmacopoeia 8 (Ph.Eur. 8, 2.5.7). For this, 200 mg oil were boiled for 1 h under reflux condensation within 25 mL ethanolic KOH. 50 mL water was added and the mixture was extracted three times with 50 mL of peroxide-free ether in a separating funnel. Exactly according to Ph.Eur., the combined ether fraction was washed three times with each 40 mL of water and potassium hydroxide solution. The washed ether phase was evaporated, the residue resolved in acetone and evaporated again. The dried residue was weighed; the unsaponifiable matter was calculated in %. The experiments were carried out in duplicates.

2.7. Fatty acid composition

The n-hexane extracts were derivatized with methanolic HCl according to Lepage and Roy (1986) but modified as suggested by Ostermann et al. (2014). 1.0 mg extract was dissolved in 250 µL n-heptane. Then, 600 µL methanolic HCl (methanol/acetylchloride 10:1 V/V) were added and heated at 95 °C for 1 h. Afterwards, 750 µL of 0.44 M potassium carbonate solution were added and after centrifugation (5700g, 5 min) the upper layer was transferred to microvials for analysis. Quantification was performed using the peak areas compared to the internal standard lignoceric acid (C24:0). Calibration of the method was done using a standard mixture of the fatty acids palmitic acid (C16:0), stearic acid (C18:0), oleic acid (C18:1), linoleic acid (C18:2) and α-linolenic acid (C18:3) in concentrations from 0.2 to 3.2 mmol L^{-1}. Derivatization of the calibration solutions was performed as described above.

Separation by gas chromatography was carried out similarly to Liebeke et al. (2008) using a 30 m × 0.25 mm DB-5MS Agilent Technologies capillary column with 0.25 µm film-thickness. The following temperature gradient was used on a 1530 Series GC instrument (Agilent, Weilbronn, Germany): 70 °C for 1 min, 70 °C to 76 °C with 1.5 °C min^{-1}, 76 °C to 330 °C with 5 °C min^{-1} and 330 °C for 10 min (total run time 65.8 min). Helium was used as carrier gas with a constant flow of 1 mL min^{-1}. 2 µL of the sample were injected with an injector kept at 230 °C, the split set to 25:1. For detection and identification electron ionization mass spectrometry was used based on the following settings: The electron ionization was performed with 70 eV and tuned automatically using PFTBA (masses 69, 219 and 502). The dwell time was set to 30 ms in the range 35 to 573 m/z with a scan rate of 2.74 s^{-1}.

3. Results and discussion

3.1. Starvation experiments

3.1.1. Nitrate starvation

S. obtusiusculus A189 was cultivated in BG-11 medium with varying N concentrations. Medium samples were analyzed for the remaining nitrate concentration over the cultivation period. Fig. 1b shows that only in cultures with the highest N concentrations, N100 and N75, respectively, N was detectable at the end of the cultivation time. In cultures with lower N concentrations, N was already exhausted between day 2 (N5) and day 9 (N50). The nitrate consumption during exponential growth (approx. day 2–10) was similar in all cultures, at a rate of 76.4 ± 5.5 mg L^{-1} d^{-1} (calculated from day 2–5, with the cultures N100–N25). Under nitrate limitation the biomass composition of *S. obtusiusculus* A189 changed significantly. The protein content decreased from 39.5% (control) to approx. 11% (N25 to N0, Fig. 1a). The

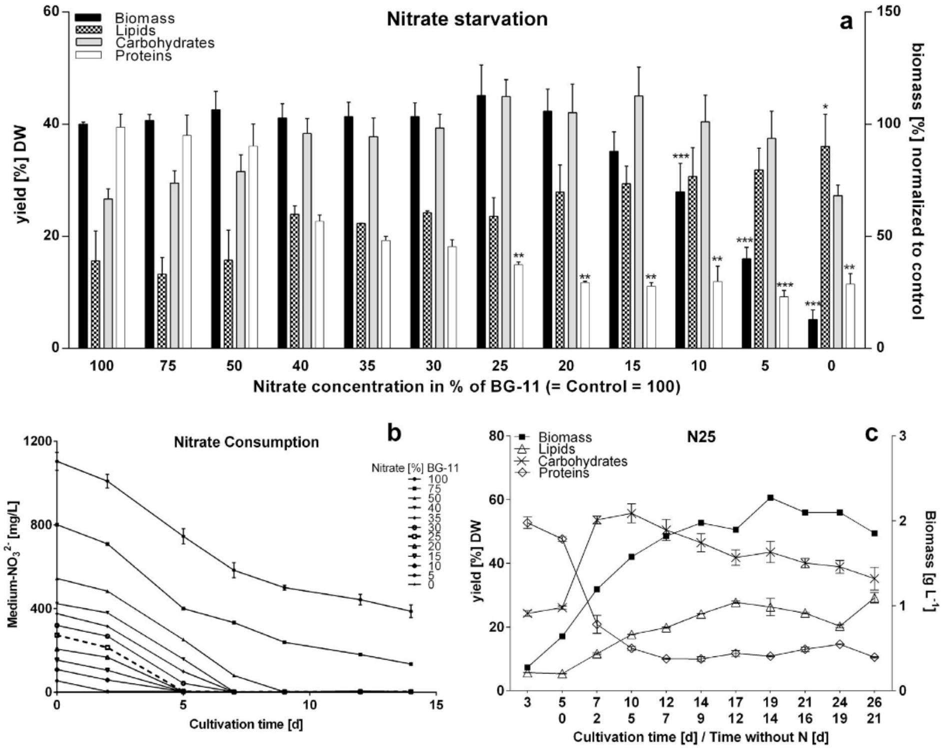

Fig. 1. Nitrate starvation experiments with *S. obtusiusculus* A189. (a) Relative biomass production and composition of *S. obtusiusculus* A189 depending on starting N concentration, mean + SEM, n = 3, Statistical tests: 2way ANOVA Dunnett's multiple comparison test; GraphPad Prism 6, California, US; * = $p < 0.05$, ** = $p < 0.005$, *** = $p < 0.001$ (compared to control = N100). (b) Nitrate concentration in medium during cultivation under different starting concentrations, mean ± SEM, n = 3. (c) Biomass production and composition of *S. obtusiusculus* A189 as a function of cultivation time with starting N concentration of 25% of control (BG-11), mean ± SEM, n = 1 (Biomass day 12–26), 2 (Biomass days 7,10), 3 (Biomass day 5, proteins, carbohydrates, lipids) or 4 (Biomass day 3).

carbohydrate content reached maximum values of around 45% from N25 to N15 and decreased again to control level (27%, N100 and N0, Fig. 1a). The lipid yield was maximal (36%) when cultivating the algae without any N; the lipid content under reference conditions was 16% (Fig. 1a). The biomass productivity (Fig. 1a) did not change significantly at N levels above 10 % of the reference concentration. At N25, the biomass yield reached a maximum value (113% compared to N100). At this point, the absolute lipid and carbohydrate yield was maximal so this N concentration was selected for further experiments.

To find the optimal harvesting point, A189 cultures with N25 were analyzed for their biochemical composition at different cultivation times. To determine how long N limitation was necessary for maximum biomass yield and the highest lipid and carbohydrate content, the nitrate concentration in the medium and the biomass composition were measured. Nitrate measurement in the medium showed that N was completely exhausted at day 5, confirming the data shown in Fig. 1b (dotted line). As Fig. 1c shows, the highest biomass concentration was reached after 19 days of cultivation (2.2 g L^{-1}), however after 12–14 cultivation days no significant increase was observed (2.0 g L^{-1}). The protein content decreased continuously in N-limited medium and reached its minimum (approx. 11%) after 12 days of cultivation. The carbohydrate yield showed a maximum of 56% at day 10 (5 days after N exhaustion) and decreased beyond again. The lipid content increased until cultivation day 17–19, then decreased again and reached its maximum value (29%) at cultivation day 26. According to this data, the optimal harvesting time was between cultivation days 12–14. Summarizing these results (Fig. 1) the optimal $NaNO_3$ medium concentration is 375 mg L^{-1} and harvesting should be done at cultivation day 14 where the culture was 9 days N-limited.

3.1.2. Phosphate and iron starvation

The phosphate starvation experiment (Fig. 2a) showed that any phosphate limitation in the medium leads to a significant decrease in biomass production. The biochemical composition is only marginally influenced, only at 10 and 0% P, lipid content increased significantly to 32% and at 50, 10, and 0% P carbohydrate yield decreased to around 27%. Protein yield was not significantly influenced by P decrease. Higher phosphate concentrations in the media (up to 62 mg L^{-1} K_2HPO_4) had no effect on biomass yield and composition (data not shown), so that the content in BG-11 medium (31 mg L^{-1} K_2HPO_4) was optimal.

Under iron starvation (Fig. 2b), the algal growth remained nearly constant from the starting concentration down to 10% of the reference value. At this concentration the carbohydrate yield was enhanced significantly from 34% (control) to 49% (Fe10), the protein content decreased (40% versus 30%) and the biomass productivity was nearly at control level, so that this concentration (0.6 mg L^{-1} ferric ammonium citrate) was considered as optimum and further used.

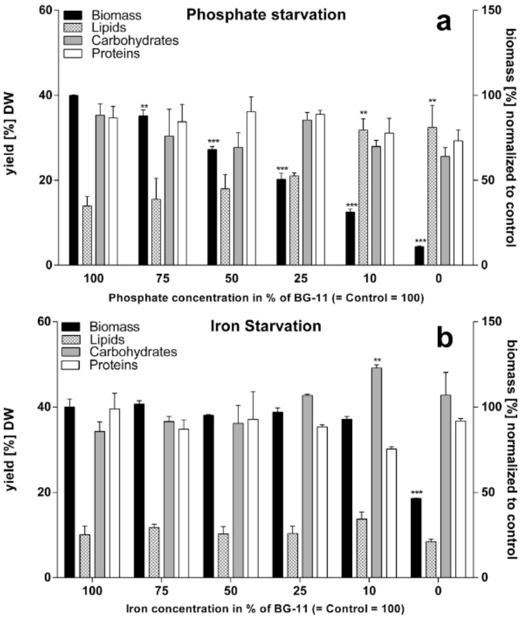

Fig. 2. Biomass production and biochemical composition of *S. obtusiusculus* A189 under P (a) and Fe (b) starvation. Mean + range, n = 2. Statistical tests: 2way ANOVA Dunnett's multiple comparison test; GraphPad Prism 6, California, US; $* = p < 0.05$, $** = p < 0.005$, $*** = p < 0.001$ compared to control (P100 or Fe 100).

3.2. Cultivation in ABV-Medium

3.2.1. Biomass production and biochemical composition

Based on the aforementioned optimization experiments the ABV1 medium was prepared with the optimal nitrate, phosphate and ferric ammonium citrate concentrations and supplemented with 0.5% (m/m) artificial sea salt in deionized water (Table 1). Fig. 3a shows that similar biomass productivities of *S. obtusiusculus* A189 were obtained in the ABV1 medium and in the standard BG-11 medium, though with significantly different biomass composition. Lipid content increased from 6.0% to 19.9% DW, and the carbohydrate yield from 45.3% to 50.3% DW. On the other hand, the protein content was reduced by half. It could be shown that the low-cost ABV1 medium leads in a one-step cultivation process to more valuable products (lipids and carbohydrates, 1.33 g L^{-1}, Fig. 3b) than the high-cost BG-11 medium (1.04 g L^{-1}).

Cultivation of A189 in the ABV2 medium, where the artificial sea salt was replaced by natural Baltic Sea water, resulted in reduced biomass yield but the lipid content was nearly the same as in BG-11 medium. Due to the reduced biomass productivity in ABV2 probably the nitrate was exhausted later, so that accumulation of lipids was lower as in the N-limited culture grown with ABV1. The carbohydrate yield significantly increased from 45.3 % DW to 51.7% (ABV2 compared to BG-11) and the protein content significantly decreased from 32.4 % to 25.3%. It seems that some components of the Baltic Sea water might inhibit algal growth. The total yield of valuable products was clearly decreased from 1.02 g L^{-1} to 0.58 g L^{-1} (BG-11 vs. ABV2). For optimal biomass composition, the starting N concentration in Baltic Sea water medium ABV2 should be reduced to induce nutrient limitation earlier, or the cultivation time should be prolonged.

The biomass yield and composition of *S. obtusiusculus* A189, cultivated in Peene River medium (freshwater) ABV3 was similar to ABV1 medium. Compared to BG-11, the biomass was slightly but not significantly reduced, whereas lipids and carbohydrates increased (6.0% to 15.0% and 45.3% to 55.5%, respectively) and proteins decreased from 32.4% to 19.7%. The total amount of valuable products was enhanced from 1.04 to 1.19 g L^{-1}.

These results clearly demonstrate that *S. obtusiusculus* A189 can be cultivated successfully in a low-cost, natural water-based medium with high yield of carbohydrates and lipids. For algal growth required micronutrients present in BG-11 can be replaced by fresh- and brackish water, respectively and after addition of optimized amounts of Nitrogen, Phosphorus and Iron the algae grew as good as in artificial BG-11 medium but with optimized biochemical composition.

The long-time cultivation of *S. obtusiusculus* A189 in the ABV1-medium showed that the biomass yield and growth rate did not decrease after ten times of harvesting and refilling a remaining stock of about 5% of the reactor volume with fresh medium in the bioreactor. This phenomenon suggested that there was no exhaustion of any other nutrients in the culture, an important issue

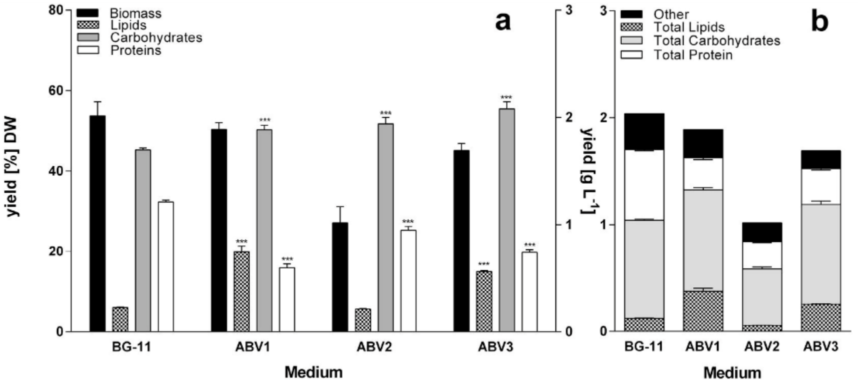

Fig. 3. *S. obtusiusculus* A189, grown in BG-11 medium in comparison to the new developed ABV media. (a) Total Biomass and relative amounts of lipids, carbohydrates and proteins (% DW); (b) Total yield of lipids, carbohydrates and proteins (g L^{-1}), "other": biomass – (lipids + carbohydrates + proteins). Mean + or - SEM, n = 3, except A189 ABV1 Biomass n = 9. Statistical tests: 2way ANOVA Dunnett's multiple comparison test; GraphPad Prism 6, California, US; $* = p < 0.05$, $** = p < 0.005$, $*** = p < 0.001$ compared to control (=BG-11).

for large-scale cultivation and improving the effectiveness of the cultivation process.

3.2.2. Carbohydrate composition

The determination of the total carbohydrate yield of *S. obtusiusculus* A189 (Fig. 3a) using thymol-sulfuric acid method revealed increase for biomass grown in ABV1, ABV2 and ABV3 in comparison to BG-11. Further investigations with LC-MS (Fig. 4) showed that the main occurring monosaccharides were glucose, galactose and mannose, but with glucose being the main component in all investigated biomasses samples. The data shows that the ratio of the monosaccharides stayed nearly unaffected by the total carbohydrate yield: in ABV1, 2, and 3 medium biomass the total yield was significantly higher than in BG-11 medium biomass, but glucose was with more than 80% the main monosaccharide, mannose yield was about 10% and galactose yield was less than 5%. These results are similar to the study of Ho et al. (2013a), they reported that 80% of the total sugars in carbohydrate-rich *Scenedesmus obliquus* was glucose.

3.2.3. Fatty acid composition

The total quantities of fatty acids (Fig. 5) in the n-hexane extracts were similar when the algae were grown in BG-11 (0.44 mg mg^{-1}) and ABV2 (0.45 mg mg^{-1}) but increased in ABV1 (0.54 mg mg^{-1}) and ABV3 (0.49 mg mg^{-1}). The fatty acid composition was different in the three ABV media compared to the BG-11 medium. Palmitic acid (C16:0) was significantly decreased from 0.17 to 0.14 mg mg^{-1} in ABV1, 2, and 3. The amount of linolenic acid (C18:3) increased from 0.047 to 0.055, 0.068, and 0.058 mg mg^{-1} in ABV1, 2, and 3, respectively. An increase in linoleic acid (C18:2) was only observed in ABV1 and ABV3, from 0.058 to 0.066 and 0.083 mg mg^{-1}, respectively. Oleic acid (C18:1) was the main fatty acid in ABV1, 2 and 3 revealing values of 0.23, 0.17, and 0.15 mg mg^{-1}, respectively, significantly higher compared to BG-11 (0.14 mg mg^{-1}). The concentration of stearic acid (C18:0) was higher in ABV1 (0.056 mg mg^{-1}) and 3 (0.052 mg mg^{-1}), but lower in ABV2 0.014 mg mg^{-1} compared to BG-11 (0.025 mg mg^{-1}). In general, the n-hexane extracts of ABV1 and ABV3 biomass were similar to each other regarding the fatty acid profile, except for oleic acid, which was lower in ABV3. The total amounts of polyunsaturated fatty acids (PUFAs, C18:2 and C18:3) in the n-hexane extracts of algae cultured in BG-11, ABV1, 2, and 3 were 24, 22, 29, and 29% of the content of all fatty acids, respectively. Regarding this, the algae oil extracted from ABV1 biomass with lower yield of PUFAs could be favorable for technical applications where high oxidative stability is required. Otherwise algal biomass with higher contents of PUFAs could be of interest for utilization in health food applications.

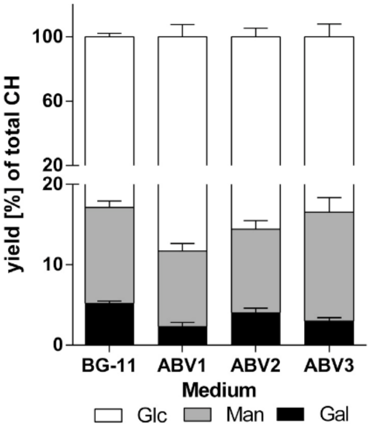

Fig. 4. Carbohydrate composition of *S. obtusiusculus* A189, cultivated in BG-11 medium compared to the new ABV media, yield in % of total carbohydrates. CH = carbohydrates, Glc = glucose, Gal = galactose, Man = mannose. Mean + SD, n = 3.

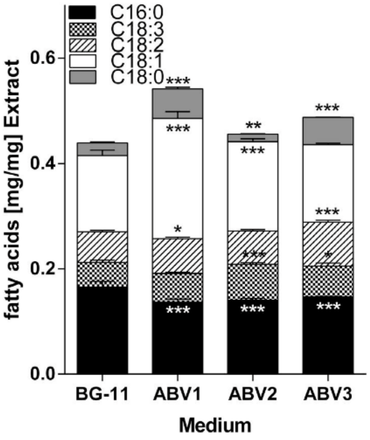

Fig. 5. Characterization of the lipid fraction. Fatty acid composition of the n-hexane extract of *S. obtusiusculus* A189, cultivated in different culture media. Mean + range, n = 2. Statistical tests: 2way ANOVA Dunnett's multiple comparison test; GraphPad Prism 6, California, US; ** = $p < 0.005$, *** = $p < 0.001$ compared to control (=BG-11).

3.2.4. Unsaponifiable matter

The unsaponifiable matter describes lipophilic, non-fatty acid compounds of oils such as sterols, terpens, pigments and others and is especially relevant in the analysis of plant oils. There are several methods described in the literature (Schröder and Vetter, 2012) with nearly the same principle. After saponification of the oil with lye, other non-polar compounds are extracted with lipophilic solvents, which are separated by evaporation and the residue is estimated gravimetrically. The unsaponifiable matter of the extracted algae oil decreased significantly (2way ANOVA, n = 2) in the biomass cultured with ABV1 medium (11.4%) and the ABV3 medium (10.3%) compared to the BG-11 medium (19.5%). The unsaponifiable matter of the lipid fraction extracted from the biomass grown in ABV2 medium decreased only marginally (16.3%). These results confirm the increased yield of fatty acids found in the n-hexane extract of *S. obtusiusculus* A189 grown in ABV1 and ABV3 medium. A reduced yield of pigments and their degradation products could be an explanation for the decreased unsaponifiable matter. Oils with a high unsaponifiable matter are unfavorable for most technical applications. A high content of sterols, terpens and pigments leads to oils with high pourpoints, low oxidative stability and high viscosity.

4. Conclusions

A one-stage cultivation process with a new cultivation medium was developed and evaluated with *Scenedesmus obtusiusculus* A189 for producing lipid- and carbohydrate-rich algal biomass. For A189, this process revealed advantages compared to cultivation in standard BG-11 medium. While biomass productivity was unchanged, the yield of valuable products (carbohydrates, lipids) was improved by 33% and 14%, when 0.5% (m/m) artificial sea water and fresh water (Peene River water), respectively, was used as basis. Baltic Sea water seems to be a less suitable basis, because of reduced growth, however species differences in growth cannot be fully ruled out.

Acknowledgements

Thanks to the Federal Ministry of Education and Research for funding the project. Special thanks to Mrs. M. Schmidt for the excellent technical support. Mr. S. Rieck is thanked for adapting the unsaponifiable matter method to algae oil.

References

Adamsson, M., 2000. Potential use of human urine by greenhouse culturing of microalgae (*Scenedesmus acuminatus*), zooplankton (*Daphnia magna*) and tomatoes (Lycopersicon). Ecol. Eng. 16, 243–254.

Aravantinou, A.F., Theodorakopoulos, M.A., Manariotis, I.D., 2013. Selection of microalgae for wastewater treatment and potential lipids production. Bioresour. Technol. 147, 130–134.

Borowitzka, M.A., 2013. High-value products from microalgae—their development and commercialisation. J. Appl. Phycol. 25, 743–756.

Cabello, J., Toledo-Cervantes, A., Sánchez, L., Revah, S., Morales, M., 2015. Effect of the temperature, pH and irradiance on the photosynthetic activity by *Scenedesmus obtusiusculus* under nitrogen replete and deplete conditions. Bioresour. Technol. 181, 128–135.

Dahmen, I., Chtourou, H., Jebali, A., Daassi, D., Karray, F., Hassairi, I., Sayadi, S., Abdelkafi, S., Dhouib, A., 2014. Optimisation of the critical medium components for better growth of Picochlorum sp. and the role of stressful environments for higher lipid production. J. Sci. Food. Agric. 94, 1628–1638.

Fabregas, J., Abalde, J., Herrero, C., Cabezas, B.V., 1985. Growth, chlorophyll a and protein of the marine microalga *Isochrysis galbana* in batch cultures with different salinities and high nutrient concentrations. Aquaculture 50, 1–11.

Feng, Y., Li, C., Zhang, D., 2011. Lipid production of *Chlorella vulgaris* cultured in artificial wastewater medium. Bioresour. Technol. 102, 101–105.

Francisco, É.C., Neves, D.B., Jacob-Lopes, E., Franco, T.T., 2010. Microalgae as feedstock for biodiesel production: carbon dioxide sequestration, lipid production and biofuel quality. J. Chem. Technol. Biotechnol. 85, 395–403.

Gao, B., Yang, J., Lei, X., Xia, S., Li, A., Zhang, C., 2015. Characterization of cell structural change, growth, lipid accumulation, and pigment profile of a novel oleaginous microalga, *Vischeria stellata* (Eustigmatophyceae), cultured with different initial nitrate supplies. J. Appl. Phycol.

Griffiths, M.J., van Hille, R.P.H., Susan, T.L., 2012. Lipid productivity, settling potential and fatty acid profile of 11 microalgal species grown under nitrogen replete and limited conditions. J. Appl. Phycol. 24, 989–1001.

Griffiths, M.J., van Hille, R.P.H., Susan, T.L., 2014. The effect of nitrogen limitation on lipid productivity and cell composition in *Chlorella vulgaris*. Appl. Microbiol. Biotechnol. 98, 2345–2356.

Ho, S.-H., Chen, W.-M., Chang, J.-S., 2010. Scenedesmus obliquus CNW-N as a potential candidate for CO_2 mitigation and biodiesel production. Bioresour. Technol. 101, 8725–8730.

Ho, S.-H., Chen, C.-Y., Chang, J.-S., 2012. Effect of light intensity and nitrogen starvation on CO_2 fixation and lipid/carbohydrate production of an indigenous microalga *Scenedesmus obliquus* CNW-N. Bioresour. Technol. 113, 244–252.

Ho, S.-H., Kondo, A., Hasunuma, T., Chang, J.-S., 2013a. Engineering strategies for improving the CO_2 fixation and carbohydrate productivity of Scenedesmus obliquus CNW-N used for bioethanol fermentation. Bioresour. Technol. 143, 163–171.

Ho, S.-H., Li, P.-J., Liu, C.-C., Chang, J.-S., 2013b. Bioprocess development on microalgae-based CO_2 fixation and bioethanol production using Scenedesmus obliquus CNW-N. Bioresour. Technol. 145, 142–149.

Kim, M.K., Park, J.W., Park, C.S., Kim, S.J., Jeune, K.H., Chang, M.U., Acreman, J., 2007. Enhanced production of Scenedesmus spp. (green microalgae) using a new medium containing fermented swine wastewater. Bioresour. Technol. 98, 2220–2228.

Kuhl, A., Lorenzen, H., 1964. Handling and culturing of chlorella. In: Prescott, D.M. (Ed.), Methods in Cell Physiology, vol. 1. Academic Press, New York and London, pp. 159–187 (Chapter 10).

Lepage, G., Roy, C.C., 1986. Direct transesterification of all classes of lipids in a one-step reaction. J. Lipid Res. 27, 114–120.

Liebeke, M., Pöther, D.-C., van Duy, N., Albrecht, D., Becher, D., Hochgräfe, F., Lalk, M., Hecker, M., Antelmann, H., 2008. Depletion of thiol-containing proteins in response to quinines in *Bacillus subtilis*. Mol. Microbiol. 69, 1513–1529.

Markou, G., Angelidaki, I., Georgakakis, D., 2012. Microalgal carbohydrates: an overview of the factors influencing carbohydrates production, and of main bioconversion technologies for production of biofuels. Appl. Microbiol. Biotechnol. 96, 631–645.

Nascimento, I.A., Marques, S.S.I., Cabanelas, I.T.D., Pereira, S.A., Druzian, J.I., de Souza, C.O., Vich, D.V., de Carvalho, G.C., Nascimento, M.A., 2013. Screening microalgae strains for biodiesel production: lipid productivity and estimation of fuel quality based on fatty acids profiles as selective criteria. Bioenerg. Res. 6, 1–13.

Ortiz-Tena, J.G., Rühmann, B., Schieder, D., Sieber, V., 2016. Revealing the diversity of algal monosaccharides: fast carbohydrate fingerprinting of microalgae using crude biomass and showcasing sugar distribution in *Chlorella vulgaris* by biomass fractionation. Algal Res. 17, 227–235.

Ostermann, A.I., Müller, M., Willenberg, I., Schebb, N.H., 2014. Determining the fatty acid composition in plasma and tissues as fatty acid methyl esters using gas chromatography – a comparison of different derivatization and extraction procedures. Prostag. Leukotr. Ess. 91, 235–241.

Pohl, P., Ohlhase, M.K., Rautwurst, S.K., Baasch, K.-H., 1987. An inexpensive inorganic medium for the mass cultivation of freshwater microalgae. Phytochemistry 26, 1657–1659.

Rodolfi, L., Chini, G.Z., Bassi, N., Padovani, G., Biondi, N., Bonini, G., Tredici, M.R., 2009. Microalgae for oil: strain selection, induction of lipid synthesis and outdoor mass cultivation in a low-cost photobioreactor. Biotechnol. Bioeng. 102, 100–112.

Schröder, M., Vetter, W., 2012. Investigation of unsaponifiable matter of plant oils and isolation of eight phytosterols by means of high-speed counter-current chromatography. J. Chromatogr. A 1237, 96–105.

Schulze, C., Wetzel, M., Reinhardt, J., Schmidt, M., Felten, L., Mundt, S., 2016. Screening of microalgae for primary metabolites including β-glucans and the influence of nitrate starvation and irradiance on β-glucan production. J. Appl. Phycol. http://dx.doi.org/10.1007/s10811-016-0812-9 (in press).

Song, M., Pei, H., Hu, W., Ma, G., 2013. Evaluation of the potential of 10 microalgal strains for biodiesel production. Bioresour. Technol. 141, 245–251.

Toledo-Cervantes, A., Morales, M., Novelo, E., Revah, S., 2013. Carbon dioxide fixation and lipid storage by *Scenedesmus obtusiusculus*. Bioresour. Technol. 130, 652–658.

Wang, L., Li, Y., Sommerfeld, M., Hu, Q., 2013. A flexible culture process for production of the green microalga *Scenedesmus dimorphus* rich in protein, carbohydrate or lipid. Bioresour Technol. 129, 289–295.

Waterbury, J.B., Stanier, R.Y., 1981. Isolation and growth of cyanobacteria from marine and hypersaline environments. In: Starr, M.P. (Ed.), The Procaryotes, vol. 1. SpringerVerlag, Berlin, pp. 221–223 (Chapt. 9).

Xia, L., Ge, H., Zhou, X., Zhang, D., Hu, C., 2013. Photoautotrophic outdoor two-stage cultivation for oleaginous microalgae *Scenedesmus obtusus* XJ-15. Bioresour Technol. 144, 261–267.

Xu, Y., Boeing, W.J., 2014. Modeling maximum lipid productivity of microalgae: review and next step. Renew. Sustain. Energy Rev. 32, 29–39.

A4.3. Enzymatic saccharification of carbohydrate-rich algal biomass

To obtain reducing sugars from carbohydrate-rich biomass from *S. obtusiusculus* (as produced in section A4.2) for their subsequent utilization (e.g., for fermentation), an enzymatic hydrolysis using commercial enzyme mixtures was evaluated. The softer conditions employed therein can help avoid sugar degradation compared to those used during chemical (e.g., TFA) hydrolysis. The general process was performed using lipid-extracted biomass as described in Figure 6. After the enzymatic treatment, the liquid and the solid remaining phase were separated by centrifugation. In this way, distinction was made between **solubilized** sugars and **insoluble** residual carbohydrates. Both phases were next analyzed towards monosaccharides (as direct analysis), and those present as short-chained oligosaccharides or long-chained polysaccharides *via* monosaccharide analysis after chemical TFA-hydrolysis.

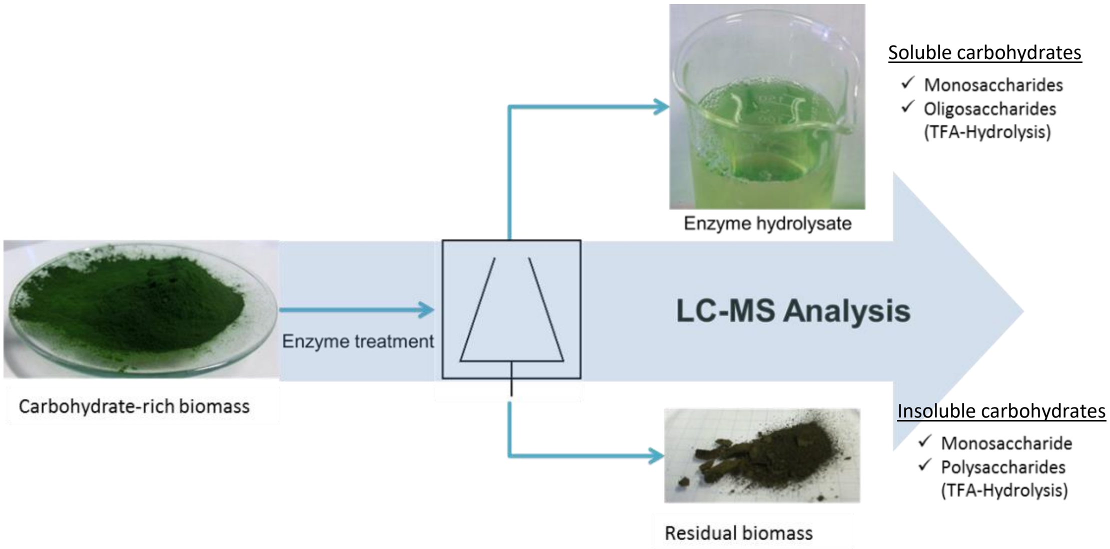
Soluble carbohydrates
✓ Monosaccharides
✓ Oligosaccharides (TFA-Hydrolysis)
Enzyme hydrolysate
LC-MS Analysis
Enzyme treatment
Carbohydrate-rich biomass
Insoluble carbohydrates
✓ Monosaccharide
✓ Polysaccharides (TFA-Hydrolysis)
Residual biomass

Figure 6 Enzymatic treatment of carbohydrate-rich biomass and its carbohydrate analysis by LC-MS

Selection of the commercial enzymes: The enzyme mixtures commercialized under the names Rohapect® UF (with declared pectinase and arabanase activity), Rohament® CL (declared cellulase activity), and Rohapect® B1L (declared pectinase, cellulase, and mannanase activity) from the company AB Enzymes® were selected for the enzymatic treatments (Table 8). These technical mixtures are readily available and find typical application in the processing of juices and pulps (to improve filterability) and in the fermentative bioethanol production from cellulosic biomass (ABEnzymes, 2011a, 2011b, 2013). The justification for their selection can be explained by the similar monosaccharide types that can be found in the polysaccharides from juice pulp and peels fruits, (e.g., gluco- and galactomannan, arabinoglucan, and pectin) in comparison to those found in the carbohydrate-rich biomass from *S. obtusiusculus* (see section A4.2).

To test the activity of the selected hemicellulases Rohapect® UF and B1L towards standard polysaccharides in advance, commercially available pectin, xylan, and galactomannan were tested as substrates (see section A3.9 – *saccharification of standard polymers*). The concentrations of monosaccharides found in each hydrolysate are listed in Table 12.

Table 12 Monosaccharides found in enzyme hydrolysates of standard polymers. Initial concentration of pectin and xylan: 50 g L^{-1}. Galactomannan: 5 g L^{-1}. For the recovery calculations, the addition of water due to hydrolysis was considered. [a] As a sucrose content of 36.7% (w/w) was measured in pectin, 34.9 g L^{-1} were accounted for a 100% recovery (including mass increase by water addition due to hydrolysis).

Standard	Monosaccharide	Rohapect® UF (g L^{-1})	Rohapect® B1L (g L^{-1})
Pectin (standardized with sucrose)	GalUA	31.4	14.4
	Gal	1.8	0.0
	Rha	0.7	0.0
	Total	33.9	14.4
	% Recovery [a]	**97%**	**41%**
	Ratio	GalUA:Gal:Rha 46.5:2.5:1	GalUA:Gal:Rha 1:0:0
Xylan	Xyl	9.9	18.1
	Glc	0.9	0.8
	Total	10.8	18.9
	% Recovery	**19%**	**33%**
	Ratio	Xyl:Glc 11:1	Xyl:Glc 24:1
Galactomannan	Gal	0.5	0.1
	Man	1.0	0.6
	Total	1.5	0.7
	% Recovery	**27%**	**13%**
	Ratio	Gal:Man 1:2	Gal:Man 1:6

The samples containing pectin and xylan were visibly less viscous after the enzyme treatment. Pectinase activity could be confirmed in both enzyme mixtures, though much stronger in Rohapect® UF (97% recovery) than B1L (41%). In addition to GalUA, lower amounts of galactose and rhamnose were also found in UF hydrolysate. These two monosaccharides have been reported within the pectin molecular structure (Pettolino et al., 2012). Furthermore, a modest xylanase activity was found for both enzymes, which was not declared by the manufacturer. 33% xylan recovery was found after treatment with Rohapect® B1L, while 19% for Rohapect® UF. As xylan is a natural product, also trace concentrations of glucose (~1% theoretical yield) were detected in both hydrolysates.

Considering its composition, gluco- and galacto-mannanase activity is an interesting parameter for the later enzymatic treatment of *S: obtusiusculus,* as presented below (Figure 7). According to the product datasheet, the employed galactomannan displays a Gal:Man ratio of 1:3.2. The enzyme manufacturer declared a mannanase activity for Rohapect® B1L only. However, this enzyme displayed a rather poor recovery of 13% towards galactomannan, with a Gal:Man ratio of 1:6. On the other hand, Rohapect® UF was able to saccharify galactomannan to a 1:2 Gal:Man mixture with an overall recovery of 27%. Thus, this enzyme showed a better cleaving of the galactose side chains than Rohapect® B1L. As both enzyme mixtures seem to act differently on galactomannan, a combination of these two enzymes may produce additive effects with *S. obtusiusculus* biomass.

Selection of lipid-extracted, carbohydrate-rich biomass from *S. obtusiusculus*: The lipid fraction of *S. obtusiusculus* carbohydrate-rich biomass (cultured similarly as described in section A4.2), was extracted using supercritical CO_2 by the industrial partner under different pressure and temperature process conditions. According to them, the lipid content of the original biomass was 10.1% w/w (101 mg g_B^{-1}) with a moisture content of 4.7% w/w. Consequently, the lipid-extracted biomasses designed as ABV6-ABV13 were available for the enzymatic hydrolysis (see Table 6). To identify the most suitable defatted biomass for saccharification, their monomeric sugar content was first analyzed using the PMP UHPLC-MS adapted method (see section A4.1) and the standard TFA hydrolysis. In all these lipid-extracted biomasses, the monomeric sugars glucose, mannose, and galactose were mainly found, similarly to biomasses ABV1-ABV3. Contrarily to these analyzed biomasses without lipid extraction, rhamnose and trace amounts of fucose and xylose were also found in the defatted material (Figure 7). Given the highest carbohydrate content found, the biomasses “ABV 10” and “ABV 11” were selected for further enzymatic treatment.

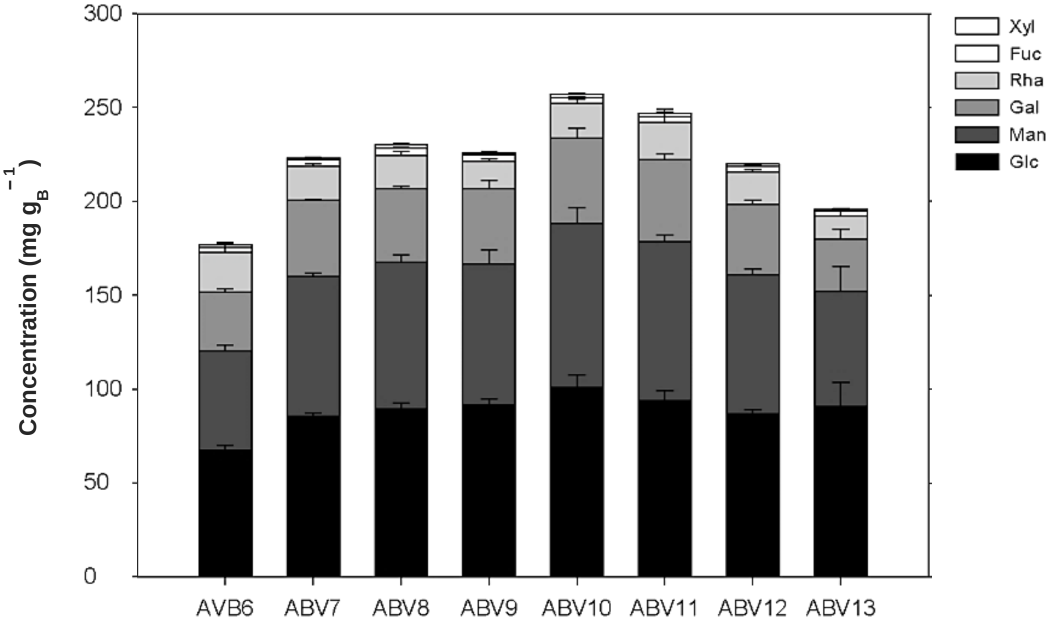

Figure 7 Carbohydrate composition of differently lipid-extracted biomass from *S. obtusiusculus* after TFA standard hydrolysis (see section A3.8). Glc: glucose; Man: mannose; Gal: galactose; Rha: rhamnose; Fuc: fucose; Xyl: xylose. n=3

To achieve a closure analysis, the protein content of the samples was examined using elementary analysis (see section A3.8). The results revealed that the biomasses ABV6-13 were composed between 37.2 – 39.2% w/w by proteins (Figure A5). Furthermore, the lipid content in the original biomass was reported by the industrial partner as 10% w/w, with extraction yields of 6.5 – 8.3% w/w. Consequently, the lipid content of the defatted biomasses ABV6-13 can be accounted to be in the range 1.7 – 3.5% w/w, with a low moisture content of around 5% w/w (biomass was dried after extraction). Accordingly, a theoretical calculated carbohydrate content of around 50% w/w (500 mg g_B^{-1}) can be expected in the defatted biomass. However, the results obtained by standard TFA hydrolysis (Figure 7) clearly revealed lower sugar concentrations than calculated. Softer hydrolysis conditions, such as enzymatic treatments, can be applied to avoid degradation and obtain higher sugar yields, as presented below.

Enzymatic hydrolysis of carbohydrates from ABV10-11 biomass: The selected enzymes Rohapect® UF, Rohapect® B1L and Rohament® CL were then tested singly on *S. obtusiusculus* carbohydrate-rich and lipid extracted biomass using three different concentrations (1, 2 and 4% $w_{protein}/w_{biomass}$). Because of their activity over the biomass polysaccharides, mono- and oligosaccharides were released into the liquid phase. After that, the solubilized monomers in the liquid phase were derivatized with PMP and quantified using the method presented in section A4.1. Further, the amount of sugars released as oligomers was determined by treating the liquid phase with 2 M TFA at 121°C, subsequent derivatization, and monomer analysis (Figure 6). To avoid carbohydrate degradation in the liquid phase and ensure an accurate sugar quantification, experiments were performed using different TFA hydrolysis times to determine at which time point a maximum sugar yield can be obtained (Figure A6). In this phase, mainly glucose, galactose and mannose were found, together with trace amounts of rhamnose (Figure A7). This correlates well with the monosaccharide composition reported after TFA hydrolysis. Besides, the content of monosaccharides and polysaccharides in the residual solid biomass was evaluated as well. The results of this enzymatic hydrolysis are presented in Figure 8.

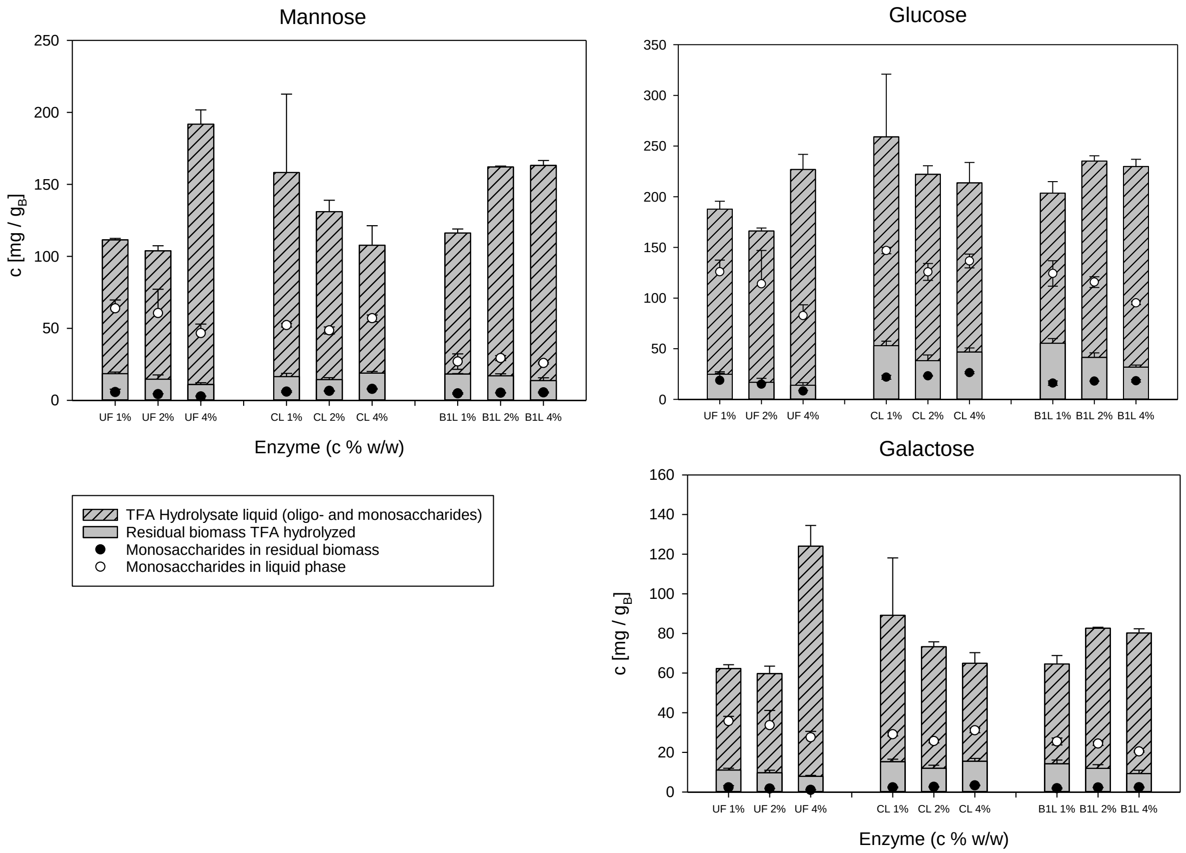

Figure 8 Carbohydrate composition of differently lipid-extracted biomass from *S. obtusiusculus* after TFA standard hydrolysis (see section A3.9). Glc: glucose; Man: mannose; Gal: galactose; Rha: rhamnose; Fuc: fucose; Xyl: xylose. n=3

In this Figure, the striped bars indicate the amount of sugar solubilized in the liquid phase including oligomers. The white dots represent the monosaccharides produced by the commercial enzymes and directly released in the liquid medium (saccharification). The results showed a very good *solubilization* of the microalgal carbohydrates by the employed enzymes. However, the *saccharification* of the soluble sugars remained incomplete, as the share of free monosaccharides in the liquid phase (○) was comparatively lower than the total carbohydrate content (stripped + gray bars). This was especially true for mannose and galactose. Noticeably, the amount of carbohydrates in the solid residual biomass (grey bars) differed with the type of enzyme. In general, a more effective carbohydrate *solubilization* could be achieved using Rohapect® UF than with Rohapect® B1L and Rohament® CL, especially for glucose.

By hydrolyzing both the enzymatically solubilized oligomers and the carbohydrates in the residual solid phase with TFA, a total carbohydrate quantification of the algal biomass can be achieved. In theory, this amount should be the same for each enzymatic treatment, independently of the enzyme used or its concentration. However, despite the good reproducibility within triplicates (CV < 10%, except Rohament® CL at 1% w/w), relatively large discrepancies were found among them. Rohapect® UF 1% and 2% w/w, for example, presented a rather lower total carbohydrate yield compared to the rest of the treatments, especially for mannose and glucose (Figure 8). The average total carbohydrate yield (sum found in the liquid and residual solid phases) accounted for all enzymatic treatments is reported in Table 13.

Table 13 Average total carbohydrate content of *S. obtusiusculus* defatted biomass after enzymatic and TFA hydrolysis. μ = mean value of all enzymatic treatments; SD: standard deviation; CV: coefficient of variation

	μ (mg g_B^{-1})	**SD (mg g_B^{-1})**	**CV (%)**
Man	139	31	22%
Glc	216	28	13%
Gal	78	20	26%
Total	432	72	17%

As explained above, the theoretical carbohydrate concentration of the biomass was calculated to be 500 mg g_B^{-1} based on lipid extraction yields and protein content. After enzymatic treatments 432 ± 72 mg g_B^{-1} average carbohydrate content was found (Table 13), so significant sugar underestimation by TFA standard hydrolysis cannot be excluded. In fact, the total carbohydrate content as well as the amount of each monosaccharide found in both biomasses ABV10 and ABV11 after enzymatic hydrolysis is higher than that obtained with standard TFA hydrolysis of the raw biomass (Figure 7). This discrepancy may be explained by the TFA hydrolysis conditions employed for solid biomass (either raw or residual), which were most probably sub-optimal for a maximized monosaccharide release. The relatively high protein content of the defatted biomass (37.2 – 39.2% w/w, Figure A5) may have promoted Maillard reactions, degrading monosaccharides during TFA hydrolysis. An especially high discrepancy was observed for glucose (100 mg g_B^{-1} in TFA hydrolysis, 216 mg g_B^{-1} enzymatic hydrolysis) and mannose (80 mg g_B^{-1} TFA and 139 mg g_B^{-1} enzymatic hydrolysis).

As shown in section A4.1 (DoE of TFA hydrolysis) for *C. vulgaris* algal biomass, 50% higher yield of neutral sugars can be obtained when softer hydrolysis conditions than the standard hydrolysis are employed (100°C, 1M TFA, 120 min, 0.5 g_B L^{-1}). Furthermore, it could be demonstrated that different TFA hydrolysis parameters (e.g., TFA and biomass concentration) play an important role for the release of different monosaccharides. A detailed discussion of this subject is presented in section A5.1. From an analytical perspective, an enzymatic biomass pre-treatment followed by TFA hydrolysis of the resulting liquid and solid fractions can help avoid underestimation of microalgal carbohydrates.

LC-MS oligosaccharide detection method: To identify additional enzymes needed for a complete saccharification of the biomass, the identity of the oligosaccharides solubilized in the liquid supernatant must be resolved. For this, a LC-MS analytical method for identifying short and middle-long chained saccharides was employed (see section A3.7). The method is based on the same derivatization principle as the HT-PMP method for monosaccharides with the main difference that the chromatographic separation is achieved with a HILIC-phase instead of a reverse phase column. After separation, each compound is analyzed by MS and MS^2. As relevant commercial standards for oligosaccharides were hardly available, the method was mainly used for a qualitative determination of short-chained carbohydrates. To verify its validity, commercially available pullulan (M_w 1,320) was employed as certified reference material. According to the supplier, this mixture consists of poly-maltotriose units (α-D-Glc-(1→4)-α-D-Glc-(1→4)-α-D-Glc) of varying length linked by α-(1→6) bonds. After chromatographic separation, the monosaccharides forming the oligosaccharides present in the sample can be elucidated by fragmenting the generated ions.

Figure 9A shows the EIC of pullulan after PMP derivatization in a concentration of around 1 g L^{-1}. The observed peaks relate to the different oligosaccharides present in this standard. Because of the interacting hydroxyl groups of the sugars with the solid phase of the LC column (1,2-dihydroxypropyl phase), the elution time increases with increasing hydrophilicity (and M_w) of the oligosaccharides. The separation resolution of the oligosaccharides in this standard of identical monomers decreases with increasing M_W, as observed by the peaks with *m/z* > 1159. These results confirm the ability of the method to separate and analyze mixtures of oligosaccharides within 12 min elution time. When the eluted peaks are fragmented in MS^2 mode, a clear pattern with identical mass intervals of 162 is observed. The lightest fragment is then a PMP derivatized hexose having *m/z* = 511 (Figure 9B-D). The mass differences reflect the glucose units (M_W = 180 – 18 for H_2O involved in the glycosidic linkage) forming the oligosaccharides of pullulan. In this way, the monosaccharide type (hexose, pentose, etc.) present, as well as its arrangement in the oligo chain can be roughly determined using this analysis. With the chromatographic configuration employed, the method allowed the detection of oligosaccharides with a chain length of up to 6 – 7 monomeric sugars.

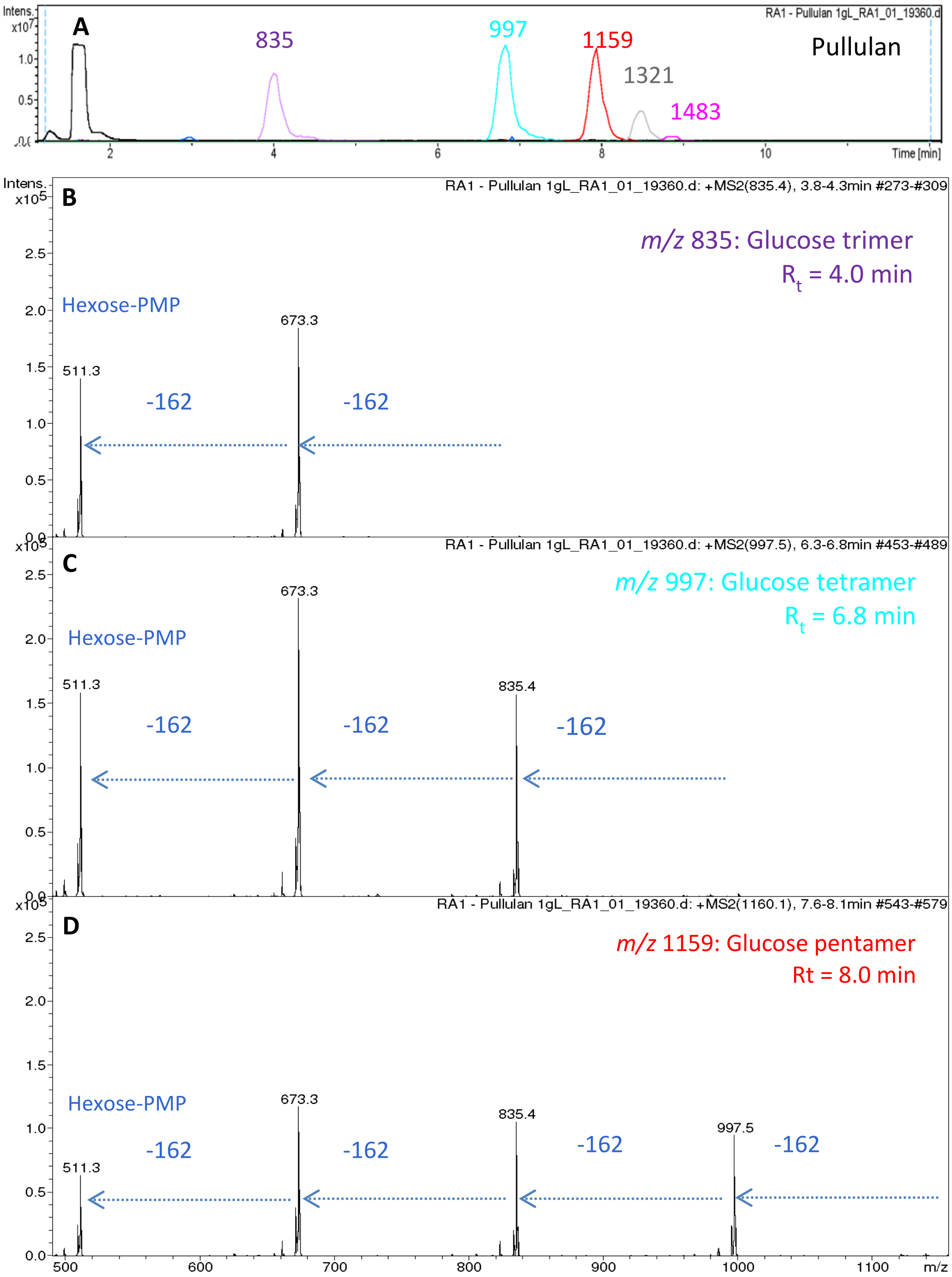

Figure 9 LC-MS analysis of pullulan 1300 as certified reference material. A. EIC of the relevant species; B. MS^2 Fragmentation analysis of *m/z* 835; C. Fragmentation analysis of *m/z* 997; D. Fragmentation analysis of *m/z* 1159

Identification of soluble oligosaccharides in enzymatic hydrolysates: As shown in Figure 8, the amount of solubilized carbohydrates in the enzymatic hydrolysates of *S. obtusiusculus* ABV10 and ABV 11 (i.e., monosaccharides detected after TFA treatment) resulted higher than that enzymatically saccharified (i.e., monosaccharides found in the same phase without the TFA hydrolysis). This suggests the presence of carbohydrates in oligomeric form in the supernatants that were not hydrolyzed to monosaccharides by the commercial mixtures employed. According to the results above, these oligomers are most probably composed of mannose, galactose, and rhamnose. Consequently, the liquid supernatants were examined with the previously presented LC-MS method for oligosaccharides. The qualitative results of the enzymatic hydrolysates are exemplary discussed for the sample treated with Rohapect® UF at 4% $w_{protein}/w_{biomass}$. The results for Rohapect® B1L and Rohament® CL are presented in the Appendix (Figure A8-9). To exclude auto-hydrolysis of the biomass or the presence of oligosaccharides in the commercial enzyme mixes, the same analysis was performed on a biomass and enzyme control, respectively.

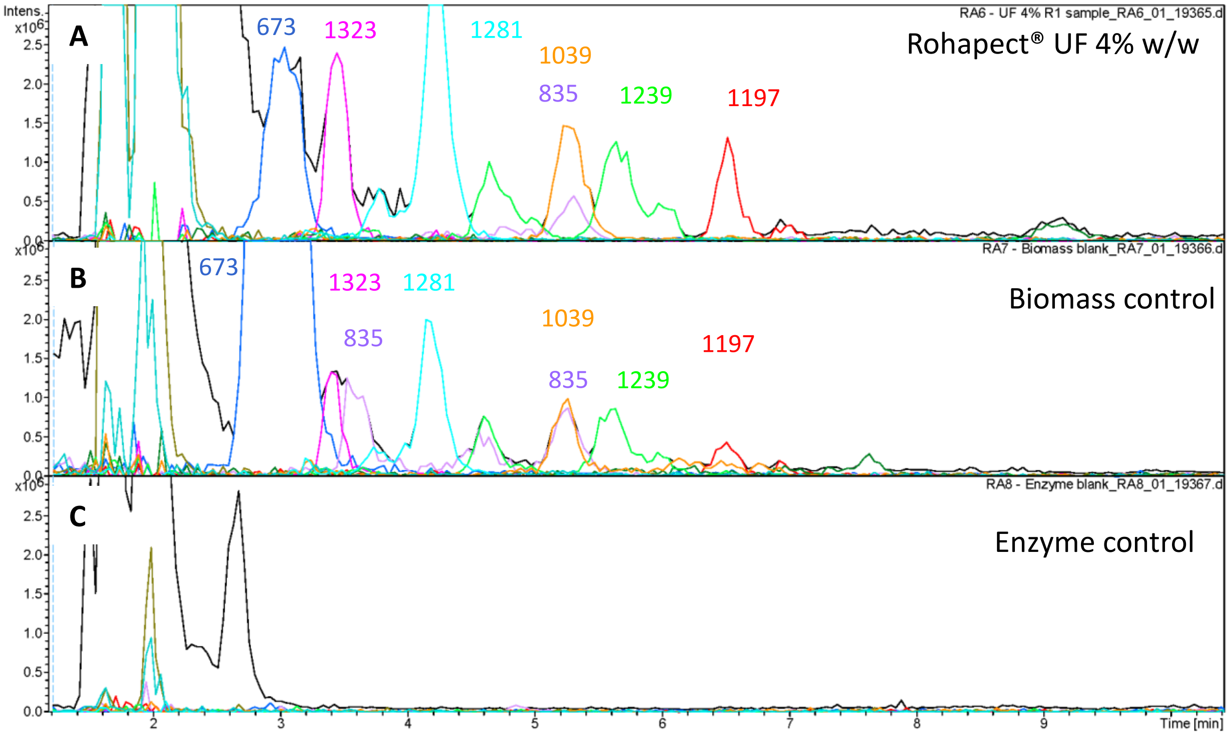

Figure 10 LC-MS analysis by EIC (color) of A. Enzyme hydrolysate (Rohapect® UF 4% w/w); B. Biomass control; C. Enzyme control. Hydrolyzed biomass *S. obtusiusculus* ABV10. In color are the represented specific masses, in black BPC (*m/z* 500 – 3,000)

As shown in Figure 10, the EIC of the treated sample revealed a complex mixture of oligosaccharides with at least 10 different peaks, with *m/z* ranging from 673 up to 1323. Most of the peaks found in the enzymatic hydrolysate were also observed in the biomass control to which no enzyme was added, but with a lower intensity. This may indicate a non-enzymatic hydrolysis of the biomass resulting most likely from factors such as mechanical forces, pH or thermal conditions. Noticeable, the very intense hexose disaccharide peak of *m/z* 673 at 3 min R_t present in the biomass control was found in the supernatant treated with hydrolase Rohapect® UF with a lower intensity. Besides, the hexose trisaccharide peak with *m/z* 835 and 3.6 min R_t of the biomass control was not found in the enzymatic hydrolysate. These results indicate enzyme activity on the corresponding sugar dimer and trimer. The control containing only the enzyme mixture did not show peaks resulting from oligosaccharides.

In contrast to the pullulan reference material, the MS^2 fragmentation pattern of the averaged peak spectra found in the enzyme hydrolysate displays irregular mass intervals (Figure 11). The peak with *m/z* 1039 and R_t 5.2 min, for example, presents a PMP derivatized hexose with *m/z* 511 followed by a fragment after a mass increment of 204, and then by two hexose increments of 162 (Figure 11A). A similar pattern is observed in the peak with *m/z* 1197, with the difference in the two monosaccharides of the non-reducing end presenting mass increments of 146 and 174 (Figure 11B).

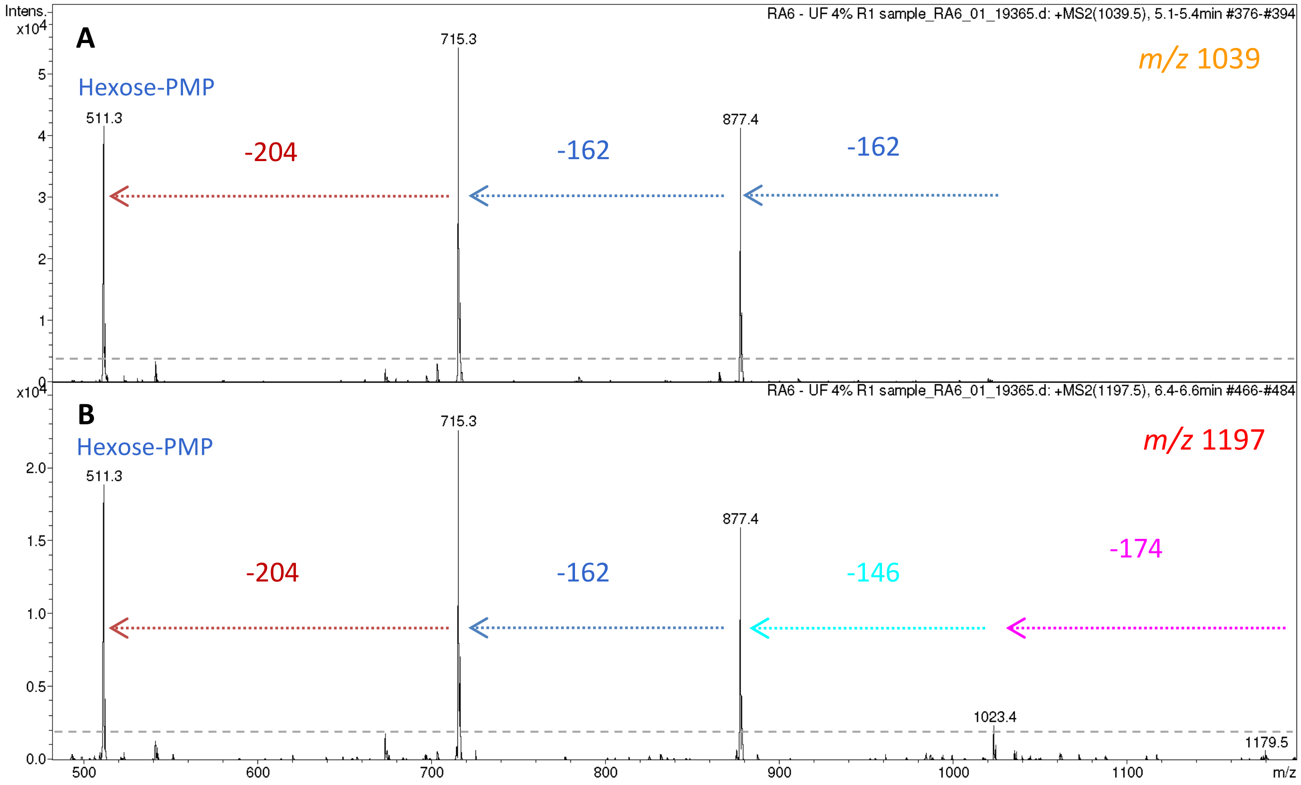

Figure 11 Averaged MS fragmentation spectra of peaks found in the enzyme hydrolysate (Rohapect® UF 4% w/w). A. *m/z* 1039 (R_t 5.2 min); B. *m/z* 1197 (R_t 6.5 min). The dotted line indicates the threshold value set for analysis (2000)

The averaged MS^2 mass spectra of all the found peaks can be found in the Appendix (Figure A10-11). The collected data, together with the information provided by chromatograms (e.g., Rt) and mass spectra including their fractionation pattern, allow the algae analyst to assume the identity of the oligosaccharides found, as discussed in detail in section A5.1.

Complementary enzymes for oligosaccharide saccharification: According to the analysis present in section A5.1, a polysaccharide esterase may assist a complete enzymatic hydrolysis of *S. obtusiusculus* ABV10 biomass. As discussed there, mainly acetylated sugars are very likely present in the saccharified biomass. Preliminary results using an acetyl xylan esterase from

Orpinomyces sp. (Megazyme, section A3.9) on the supernatants obtained from the enzymatic treatment with Rohapect® UF 4% $w_{protein}/w_{biomass}$ showed a significant concentration increase of 38% mannose, 36% glucose, and 21% galactose. While these results are to be further verified on the rest of the hydrolase supernatants, they highlight the potential of this approach for designing targeted hydrolysis strategies.

A5. Discussion

A5.1. PMP carbohydrate analysis for algal biomass: advantages, limitations and application in biomass development

One of the main challenges in the analytical field for microalgal carbohydrates is the identification and characterization of unknown or rare monosaccharides. The methodology presented in section A4.1 (Ortiz-Tena et al., 2016) offers important advantages over existing analysis methods for studying carbohydrates from algal biomass. Earlier to this work, other authors (Templeton et al., 2012) evaluated the performance of various analytical procedures using HPLC, HPAEC, and GC for analyzing microalgal carbohydrates. There, different microalgal strains were analyzed and several unknown peaks were identified in the corresponding hydrolysates, even five in *Chlorella vulgaris*. Thus, the authors concluded that under- or overestimation of monosaccharides could not be excluded with the evaluated methods, e.g., due to likely co-elution of such unidentified compounds.

Unknown compound qualification by MS has become a very powerful and sensitive tool for different applications. Data analysis can be performed within a very short time compared to other methods, such as NMR spectroscopy. For example, GC coupled to MS is commonly used for the determination of unknown volatile compounds. A significant drawback for its use in carbohydrate analysis, however, is the challenging volatilization of sugars, which ultimately increase sample preparation in most cases. Commonly, trimethyl silane (TMS) or alditol acetate derivatives are generated for GC analysis of biomass samples. However, this strategy is sometimes hard to apply for charged sugars, i.e. uronic acids or amino sugars. A significant advantage of the PMP derivatization in liquid chromatography is its applicability to a wider range of sugar compounds, including uronic acids, amino, and sulfated sugars, as demonstrated in this work. An important limitation of this type of derivatization is the fact that only aldoses can be detected, as the chemical reaction occurs in the aldehyde group of the sugar. Lacking this group, important ketoses (e.g., fructose and sorbose) cannot be determined, so that verification with corresponding methods is advisable.

In general, derivatization steps in analytical methods are rather undesired, as they are usually time consuming and the compound detection may not be accurate. In the case of the PMP method transferred, derivatizing the sugars is a worthwhile step, because the sugars can be analyzed by UV-absorbance and become at the same time ionizable for MS quantification. This double detection is very sensitive and enables identification of sugar compounds in similar measurement ranges. Therefore, cross-verification of each compound is possible, rendering the method an additional proof of quality. Co-eluting and unknown compounds can be easily identified by analyzing corresponding MS fragmentation patterns. Lastly, the separation time of 12 min allows saving eluents in comparison to other methods, such as HPAEC.

Since the PMP derivatization and sample preparation (i.e., derivative stabilization and sample filtering) prior to chromatographic separation are conducted in 96-well format, the implementation of the method in HT format is feasible (Rühmann et al., 2015). In this work, carbohydrate determination from microalgae was rather performed in a medium throughput mode, as the hydrolysis and neutralization steps were carried out in glass tubes. In order to truly perform HT analysis of dry biomass, a grinding and weighing platform for biomass samples could be employed, as previously demonstrated for lignocellulosic material (Whitehead et al., 2012). A faster and more elegant analysis procedure may include the hydrolysis of the algal culture directly from the bioreactor, followed by PMP derivatization and sugar quantification. For this, a threshold for biomass concentration of 1 g L^{-1} would be required to perform the analysis with the conditions described here.

A central aspect of the analytical transfer was the qualification and verification of the procedure for its suitability and feasibility to analyze microalgal biomass. The suitability of the PMP method on microalgal biomass was validated by determining the monosaccharide recovery after spiking different algal hydrolysates and process fractions with good results. A more comprehensive validation of the method should include the analysis of an external reference material, as commonly employed for lignocellulosic materials (Templeton et al., 2016). However, due to the very different chemical composition compared to microalgae, the use of a terrestrial biomass as reference material (such as sugarcane bagasse or wheat straw from the NIST, USA), would not really validate the quantification presented here. Presently, this is a challenging task for algae analysts, as no standard microalgal biomass reference material is available yet (ABO, 2017). If this material becomes available in the future, its analysis could complement the method validation.

TFA Chemical hydrolysis of algal biomass: The chemical hydrolysis applied to release monosaccharides from biomass is a crucial step in any analytical procedure for carbohydrates. At the conditions needed to attain chemical hydrolysis of polysaccharides (i.e., elevated temperature, low pH), complex chemical processes occur that are very difficult to predict. At such conditions, monosaccharides are not only released but also degraded or become reactive with other components present in the sample. The degradation of monosaccharides present in a pure mixture cannot be compared to that taking place with polysaccharides in solution (Rühmann, 2016). This indicates that the energy needed to cleave the glycosidic bonds plays an important role in monosaccharide degradation. Similarly, other molecules present in biomass, such as proteins and lipids, may interact with the released monomeric sugars to form complex degradation products, e.g., as occurs during the Maillard reactions.

A detailed investigation of such phenomena lies beyond the scope of this work. However, the standard TFA hydrolysis employed was critically evaluated using the DoE methodology (section A4.1). There, four different hydrolysis parameters (hydrolysis time, temperature, TFA and biomass concentration) were varied for sugar quantification in the model microalga *C. vulgaris*. The results of the analysis confirmed that each input parameter promotes the release of monosaccharides differently. The yield of glucose, for instance, can be maximized within the investigated range at 119°C and 1.8 g L^{-1} biomass. The parameters hydrolysis time and TFA concentration yielded a maximum at the highest and lowest value within the investigated range (120 min and 1 M, respectively). From explorative additional samples analyzed beyond these values, it can be inferred that a global optimum may most probably be found between 120 – 180 min and 0.5 – 1 M TFA. Being a statistically significant parameter, TFA concentration should have a stronger impact in glucose yield than the hydrolysis time and could be chosen first to expand in a closer DoE range towards glucose maximization.

In summary, the DoE allowed to identify the hydrolysis conditions at its CP (90 min, 121°C, 2 M TFA, 2.5 $g_{Biomass}$ L^{-1}) as a good starting point for an explorative carbohydrate analysis of *C. vulgaris*, as all the output sugars could be detected. Noticeably, hydrolysis temperature and concentration of algal biomass were statistically significant for three out of four output variables (Table 11). As biomass concentration directly correlates with the protein content in the hydrolysis mixture, its strong influence in the DoE can be associated to Maillard reactions in which the ratio of protein to TFA concentration may be involved. Therefore, varying temperature and biomass concentration is most suitable to achieve better output yields for the tested sugars, in contrast to hydrolysis time and TFA concentration.

In total, 25 different hydrolysis conditions were investigated to determine carbohydrates with the PMP UHPLC-MS method in *C. vulgaris*. Summing up the maximum yield for each sugar output obtained from these samples, 392 mg g_B^{-1} total carbohydrate concentration can be reported. This value is 30% higher than the total sugar yield obtained with the standard hydrolysis conditions (295 mg g_B^{-1}) and the CP of the DoE (302 mg g_B^{-1}). The largest difference was observed in neutral sugars, for which the yield obtained at the CP and with standard hydrolysis conditions (63 and 60 mg g_B^{-1}, respectively) was 50% lower than the softer conditions employed in sample 6 of the DoE. These results indicate a significant and unavoidable underestimation of monosaccharides in *C. vulgaris* biomass using TFA hydrolysis, most probably due to sugar degradation (e.g., Maillard reactions). Consequently, chemical hydrolysis must be carefully interpreted as reference for determining saccharification yields (e.g., in enzymatic treatments, as observed in section A4.3). Strictly speaking, a DoE analysis is advisable to avoid monosaccharide underestimation in microalgal biomass due to sub-optimal hydrolysis conditions. Lastly, PMP carbohydrate analysis should be supported by protein and lipid examination to ensure 100% biomass closure.

Further applications of the PMP monosaccharide analysis method: As discussed above, a very important aspect for the design and development of a microalgal bio refinery is the modulation of the biomass carbohydrate content. A common culture strategy for this consists in limiting the nitrogen availability in the culture media in order to suppress the formation of proteins in the biomass (Christian Schulze, Wetzel, et al., 2016). The PMP derivatization and analysis method has been used for evaluating strategies to control the carbohydrate content of cultured microalgae (Sinzinger, 2016). In his work, Sinzinger determined the sugar content of microalgal biomass grown by the author under nitrogen deplete and replete conditions as reported in Table 7. While *Chaetoceros muelleri* and *Isocrysis galbana* did not show significant increase in the carbohydrate content under nitrogen limitation, *Tetraselmis* sp. and *Spirulina* sp. triplicated their sugar content when no nitrogen was supplemented.

Another interesting aspect for biomass culture is the type of light employed in the cell growth phase. The sugar formation in certain chrysolaminarin-producing microalgal strains, e.g., *Phaeodactylum tricornutum*, seems to be highly dependent on light conditions and day-night cycles (Kroth et al., 2008). Sinzinger also applied the PMP method to evaluate the carbohydrate content of this strain cultivated under different light conditions (Table 7). According to his results, culturing under white and green light increased the sugar content from 80 mg g_B^{-1} to 150 mg g_B^{-1} compared to sunlight. The use of low-energy red light mainly increased the sugar concentration to 180 mg g_B^{-1}, mostly promoting the formation of glucose.

LC-MS oligosaccharide detection: In addition to the monomer sugar detection method transferred for microalgal carbohydrate analysis, the PMP derivatization and MS analysis can also be applied to oligosaccharides with reducing ends. A significant advantage of this method is the possibility to ionize and fragment short chained sugars for a qualitative composition determination. As shown in section A4.3, pullulan and the oligosaccharides released by the hydrolase mixture Rohapect® UF can be analyzed. In this section, a general evaluation and interpretation of these unknown oligo sugars is presented.

The mass fragments (MS^2) obtained from all the observed peaks in the hydrolysate of Rohapect® UF 4% $w_{protein}/w_{biomass}$ are summarized in Table 14 (corresponding averaged MS^2 spectra are shown in Figure 11 and in the Appendix, Figure A10-11). According to the results, all the oligosaccharides found displayed a very similar fragmentation pattern, especially concerning the section of the spectra with the lowest *m/z* ratio. Noticeably, the fragments having *m/z* 715 and 877 (Δ*m/z* 162) were observed in almost all cases. This indicates the presence of a chain pattern that may relate to the resistance of the oligosaccharides towards enzymatic hydrolysis by the commercial mixtures employed. The higher mass fragments diverge among the peaks with different *m/z* values. Remarkably, the four peaks found with *m/z* 1239 (green chromatogram in Figure 10) present slightly different fragmentation masses with varying intensity (Figure A10). Their distinct retention times may suggest a variable monosaccharide arrangement within the chain (e.g., branching), as they interact differently with the hydrophilic phase in the chromatographic column. For all the oligomers found, a postulation concerning the chain length and (substituted) monomers was made in accordance to the number of defined significant fragments (intensity > 2,000, ca. one tenth of maximal intensity found) observed in their MS^2.

Table 14 MS^2 fragments of the peaks found in the liquid supernatant of the biomass treatment with Rohapect® UF 4% w/w. Hex: hexose, Pen: pentose, Ac: acetylated, d-Hex: deoxy-hexose. [a]Threshold intensity of significant fragments: 2000. [b]Identity of monosaccharides was assumed based on fragments with lower intensity than threshold. [d]Fragment resulted from loss of water of fragment 1149. [u]Unidentified fragment with Δ*m/z* 82.

MS *m/z*	**R_t range** **min**	**MS^2 mean significant fragments^{a}** *m/z*									**Oligosaccharide**	
673	2.8 – 3.2	511	-	-	-	-	-	-	-	-	2 x Hex	Dimer
835	5.0 – 5.4	511	673	-	-	-	-	-	-	-	3 x Hex	Trimer
1039	5.1 – 5.4	511	-	715	877	-	-	-	-	-	1 x Hex 1 x Ac-Hex 2 x Hex	Tetramer
1197	6.4 – 6.6	511	-	715	877	-	1023	-	-	-	1 x Hex 1 x Ac-Hex 1 x Hex 1 x d-Hex 1 x Ac-Pen	Pentamer
1197	6.9 – 7.1	511	-	715	877	-	1023	-	-	-	1 x Hex 1 x Ac-Hex 1 x Hex 1 x d-Hex 1 x Ac-Pen	Pentamer
1239	4.5 – 4.8	511	-	715	877	-	-	1065	-	-	1 x Hex 1 x Ac-Hex 1 x Hex 1 x Ac-d-Hex 1 x Ac-Pen	Pentamer
1239	4.8 – 5.1	511	-	715	-	919	-	-	-	-	1 x Hex 1 x Ac-Hex 1 x Ac-Hex 1 x d-Hex ^{b} 1 x Ac-Pen ^{b}	Pentamer
1239	5.5 – 5.7	511	-	715	877	-	-	1065	-	-	1 x Hex 1 x Ac-Hex 1 x Hex 1 x Ac-d-Hex 1 x Ac-Pen	Pentamer
1239	6.0 – 6.2	511	673	-	-	-	-	-	-	-	2 x Hex 1 x Ac-Hex ^{b} 1 x Ac-d-Hex ^{b} 1 x Ac-Pen ^{b}	Pentamer
1281	3.7 – 4.0	511	-	715	-	919	-	-	-	-	1 x Hex 1 x Ac-Hex 1 x Ac-Hex 1 x Ac-d-Hex ^{b} 1 x Ac-Pen ^{b}	Pentamer
1281	4.0 – 4.2	511	-	715	-	-	-	-	1107	-	1 x Hex 1 x Ac-Hex 1 x Hex ^{b} 1 x Ac-Ac-d-Hex ^{b} 1 x Ac-Pen	Pentamer
1323	3.3 – 3.6	511	-	715	-	-	-	-	-	1131^{d} 1149 1241^{u}	1 x Hex 1 x Ac-Hex 1 x Ac-Hex ^{b} 1 x Ac-Ac-d-Hex ^{b} 1 x Ac-Pen	Pentamer

Several significant EIC peaks with a clear fragmentation pattern were identified in the above-mentioned hydrolysate. The fact that all hydrolysate peaks eluted faster compared to those present in the reference pullulan (Figure 9) suggests a hydrophobic character of the oligosaccharides. This may occur because of two reasons: either the absence of hydroxyl groups in the sugar structures (e.g., deoxy-sugars) or hydrophobic substituents present in the oligomeric chain. As the peaks found in the enzymatic hydrolysate present higher *m/z* ratios than those from the pullulan standard, the later seems more plausible (Table 14).

In the shortest oligosaccharide of this type found (*m/z* 1039), the fragment sequence *m/z* 511-715-877-1039 suggests a tetrameric structure consisting of three hexoses (3 x Δ*m/z* 162) and one substituted monosaccharide (Δ*m/z* 204). Given the shorter elution time of this unknown tetramer compared to the glucose tetramer present in the pullulan reference material (5.2 < 6.8 min), a hydrophobic group bound to the substituted monosaccharide seems possible. The mass difference of this unknown sugar compared to a hexose is *m/z* = 204 – 162 = 42, which exactly corresponds to the mass of an acetyl group (Table 14).

The next oligomers found present a *m/z* 1197. Again, their shorter retention time compared to that of the glucose pentamer in pullulan (6.5 and 6.9 < 8.0 min) suggests the presence of hydrophobic substituents within the chain. From its fragmentation pattern, it can be inferred that this oligosaccharide is a sugar pentamer with four different types of monomers (Figure 11). The oligomeric structure seems to be formed by the same acetyl hexose flanked by two hexoses (fragment sequence *m/z* 511-715-877). The fourth and fifth sugar counted from the derivatized end presented mass increments of Δ*m/z* 146 and 174, respectively. The first mass increment of 146 corresponds well to a deoxy-hexose, such as fucose or rhamnose. Noticeable, both monosaccharides were found in TFA hydrolysates of the raw, lipid-extracted biomass ABV10 (Figure 7). Rhamnose was even detected in the enzymatic hydrolysates after TFA hydrolysis (Figure A7). The second mass increment of 174 may indicate an acetylated pentose, given its mass difference compared to a bound pentose (Δ*m/z* = 174 – 132 = 42). As two peaks were found with this *m/z* at different retention times, branching seems possible.

A similar analysis can be performed for the rest of the oligosaccharides, as presented in Table 14. Two of the peaks with *m/z* 1239 presented significant fragments with Δ*m/z* = 1065 – 877 = 188, which fits well with an acetylated deoxy-hexose. For the peaks with *m/z* 1281 and 1323, fragments with rather low intensity were found in the upper region (*m/z* ~ 1000) of the spectrum (Figure A11). Therefore, assumptions were made based on fragments with lower intensity than the threshold of 2,000. Here, a Δ*m/z* 230 was found, which may indicate a doubled-acetylated deoxy hexose. Furthermore, the fragment with *m/z* 1131 reflects the loss of water of fragment 1149 (Δ*m/z* 18). In fact, the very short R_t of these peaks (4.2 and 3.4 min, respectively) indicates a much stronger hydrophobic character compared with non- (8.0 min), and lower-grade-acetylated pentamers (6.9 min). To confirm this assumption, using a lower fragmentation energy in the ion trap may provide a clearer picture, which could also explain the unidentified fragment 1241 (Δ*m/z* 82).

As mentioned above, the Δ*m/z* 204 next to the derivatized hexose (*m/z* 511) and the subsequent fragment was found in all the oligomers, yielding ion fragments of *m/z* 715 and 877. According to its fragmentation (Figure 11) the block units in Figure 12 seem plausible.

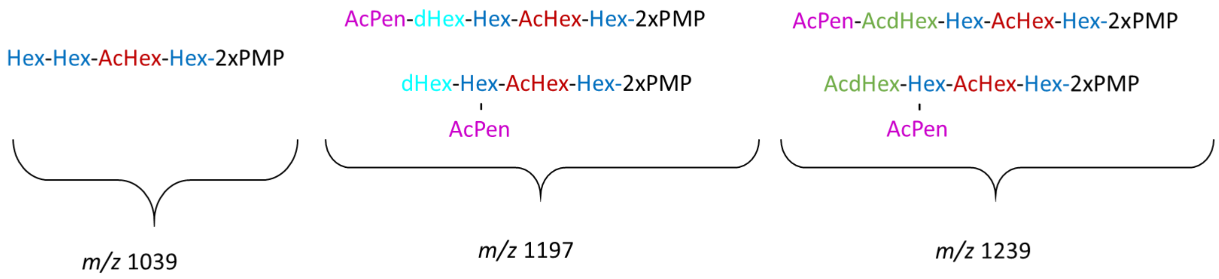
Hex-Hex-AcHex-Hex-2xPMP
AcPen-dHex-Hex-AcHex-Hex-2xPMP
dHex-Hex-AcHex-Hex-2xPMP
AcPen
AcPen-AcdHex-Hex-AcHex-Hex-2xPMP
AcdHex-Hex-AcHex-Hex-2xPMP
AcPen
m/z 1039
m/z 1197
m/z 1239

Figure 12: Possible oligomeric sugar structure of the peaks found (*m/z* 1039, 1197 and 1239) in the enzymatic supernatant (Rohapect® UF 4% w/w) of the algal biomass of *S. obtusiusculus* ABV 10. Hex: hexose, Pen: pentose, Ac: acetylated, dHex: deoxy-hexose

The MS^2 spectrum of these compounds, however, does not allow a clear conclusion whether their structure is linear or branched, as well as about the exact position of the substituted groups. The low intensity fragments found in the upper region (*m/z* ~ 1000) of the spectrum (Figure 11) may indicate a branched structure. The presence of branched oligo structures seems possible, as four different peaks having *m/z* 1239 and two with *m/z* 1197 were found, each presenting differing retention times and fragment intensities in the MS^2 pattern.

The fragmentation pattern of all oligosaccharides exhibits a combination of the same mass increments 230, 204, 188, 174, and 146. Most probably, highly acetylated oligosaccharides are present in the microalgal biomass. Such oligosaccharides may act as protection against hydrolytic enzymes. In fact, acetylated hemicelluloses are commonly present in the cell wall of different terrestrial plants and some marine organisms, which serve the cells as defense against enzymatic degradation (Loft et al., 2009). A more detailed analysis using complementary methods should still be carried out (e.g., NMR, IR) to confirm this hypothesis.

The analysis presented here demonstrates the feasibility of the PMP oligosaccharide method for detecting partially hydrolyzed carbohydrates from microalgal biomass. This enables the identification of complementary activities for a complete saccharification, as discussed in the next section. Accordingly, a much more targeted strategy can be designed to release monosaccharides enzymatically from carbohydrate-rich biomass.

A5.2. Enzymatic hydrolysis of microalgal carbohydrates

The results presented above demonstrate the feasibility of the proposed approach to design a targeted hydrolysis of microalgal biomass by analyzing eventually lacking activities. Concretely, the LC-MS oligosaccharide analysis employed here on the Rohapect® UF supernatant provides an effective tool for identifying complementary hydrolytic activities for increasing sugar monomerization. Highly acetylated oligosaccharides were detected after enzymatic hydrolysis of carbohydrate-rich and defatted biomass of *S. obtusiusculus* using the above-mentioned commercial hemicellulase. Preliminary experiments using a commercial acetyl xylan esterase on the produced hydrolysates yielded positive results towards a complete biomass hydrolysis (section A4.3).

This approach has been performed for testing the PMP mono- and oligosaccharide method to achieve complete enzymatic saccharification using glucomannan and galactomannan as polysaccharide standards (Sinzinger, 2016). In his work, ca. 600 mg g_B^{-1} total monosaccharide was found in glucomannan hydrolysates of Rohapect® UF and around 350 mg g_B^{-1} of B1L and Rohament® CL. The reason for the improved activity of Rohapect® UF remained unclear, given the fact that Rohapect® B1L has a declared mannanase activity. Furthermore, similar hydrolytic activity on galactomannan were found. As solubilized galactose was detected in the biomass hydrolysates generated with both enzymes, it can be inferred that the enzymes are active on the glycosidic bond Gal-β-(1→6)-Man of the galactomannan side chain, as described here. These types of linkages may also be present in the polysaccharides of *S. obtusiusculus* and could have been hydrolyzed as well, as free galactose was observed in the hydrolysate. Furthermore, Sinzinger employed this method for optimizing the saccharification of carbohydrate-rich and defatted *S. obtusiusculus* grown on pilot scale with an approach that included the use of amylase, allowing a distinction between storage and cell walls polysaccharides (Sinzinger, 2017).

To date, numerous studies addressing the enzymatic hydrolysis of plant and algal carbohydrates have been reported (Demuez et al., 2015). In addition to the saccharification of biomass for subsequent fermentations or bio transformations, enzymatic treatments can be applied to assist extraction processes (e.g., for lipids or bioactive compounds) (Zuorro et al., 2016) or for improving the production of biogas from biomass (Mahdy et al., 2015). Whatever the goal of the treatment, when it comes to employing enzymes for degrading microalgal polysaccharides, promising hydrolase candidates are usually more or less arbitrarily selected. The enzymes are employed either singly or combined and the saccharification yield is determined by calculating the monosaccharide released by the hydrolases compared to those found by chemical hydrolysis. Besides, carbohydrate losses resulting from suboptimal hydrolysis conditions are not considered. Thereby, partially hydrolyzed carbohydrates released into the liquid phase in form of (substituted) oligosaccharides are not considered, which is translated in suboptimal saccharification processes. The methods and analysis presented here highlight the need for more accurate and systematic choice of enzymes for algal biomass saccharification.

A6. Conclusions and Perspectives

In the first part of this work, the previously developed HT-PMP carbohydrate analytical method for bacterial exopolysaccharides was successfully transferred to analyze microalgal biomass. The overall performance was very positive and, most importantly, unidentified monosaccharides (e.g., amino, methylated and sulfated sugars) could be newly reported in relevant microalgal strains. Further, the feasibility of the analytical procedure was demonstrated by generating a carbohydrate distribution profile of the model microalga *C. vulgaris*. The biomass fractioning procedure employed for this purpose may well be expanded to any other strain for its comprehensive characterization, or also for the screening and analysis of microalgal exopolysaccharides. On the other hand, the method was successfully applied to investigate the carbohydrate formation of various microalgal strains using currently employed strategies for biomass formation, such as nitrogen starvation or light modulation.

Considering the enormous diversity of still unexplored microalgal strains, the procedure presented here provides a powerful tool for a fast evaluation of important selection and culture parameters. If appropriate hydrolysis conditions for microalgal biomass in a plate format are designed, a complete automatized carbohydrate analysis platform integrating this method seems possible. The main steps may include: microalgal inoculation, growth in plate format, micro TFA hydrolysis, and HT-PMP analysis. With the advance of powerful gene editing technologies for microalgae, such as CRISPR-CAS9, high-throughput phenotyping of carbohydrate production (especially rare sugars) can become much simpler with the HT-PMP method.

The possibility of analyzing oligosaccharides using the same derivatization conditions as for monosaccharides offers important advantages for the conversion of algal carbohydrates. A complete saccharification strategy, for instance, could be accelerated by selecting the appropriate enzymes when substituted mono or oligo sugars are presented (e.g., sulfated, methylated, or acetylated). In this framework, first results treating the analyzed oligosaccharides with an acetyl xylan esterase showed a significant yield increase of 38% mannose, 36% glucose, and 21% galactose in comparison to those treated only with the commercial hydrolases. While these results are to be further verified on the rest of the hydrolase supernatants generated, they highlight the potential of this approach for designing targeted hydrolysis strategies.

As a very fast processing of samples is possible, different saccharification conditions for enzyme combinations may be tested, including pH, temperature, buffer type, enzyme concentration, etc. For this, an integration of all procedure steps for both types of sugars (mono and oligosaccharides) into one working scheme is required. To make the process more economic, however, a comprehensive analysis and optimization of consumables (such as separation columns, buffers, and plate types) should be performed.

B. Macroalgae

B1. Literature review

B1.1. Macroalgal biomass

Macroalgae, commonly referred as seaweed, represent a wide group of multicellular, macroscopic marine organisms that grow in very diverse environments. In contrast to microalgae, which are capable to freely float in water, most of the macroalgae require a firm attachment point to the marine ground. This is achieved by a part of the seaweed called holdfast, a specialized basal structure providing anchoring to a surface, often a rock or another alga (Hurd et al., 2014). The size of these photosynthetic organisms ranges from a few centimeters up to 60 m. Macroalgae are ecologically very relevant, especially in littoral zones, as they participate in the nutrient recycling that form the basis for primary production and food chains (Kirkman & Kendrick, 1997).

Initially, macroalgae were collected from bare coastal accumulations, but in the last years the production of seaweed (i.e., aquaculture) has become a true marine agronomic activity on large scale. These achievements could be attained in part thanks to the micro-propagation technique applied to seaweeds, which allowed a selective breeding of individuals with traits of interest (Reddy et al., 2017). The most relevant parameters for production in cultivars include light intensity, temperature, water salinity, nutrients and water motion. Recently, various promising approaches for the sustainable production of seaweed have been developed, such as the integrated multi-trophic aquaculture, in which different species are grown in a single area for nutrient recycling (Azanza & Ask, 2017).

The early uses of macroalgal biomass were limited to human consumption as dried sheets for preparing soups, sushi wraps, or rice balls, especially in Asian countries. In the early 60’s and 70’s, commercial seaweed production arose in the indo-pacific region to cover the demand for hydrocolloids, one of the main products from seaweeds (Neish et al., 2017). Since the 2000’s, the annual seaweed production increased considerably at rates of ca. 10% p.a. as a result of the rapid industrial expansion and the development of new applications (Cottier-Cook et al., 2016). These include the production of several bioactive (e.g., antiviral, antibiotic, anti-inflammatory) compounds, toxins, and enzyme inhibitors for relevant diseases (Smit, 2004).

Different types of products can be obtained from macroalgae, depending on the species, harvesting time, weather conditions, etc. Similarly to microalgae, standardization procedures for production and processing are required to open the market for new fields (Hafting et al., 2015). Although the composition of macroalgae cannot be influenced so easily as for microalgae (and consequently the products obtained from them), they have conquered well established markets. Brown algae, such as *Laminaria* sp., have been used for several decades for producing fucoidan and alginic acid. *Chondrus* sp., a red alga, is cultured to obtain carrageenan, and carotenoids are extracted from green algae, e.g., *Ulva* sp. (Holdt & Kraan, 2011). An overview of the most significant compounds produced from seaweeds is given in Table 15.

Table 15 Main products obtained from seaweeds. Condensed from (Holdt & Kraan, 2011)

Seaweed	Species	Carbohydrates	Proteins	Lipids	Pigments
Brown	*Laminaria* *Fucus* *Ascophylum* *Undaria* *Sargassum*	Alginates Fucoidan Laminarin Mannitol	Limited	PUFA Glycolipids Sterols	Fucoxanthin Violaxanthin Carotenes
Green	*Ulva*	Ulvan	Lectins	Limited	Chlorophyll
Red	*Chondrus* *Porphyra* *Gracilaria* *Kappaphycus*	Porphyran Starch Agar Carrageenan	Phycobiliproteins	Saturated acids Phospholipids Sterols	Lutein Zeaxanthin

Carbohydrates in the form of polysaccharides are the most abundant component present in macroalgae, making up to 65% of the dry weight of some species (Holdt & Kraan, 2011). These compounds can easily be extracted with hot water or alkali solutions, which at the same time modifies their rheological properties (Azevedo et al., 2015). These polymeric sugars behave in solution as hydrocolloids, forming gels and emulsions with differing properties depending on different factors, such as chemical structure, temperature, and pH. This property is very convenient for their use in diverse industrial fields, including food, feed, chemical, and pharmaceutical. Therefore, it is not surprising that seaweeds are especially cultured to produce polysaccharides in large scale (Trivedi et al., 2016).

The most important seaweed hydrocolloids to date include agar, alginates, and carrageenan. Together, these three products reached volume sales of around 1,000 million US$ in 2009, a very significant growth compared with the 644 million US$ in 1999 (Bixler & Porse, 2011). In the last years, however, these numbers have become stagnant to modest growth rates of around 3% p.a. due to different reasons, such as price competition and cost increases (Porse & Rudolph, 2017). Thus, solutions to increase value added of seaweed processing as well as a market diversification of the established products towards new applications are required to change this scenario. Both aspects are addressed in the next sections for carrageenan, one of the most industrially relevant hydrocolloid.

B1.2. Carrageenan and More: Biorefinery Approaches with Special Reference to the Processing of *Kappaphycus*

The increasing global population and its accompanying raising demand for commodities require not only the development of novel sustainable alternatives, but also the improvement of already existing processing technologies. This book chapter is devoted to one of the most important products from marine resources: carrageenan. This carbohydrate polymer with valuable gelling and thickening properties is mainly obtained from red seaweeds, especially from the genus *Kappaphycus*. The first part of the chapter thus presents a literature research concerning the reported chemical composition of the seaweed as well as some culturing strategies. Next, the physical-chemical properties of the main types of carrageenan (κ-, ι-, λ-) are discussed, together with the most important applications in the food industry currently. Besides, some promising valorization strategies for the chemical and pharmaceutical sector (e.g., drug delivery) are presented and discussed.

The second half of the chapter provides an overview on conventional carrageenan extraction and refining processes performed in different parts of the world together with numbers on diverse commercialized qualities in the market. Most importantly, an evaluation on the by-products generated is presented, as well as possible utilization paths with the objective of delineating strategies for a bio refinery of this macroalga. Thanks to the gained insights, biotechnological approaches, such as enzymatic processing of the seaweeds and carrageenan itself, were identified to increase the value added.

The author conducted most of the literature research, provided relevant sources and summarized the data for the chapter. The co-authors contributed to sources, content, and language. The chapter was written on explicit invitation from expert researchers in the field and book editors.

Carrageenan and More: Biorefinery Approaches with Special Reference to the Processing of *Kappaphycus*

José G. Ortiz-Tena, Doris Schieder, and Volker Sieber

In book: Tropical Seaweed Farming Trends, Problems and Opportunities
Developments in Applied Phycology Book Series (Vol. 9)
Springer 2017

Reproduced with permission, license number: 4227220860626
DOI: 10.1007/978-3-319-63498-2_10

Carrageenan and More: Biorefinery Approaches with Special Reference to the Processing of *Kappaphycus*

10

José G. Ortiz-Tena, Doris Schieder, and Volker Sieber

Abstract

In the age of increasing awareness of our planet's limited resources, utilization of plant biomass not only for food but also for fuel and chemicals becomes an essential part of a more sustainable economy. Marine plants such as seaweeds have an especially high potential compared to land plants as the earth's surface is mainly covered by water and they can be considered still under-utilized. This scenario is currently changing with the increasing areas of seaweed farms close to the shore in the Indo-Pacific area as well as the development of off-shore concepts on floats in the Atlantic Ocean. Of the different types of seaweeds brown and red seaweed have been utilized most so far. The major products obtained from red seaweeds today are carrageenans. *Kappaphycus* here plays a central role as it is the dominant source for kappa-carrageenan. While *Kappaphycus*, as any other seaweed, contains many more components, the production process is optimized for highest carrageenan yields. The modern zero-waste policy, however, requires production processes that will allow utilization of any by-product. Biorefinery approaches have been developed for many land plants over the last decade. Can these concepts be transferred to seaweeds as well? This chapter evaluates the challenges and opportunities for optimal utilization of the crude biomass from *Kappaphycus* seaweeds, with special focus on the latest applications and processing technologies for its main components, including carrageenan as a major valorization product.

10.1 Constituents of *Kappaphycus*

From a general valorization perspective, seaweed biomass can be conveniently divided into: (a) insoluble polymeric material that confers structural support or serves as energy storage in the cell (i.e. carbohydrates and proteins), and (b) low molecular weight compounds, which, for example, may act as defenses against pathogens, or as enzyme co-factors. Polymers can either be hydrolyzed to their monomeric components or directly extracted and utilized in different applications, depending on their physical and chemical properties. Furthermore, the small molecules are usually extracted using organic solvents and then concentrated by thermal or filtration processes. The biomass from marine origin differs considerably in composition from terrestrial feedstock e.g. wood, straw, grasses, etc., and also requires different processing techniques (Jung et al. 2013). It is known that the chemical composition of *Kappaphycus* seaweeds varies according to many factors, including the weed strain, growth conditions (duration) and especially harvesting season (Zuldin et al. 2016; Suresh Kumar et al. 2015; Yong et al. 2015) (Table 10.1). In general, carbohydrates are the most abundant class of polymer present in red algae, such as *K. alvarezii*, (at least 30% DW). The major monosaccharides

---

J.G. Ortiz-Tena • D. Schieder
Chemistry of Biogenic Resources, Technical University of Munich,
16 Schulgasse, 94315 Straubing, Germany

V. Sieber (✉)
Chemistry of Biogenic Resources, Technical University of Munich,
16 Schulgasse, 94315 Straubing, Germany

Fraunhofer IGB, Straubing Branch BioCat, Straubing, Germany
e-mail: Sieber@tum.de

© Springer International Publishing AG 2017

A.Q. Hurtado et al. (eds.), *Tropical Seaweed Farming Trends, Problems and Opportunities*, Developments in Applied Phycology 9, DOI 10.1007/978-3-319-63498-2_10

Table 10.1 Reported composition of *Kappaphycus* in the recent literature (% DW)

Carbohydrates[a]	Proteins	Lipids + insoluble aromatics	Ash	Species	Comments	References
46–59	5	NR	20–23	*K. striatum* *K. alvarezii*	Culture in customized tank systems	Zuldin et al. (2016)
52–56	2–4	2–4	15–17	*K. alvarezii*	Red, brown, green and G11 strains	Masarin et al. (2016)
30–55	12–22	0.4–0.9	21–34	*K. alvarezii*	Evaluation of seasonal variation	Suresh Kumar et al. (2015)
NR	9.9	2–3	38	*K. alvarezii*	Comparison of farm and micro-propagated cultures	Yong et al. (2015)
56.8	16.2	0.8	19.7	*K. alvarezii*	Samples collected from the west coast of India	Fayaz et al. (2005)

[a]Carbohydrates accounts as the sum of reported sugars and fiber content
NR not reported

present in acid hydrolysates are galactans from carrageenan (ca. 73% of total carbohydrates), followed by glucans from cellulose (ca. 23% total carbohydrates). Mannose and xylose are also present in lower concentrations (Masarin et al. 2016). The protein amounts reported in the literature vary, ranging from 2–6% DW (Masarin et al. 2016; Zuldin et al. 2016) up to 20% DW, depending on the specific strain and collecting season (Suresh Kumar et al. 2015). Compared to other types of biomass, the inorganic ash content is relatively high, from 20% DW up to 38% DW being reported (Fayaz et al. 2005; Yong et al. 2015). A substantial part of this is derived from sulphate, which is bound to the galactans forming the carrageenan and essentially increasing the carbohydrate content when included in the weight analysis. Lipids and other small molecules constitute barely 3% DW of the biomass (Masarin et al. 2016).

Kappaphycus species and variants also contain a number of low molecular weight compounds, which are bioactive and as such of interest for valorization. Extracts of seaweeds made with water, alcohols (methanol, ethanol), ether or acetone have been found to possess anti-oxidant, anti-microbial, anti-tumor or neurotrophic activity (Ling et al. 2013; Lau et al. 2014; Tirtawijaya et al. 2016). Phenols and flavonoids are responsible for parts of these activities but the general analysis of the chemical structures of isolated compounds of this genus is rare. Only one patent referring to a bromophenol describes a specific compound with biological activity (Rajasulochana et al. 2012; Rajasulochana et al. 2015). Valorization of simple extracts to be used as nutritional supplements should be possible without knowing the identity of each compound, however.

10.2 Carrageenan – Types and Uses

Over the last 50 years, carrageenan has been the main product extracted from *Kappaphycus* seaweeds, especially for their application in the food industry as thickener, gelling agent, emulsion stabilizer and recrystallization inhibitor (also elsewhere in this book) (De Ruiter and Rudolph 1997; Seta et al. 2013; Leiter et al. 2017). Carrageenan constitutes a very broad group of sulphated polysaccharides made up of galactans. The disaccharide repeating unit, carrabiose consists of alternating 3-linked β-D-galactopyranose (G-units, also referred to as "A-residue") bonded to 4-linked α-D-galactopyranose (D-units), or to 3,6-anhydro-α-D-galactopyranose (DA-units), either being also called "B-residue". Depending on the sulphation grade of the repeating disaccharide, the major carrageenans are classified as kappa (κ)-, iota (ι)- and theta (θ)- carrageenan (G plus DA-unit) and the corresponding, mu (μ)-, nu (ν)-, and lambda (λ)-carrageenan (G plus D unit) (Fig. 10.1) (Campo et al. 2009). This sulphation grade, as well as the presence of the DA-unit, are determining parameters for the physical and chemical properties and therefore for applications in different fields. *Kappaphycus* sp. and variant strains contain predominantly κ – (90–93%) with some minor amounts of ι – carrageenan (7–10%) including varying amounts of their corresponding precursors (μ and ν) depending on the plant condition at harvest (van de Velde et al. 2005). Kappa carrageenan forms strong gels in the presence of potassium ions, and rather brittle, stiff gels with calcium ions. Very low concentrations are enough for gel formation to occur (0.5% in water, 0.2% in milk) (Campo et al. 2009). Small amounts of kappa (0.01–0.05%) are commonly added to cheese, ice cream or cocoa beverages to prevent separation of whey proteins and to control stability. Other applications include thickener in low-calorie foods (e.g., jellies, salad dressings, sorbets), as fat replacer in sausages, ingredient in pet food

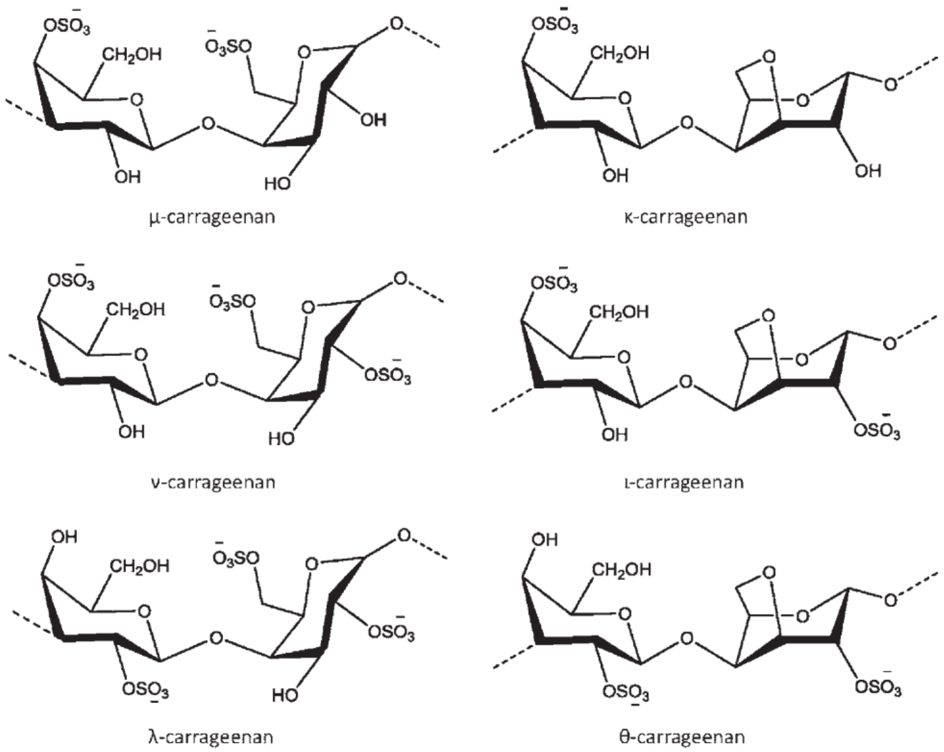

μ-carrageenan κ-carrageenan

ν-carrageenan ι-carrageenan

λ-carrageenan θ-carrageenan

Fig. 10.1 Chemical structure of the major building blocks of different types of carrageenan

and air freshener gels (McHugh 2003). On the other hand, ι – carrageenan forms better gels with calcium than with potassium ions and are rather soft, resilient and free of bleeding. They have the advantage of being stable to freeze-thaw cycles and display thixotropic flow. This property is desirable in toothpaste, because the gel should stand but also flow when pressure is applied. For this reason iota is added in about 1% concentration. Further, ground beef can be treated with iota to provide meat with fat-like characteristics, such as moisture retention for better product acceptance (McHugh 2003). Finally, lambda is a good thickening agent and is used mainly in combination with the other types of carrageenan.

Prior to carrageenan extraction, seaweeds are usually dried using different methods (freeze-, shade- and sun-drying), which have an effect on the chemical composition and properties of the final product (Vairappan et al. 2014). The extraction process plays a significant role for the quality of the carrageenan extracted and its subsequent applications. If the extraction of the hydrophilic carrageenan is performed in hot water, the carrageenan removed displays poor gel strength. One reason for this is the presence of significant amounts of μ – carrageenan, the precursor of kappa. Therefore, the dried seaweeds are subjected to alkali at high temperatures with either KOH, NaOH or $Ca(OH)_2$ to improve the gel strength (Mishra et al. 2006). Under such alkaline conditions, an intra-ring cyclization of the D-units occurs to form the 3,6-anhydro bridge of the DA-units (van de Velde et al. 2002) and μ – and ν – are converted into κ – and ι – carrageenan, respectively. The desired properties (e.g. gelling or viscosity behaviour) can be tailored by choosing the key parameters, such as time, temperature and alkali concentration (Azevedo et al. 2013, 2015). Alternative extraction procedures have been proposed without alkali treatment, such as atomization drying and the use of deep eutectic solvents (Webber et al. 2012; Das et al. 2016). One of the most commercialized types of carrageenan is the so called hybrid carrageenan, or “Kappa-2”. It was largely debated whether this type of carrageenan was made of mixtures of κ – and ι – homo-polymers or if both types were present in a single chain forming a copolymer (Hilliou 2014). It was only recently demonstrated that this product is actually a block copolymer comprising iota and kappa with different lengths and distributions within the chain (Guibet et al. 2008). The gel formation of this blend depends on the block pattern of the conforming units, showing an intermediate gelation strength between κ – and ι – carrageenan (van de Velde et al. 2005). Other properties, such as the cation type used for gel formation, gel setting or temperature do not differ from the homo-polymer (van de Velde et al. 2005; Hilliou et al. 2014). This "technical grade carrageenan" is employed in different applications within the food industry, such as milk beverages (Bixler et al. 2001) and as edible films with enhanced properties (Larotonda et al. 2016).

On the other hand, the anionic character of carrageenan allows its electrostatic interaction with various interesting molecules which can be targeted to useful applications, such as methylene blue for colorimetric oxygen indicators in food packaging (Vu and Won 2014). The more common polysaccharides, i.e. starch and cellulose are often chemically modified to improve their performance for specific purposes, such as flocculation or wet-end additives. This type of processing is also feasible for seaweed polysaccharides. Barahona et al. (2015) created an amphoteric carrageenan by adding 3-chloro-2-hydroxypropyltrimethylammonium chloride, a cation that substitutes the hydroxyl groups of the galactan units to different degrees. Another example includes the complexing of ι -carrageenan with ammonium bromide to improve its conductivity towards the production of biofilms for fuel cell applications (Karthikeyan et al. 2016). Furthermore, a graft carrageenan polymer with N-isopropylacrylamide which exhibited thermo-sensitive properties and improved interaction with cationic species was produced (Gaweł et al. 2013). This type of polymer finds applications in water treatment or metabolite encapsulation. Consequently, the interest for carrageenan in the pharmaceutical industry has increased over the last few years for two main reasons. Firstly, diverse biomaterials applications have been devised, such as vehicle for drug delivery in oral formulations and tissue engineering (Liu et al. 2015). This has been driven by novel developments of carrageenan-based, nano-structures, which can be produced either from partially degraded pure carrageenan (Sun et al. 2016) or by electrostatic interactions with different cationic species, such as chitosan or protamine (Dul et al. 2015; Long et al. 2015). Secondly, diverse biological activities of carrageenan in polymeric and oligomeric form have been published, including anti-tumor, anti-coagulant, anti-hyperlipidemic, antiviral and immune-modulatory properties (Campo et al. 2009; Hu et al. 2006). The requirements for the use of carrageenan in medical applications are much stricter than in the food industry, since the chemical composition can have significant effects in the desired property. The sulphate regiochemistry, for instance, has a considerable influence in the anti-coagulant activity and cyto-toxicity of carrageenans (Liang et al. 2014; de Araújo et al. 2013). For this reason, the technical hybrid carrageenans must be refined to the pure homo-polymeric forms for pharmaceutical applications. In the recent past, the bio-catalytic potential of diverse marine micro-organisms has been explored to specifically modify the chemical structure of carrageenan (Helbert 2012). Diverse carrageenan sulphatases that modify the sulphation pattern of the carrabiose repeating units of κ -, ι – and hybrid carrageenans have been isolated from cell lysates of various species of *Pseudoalteromonas* and recombinants produced (Genicot et al. 2014; Préchoux et al. 2016, 2013). This opens the possibility of further genetic exploration of similar marine organisms for the biotechnological utilization of this valuable polysaccharide. In addition to the afore-mentioned applications of carrageenan as a polymer, monomeric sugars can be obtained by chemical or enzymatic hydrolysis, which increases its valorization potential as a fermentation source for the production of commodity chemicals and biofuels (Yun et al. 2016). This strategy is addressed in detail in Sect. 10.4.

10.3 Classic Processing of Carrageenan Containing Seaweeds

Today, commercial carrageenans from *K. alvarezii* are produced by alkaline treatment of the algal biomass using different methods (Fig. 10.2). "Refined carrageenans (RC)" are recovered by extracting carrageenan from cleaned and washed seaweed using hot alkaline solutions at around 95–110 °C. The alkaline solution not only helps in dissolving the carrageenan but also achieves the transformation of the precursors μ – carrageenan and ν – carrageenan into κ – carrageenan and ι – carrageenan, respectively. Subsequent filtering removes the remaining seaweed matrix, and then carrageenan is precipitated by adding alcohol (mainly isopropanol), or by gel forming in potassiumchloride solution (i.e. "gel press process"). In the gel press pathway, the major part of water is removed after gelling by squeezing or freeze-thawing. In contrast to the alcohol precipitated product, the gel press product therefore usually contains higher amounts of potassiumchloride. After precipitation, the carrageenans are dried and milled. Semi-refining is the "younger" technology, which does not extract the carrageenan from the seaweed matrix, but treats the matrix with aqueous potassium hydroxide at around 75 °C to dissolve and remove soluble compounds other than carrageenan, i.e. mainly salts, soluble proteins, and soluble sugars. The embedded carrageenan is kept in the gel state and does not dissolve into the solution, since the process is operated with salt concentrations that keep the carrageenan below its gel melting temperature. Nevertheless, the transformation of the precursors from μ – carrageenan to κ – carrageenan is still taking place. The semi-refining technology is less expensive than the RC extraction process, since the costs for carrageenan precipitation or solvent recovery are avoided. The extracted primary

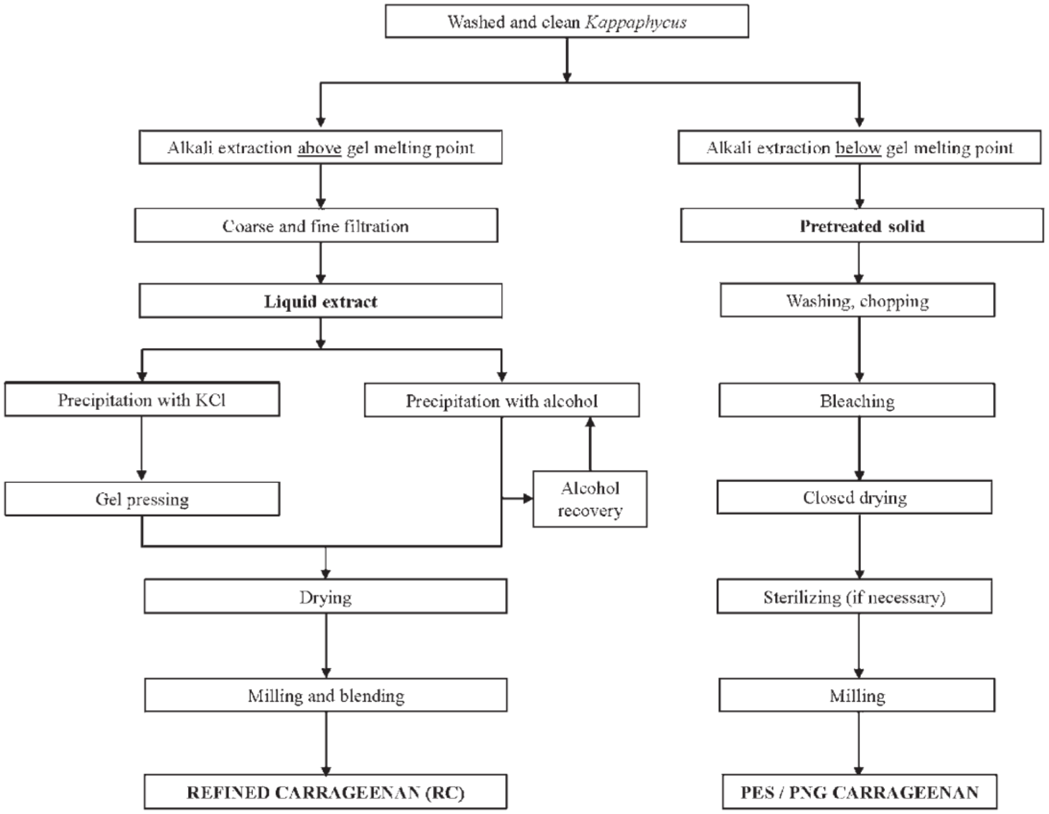

Washed and clean *Kappaphycus*
Alkali extraction above gel melting point
Alkali extraction below gel melting point
Coarse and fine filtration
Pretreated solid
Liquid extract
Washing, chopping
Precipitation with KCl
Precipitation with alcohol
Bleaching
Alcohol recovery
Gel pressing
Closed drying
Drying
Sterilizing (if necessary)
Milling and blending
Milling
REFINED CARRAGEENAN (RC)
PES / PNG CARRAGEENAN

Fig. 10.2 Carrageenan production processes (Modified from McHugh 2003 and Phillips 1996)

product of the semi-refining process is dried and milled to yield a product of lower quality termed "seaweed flour", "alkali modified flour (AMF)", or "semi-refined carrageenan (SRC)", which is not suitable for human food application but is destined for pet food production. Higher qualities of SRC, termed "Processed *Eucheuma* Seaweed – PES" or "Philippine Natural Grade – PNG", which are suitable for food use, are achieved by an optional, additional bleaching or a drying step in a closed system to maintain low levels of microbial contamination. In contrast to RC, PES/PNG still contains the cellulose of the original seaweed. This distinction is also made in the European legislation for food, where PES is represented by its own number (e.g. E407a in contrast to E407 for RC), and is allowed to contain up to 15% cellulose (McHugh 2003; Phillips 1996; Rhein-Knudsen et al. 2015; McHugh 1987; Commission 1996).

RC has been, and is still mainly, produced in Europe and the US, while semi-refined products are mainly produced in Asia. In the decade 1999–2009 the major commercial production shifted slightly from alcohol precipitated to gel press process carrageenan due to lower production costs, and it shifted also considerably from low quality SRC to PES. The production of PES increased from 9,200 MT in 1999 to 20,500 MT in 2009, an increase from 22 to 41% of the global carrageenan production. The total global carrageenan production was estimated to be 50,000 MT in 2009 and 60,000 MT in 2015 (US$ 626 million) (Rhein-Knudsen et al. 2015; Bixler and Porse 2011).

10.4 Lessons from a Lignocellulose Bio-Refinery: Options for a Red Seaweed Bio-Refinery

Since the industrial production of carrageenan from *Kappaphycus* is a mature and well-established technology and the recovered carrageenan is well-established on the global market, *Kappaphycus* bio-refinery systems should be primarily based on carrageenan production. Yet, an integrated sustainable bio-refinery should aim to use as many compounds of the harvested algal biomass as possible, for production of valuable products.

Effluent solutions from carrageenan recovery containing mineral salts may be used for fertilizer. The use of seaweed for fertilizer and soil conditioner is generally well known and traditionally practiced (McHugh 2003). Seaweed extracts of various species are also well known to stimulate plant growth, a phenomenon which is attributed to growth regulators (Chapman and Chapman 1980; Crouch and van Staden 1993). In the "juice" of *K. alvarezii*, plant growth regulators such as indole 3-acetic acid, gibberellin GA3, kinetin and zeatin have been identified (Prasad et al. 2010; Zodape et al. 2009). A method was proposed for the recovery of seaweed juice for fertilizer and foliar spray application in addition to carrageenan production from the seaweed solid (Eswaran et al. 2005). For that, the juice, containing various minerals, mainly sodium, potassium, chloride and sulphate, as well as 1–1.4% organic matter (Zodape et al. 2009), is separated by crushing and filtering the freshly harvested seaweed. After separation of the juice, the remaining seaweed matter is dried and further processed by state-of-the-art carrageenan recovery methods (Eswaran et al. 2005). Amongst others, the main benefit of this method may lie in the fact that the juice is not subject to harsh conditions such as alkaline treatment, which might decompose parts of the dissolved organic compounds. Besides direct use for fertilizer, further valorization of the juice, e.g. by recovery of bioactives or pigments, may be an option.

Reddy et al. (2015) proposed a seaweed bio-refinery that starts with aqueous extraction of the fresh seaweed to get pigments from the extract by precipitation with ammonium sulphate. The algal matter is then subjected to lipid extraction with a chloroform-methanol solvent mixture. If *Kappaphycus* is processed, the extracted solid is treated with KOH solution to dissolve and precipitate the carrageenan while cellulose can be obtained from the residual solid of the carrageenan recovery (Reddy et al. 2015).

The major part of carrageenan in *K. alvarezii* is hydro-soluble, while the cellulose is mainly hydro-insoluble (Lechat et al. 1997). Insoluble residues after carrageenan extraction consequently contain mainly cellulose, small amounts of mannose and xylose-based polymers, as well as residual galactose and anhydro-galactose, depending on the efficiency of the carrageenan extraction process (Phillips 1996; Masarin et al. 2016). In native *Kappaphycus*, cellulose contributes to less than 15% to the dry matter (Phillips 1996). Cellulose can be enzymatically hydrolyzed to obtain glucose to be used as a fermentation substrate (Reddy et al. 2015), since there are different fermentation pathways using glucose as a carbon source, e.g. production of bioethanol, biobutanol, lactic acid, succinic acid, or poly-hydroxy-alcanoates (PHA). The cellulose fraction in the laboratory-scale production of SRC for instance, was reported to be nearly completely hydrolyzed by commercially available cellulases (Masarin et al. 2016).

Proteins could be another interesting by-product, since they make up a considerable share of the *Kappaphycus* dry matter (Table 10.1). The protein quality of seaweeds in terms of essential amino acids is reported to be comparable or even superior to traditional protein sources, such as soybean meal, or fish meal. However, the concentration of essential amino acids in the seaweed dry matter is lower, and the variations between different species are high, requiring development of suitable standardization technologies for protein concentration and extraction (Angell et al. 2016). During the alkaline treatments used for conventional carrageenan production, any soluble proteins are usually dissolved in the extraction solutions. In a recent semi-refining type laboratory-scale study, for example, a reduction in protein content of about 90% was reported for KOH (6% w/v aqueous solution) treated *K. alvarezii*strains (Masarin et al. 2016). Yet, alkaline conditions lead to denaturation and hydrolysis of proteins. The recovery of native proteins thus should be performed prior to alkaline treatment. An alternative valorization, which might be less affected by the pre-hydrolyzation of proteins, could be the conversion of amino acids to N-containing chemicals, e.g. glutamic acid conversion to products such as N-methypyrrolidine, succinonitril, or acetonitrile (Lammens et al. 2012).

Apart from the alkaline-based technologies, advanced alternative methods for the recovery of carrageenan have been proposed in recent years. Accordingly carrageenans can be successfully enzymatically extracted using proteases and cellulases. Even several decades ago this approach was considered as an alternative production route (Niwano 1970; Amat et al. 2000; Zamorano Palma et al. 2002). However, transfer to production-scale was not economical at that time. The strong decrease in enzyme costs for degradation of lignocellulose in the last decade, however, might now open this route for commercialization. In addition, sulphurylases, the enzymes that naturally catalyze the transformation of D- into DA-units, have been tested to convert the precursors to κ – or ι – carrageenan, which would allow the elimination of alkaline conditions (Genicot-Jancour et al. 2009). Unfortunately, no recombinant production of this enzyme has been described so far, which would be a requirement for it application at low cost. Rhein-Knudsen et al. (2015) recently summarized strategies for enzyme-based processes. Besides the recovery of carrageenan, enzyme-based technologies may also offer new perspectives for enhanced by-product separation and valorization.

Figure 10.3 outlines an integrated bio-refinery for advanced enzyme-based processing with respect to the state of knowledge discussed above. The particular steps proposed

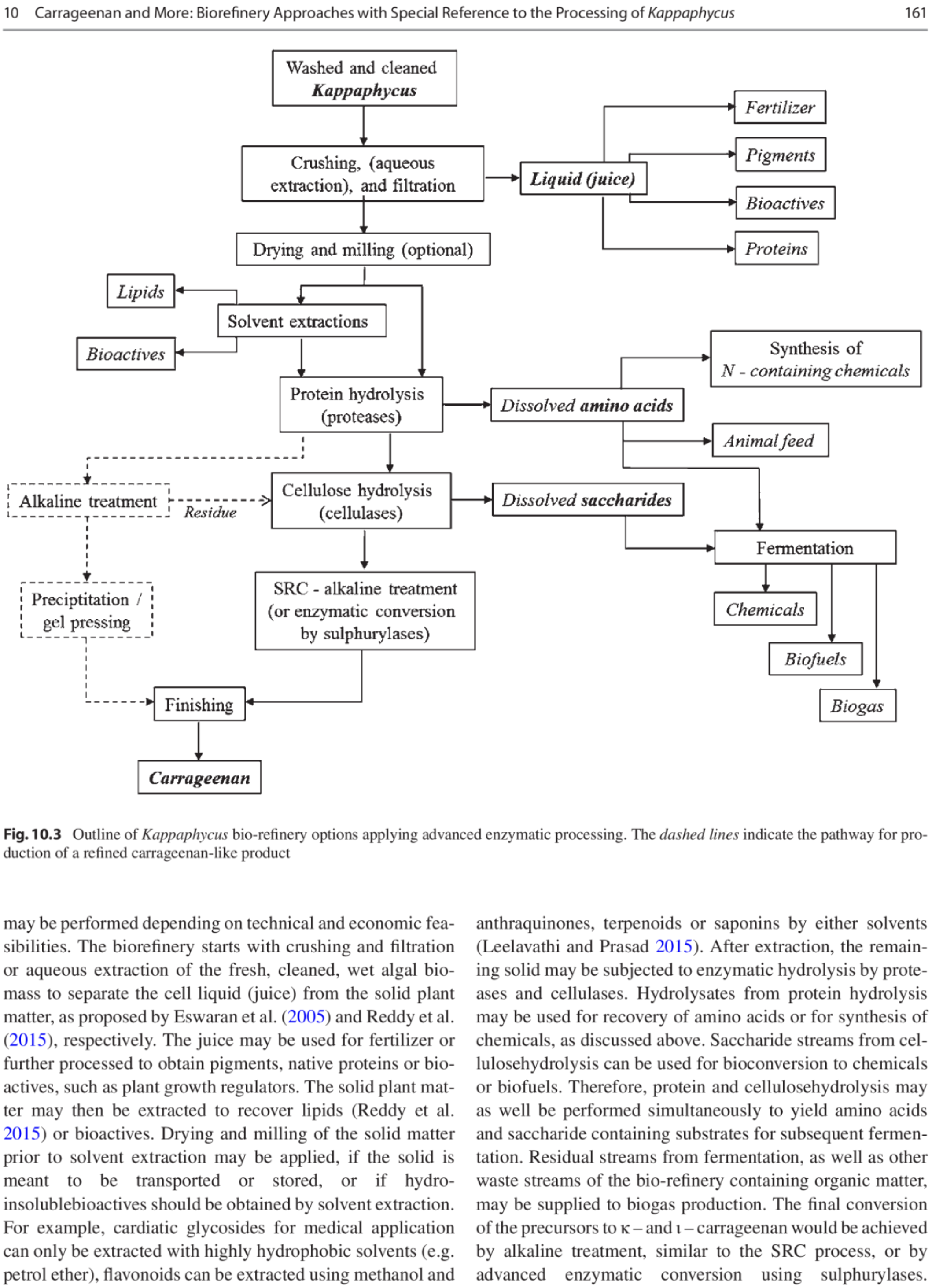

Washed and cleaned **Kappaphycus**
Crushing, (aqueous extraction), and filtration
Liquid (juice)
Fertilizer
Pigments
Bioactives
Proteins
Drying and milling (optional)
Lipids
Solvent extractions
Bioactives
Protein hydrolysis (proteases)
Dissolved ***amino acids***
Synthesis of *N - containing chemicals*
Animal feed
Alkaline treatment
Residue
Cellulose hydrolysis (cellulases)
Dissolved ***saccharides***
Fermentation
Chemicals
Biofuels
Biogas
Preciptitation / gel pressing
SRC - alkaline treatment (or enzymatic conversion by sulphurylases)
Finishing
Carrageenan

Fig. 10.3 Outline of *Kappaphycus* bio-refinery options applying advanced enzymatic processing. The *dashed lines* indicate the pathway for production of a refined carrageenan-like product

may be performed depending on technical and economic feasibilities. The biorefinery starts with crushing and filtration or aqueous extraction of the fresh, cleaned, wet algal biomass to separate the cell liquid (juice) from the solid plant matter, as proposed by Eswaran et al. (2005) and Reddy et al. (2015), respectively. The juice may be used for fertilizer or further processed to obtain pigments, native proteins or bioactives, such as plant growth regulators. The solid plant matter may then be extracted to recover lipids (Reddy et al. 2015) or bioactives. Drying and milling of the solid matter prior to solvent extraction may be applied, if the solid is meant to be transported or stored, or if hydro-insolublebioactives should be obtained by solvent extraction. For example, cardiatic glycosides for medical application can only be extracted with highly hydrophobic solvents (e.g. petrol ether), flavonoids can be extracted using methanol and anthraquinones, terpenoids or saponins by either solvents (Leelavathi and Prasad 2015). After extraction, the remaining solid may be subjected to enzymatic hydrolysis by proteases and cellulases. Hydrolysates from protein hydrolysis may be used for recovery of amino acids or for synthesis of chemicals, as discussed above. Saccharide streams from cellulosehydrolysis can be used for bioconversion to chemicals or biofuels. Therefore, protein and cellulosehydrolysis may as well be performed simultaneously to yield amino acids and saccharide containing substrates for subsequent fermentation. Residual streams from fermentation, as well as other waste streams of the bio-refinery containing organic matter, may be supplied to biogas production. The final conversion of the precursors to κ – and ι – carrageenan would be achieved by alkaline treatment, similar to the SRC process, or by advanced enzymatic conversion using sulphurylases.

Alternatively, carrageenan may be extracted after proteinhydrolysis by an alkaline solution and precipitated to get a refined carrageenan - like product. In that case, saccharides would be recovered from the solid residue of alkaline extraction, as proposed by Reddy et al. (2015).

An alternative to the afore-mentioned strategies for valorization of the red algal biomass could be the strategy of complete saccharification of polysaccharides (including carrageenan) to generate sugars for the subsequent production of bioethanol or commodity chemicals via fermentation, similar to lignocellulosic bioethanol production. The difference to lignocellulosic treatment lies in the milder conditions for hydrolysis needed to release reducing monosaccharides (0.2 M H_2SO_4, 15 min, 130 °C) from algae (Meinita et al. 2012). This is possible due to the absence of lignin and the lower concentrations of crystalline cellulose. Chemical heterogeneous catalysts such as Amberlyst™ -15 can also be used to hydrolyze carbohydrates, making it easier to recover, but with lower yields (Tan et al. 2013). In general, lower fermentation product yields are obtained from seaweeds for two reasons. Firstly, ordinary fermentative microorganisms (e.g. *Saccharomyces cerevisiae, Zymomonas mobilis*) are not capable of catabolizing 3,6-anhydro-galactose. However, the recent discovery and recombinant production of the two key catabolic enzymes of 3,6-anhydro-galactose from marine bacteria enabled ethanologenic strains of *E. coli* to grow and produce ethanol in agarose hydrolysates (Yun et al. 2015). Secondly, the galactose present in carrageenan is metabolized more slowly than glucose in classic fermentative organisms. This can be overcome by pre-culturing the yeasts in galactose medium, which diminishes the glucose inhibition and prepares the galactose metabolism in the cell (Hargreaves et al. 2013). Khambhaty et al. (2012) produced ethanol from the solid residues of pressed *Kappaphycus* with the yeast *S. cerevisiae*, reporting ethanol conversion of ca. 80% of reducing sugars after acid hydrolysis. Enzymatic hydrolysis using commercial enzymes for saccharification and subsequent fermentation has also been demonstrated. However, a modest hydrolysis yield of 62% was obtained, suggesting the need for specific carrageenases (Abd-Rahim et al. 2014). Other studies proved that simultaneous saccharification and fermentation of a cellulose containing stream separated from a liquid galactose stream could improve ethanol production, obtaining 105 L of ethanol per ton of seaweed (Hargreaves et al. 2013). More recently, this two-stream model was applied to generate concentrated sugar hydrolysates (98.7 g L^{-1}), by a combined approach, using a solid catalyst (Dowex™ Dr.-G8) and a commercial cellulase, yielding 11.6 g L^{-1}bioethanol from each fraction. After performing an economic analysis, the authors concluded that the fixed price of bioethanol produced from red seaweed was competitive with that obtained from other feedstocks (Tan and Lee 2016). However, despite the successful examples for the production of bioethanol from *Kappaphycus*, the economic viability of all these carrageenan hydrolyzing and fermenting strategies has to be assessed in contrast to the production of RC or SRC. With the carrageenan market prices (e.g. 6–15 US$ per kg in 2009, depending on quality grade (Bixler and Porse 2011); retail price of ca. 10.4 US$ per kg in 2015 (Rhein-Knudsen et al. 2015), similar profitable products from the hydrolysis and fermentation of carrageenan should be established that justify this process strategy.

References

Abd-Rahim F, Wasoh H, Zakaria MR, Ariff A, Kapri R, Ramli N, Siew-Ling L (2014) Production of high yield sugars from *Kappaphycus alvarezii* using combined methods of chemical and enzymatic hydrolysis. Food Hydrocoll 42:309–315

Amat M, Masoyer J, Demande F (2000) Method for purifying carrageenans FR 2794474 A1 20001208. FR 2794474 A1 2000120

Angell AR, Angell SF, de Nys R, Paul NA (2016) Seaweed as a protein source for mono-gastric livestock. Trends Food Sci Technol 54:74-84. doi:http://dx.doi.org/10.1016/j.tifs.2016.05.014

Azevedo G, Hilliou L, Bernardo G, Sousa-Pinto I, Adams RW, Nilsson M, Villanueva RD (2013) Tailoring kappa/iota-hybrid carrageenan from *Mastocarpus stellatus* with desired gel quality through pre-extraction alkali treatment. Food Hydrocoll 31(1):94–102

Azevedo G, Torres MD, Sousa-Pinto I, Hilliou L (2015) Effect of pre-extraction alkali treatment on the chemical structure and gelling properties of extracted hybrid carrageenan from *Chondrus crispus* and *Ahnfeltiopsis devoniensis*. Food Hydrocoll 50:150–158

Barahona T, Prado HJ, Bonelli PR, Cukierman AL, Fissore EL, Gerschenson LN, Matulewicz MC (2015) Cationization of kappa- and iota-carrageenan – characterization and properties of amphoteric polysaccharides. Carbohydr Polym 126:70–77

Bixler HJ, Porse H (2011) A decade of change in the seaweed hydrocolloids industry. J Appl Phycol 23(3):321–335

Bixler HJ, Johndro K, Falshaw R (2001) Kappa-2 carrageenan: structure and performance of commercial extracts: II. Performance in two simulated dairy applications. Food Hydrocoll 15(4–6):619–630

Campo VL, Kawano DF, Silva DB Jr, Carvalho I (2009) Carrageenans: biological properties, chemical modifications and structural analysis – a review. Carbohydr Polym 77(2):167–180

Chapman VJ, Chapman DJ (1980) Chapter 2. In: Seaweeds and their uses, 3rd edn. Chapman and Hall, London, pp 334–339

Commission Europena (1996) Commission directive 96/77/EC of laying down specific purity criteria on food additives other than colours and sweeteners. The European Commission

Crouch IJ, van Staden J (1993) Evidence for the presence of plant growth regulators in commercial seaweed products. Plant Growth Regul 13(1):21–29

Das AK, Sharma M, Mondal D, Prasad K (2016) Deep eutectic solvents as efficient solvent system for the extraction of κ-carrageenan from *Kappaphycus alvarezii*. Carbohydr Polym 136:930–935

de Araújo CA, Noseda MD, Cipriani TR, Gonçalves AG, Duarte MER, Ducatti DRB (2013) Selective sulfation of carrageenans and the influence of sulfate regiochemistry on anticoagulant properties. Carbohydr Polym 91(2):483–491

De Ruiter GA, Rudolph B (1997) Carrageenan biotechnology. Trends Food Sci Tech 8(12):389–395

Dul M, Paluch KJ, Kelly H, Healy AM, Sasse A, Tajber L (2015) Self-assembled carrageenan/protamine polyelectrolyte nanoplexes—investigation of critical parameters governing their formation and characteristics. Carbohydr Polym 123:339–349

Eswaran K, Ghosh PK, Siddhata AK, Patolia JS, Periyasamy C, Mehta AS, Mody KH, Ramavat BK, Prasad K, Rajyaguru MR, Reddy CRK, PAndya JB, Less AT (2005) Integrated method for production of carrageenan and liquid fertilizer from fresh seaweeds. USA Patent US6893479 B2

Fayaz M, Namitha KK, Murthy KNC, Swamy MM, Sarada R, Khanam S, Subbarao PV, Ravishankar GA (2005) Chemical composition, iron bioavailability, and antioxidant activity of *Kappaphycus alvarezii* (Doty). J Agric Food Chem 53(3):792–797

Gaweł K, Karewicz A, Bielska D, Szczubiałka K, Rysak K, Bonarek P, Nowakowska M (2013) A thermosensitive carrageenan-based polymer: synthesis, characterization and interactions with a cationic surfactant. Carbohydr Polym 96(1):211–217

Genicot SM, Groisillier A, Rogniaux H, Meslet-Cladière L, Barbeyron T, Helbert W (2014) Discovery of a novel iota carrageenan sulfatase isolated from the marine bacterium *Pseudoalteromonas carrageenovora*. Front Chem 26:1–15

Genicot-Jancour S, Poinas A, Richard O, Potin P, Rudolph B, Kloareg B, Helbert W (2009) The cyclization of the 3,6-anhydro-galactose ring of ι-carrageenan is catalyzed by two D-galactose-2,6-sulfurylases in the red alga *Chondrus crispus*. Plant Physiol 151(3):1609–1616

Guibet M, Boulenguer P, Mazoyer J, Kervarec N, Antonopoulos A, Lafosse M, Helbert W (2008) Composition and distribution of carrabiose moieties in hybrid κ−/ι-carrageenans using carrageenases. Biomacromolecules 9(1):408–415

Hargreaves PL, Barcelos CA, Costa ACA, Junior NP (2013) Production of ethanol 3G from *Kappaphycus alvarezii*: evaluation of different process strategies. Bioresoure Technol 134:257–263

Helbert W (2012) Analysis and modification of carrageenan structure using enzymes. In: Gums and stabilisers for the food industry 16. Royal Society of Chemistry, Cambridge, pp 19–25

Hilliou L (2014) Chapter two – hybrid carrageenans: isolation, chemical structure, and gel properties. In: Se-Kwon K (ed) Adv Food Nutr Res 72:17–43

Hilliou L, Sereno AM, Gonçalves MP (2014) Gel setting of hybrid carrageenan solutions under steady shear. Food Hydrocoll 35:531–538

Hu X, Jiang X, Aubree E, Boulenguer P, Critchley AT (2006) Preparation and *in vivo* antitumor activity of κ-carrageenan oligosaccharides. Pharm Biol 44(9):646–650

Jung KA, Lim S-R, Kim Y, Park JM (2013) Potentials of macroalgae as feedstocks for biorefinery. Bioresour Technol 135:182–190

Karthikeyan S, Selvasekarapandian S, Premalatha M, Monisha S, Boopathi G, Aristatil G, Arun A, Madeswaran S (2016) Proton-conducting I-Carrageenan-based biopolymer electrolyte for fuel cell application. Ionics:1–6. doi:10.1007/s11581-016-1901-0

Khambhaty Y, Mody K, Gandhi MR, Thampy S, Maiti P, Brahmbhatt H, Eswaran K, Ghosh PK (2012) Kappaphycus alvarezii as a source of bioetanol. Bioresour Technol 103

Lammens TM, Franssen MCR, Scott EL, Sanders JPM (2012) Availability of protein-derived amino acids as feedstock for the production of bio-based chemicals. Biomass Bioenergy 44:168–181

Larotonda FDS, Torres MD, Gonçalves MP, Sereno AM, Hilliou L (2016) Hybrid carrageenan-based formulations for edible film preparation: benchmarking with kappa carrageenan. J Appl Polym Sci 133 (2). doi:10.1002/app.42263

Lau TY, Vittal DF, Chew CSY, Yong WTL (2014) Antiproliferative potential of extracts from *Kappaphycus* seaweeds on HeLa cancer cell lines. Sains Malays 43(12):1895–1900

Lechat H, Amat M, Mazoyer J, Gallant DJ, Buléon A, Lahaye M (1997) Cell wall composition of the carrageenophyte *Kappaphycus alvarezii* (Gigartinales, Rhodophyta) partitioned by wet sieving. J Appl Phycol 9(6):565–572

Leelavathi MS, Prasad MP (2015) Comparative analysis of phytochemical compounds of marine algae isolated from Gulf of Mannar. World J Pharm Pharm Sci 4(5):640–654

Leiter A, Ludwig A, Gaukel V (2017) Influence of heating temperature, pH and ions on recrystallization inhibition activity of κ-carrageenan in sucrose solution. J Food Eng 195:14–20. doi:http://dx.doi.org/10.1016/j.jfoodeng.2016.09.016

Liang W, Mao X, Peng X, Tang S (2014) Effects of sulfate group in red seaweed polysaccharides on anticoagulant activity and cytotoxicity. Carbohydr Polym 101:776–785

Ling ALM, Yasir SM, Matanjun P, Abu Bakar MF (2013) Antioxidant activity, total phenolic and flavonoid contents of selected commercial seaweeds of Sabah, Malaysia. Int J Pharm Phytopharm Res 3(3):234–238

Liu J, Zhan X, Wan J, Wang Y, Wang C (2015) Review for carrageenan-based pharmaceutical biomaterials: favourable physical features versus adverse biological effects. Carbohydr Polym 121:27–36

Long J, Yu X, Xu E, Wu Z, Xu X, Jin Z, Jiao A (2015) In situ synthesis of new magnetite chitosan/carrageenan nanocomposites by electrostatic interactions for protein delivery applications. Carbohydr Polym 131:98–107

Masarin F, Cedeno FRP, Chavez EGS, de Oliveira LE, Gelli VC, Monti R (2016) Chemical analysis and biorefinery of red algae *Kappaphycus alvarezii* for efficient production of glucose from residue of carrageenan extraction process. Biotechnol Biofuels 9(1):1–12. doi:10.1186/s13068-016-0535-9

McHugh DJ (1987) Production and utilization of products from commercial seaweeds. FAO Fisheries Technical Paper No 288

McHugh DJ (2003) A guide to the seaweed industry. FAO Fisheries Technical Paper No 441:61–72

Meinita MDN, Yong YK, Kang GT, Jeong GT, Koo HM, Park SM (2012) Bioethanol production from the acid hydrolysate of the carrageenophyte *Kappaphycus alvarezii* (cottonii). J Appl Phycol 24:857–862

Mishra PC, Jayasankar R, Seema C (2006) Yield and quality of carrageenan from *Kappaphycus alvarezii* subjected to different physical and chemical treatments. Seaweed Res Util 28(1):113–117

Niwano S (1970) Carrageenan JP 1970-92570. JP:1970–92570

Phillips GO (1996) The chemical identification of PNG-carrageenan. In: Phillips GO, Williams PA, Wedlock DJ (eds) Gums and stabilisers for the food industry, vol 8. IRL, Oxford, p 403

Prasad K, Das AK, Oza MD, Brahmbhatt H, Siddhanta AK, Meena R, Eswaran K, Rajyaguru MR, Ghosh PK (2010) Detection and quantification of some plant growth regulators in a seaweed-based foliar spray employing a mass spectrometric technique sans chromatographic separation. J Agric Food Chem 58(8):4594–4601

Préchoux A, Genicot S, Rogniaux H, Helbert W (2013) Controlling carrageenan structure using a novel Formylglycine-dependent sulfatase, an Endo-4S-iota-carrageenan sulfatase. Mar Biotechnol 15(3):265–274. doi:10.1007/s10126-012-9483-y

Préchoux A, Genicot S, Rogniaux H, Helbert W (2016) Enzyme-assisted preparation of furcellaran-like κ−/β -carrageenan. Mar Biotechnol 18(1):133–143. doi:10.1007/s10126-015-9675-3

Rajasulochana P, Krishnamoorthy P, Dhamotharan R (2012) Experimental studies to determine various vitamins available in *Kappaphycus alvarezii*. J Chem Pharm Res 4(12):5176–5179

Rajasulochana P, Kumar S, Krishnamoorthy P (2015) A new antimicrobial bromophenol from *Kappaphycus alvarezii.* IN2014CH00602A

Reddy CRK, Baghel RS, Trivedi N, Kumari P, Gupta V, Prasad K, Meena R (2015) An integrated process to recover a spectrum of bioproducts from fresh seaweeds. Patents WO 2015102021 A1

Rhein-Knudsen N, Ale M, Meyer A (2015) Seaweed hydrocolloid production: an update on enzyme assisted extraction and modification technologies. Mar Drugs 13(6):3340

Seta L, Baldino N, Gabriele D, Lupi FR, de Cindio B (2013) The influence of carrageenan on interfacial properties and short-term stability of milk whey proteins emulsions. Food Hydrocoll 32(2):373–382

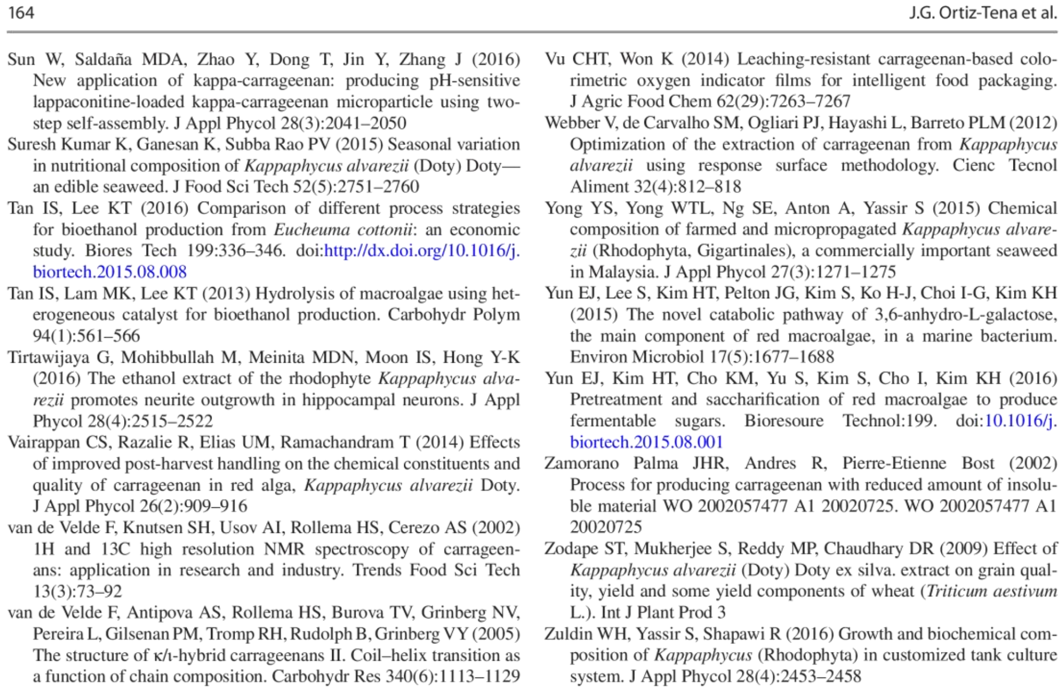

Sun W, Saldaña MDA, Zhao Y, Dong T, Jin Y, Zhang J (2016) New application of kappa-carrageenan: producing pH-sensitive lappaconitine-loaded kappa-carrageenan microparticle using two-step self-assembly. J Appl Phycol 28(3):2041–2050

Suresh Kumar K, Ganesan K, Subba Rao PV (2015) Seasonal variation in nutritional composition of *Kappaphycus alvarezii* (Doty) Doty—an edible seaweed. J Food Sci Tech 52(5):2751–2760

Tan IS, Lee KT (2016) Comparison of different process strategies for bioethanol production from *Eucheuma cottonii*: an economic study. Biores Tech 199:336–346. doi:http://dx.doi.org/10.1016/j.biortech.2015.08.008

Tan IS, Lam MK, Lee KT (2013) Hydrolysis of macroalgae using heterogeneous catalyst for bioethanol production. Carbohydr Polym 94(1):561–566

Tirtawijaya G, Mohibbullah M, Meinita MDN, Moon IS, Hong Y-K (2016) The ethanol extract of the rhodophyte *Kappaphycus alvarezii* promotes neurite outgrowth in hippocampal neurons. J Appl Phycol 28(4):2515–2522

Vairappan CS, Razalie R, Elias UM, Ramachandram T (2014) Effects of improved post-harvest handling on the chemical constituents and quality of carrageenan in red alga, *Kappaphycus alvarezii* Doty. J Appl Phycol 26(2):909–916

van de Velde F, Knutsen SH, Usov AI, Rollema HS, Cerezo AS (2002) 1H and 13C high resolution NMR spectroscopy of carrageenans: application in research and industry. Trends Food Sci Tech 13(3):73–92

van de Velde F, Antipova AS, Rollema HS, Burova TV, Grinberg NV, Pereira L, Gilsenan PM, Tromp RH, Rudolph B, Grinberg VY (2005) The structure of κ/ι-hybrid carrageenans II. Coil–helix transition as a function of chain composition. Carbohydr Res 340(6):1113–1129

Vu CHT, Won K (2014) Leaching-resistant carrageenan-based colorimetric oxygen indicator films for intelligent food packaging. J Agric Food Chem 62(29):7263–7267

Webber V, de Carvalho SM, Ogliari PJ, Hayashi L, Barreto PLM (2012) Optimization of the extraction of carrageenan from *Kappaphycus alvarezii* using response surface methodology. Cienc Tecnol Aliment 32(4):812–818

Yong YS, Yong WTL, Ng SE, Anton A, Yassir S (2015) Chemical composition of farmed and micropropagated *Kappaphycus alvarezii* (Rhodophyta, Gigartinales), a commercially important seaweed in Malaysia. J Appl Phycol 27(3):1271–1275

Yun EJ, Lee S, Kim HT, Pelton JG, Kim S, Ko H-J, Choi I-G, Kim KH (2015) The novel catabolic pathway of 3,6-anhydro-L-galactose, the main component of red macroalgae, in a marine bacterium. Environ Microbiol 17(5):1677–1688

Yun EJ, Kim HT, Cho KM, Yu S, Kim S, Cho I, Kim KH (2016) Pretreatment and saccharification of red macroalgae to produce fermentable sugars. Bioresoure Technol:199. doi:10.1016/j.biortech.2015.08.001

Zamorano Palma JHR, Andres R, Pierre-Etienne Bost (2002) Process for producing carrageenan with reduced amount of insoluble material WO 2002057477 A1 20020725. WO 2002057477 A1 20020725

Zodape ST, Mukherjee S, Reddy MP, Chaudhary DR (2009) Effect of *Kappaphycus alvarezii* (Doty) Doty ex silva. extract on grain quality, yield and some yield components of wheat (*Triticum aestivum* L.). Int J Plant Prod 3

Zuldin WH, Yassir S, Shapawi R (2016) Growth and biochemical composition of *Kappaphycus* (Rhodophyta) in customized tank culture system. J Appl Phycol 28(4):2453–2458

B1.3. Biotechnological processing of hydrocolloids

In the previous chapter, the importance of finding new methods for adding value to seaweed biomass and its products was emphasized. The bio refinery concept is a promising alternative not only for red but also for brown seaweed (Kostas et al., 2017). In this context, the application of enzymes plays a key role in the development of such processes, as the extraction of bioactive compounds, for example, can be performed under much milder conditions (Charoensiddhi et al., 2017). Furthermore, bio catalysis allows a much more targeted modification of the substrate of interest than a classical chemical conversion. For example, carbohydrate-active enzymes have enabled the advancement of valuable products for the food industry, such as cyclodextrin, isomaltulose, high fructose corn syrup, and glucuronic acid. An overview of the most industrial relevant enzymes for carbohydrates is shown in Table 16.

Table 16: Carbohydrate-active enzymes of industrial relevance

Enzyme name	Enzyme type	Substrate	Product	Application
Cyclodextrin Glycosyl transferase	Transferase	Liquefied Starch	Cyclodextrin	Drug delivery (pharma) Odor absorber
Sucrose glycosyl mutase	Isomerase	Sucrose	Isomaltulose (Palatinose®)	Sweetener
Invertase	Hydrolase	Sucrose	Invert sugar	Beverages
Glucose oxidase	Oxidase	Glucose	Glucuronic acid	Energy drinks
Pectinase	Hydrolase	Pectin	Galacturonic acid	Juice industry
β-Galactosidase	Hydrolase	Lactose	Glucose + Galactose	Lactose-free dairy products

The examples presented above are well established bio catalysts that are active on substrates from terrestrial biomass sources. Conversely, the discovery and development of enzymes active on marine hydrocolloids exhibited little advances in the past years. Similarly to microalgae, current methods involve the sheer application of commercially available enzyme mixtures developed for other substrates, especially hydrolases (Rhein-Knudsen et al., 2015). Thus, a need for specific enzymes active on hydrocolloids has been identified. Carrageenases, for example, can generate sulfated oligosaccharides with bioactive properties for the pharmaceutical industry. Other potential applications include: bioethanol production, detergent additives, textiles, and generation of protoplasts from algae for their study (Chauhan & Saxena, 2016).

Further enzymes apart from hydrolases and transferases have become relevant for processing carbohydrates, such as polysaccharide lyases, carbohydrate esterases, oxidases, and sulfatases (Cantarel et al., 2009; Gurpilhares et al., 2016). Due to their ability to modify the chemical structure of the sugar chain without breaking it, such enzymes are very promising for developing new products or even improving the properties of existing ones. Carbohydrate sulfatases and sulfurylases that act with a high degree of regioselectivity on carrageenan, for example, could be used to tailor the rheological properties of this product (Hanson et al., 2004). Thanks to the improvements in bioinformatics, numerous potential sources for sulfatases have been annotated in the last decades, especially from marine organisms (Barbeyron et al., 2016; Wegner et al., 2013). Based on these sequences, endo-sulfatases for converting κ- and ι- carrageenan into hybrid forms were recently purified from the marine bacteria *Pseudoalteromonas atlantica* and *Pseudoalteromonas carrageenovora* (Genicot et al., 2014; Prechoux et al., 2016). However, this was achieved with moderate success, as the activity of the recombinant variant showed a much lower activity than the variant directly isolated from the marine bacteria. Most importantly, their discovery and purification involved numerous chromatographic steps as well as activity analysis using ion chromatography, so that these issues remain important limiting factors for a faster development (Helbert, 2017).

As for other type of enzymes, this problem can be solved by applying medium- and high-throughput methods to detect relevant activity, as has been shown for different types of carbohydrate-active enzymes (Fer et al., 2012). At the same time, such methods allow the application of functional screening using metagenomics. This is achieved by extracting and isolating DNA from environmental samples, size selection and insertion in fosmids, which can be then expressed in suitable systems (Lam et al., 2015). The use of metagenomics has been successfully applied for discovering different types of enzymes, such as cellulases (Leis et al., 2015). For a screening procedure to be successful, appropriate assays for detecting enzyme activity must be developed. This is an especially challenging task for sulfatases, as the available sulfate detection methods are either low-throughput (i.e., ion chromatography) or not enough sensitive for such screenings. An assay compatible with suitable screening platforms would greatly facilitate discovering and even engineering sulfatases for the biotechnological processing of hydrocolloids from macroalgae, which would increase their value added in different fields.

B2. Scope of the work

The main goal of the second part of this work was to develop, evaluate and validate a detection assay for screening sulfatase activity. The assay is aimed to simplify the discovery of carrageenan-active sulfatases from promising microorganisms, such as marine bacteria. Although some sulfatase screening assays are readily available, their application is limited to chromogenic substrates, such as *p*-nitrophenyl sulfate. This does not guarantee activity on other substrates of interest like sulfated polysaccharides. Therefore, the devised procedure should fulfill special requirements. Firstly, the assay must avoid the use of synthetic substrates, i.e., it should directly detect sulfate as product to generalize its implementation for any kind of sulfatase. Secondly, the assay throughput shall be high enough to screen hundreds of samples within few hours, making it compatible with currently employed robotics. As this requirement excludes chromatographic techniques, an enzymatic colorimetric assay based on known robust reactions was selected. Once the detection strategy is established, it should be improved and adapted for detecting sulfate directly in relevant matrixes for sulfatase reactions, such as organic solvents, enzyme buffers and, most importantly, bacterial cell lysates. The applicability of the assay for screening sulfatases should be finally demonstrated using known and well-established sulfatases. The developed procedure is intended to facilitate the exploration of the bio catalytic potential of marine microbial communities. Thereby, a more efficient conversion of sulfated polysaccharides from macroalgae can be achieved, which enables an added value in different fields.

B3. Materials and Methods

The employed equipment, software, commercial enzymes and consumables for the development of the sulfate assay can be found in section A3.1-4.

B3.1. Cloning

Table 17 provides an overview of the molecular biology tools for cloning the genes involved in the development and validation of the sulfatase assay.

Table 17 Molecular biology tools for cloning the enzymes' genes involved in the sulfatase assay

Enzyme	Gene ID	Gene length (bp)	Organism	Expression vector	Cloned by	Ref.
PPDK	AJ549196	2 667	*Propionibacterium freudenreichii* NBRC 12426	pET-28a(+)	GeneScript	(Kameya et al., 2014)
ATPs / GTPase	*cysDN*	2 344	*Escherichia coli* K12	pET-28a(+)	Self-cloned*	(Sun & Leyh, 2005)
APSk	MET14	614	*Saccharomyces cerevisiae*	pET-28a(+)	GeneScript	(Wei et al., 2002)
PAS	atsA	1 602	*Pseudomonas aeruginosa*	pASK-IBA5 plus	Kurt Faber (TU Graz)	(Schober et al., 2013)
PISA	pisa1	1 989	*Pseudomonas* sp. DSM6611	pET-21a(+)	Kurt Faber (TU Graz)	(Schober et al., 2011)

* Primers for the amplification of *E. coli cysDN* genes:

fw5'-ATATATCTCGAGTTTATCCCCCAGC-3'
rev5'-TATATACCATATGGATCAAATACGAC-3'

B3.2. Heterologous enzyme production

After amplifying the expression vectors using the *E. coli* cloning strain XL1-Blue (transformation by electroporation), the plasmids were purified using the GeneJET^{TM} Plasmid Miniprep kit (Thermo Fischer Scientific). 100 – 300 ng of vector DNA was then transferred into expression strains *via* chemical-transformation or electroporation according to Table 18. The transformed cells were incubated in SOC medium at 37°C for 1 hour. 100 µL of the transformed cells were cultured in LB agar plates at 37°C overnight and one colony was picked and inoculated into 40 mL LB culture medium containing the corresponding selection antibiotic. This pre-culture was grown overnight at

37°C and 20 mL were transferred into 1 L LB medium. When the expression culture reached OD_{600}=0.6, the cells were induced according to Table 18 and the expression was performed at the given time and temperature.

Table 18: Materials employed for over-expressing the enzymes employed for the sulfatase assay

Enzyme	Expression strain	Selection antibiotic	Induction agent	Expression conditions
PPDK	BL21 (DE3) – electrocompetent cells	Kanamycin	IPTG (500 µM)	4 h at 16°C
ATPs / GTPase	BL21 (DE3) – electrocompetent cells	Kanamycin	IPTG (400 µM)	2 h at 37°C
APSk	BL21-Codonplus (DE3) – RIL chemical competent	Kanamycin	IPTG (600 µM)	Overnight at 16°C
PAS	BL21 (DE3) – chemical competent	Carbenicillin	Tetracycline hydrochloride (200 ng μL^{-1})	4 h 37°C and 16°C tested
PISA	BL21 (DE3) – chemical competent	Ampicillin	IPTG (500 µM)	Overnight at 20°C

After expression, the cells were collected by centrifugation (30 min at 6,000 x g) and the pellets were re-suspended (50 – 100 g L^{-1}) in the corresponding washing buffer (Table 19). The cell suspension was then disrupted by sonication using a sonotrode for 25 min, 70% performance with 0.5 seconds intervals in ice. After cell disruption, the debris suspension was centrifuged in high speed centrifugation tubes at 40,000 x g and the tagged, over-expressed proteins were purified by affinity chromatography. Table 19 provides an overview of the columns and buffers used for protein purification. All fractions were analyzed by SDS electrophoresis (see Appendix, Figure A12-15) and the purified fractions were mixed with glycerol at 20% (v/v) final concentration.

Table 19: Materials employed for purifying the enzymes employed for the sulfatase assay. N.A. not applied

Enzyme	Purification column	Washing buffer	Elution buffer	Desalting
PPDK	Affinity Nickel	pH 8 Tris-HCl 20 mM NaCl 300 mM Imidazole 50 mM	pH 8 Tris-HCl 20 mM NaCl 300 mM Imidazole 500 mM	N.A.
ATPs / GTPase	Affinity Nickel	pH 8 Tris-HCl 20 mM NaCl 300 mM Imidazole 50 mM	pH 8 Tris-HCl 20 mM NaCl 300 mM Imidazole 500 mM	pH 8 Hepes 50 mM
APSk	Affinity Nickel	pH 8 Hepes/K^+ 50 mM NaCl 300 mM Imidazole 5 mM	pH 8 Hepes/K^+ 50 mM NaCl 300 mM Imidazole 500 mM	pH 8 Hepes 50 mM
PAS	Affinity Streptavidin (Gravity)	pH 8 Tris-HCl 100 mM NaCl 150 mM	pH 8 Tris-HCl 100 mM NaCl 150 mM EDTA 1 mM Desthiobiotin 2.5 mM	pH 8 Tris 100 mM

Enzyme	Purification column	Washing buffer	Elution buffer	Desalting
PISA	Affinity Nickel	pH 8.2 NaH_2PO_4 50 mM NaCl 300 mM Imidazole 10 mM	pH 8.2 NaH_2PO_4 50 mM NaCl 300 mM Imidazole 150 mM	pH 8.2 Tril-HCl 100 mM

The purified fractions were aliquoted in 1 mL tubes, introduced in liquid nitrogen, and stored until use at –20°C. The concentration was determined using a nanophotometer using the parameters reported in Table 20.

Table 20: Parameters for determining the concentration of purified enzymes prior to addition of glycerol to 20% (v/v) final concentration

Enzyme	ε_{280} (L mol^{-1} cm^{-1})	M (kDa)	c (mg mL^{-1})
PPDK	54,360	98.0	1.62
ATPs / GTPase	93,300	87.7	1.59
APSk	21,500	23.0	4.87
PAS	102,790	59.8	1.89
PISA	82,280	73.9	2.80

B3.3. Synthesis of PISA1 substrate 2-heptyl-sulfate

The synthesis of 2-heptyl-sulfate was carried out as previously described (G. F. White et al., 1980) using the sulfur trioxide triethylamine complex as sulfation agent of the sodium alkoxide (4-fold amounts). Following modifications were performed:

A. The sodium suspension was prepared by adding small pieces of metallic sodium into stirred dry toluene in oxygen-absent conditions (instead of mineral oil dispersion).
B. The sodium alkoxide of 2-heptanol was prepared by adding 16 mmol of 2-heptanol dropwise to the sodium suspension and stirred at 100°C for 30 min, and then overnight at 40°C.
C. The sulfation agent was added to the alkoxide solution at room temperature and stirred overnight (instead of 1h).

The subsequent purification procedure was performed as described by White et. al. (1980).

B3.4. Sulfate analysis of carrageenan TFA hydrolysates

6 mL carrageenan solution (1 g L^{-1}) was prepared in glass tubes and hydrolyzed using 2 M TFA for 90 min at 121°C in a heating block. The resulting hydrolysate was neutralized to pH ~ 8 using a NH_4OH solution (3.2% v/v). The neutralized hydrolysates were further diluted to a final factor of 20 for analysis with the developed enzymatic assay as follows: 50 µL were taken and mixed with 50 µL master mix 1 (HEPES 12.5 mM pH 7.8, GTP and ATP 1 mM, $MgCl_2$ 3 mM, ATPs 0.46 µM,

APSk 5.3 µM) into a micro titer plate. An incubation step at 25°C for 45 min followed and then 100 µL of master mix 2 was added (K_2HPO_4 100 mM pH 6.5, DA-64 100 µM, TPP 50 µM, $MgCl_2$ 100 µM, PEP 500 µM, AMP 500 µM, PPDK 50 mU, POX 50 mU, HRP 200 mU). The plate was then incubated for 30 min at 37°C and $A_{727–540}$ was computed. The resulting signals were compared to a sulfate calibration curve using K_2SO_4 as standard in the range 2.5 – 250 µM, which contained the neutralized TFA matrix.

B4. Results

B4.1. Colorimetric determination of sulfate *via* an enzyme cascade for high-throughput detection of sulfatase activity

In the omics era, HT analyses are essential for discovering, studying, and engineering biocatalysts of medical and synthetic relevance. Carbohydrate sulfatases are one of the most interesting and promising enzymes for the processing of carrageenan, a very important polysaccharide present in macroalgae. Several annotated DNA sequences for this type of enzymes have been reported in various marine bacteria, such as *Rhodopirellula baltica* or *Pseudoalteromonas carrageenovora*. A classical approach for their *de novo* isolation would include tedious steps, such as bacterial culture optimization, enhancement of protein expression, and chromatographic analysis.

To accelerate the discovery of sulfatases from such marine bacteria using functional (meta) genomics, fast and robust sulfate assays are needed. The conventional sulfate detection methods, such as turbidimetry with barium chloride or ion chromatography, are considerably limited for screening sulfatases, as discussed in the publication. On the other hand, the current development of sulfatases is restricted to enzyme activity detection using artificial substrate analogs (e.g., *p*-nitrophenyl sulfate). However, sulfatases acting on polysaccharides such as carrageenan or fucoidan are unlikely to show activity using such substrate analogs. Therefore, alternatives for a rapid detection of sulfate that are compatible with sulfatase screening platforms are required.

In this paper, the optimization of an enzymatic cascade for the sensitive detection of sulfate is firstly shown. The developed method was then validated and characterized using pertinent compounds commonly used for sulfatase reactions, such as buffers, organic solvents, and metallic ions. Lastly, the analytical procedure was adapted for determining sulfate in bacterial lysates. To demonstrate its application for screening sulfatases, the assay was performed as part of an automatable workflow using *E. coli* as expression system. The activity of an aryl sulfatase from *Pseudomonas* sp. (PAS) could be thus confirmed in 96-well format and cross-verified by the photometric analysis of *p*-nitrophenol, the corresponding de-sulfated product. Similarly, the activity of an alkyl sulfatase (PISA1) towards 2-heptyl-sulfate could be verified with an outstanding assay quality for discerning positive hits form negative clones. This method provides an excellent alternative for detecting sulfatase activity directly from bacterial lysates, which set the basis for a much more accelerated study of carrageenan sulfatases.

The author designed and conducted all the experiments and wrote the manuscript under supervision of the paper co-authors, which contributed to content and language of the article.

Colorimetric determination of sulfate *via* an enzyme cascade for high-throughput detection of sulfatase activity

José G. Ortiz-Tena, Broder Rühmann, and Volker Sieber

Analytical Chemistry
2018

Reproduced with permission
DOI: 10.1021/acs.analchem.7b03719

analytical chemistry
Article
Cite This: *Anal. Chem.* XXXX, XXX, XXX−XXX
pubs.acs.org/ac

Colorimetric Determination of Sulfate via an Enzyme Cascade for High-Throughput Detection of Sulfatase Activity

Jose G. Ortiz-Tena,[†] Broder Rühmann,[†] and Volker Sieber*[,†,‡,§,∥]

[†]Chair of Chemistry of Biogenic Resources, Technische Universität München, 94315 Straubing, Germany
[‡]Fraunhofer IGB, Straubing Branch BioCat, 94315 Straubing, Germany
[§]TUM Catalysis Research Center, Ernst-Otto-Fischer-Straße 1, 85748 Garching, Germany
[∥]The University of Queensland, School of Chemistry and Molecular Biosciences, 68 Copper Road, St. Lucia 4072, Australia

Supporting Information

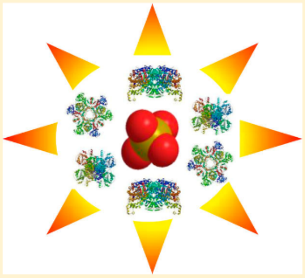

ABSTRACT: High-throughput screening (HTS) methods have become decisive for the discovery and development of new biocatalysts and their application in numerous fields. Sulfatases, a broad class of biocatalysts that hydrolyze sulfate esters, are involved in diverse relevant cellular functions (e.g., signaling and hormonal regulation) and are therefore gaining importance, particularly in the medical field. Additionally, various technical applications have been recently devised. One of the major challenges in the field of enzyme development is the sensitive and high-throughput detection of the actual product of the biocatalyst of interest without the need for chromophore analogues. Addressing this issue, a colorimetric assay for sulfatases was developed and validated for detecting sulfate through a two-step enzymatic cascade, with a linear detection range of 3.3 (limit of detection) up to 250 μM. The procedure is compatible with relevant compounds employed in sulfatase reactions, including cosolvents, cations, and buffers. The assay was optimized and performed as part of a 96-well screening workflow that included bacterial growth, heterologous sulfatase expression, cell lysis, sulfate ester hydrolysis, inactivation of cell lysate, and colorimetric sulfate determination. With this procedure, the activity of an aryl and an alkyl sulfatase could be confirmed and validated. Overall, this assay provides a simple and fast alternative for screening and engineering sulfatases from DNA libraries (e.g., using metagenomics) with medical or synthetic relevance.

Current advances in enzyme discovery and engineering rely highly on the analytical screening methods used. The decision on how to screen large mutant or metagenomic libraries is a crucial step for the success of any enzyme optimization or search procedure.[1] Microplate assays play a key role in the screening phase because the existing compatible robotics enables fast processing of a large number of enzyme variants. Recently, sulfatases (EC 3.1.6.X) have attracted the interest of various disciplines from the scientific community owing to both their biological relevance and the technical applications devised in different fields.[2] Sulfatases represent a very broad family of enzymes that catalyze the hydrolysis of sulfate esters from a wide spectrum of substrates. These enzymes are involved in numerous cellular functions, such as cell signaling, cellular degradation, hormone regulation, and pathogenesis.[2] As they play an essential role in several diseases, their relevance in human health has been increasingly recognized.[3] Given that the sulfation degree of their substrates is decisive for, e.g., ligand activity (which appears to be strongly related to certain types of cancer[4]), the inhibition and modulation of sulfatases' activity toward signaling molecules have been increasingly studied.[5,6] Furthermore, several technical applications of sulfatases have been developed, such as the enantioselective production of *sec*-alcohols from alkyl sulfates[7] or the regioselective cleavage of sulfate groups from different types of carrageenan to control its gelling or texturizing properties.[8] The increasing importance of this type of biocatalyst is reflected in the recent creation of a sulfatase classification database,[9] which arranges enzymes according to their substrate specificity into alkyl or aryl sulfatases. Given the enormous diversity of sulfated substrates, enzyme HTS procedures are far from being straightforward. The substrates used as standards to detect sulfatases' activity include *p*-nitrophenyl- or *p*-nitrocatechol-sulfate for aryl sulfatases and chromogenic substrate analogues for alkyl sulfatases.[10] For example, a very sensitive sulfatase activity assay was recently proposed in which the fluorescent compound *N*-methylisoindole is produced after sulfatase cleavage of a corresponding sulfated chromophore.[11] However, these assays are only selective for sulfatases that are active on the non-natural substrates that contain such pro-fluorescent probes. Although the easy colorimetric or UV detection of the corresponding desulfated products makes their use very convenient, this strategy does not necessarily guarantee activity on the actual substrate of interest, and the analogues are usually expensive. If

Received: September 11, 2017
Accepted: January 8, 2018
Published: January 8, 2018

ACS Publications © XXXX American Chemical Society

DOI: 10.1021/acs.analchem.7b03719
Anal. Chem. XXXX, XXX, XXX−XXX

the desulfated product is not chromogenic, instrumental analytical techniques (liquid or gas chromatography, mass spectrometry, and nuclear magnetic resonance) are required to detect the hydrolyzed product, which impedes high-throughput processing of large enzyme libraries. Direct sulfate detection would enable the screening and discovery of sulfatases regardless of the substrate type. For a wide range of common food and environmental applications (e.g., sludge or drinking water analyses), sulfate is sensitively detected (0.1 mg L^{-1}) and quantified using ion chromatography or lead ion-selective electrodes.[12,13] Given the long experimental times, large eluent volumes, and tedious sample preparation associated with such procedures, they are rather unsuitable to realize HTS. Turbidimetric determination of sulfate precipitates with barium chloride has become the method of choice when large amounts of samples are measured because the procedure is straightforward and compatible with the microplate format. Several variants of this method have been developed for different applications, e.g., bacterial cultures,[14] human urine,[15] or industrial effluents,[16] and commercial kits are readily available. However, the precipitation of barium sulfate for generating a turbidimetric signal is strongly dependent on multiple factors, e.g., suspension stabilizing reagent used, ionic strength of the sample, and protein concentration.[14] Therefore, the application of turbidimetry using barium chloride for screening sulfatases from cell lysates is somewhat inappropriate because organic components, such as glycosaminoglycans and peptides, strongly inhibit the precipitation of $BaSO_4$.[17] Recently, a study on a sensitive colorimetric assay for sulfate detection was published in which cysteamine-coated gold nanoparticles aggregated in the presence of SO_4^{2-} ions, inducing a detectable absorption shift in the range of 0.34−30 μM, with a sigmoidal sulfate calibration curve.[18] Also, highly sensitive phosphatase assays have been recently developed on the basis of the application of various nanostructures. The output signal of these methods, which in part involve substrate-coordinated compounds, ranges from colorimetry to fluorescence and voltammetry. Unfortunately, their utilization for the analysis of sulfatases has not been shown.[19−21] In this study, addressing the need for a reliable, sensitive, and inexpensive alternative for screening sulfatase libraries with a broad detection range, a colorimetric assay was developed and validated for sulfate determination based on a two-step enzymatic cascade. After optimizing the relevant reaction parameters of the enzymatic cascade, the assay was validated and the influence thereon of pertinent compounds was evaluated. Sample preparation was then adjusted for optimal sulfate detection in bacterial lysates, and the application of the assay for HTS of sulfatase activity was demonstrated by determining the activity of heterologously expressed aryl and alkyl sulfatases in *E. coli* in microplate format.

■ EXPERIMENTAL SECTION

Chemicals and Enzymes. All chemicals were of analytical grade and were purchased from Sigma-Aldrich, Merck KGaA, and Carl Roth GmbH. Pyruvate oxidase (POX) and horseradish peroxidase (HRP) were obtained from Sigma-Aldrich. The leuco dye *N*-(carboxymethylaminocarbonyl)-4,4′-bis-(dimethylamino)diphenylaminesodium salt (DA-64) was acquired from Wako. The genes for pyruvate phosphate dikinase from *Propionibacterium freudenreichii* (PPDK) and APS kinase (APSk) from *S. cerevisiae* were purchased from Genscript in pET-28a(+) expression vectors; they were heterologously produced in *E. coli* BL21 DE3 and purified using affinity chromatography according to published protocols.[22,23] The *cysDN* gene encoding ATP sulfurylase (ATPs) with GTPase activity was amplified from *E. coli* genomic DNA using designed primers (see Supporting Information), cloned into pET-28a(+), and purified via affinity chromatography with a Ni-NTA column (Aekta, GE). Aryl sulfatase from *P. aeruginosa* (PAS) and alkyl sulfatase from *Pseudomonas sp.* DSM6611 (PISA1) were purified as previously described.[7,24] The concentrations of the purified enzymes were determined using a nanophotometer (Implen, P-330) by employing the parameters from the online tool ProtParam (SIB, Switzerland; Table S1). All purified enzymes and assay reactants were aliquoted, stored at −20 °C, and used only once. 2-Heptyl sulfate (PISA1 substrate) was synthesized as previously described[25] with modifications (see Supporting Information).

Assay Optimization. The colorimetric assay was subsequently optimized by evaluating a K_2SO_4 calibration curve constructed in the range 2.5−250 μM. Because reaction 2 of the assay (Scheme 1) is already established for determining pyrophosphate and pyruvate,[22,26] the optimization was focused on reaction 1 and each optimization round served as basis for the next. Optimization reactions were performed in duplicate by mixing 50 μL of K_2SO_4 standard and 50 μL of master mix 1. After incubation at 25 °C for varying times depending on the optimization round (see below), 100 μL of master mix 2 (K_2HPO_4 100 mM pH 6.5, DA-64 100 μM, thiamine pyrophosphate (TPP) 50 μM, $MgCl_2$ 100 μM, phosphoenolpyruvate (PEP) 500 μM, adenosine monophosphate (AMP) 500 μM, PPDK 50 mU, POX 50 mU, and HRP 200 mU; concentrations in reaction) was added to the above-mentioned solution. The mixture was then incubated at 37 °C for 30 min. In all cases, the absorbance (A) was measured at 727 and 540 nm (Varioskan, Thermo Scientific), and $A_{727-540}$ was computed for each standard and a sulfate blank. The calibration curve was then calculated by subtracting the sulfate blank absorbance value from each calibration point ($\Delta A_{727-540}$). The first optimization round focused on finding the best enzymatic concentrations for reaction 1 in HEPES (4−2-hydroxyethyl-1-piperazineethanesulfonic acid) 12.5 mM pH 7.8, GTP 2 mM, ATP 1 mM, and $MgCl_2$ 3 mM (final concentrations, incubation time 45 min). Next, GTP and ATP concentrations were varied (HEPES 12.5 mM pH 7.8, $MgCl_2$ 3 mM, ATPs 0.46 μM, and APSk 5.3 μM; final concentrations, incubation time 45 min). The optimal reaction time was determined from four equal intervals between 15 and 90 min using the previously found optimal concentrations (HEPES 12.5 mM pH 7.8, GTP and ATP 1 mM, $MgCl_2$ 3 mM, ATPs 0.46 μM, and APSk 5.3 μM, concentrations in reaction).

Assay Validation and Characterization. All the data obtained were verified for normal distribution via standard skewness and kurtosis tests. For intraday repeatability and interday reproducibility validation, the standard deviation (SD) and precision were calculated using the Student's t-test (P = 95%, n = 4 and 6, respectively). The limit of detection (LOD) was calculated as $b \pm 3\sigma_{\text{Blank}}$ and the limit of quantification (LOQ) was $b \pm 10\sigma_{\text{Blank}}$, where b is the y-intercept of the calibration curve. The effect of 100, 50, and 25 mM HEPES, TRIS (2-amino-2-(hydroxymethyl) propane-1,3-diol), MOPS (3-morpholinopropane-1-sulfonic acid), citrate, and phosphate buffers at the corresponding pK_a was evaluated by first spiking the samples with a K_2SO_4 solution (100 μM) and then adding the buffers to a complete calibration curve. The influence of

DOI: 10.1021/acs.analchem.7b03719
Anal. Chem. XXXX, XXX, XXX−XXX

various metal ions at different concentrations (1.0, 0.1, and 0.01 mM) was also investigated by spiking with 100 μM K_2SO_4 solutions and calculating the recovery. Different solvents at 5% v/v (final concentration in assay) were spiked with 100 μM sulfate as well.

Assay Application in Sulfatase Reactions. First, the applicability of the developed assay for screening sulfatase activity was assessed using purified PAS and PISA1. The reaction for PAS (3.0 nM) was performed using *p*-nitrophenyl sulfate (250 μM) as the model substrate in TRIS 100 mM (pH 8, 1 mL reaction volume) at 57 °C overnight. The concentration of *p*-nitrophenol produced was determined from the absorbance at 400 nm, quantifying against a standard calibration curve. The reaction for PISA1 (1.8 μM) was performed with 2-heptyl-sulfate as previously described.[27] The concentration of sulfate released by both enzymes was quantified using the optimized colorimetric assay.

The influence of different cell lysis methods on the assay was tested. For this, *E. coli* BL21 DE3 bearing the pET-28a(+) empty vector were cultured overnight at 37 °C. The cells were centrifuged and resuspended in HEPES (100 mM, pH 8) containing either B-Per (Thermo Scientific) or BugBuster (Merck) according to manufacturer's instructions, lysozyme (2.5 mg mL^{-1}), and DNase (10 μg mL^{-1}). The cells were incubated for 1 h at 37 °C, and the sulfate content was measured in spiked dilutions prior to and after a 5 min incubation step at 70 °C. In a second experiment, different inactivation times were evaluated over the whole calibration range. As large signal variability was observed in bacterial lysates with encoding sulfatases, the stabilizing effect of bovine serum albumin (BSA) at different concentrations in the lysis solution was evaluated.

Sulfatase Screening Procedure. *E. coli* BL21 DE3 colonies bearing the expression vectors pASK-IBA5+_PAS and pET-21(+)_PISA1 and a corresponding empty vector were picked from lysogeny broth (LB) agar plates (RapidPick CP-7200, Hudson). The colonies were then inoculated into a preculture deep well plate (Greiner) containing 1.2 mL of LB medium with carbenicillin (100 μg mL^{-1}) and grown at 37 °C overnight. Twenty microliters of the preculture was then used to inoculate an expression plate, and the cells were incubated for 2 h at 37 °C. The expression of PAS was induced with anhydrotetracycline (200 μg L^{-1}) at 30 °C for 2 h.[7] The PISA1-bearing cells were induced with IPTG (0.5 mM), expression conducted at 20 °C for 10 h.[28] After collecting the cell pellet by centrifugation (3000 g, 15 min), 500 μL of lysis solution containing HEPES 100 mM, Bugbuster protein extraction reagent (according to manufacturers' instructions), lysozyme (2.5 mg mL^{-1}), DNase (10 μg mL^{-1}), and BSA (2.5 g L^{-1}) was added to each well, and the plate was incubated for 1 h at 37 °C and 1000 rpm. After centrifugation of cell debris (4000 g, 15 min), 450 μL of cell lysates were transferred to a new U-bottom plate (Riplate, Ritter), 50 μL substrate were added, and incubated at the respective T_{opt} for each sulfatase (57 °C and 1 h for PAS $c_{pNP\text{-}Sulfate}$ = 1 mM[29] and 25 °C and 10 h for PISA1 $c_{2\text{-}heptyl\text{-}Sulfate}$ = 5 mM). At the end of the reaction, cell lysates were inactivated in a water bath at 70 °C for 30 min. The concentration of the *p*-nitrophenol produced by PAS was determined at 400 nm and quantified against a standard calibration curve in micro titer plates (Greiner) using a 20-μL sample. The content of the sulfate released by both enzymes was quantified using the optimized assay with 5-μL samples.

Optimized Assay. The final assay was performed by mixing 50 μL of the sample or standard with 50 μL of master mix 1 (HEPES 12.5 mM pH 7.8, GTP and ATP 1 mM, $MgCl_2$ 3 mM, ATPs 0.46 μM, APSk 5.3 μM). An incubation step at 25 °C for 45 min followed and then 100 μL of master mix 2 was added (K_2HPO_4 100 mM pH 6.5, DA-64 100 μM, TPP 50 μM, $MgCl_2$ 100 μM, PEP 500 μM, AMP 500 μM, PPDK 50 mU, POX 50 mU, HRP 200 mU). The plate was then incubated for 30 min at 37 °C, and $A_{727-540}$ was computed.

■ RESULTS AND DISCUSSION

For any assay aiming to identify an analyte of interest, a recognition element is required in the detection system, followed by a transducer element, e.g., colorimetric signal, whose intensity correlates to the analyte's concentration. Owing to their outstanding specificity, enzymes offer unique advantages as molecular recognition elements in analytical chemistry.[30] As sulfate ion is the analyte of interest in this case, an enzyme that utilizes it as a substrate is required as the recognition element. However, the unreactive nature of sulfate makes the selection of this enzyme challenging. ATP sulfurylase (ATPs, EC 2.7.7.4) catalyzes the universal starting step in the sulfur metabolism in vivo, "activating" SO_4^{2-} by transferring it to adenosine triphosphate (ATP) through a highly endergonic reaction ($\Delta G^{\circ\prime}$ = 19.5 kcal mol^{-1}).[31] Adenosine-5′-phosphosulfate (APS) and inorganic pyrophosphate (PP_i) are formed as the products in a reaction whose equilibrium favors the reactant side ($K = 10^{-8}$).[32] This issue is solved in vivo by many organisms through channeling complexes, in which APS is immediately transferred from the active site of the ATPs to an embedded APS kinase (APSk, EC 2.7.1.25), which in turn phosphorylates APS, shifting the equilibrium to the product side.[33] A promising alternative for performing this reaction in vitro, without the need of such a complex, is the ATPs/GTPase from *E. coli*.[34] This enzyme can couple the chemical potential of guanosine triphosphate (GTP) hydrolysis with the unfavorable activation of sulfate to produce APS, PP_i, and GDP. This particular feature is not displayed by ATPs from other organisms, e.g., *S. cerevisiae*.[35] Given this advantage, the ATPs/GTPase reaction was selected as the starting step of the proposed cascade for sulfate detection (Scheme 1). This reaction can be further driven toward completion by the immediate phosphorylation of APS to afford 3′-phosphoadenosine 5′-phosphosulfate (PAPS) using APSk from *S. cerevisiae*. Of all the products formed to this point, the resulting equimolar production of PP_i from sulfate enables the possibility of connection to a transducer element. Its detection is possible owing to a second set of enzyme-catalyzed reactions, which rely on the previously described assays for amino acids based on PP_i detection using pyruvate phosphate dikinase (PPDK) from *Propionibacterium freudenreichii*.[36] The PP_i released by ATPs/GTPase reacts with adenosine monophosphate (AMP) and phosphoenolpyruvate (PEP) to produce pyruvate, which is in turn oxidized by pyruvate oxidase (POX) to afford H_2O_2. In the last reaction of the cascade, horseradish peroxidase (HRP) catalyzes the oxidation of the dye DA-64 to produce Bindschedler's green using the H_2O_2 present, yielding a colorimetric signal at 727 nm, which is proportional to the sulfate concentration in the sample. The measurement at this particular wavelength avoids detection in the yellow region of the spectra, in which several disturbing compounds or matrices exhibit absorbance (e.g., bacterial culture media or aromatic compounds).

DOI: 10.1021/acs.analchem.7b03719

Scheme 1. Enzymatic Cascade for Colorimetric Detection of Inorganic Sulfate.[a]

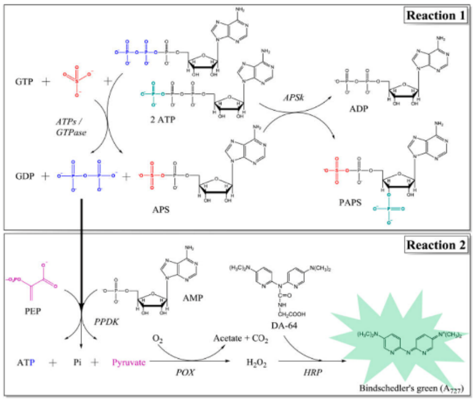

[a] *ATPs*: ATP sulfurylase; *APSk*: APS kinase; *PPDK*: pyruvate phosphate dikinase; *POX*: pyruvate oxidase; *HRP*: horseradish peroxidase; DA-64: *N*-(carboxymethylaminocarbonyl)-4,4′-bis (dimethylamino) diphenylaminesodium. The equilibrium of the two reactions lies strongly on the product side.

Assay Optimization. Owing to the complexity of the reaction cascade, a number of variables need to be explored for the assay to achieve good linearity and reproducibility over the intended detection range. Most importantly, note that the reaction parameters are not compatible for all the enzymes. ATPs/GTPase and APSk act optimally at pH ∼ 8 and 25 °C, while the optimal conditions for the reaction cascade for detecting PP_i are pH 6.5 and 37 °C; therefore, a change of buffer is necessary. Since determination of PP_i is already a well-established procedure,[36] the optimization focused on the first reaction. The concentration and ratio of enzymes employed in analytical assays are parameters relevant for their robustness. In this case, the molar ratio of ATPs and APSk was set to ∼1:10 so that virtually every APS produced by ATPs is immediately converted to PAPS by APSk. The concentration of these enzymes was varied as shown in Figure S1A. Both 0.46 μM ATPs and 5.3 μM APSk were selected because higher and lower concentrations led to lower signals with 250 μM sulfate, decreasing the assay linearity. Next, different GTP and ATP concentrations were explored. This parameter is very important for initiating the ATPs reaction. Ideally, a GTP:ATP molar ratio of 1:2 is expected to generate a steady flowing cascade as 2 ATP molecules are needed in the first reaction: one producing APS and the other for APS phosphorylation to yield PAPS with GDP as the byproduct. However, the accumulation of GDP in the system decreases the ATPs efficiency for coupling GTP hydrolysis to APS synthesis and PP_i release, as competitive inhibition of the guanine nucleotide binding site occurs between GDP and GTP.[37] Accordingly, the concentration of GTP needed to direct the reaction toward SO_4^{2-} consumption must be increased and was, therefore, set to at least a 1:1 GTP:ATP molar ratio. The GTP and ATP concentration that best fitted the curve in the desired calibration range was 1 mM (Figure S1B). By setting a higher GTP concentration (2 mM), the linearity of the assay decreases in the low-concentration range. Lastly, different times for reaction 1 were tested (Figure S1C). The sensitivity of the calibration curve increased as reaction time increased (15, 30, and 45 min) and then decreased again at 60 and 90 min. Too-short times may not be adequate for the complete reaction of sulfate, especially at the higher concentrations in the calibration curve. On the other hand, too-long times might shift the equilibrium back to the production of ATP and SO_4^{2-}, as previously described for the ATPs reaction.[37] Thus, a reaction time of 45 min was considered optimal and employed. As a result of the optimization procedure, a linear calibration curve was obtained: $y = 0.0057x + 0.0194$ with $R^2 = 0.9983$, in the range of 5.0−250 μM SO_4^{2-}. The sulfate blank of the calibration curve in water presented a moderate $A_{727-540}$ value of ∼ 0.32 in deep well plates (V_{sample} = 200 μL), which was attributed to auto hydrolysis of the nucleotides to form PP_i, ATPs-catalyzed nonsulfate-dependent hydrolysis of ATP to yield PP_i and AMP, and PEP degradation to produce pyruvate and phosphate over the course of reaction 2.

Assay Validation and Characterization. After confirming the normal distribution of the data using the standard skewness and kurtosis tests, validation analysis was performed. The calculated LOD and the LOQ were 3.3 μM and 10.9 μM, respectively. It is worth noting that commercial turbidimetric assays with barium chloride allow a detection limit of 5 mg L^{-1} (52 μM),[38] while the previously reported sulfate assay using gold nanoparticles exhibited a LOD of 0.34 μM, allowing quantification up to 30 μM with a sigmoidal response curve.[18] The present assay allows linear measurement of a broader range, which renders it more sensitive over the whole calibration range. The SD, precision, and accuracy for determining the intraday repeatability and interday reproducibility are shown in Table 1. The precision, as calculated by the Student's *t*-test (P = 95%), ranges from 1% for 250 μM sulfate to 15% near the LOQ, while the accuracy bias varies from −1% for the highest calibration point to 23% around the LOQ. These results are similar to those reported for the gold nanoparticle method and ion chromatography for real samples (>95% accuracy for samples spiked with 25 and 50 ppm sulfate)[18] and indicate an excellent performance in the upper working range that tends to decrease at sulfate concentrations lower than 25 μM.

Table 1. Analytical Performance of the Proposed Assay

	intraday repeatability			
SO_4^{2-} μM	mean μM	SD	precision[a]	accuracy bias[a]
250	247	2.0	1.3%	−1.2%
100	106	3.0	4.5%	6.6%
25	24.3	1.8	11.9%	−2.9%
10	7.7	0.7	14.6%	−23%
	interday reproducibility			
SO_4^{2-} μM	mean μM	SD	precision[b]	accuracy bias[b]
250	247	0.5	0.2%	−1.1%
100	106	1.5	1.5%	6.3%
25	23.8	1.1	4.7%	−4.9%
10	7.8	0.4	5.6%	−22%

Calculated using the Student's *t*-test with: [a]n = 4. [b]n = 6.

The influence of commonly employed compounds in sulfatase reactions was also evaluated on the enzymatic assay. First, the detection of 100 μM sulfate was assessed in the presence of different buffers (25, 50, and 100 mM, Figure 1A).

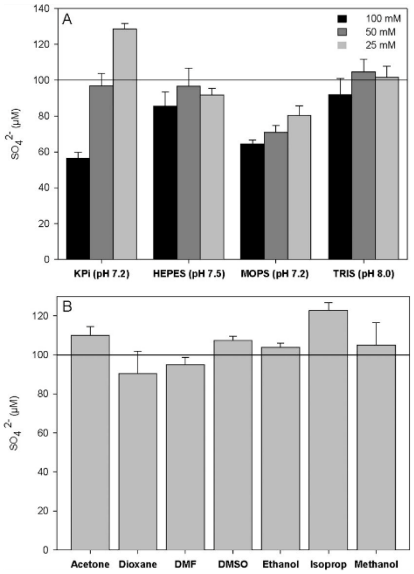

Figure 1. Sulfate determination in the presence of various compounds commonly employed in sulfatase reactions. The solid line indicates the amount of sulfate spiked. (A) Buffers at different concentrations. (B) Organic solvents at 5% (v/v, assay concentration).

Citrate buffer at the tested concentrations was not compatible with the assay as no signal was detected. The recovery of sulfate in MOPS increased from 65% at 100 mM to 81% at 25 mM. The phosphate buffer had the most considerable effect at different concentrations, with recoveries ranging from 56 to 128%. TRIS and HEPES afforded the best sulfate recoveries, 86−105%, at the tested concentrations. To investigate whether the observed effect was dependent on sulfate concentration, calibration curves containing the buffers were analyzed (Figure S2A). An absorption signal lower than that of pure water was observed in samples containing 100 mM MOPS, TRIS, and HEPES over the whole calibration range; its effect in the quantification may be hence compensated by preparing the calibration curve in these buffers or by diluting the samples to improve recovery. Conversely, the phosphate buffer has a great impact in the assay, as the absorption values of the sulfate blank at 100 mM and 25 mM were higher than that for the above-mentioned buffers, and nearly no sulfate-dependent increase in absorbance was detected. A more pronounced slope was evident in the calibration curve at concentrations between 0.5 and 2.0 mM phosphate with $A_{727-540}$ signals higher than that for the curve prepared in water. This effect could lead to false positive results (Figure S2B). Considering that reaction 2 occurs in a phosphate buffer, it is likely that phosphate has a great effect on reaction 1 at low sulfate concentrations. This suggests that competitive inhibition between phosphate and sulfate may occur in the active site of ATPs, causing a nonsulfate-dependent release of PP_i, thus producing the higher signals observed. Therefore, it is not recommended to perform the assay when samples contain phosphate at concentrations exceeding 0.1 mM (Figure S2B). This limitation should be considered when preparing sulfatase samples.

Organic solvents are commonly employed in sulfatase reactions at 20% v/v to solubilize hydrophobic sulfated substrates and to increase the selectivity of some sulfatases.[10] Therefore, the tolerance of the assay toward different solvents at 5% v/v was tested (Figure 1B). Ethanol, methanol, DMF, and DMSO exhibited good compatibility with the assay, with recoveries of 100 ± 10% for 100 μM sulfate. Accordingly, samples containing these organic solvents could be measured after dilution by a factor of 4. With a concentration of sulfated substrates of 1 mM, sulfatase activities between 10%−100% could be easily detected. Moreover, metal ions play an important role in some sulfatase reactions, acting as activators[2] (e.g., Ca^{2+} at 1−5 mM) and inhibitors (e.g., Zn^{2+} at 1 mM) and even influencing the hydrolysis enantioselectivity of *sec*-alkyl sulfates (Fe^{2+} and Co^{2+} at 1−10 mM).[39,40] The determination of 100 μM sulfate was thus evaluated in the presence of various cations at different concentrations (Figure S3). Ni^{2+}, Zn^{2+}, and Cu^{2+} enable good detection at ≤ 0.01 mM; Fe^{2+} at 0.1 mM (∼75% recovery); Co^{2+} and Rb^{+} at ≤ 1 mM, and Ca^{2+} even at 5 mM. Nickel, zinc, and cupper are frequently present in bacterial cultures as trace elements at concentrations between 0.1 and 0.5 mM. Owing to the low tolerance of the assay to iron, a removal strategy, e.g., precipitation, may be necessary to perform the assay at concentrations higher than 0.1 mM. Overall, the cation concentration can be adjusted by diluting the samples according to each case.

Assay Application in Sulfatase Reactions. After evaluating the performance of the optimized sulfate assay, determination of the enzymatic activity was tested using the aryl sulfatase from *P. aeruginosa* (PAS). This enzyme catalyzes the hydrolysis of *p*-nitrophenyl sulfate, the model substrate for the screening of sulfatases. This reaction generates free sulfate and *p*-nitrophenol, a chromophoric product that can be readily detected at 400 nm in alkaline media. Accordingly, a parallel photometric determination of both products at well-separated wavelengths of the visible spectrum is possible after performing the optimized sulfate assay. The initial substrate concentration was set to 250 μM; after the reaction, 203 μM *p*-nitrophenol (82% conversion) and 188 μM sulfate (75% conversion) were quantified, indicating an accuracy bias of −7% between both determination methods. The absorption spectrum of the reaction containing both products after performing the sulfate assay (Figure 2, solid line) reveals two peaks: one at 400 nm, corresponding to *p*-nitrophenol (A_{400} = 0.53, l = 1 cm) and another more intense peak at 727 nm resulting from the enzymatic conversion of sulfate to Bindschedler's green through the cascade (A_{727} = 2.61, l = 1 cm). When the substrate is absent (Figure 2, dashed line), no peak is observed at 400 nm, and the intensity of the peak at 727 nm decreases (A_{727} = 0.70, l = 1 cm), as was observed for the sulfate blank in the calibration curve. Under these conditions, a molar extinction coefficient of 10 160 M^{-1} cm^{-1} was calculated for Bindschedler's green, which is directly related to the concentration of sulfate. This coefficient is 4 times higher than that of *p*-nitrophenol (2 611 M^{-1} cm^{-1}), rendering sulfate colorimetric detection more sensitive than the determination of *p*-nitrophenol under the sulfatase reaction conditions. For aryl sulfatases, the cleavage of the sulfate ester bond is initiated by a nucleophilic attack of the sulfur atom. However, there are also sulfatases acting on alkyl sulfates, where the ester cleavage is achieved by nucleophilic substitution at the carbon atom (Figure S4). Such enzymes exhibit no activity with *p*-nitrophenyl sulfate and cannot be assayed as easily as aryl

DOI: 10.1021/acs.analchem.7b03719

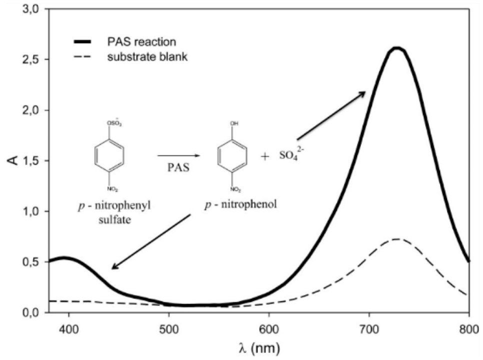

Figure 2. Spectra of the reaction of *P. aeruginosa* arylsulfatase (PAS) on *p*-nitrophenyl sulfate measured in cuvettes, $l = 1$ cm. Reactions performed overnight in TRIS 100 mM, pH 8 at 57 °C.

sulfatases. To demonstrate the detection of sulfate released from alkyl sulfatases, in which no chromogenic substrate is involved, PISA1 was purified and its activity was tested toward *rac*-2-heptyl-sulfate. The initial substrate concentration was set to 22 mM.[28] The measured sulfate concentration after a proper dilution was 9.9 mM. This represents an enzymatic conversion of 45% as previously reported; it is worth recalling the high enantioselectivity of PISA1 ($E > 200$) toward *R*-2-heptyl-sulfate.[28]

Sulfatase Screening Procedure. As the screening and engineering of enzymes is conducted in bacterial lysates of expression strains, the assay was applied for quantifying sulfate in cell lysates in order to evaluate and correct potential matrix effects. The most common method for disrupting bacterial cells is the use of detergents that solubilize the cell membrane in combination with hydrolytic enzymes, such as lysozyme and DNase. First, the determination of spiked sulfate was conducted in various dilutions of cell lysates produced with the two commercially available detergents B-Per and BugBuster (Figure S5A). The spiked sulfate could not be detected in 1:10 and 1:50 dilutions, and a poor recovery of 50% was obtained at 1:100. This suggests that the surfactant compounds of the lysis solution and the released cell components interfere with the assay either by inhibiting or denaturing the enzymes involved or by interacting with the intermediates (Scheme 1). In order to precipitate potentially interfering *E. coli* proteins, the cell lysates were incubated at 70 °C for 5 min. Afterward, nearly 100% of sulfate recovery (100 μM) was reached at 1:50 and 1:100 dilutions, but only 50%−60% was reached at 1:10. When increasing the incubation time to at least 20 min in 1.5 mL tubes (Figure S5B) and 30 min in 96-deep well plates (data not shown), the detection of sulfate in 1:10 diluted cell lysates was possible over the whole calibration range.

The experiments mentioned above were performed with *E. coli* cells bearing a pET-28a(+) empty plasmid. However, large signal variability was observed when vectors encoding sulfatases were used (data not shown). In such cases, the matrix effects influencing enzymatic assays are difficult to predict, and it was assumed that this resulted from varying cell metabolism or intracellular protein concentrations. Therefore, the protein content of *E. coli* cell lysates bearing the pASK_PAS plasmid was normalized by adding bovine serum albumin (BSA) at different concentrations, spiked with sulfate, and then inactivated at 70 °C for 30 min. BSA significantly improved the detection of sulfate in the cell lysates with expressed sulfatases over the whole calibration range at concentrations above 1 g L^{-1}, with the best linearity at 2.5 g L^{-1} BSA (Figure 3). The samples were analyzed by gel electrophoresis before and after incubation at 70 °C (Figure S6), and the presence of BSA was confirmed in the incubated samples containing at least 1 g L^{-1} BSA. Although the thermo-stabilizing effect of BSA toward enzymes has been described previously,[41] it is not fully clear whether its presence facilitates the thermal precipitation of disturbing *E. coli* components or if it stabilizes the assay enzymes.

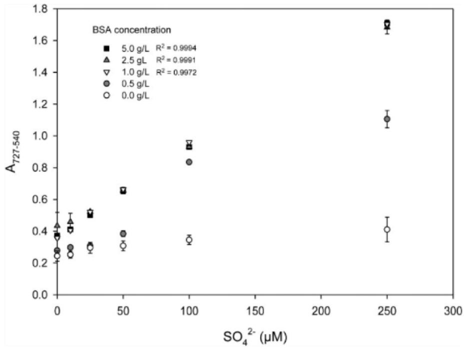

Figure 3. Sulfate calibration curve in cell lysates of *E. coli* bearing pASK_PAS plasmid containing BSA at different concentrations.

Once the optimal conditions for sulfate detection in bacterial lysates were established, a 96-well workflow was designed to create a wild-type landscape of PAS and PISA1 with their respective substrates. While PISA1 has no activity with the chromophore containing *p*-nitrophenyl sulfate, the detection of the sulfate released by the PAS clones can be cross-validated by quantifying *p*-nitrophenol as described above. Figure 4 shows the absorption signals of the products released by both enzymes. The volumes used for each product (20 μL *p*-nitrophenol and 5 μL sulfate) were chosen so that the signals would fit in the corresponding calibration curve. Black dots indicate *E. coli* sulfatase clones and white circles represent empty vector clones (pASK-IBA5+). The output signal $A_{727-540}$ obtained using the assay was 0.82 ± 0.05 (Figure 4A2), which was quantified as 0.97 mM SO_4^{2-}, while the A_{400} signal for *p*-nitrophenol obtained was 0.97 ± 0.07 (Figure 4A1), resulting in a concentration of 0.95 mM, which represents a 2% bias compared to sulfate. This reflects a conversion of ca. 96% under the screening conditions, considering that the initial concentration of *p*-nitrophenyl sulfate was 1 mM. The absorbance values for the negative controls of both procedures were 0.32 ± 0.02 for the sulfate assay and 0.08 ± 0.02 for *p*-nitrophenol.

A relevant parameter for the qualitative evaluation of HTS assays is the Z' factor (equation 1).[42] This dimensionless number evaluates the ability of an assay to discern active clones from inactive ones with high fidelity by computing the signal difference between positive and negative controls in relation to the sum of their standard deviations (noise) and is given by the following equation:

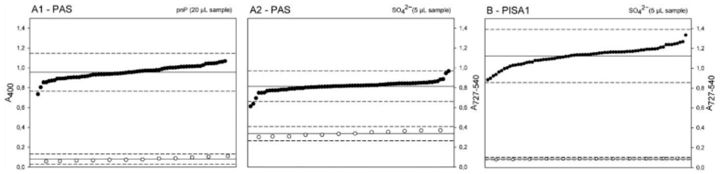

Figure 4. Absorption signals of sulfatase products. A1. pnP: *p*-nitrophenol (400 nm). A2. Sulfate (727−540 nm) from PAS. B. Sulfate (727−540 nm) from PISA1 ●: Positive clones. ○: Empty vector clones. Solid line: mean (μ); dashed lines $\mu \pm 3\sigma$ (standard deviation).

$$Z' = 1 - \frac{(3_{\sigma_{c+}} + 3_{\sigma_{c-}})}{|\mu_{c+} - \mu_{c-}|} \tag{1}$$

where μ is the mean and σ the standard deviation of the signals from positive (c+) and empty vector clones (c−). HT assays with a Z' factor of 1 are considered ideal; for assays where $1 > Z' \geq 0.5$, the separation band between positive and negative clones is considered large, and the assay provides reliable screening conditions. However, if $Z' < 0.5$, the separation band is small and the assay is considered as a double assay; therefore, it is nonpractical for distinguishing positive clones from negative ones with high precision. The detection of *p*-nitrophenol at 400 nm under the presented conditions yielded an excellent Z' value, 0.71, which results from a large signal difference between positive and negative clones. Furthermore, a value of $Z' = 0.51$ was obtained for the colorimetric detection of sulfate, as the separation band between positive and negative clones in this case is smaller than that for *p*-nitrophenol. This value reflects the suitability of the assay for screening aryl sulfatases via the detection of sulfate in the calibration range with a very good correlation with the determination of *p*-nitrophenol. As the volume used for *p*-nitrophenol was 4 times higher than that for sulfate (see above), the two Z' values cannot be compared to each other. The assay user can choose an appropriate sample volume depending on a desired threshold for the reaction yield of positive clones.

The potential of the assay developed becomes evident when such a screening workflow is applied to alkyl sulfatases, e.g., PISA1, as chromogenic substrates are hardly available and do not actually reflect the activity on the compound of interest (Figure 4B). The output sulfate signal $A_{727-540}$ with this enzyme toward *rac*-2-heptyl-sulfate was 1.12 ± 0.09 for positive clones and 0.09 ± 0.00 for empty vector clones. The amount of sulfate released was 1.8 mM, indicating 36% of conversion from a maximum of 50% enantioselective yield (initial substrate concentration, 5 mM). As the clones bearing the empty vector pET-21+ displayed lower absorbance ($A_{727-540} = 0.09$) than those used in the PAS screening ($A_{727-540} = 0.32$), a broader separation band between positive and negative clones enabled better assay performance, as indicated by $Z' = 0.73$. The lower values obtained with different empty vectors may result from differing induction and growing cell conditions for PAS and PISA1, e.g., anhydrotetracycline vs IPTG or the addition of zinc in the PISA1 culture. These results demonstrate the efficacy of the assay for discovering new sulfatases at the DNA level by, e.g., using metagenomic libraries. With this assay, one can avoid the tedious and time-consuming screening of novel sulfatase activity at the protein level in which a large amount of microorganism, plant, or animal cells have to be cultured and numerous extraction and drying steps have to be executed to detect desulfated products via chromatography, as was the case for the de novo discovery of PISA1.[43]

■ CONCLUSIONS

In this study, a colorimetric assay for detecting sulfate based on a two-step enzymatic cascade was designed, optimized, and experimentally validated. The linearity of the assay in the range 10−250 µM renders it comparable to chromatographic methods in terms of sensitivity (LOD = 3.3 µM sulfate) and superior to established plate procedures such as barium sulfate precipitation or utilization of chromogenic substrates. The proposed method demonstrated good precision and accuracy. Sulfate determination was possible in the presence of pertinent buffers, organic solvents, and metal ions at concentrations relevant for sulfatase reactions. A significant advantage of this assay is its feasibility for screening sulfatase activity in cell lysates, as optimized and demonstrated here for aryl and alkyl sulfatases in an automatable 96-well workflow. The assay showed a very good stability in such a plate workflow ($Z' > 0.5$). Further, the enzymes employed in the assay were still active 3 months after purification when stored at −20 °C. The assay provides a reliable alternative for sulfate analysis and sulfatase activity screening regardless of the substrate type and without the need for chromophore derivatives. The procedure presented herein can be employed for the HTS of large variant libraries (e.g., from mutagenesis or metagenomes). In addition, the assay might also be considered for the general determination of sulfate in different types of samples such as drinking water, bacterial and algal cultures, blood or urine, for which high throughput is of advantage.

■ ASSOCIATED CONTENT

Ⓢ Supporting Information

The Supporting Information is available free of charge on the ACS Publications website at DOI: 10.1021/acs.analchem.7b03719.

> Additional information regarding enzyme production and purification, as well as assay optimization and sample adjusting to cell lysates is available as noted in the text (PDF)

■ AUTHOR INFORMATION

Corresponding Author

*Phone: +49 (9421) 187-300. E-mail: Sieber@tum.de.

ORCID

Volker Sieber: 0000-0001-5458-9330

Author Contributions

The manuscript was written through contributions of all authors.

Notes

The authors declare no competing financial interest.

■ ACKNOWLEDGMENTS

The project was founded by the German Federal Ministry of Education and Research, Project ABV 03SF0446A. Special gratitude is expressed to Kurt Faber, Michael Tösch, and Tamara Reiter (TU Graz, Austria) for providing the PAS and PISA1 genes. The authors are extremely thankful to Dr. Josef Sperl for assisting with the amplification and cloning of *cysDN* and to Petra Lommes for conducting the synthesis of 2-heptyl-sulfate.

■ REFERENCES

(1) Bloom, J. D.; Meyer, M. M.; Meinhold, P.; Otey, C. R.; MacMillan, D.; Arnold, F. H. *Curr. Opin. Struct. Biol.* **2005**, *15*, 447−452.
(2) Hanson, S. R.; Best, M. D.; Wong, C. H. *Angew. Chem., Int. Ed.* **2004**, *43*, 5736−5763.
(3) Diez-Roux, G.; Ballabio, A. *Annu. Rev. Genomics Hum. Genet.* **2005**, *6*, 355−379.
(4) Vivès, R. R.; Seffouh, A.; Lortat-Jacob, H. *Front. Oncol.* **2014**, *3*, 1−11.
(5) Schelwies, M.; Brinson, D.; Otsuki, S.; Hong, Y. H.; Lotz, M. K.; Wong, C. H.; Hanson, S. R. *ChemBioChem* **2010**, *11*, 2393−2397.
(6) Reuillon, T.; Alhasan, S. F.; Beale, G. S.; Bertoli, A.; Brennan, A.; Cano, C.; Reeves, H. L.; Newell, D. R.; Golding, B. T.; Miller, D. C.; Griffin, R. J. *Chem. Sci.* **2016**, *7*, 2821−2826.
(7) Schober, M.; Toesch, M.; Knaus, T.; Strohmeier, G. A.; Van Loo, B.; Fuchs, M.; Hollfelder, F.; Macheroux, P.; Faber, K. *Angew. Chem., Int. Ed.* **2013**, *52*, 3277−3279.
(8) Prechoux, A.; Genicot, S.; Rogniaux, H.; Helbert, W. *Mar. Biotechnol.* **2013**, *15*, 265−274.
(9) Barbeyron, T.; Brillet-Guéguen, L.; Carré, W.; Carrière, C.; Caron, C.; Czjzek, M.; Hoebeke, M.; Michel, G. *PLoS One* **2016**, *11*, e0164846.
(10) Toesch, M.; Schober, M.; Faber, K. *Appl. Microbiol. Biotechnol.* **2014**, *98*, 1485−1496.
(11) Yoon, H. Y.; Hong, J.-I. *Anal. Biochem.* **2017**, *526*, 33−38.
(12) Petersen, S. P.; Ahring, B. K. *J. Microbiol. Methods* **1990**, *12*, 225−230.
(13) Tang, T.-C.; Huang, H.-J. *Anal. Chem.* **1995**, *67*, 2299−2303.
(14) Kolmert, Å.; Wikström, P.; Hallberg, K. B. *J. Microbiol. Methods* **2000**, *41*, 179−184.
(15) Lundquist, P.; Mårtensson, J.; Sörbo, B.; Ohman, S. *Clin. Chem.* **1980**, *26*, 1178−1181.
(16) van Staden, J. F.; Taljaard, R. E. *Anal. Chim. Acta* **1996**, *331*, 271−280.
(17) Sörbo, B. *Methods Enzymol.* **1987**, *143*, 3−6.
(18) Zhang, M.; Liu, Y.-Q.; Ye, B.-C. *Analyst* **2011**, *136*, 4558−4562.
(19) Gao, Z.; Deng, K.; Wang, X.-D.; Miró, M.; Tang, D. *ACS Appl. Mater. Interfaces* **2014**, *6*, 18243−18250.
(20) Zhou, Q.; Lin, Y.; Xu, M.; Gao, Z.; Yang, H.; Tang, D. *Anal. Chem.* **2016**, *88*, 8886−8892.
(21) Lin, Y.; Zhou, Q.; Li, J.; Shu, J.; Qiu, Z.; Lin, Y.; Tang, D. *Anal. Chem.* **2016**, *88*, 1030−1038.
(22) Kameya, M.; Himi, M.; Asano, Y. *Anal. Biochem.* **2014**, *447*, 33−38.
(23) Wei, J.; Tang, Q.-X.; Varlamova, O.; Roche, C.; Lee, R.; Leyh, T. S. *Biochemistry* **2002**, *41*, 8493−8498.
(24) Knaus, T.; Schober, M.; Kepplinger, B.; Faccinelli, M.; Pitzer, J.; Faber, K.; Macheroux, P.; Wagner, U. *FEBS J.* **2012**, *279*, 4374−4384.
(25) White, G. F.; Lillis, V.; Shaw, D. J. *Biochem. J.* **1980**, *187*, 191−196.
(26) Rühmann, B.; Schmid, J.; Sieber, V. *J. Visualized Exp.* **2016**, *2016*, 110.
(27) Schober, M.; Knaus, T.; Toesch, M.; Macheroux, P.; Wagner, U.; Faber, K. *Adv. Synth. Catal.* **2012**, *354*, 1737−1742.
(28) Schober, M.; Gadler, P.; Knaus, T.; Kayer, H.; Birner-Grünberger, R.; Güllly, C.; MacHeroux, P.; Wagner, U.; Faber, K. *Org. Lett.* **2011**, *13*, 4296−4299.
(29) Beil, S.; Kehrli, H.; James, P.; Staudenmann, W.; Cook, A. M.; Leisinger, T.; Kertesz, M. A. *Eur. J. Biochem.* **1995**, *229*, 385−394.
(30) Staiano, M.; Pennacchio, A.; Varriale, A.; Capo, A.; Majoli, A.; Capacchione, C.; D'Auria, S. In *Methods in Enzymology*; Richard, B. T., Carol, A. F., Eds.; Academic Press: San Diego, 2017; pp 115−131.
(31) Leyh, T. S.; Taylor, J. C.; Markham, G. D. *J. Biol. Chem.* **1988**, *263*, 2409−2416.
(32) Mueller, J. W.; Shafqat, N. *FEBS J.* **2013**, *280*, 3050−3057.
(33) Sun, M.; Leyh, T. S. *Biochemistry* **2006**, *45*, 11304−11311.
(34) Sun, M.; Leyh, T. S. *Biochemistry* **2005**, *44*, 13941−13948.
(35) Karamohamed, S.; Nilsson, J.; Nourizad, K.; Ronaghi, M.; Pettersson, B.; Nyrén, P. *Protein Expression Purif.* **1999**, *15*, 381−388.
(36) Kameya, M.; Asano, Y. *Enzyme Microb. Technol.* **2014**, *57*, 36−41.
(37) Liu, C.; Wang, R.; Varlamova, O.; Leyh, T. S. *Biochemistry* **1998**, *37*, 3886−3892.
(38) Morais, I. P. A.; Rangel, A. O. S. S.; Souto, M. R. S. *J. AOAC Int.* **2001**, *84*, 59−64.
(39) Tokheim, A. M.; Spannaus-Martin, D. J.; Martin, B. L. *BioMetals* **2005**, *18*, 537−540.
(40) Pogorevc, M.; Strauss, U. T.; Riermeier, T.; Faber, K. *Tetrahedron: Asymmetry* **2002**, *13*, 1443−1447.
(41) Chang, B.; Mahoney, R. *Biotechnol. Appl. Bioc.* **1995**, *22*, 203−214.
(42) Zhang, J. H.; C, T.; Oldenburg, K. R. *J. Biomol. Screening* **1999**, *4*, 67−73.
(43) Gadler, P.; Faber, K. *Eur. J. Org. Chem.* **2007**, *2007*, 5527−5530.

DOI: 10.1021/acs.analchem.7b03719
Anal. Chem. XXXX, XXX, XXX−XXX

Appendix: Supplementary Data

Supporting information – Cover Page

Colorimetric determination of sulfate *via* an enzyme cascade for high-throughput detection of sulfatase activity

Jose G. Ortiz-Tena[a], Broder Rühmann[a], Volker Sieber[a,b,c,d*]

[a]Chair of Chemistry of Biogenic Resources, Technische Universität München, Straubing, Germany
[b]Fraunhofer IGB, Straubing Branch BioCat, Straubing, Germany
[c]TUM Catalysis Research Center, Ernst-Otto-Fischer-Straße 1, 85748, Garching, Germany
[d]The University of Queensland, School of Chemistry and Molecular Biosciences, 68 Copper Road, St. Lucia 4072, Australia
*Corresponding author. Phone: +49 (9421) 187-300. E-mail: Sieber@tum.de

Table of contents

Primers for amplification of *E. coli cysDN* gene
Table S1. Parameters for determining enzyme concentration
Synthesis of PISA1 substrate 2-heptyl-sulfate
Figure S1. Optimization procedure of reaction 1
Figure S2. Sulfate calibration curve in the presence of buffers
Figure S3. Analysis of sulfate in the presence of metallic ions
Figure S4. Simplified mechanism of the two types of sulfatases
Figure S5. Sulfate determination in incubated cell lysates
Figure S6. Polyacrylamide gel electrophoresis of cell lysates

Primers for amplification of *E. coli cysDN* genes.

5’-ATATATCTCGAGTTTATCCCCCAGC-3’
5’-TATATACCATATGGATCAAATACGAC-3’

Table S1. Parameters for determining the concentration of purified enzymes prior to addition of glycerol (1:2) to 20% (v/v) final concentration

Enzyme	ε_{280} (L mol^{-1} cm^{-1})	M (kDa)	c (mg mL^{-1})
PPDK	54 360	98.0	1.62
ATPs	93 300	87.7	1.59
APSk	21 500	23.0	4.87
PAS	102 790	59.8	1.89
PISA1	82 280	73.9	2.8

Synthesis of PISA1 substrate 2-heptyl-sulfate

The synthesis of 2-heptyl-sulfate was carried out as proposed by White *et. al.*[1] using the sulfur trioxide triethylamine complex (Sigma-Aldrich, Germany) as sulfation agent of the sodium alkoxide (4-fold amounts). Following modifications were performed:

a) The sodium suspension was prepared by adding small pieces of metallic sodium (Sigma-Aldrich, Germany) into stirred dry toluene in oxygen-absent conditions (instead of mineral oil dispersion).
b) The sodium alkoxide of 2-heptanol was prepared by adding 16 mmol of 2-heptanol dropwise to the sodium suspension and stirred at 100°C for 30 min, and then overnight at 40°C.
c) The sulfation agent was added to the alkoxide solution at room temperature and stirred overnight (instead of 1h)

The subsequent purification procedure was performed as described by White *et. al.*[1]

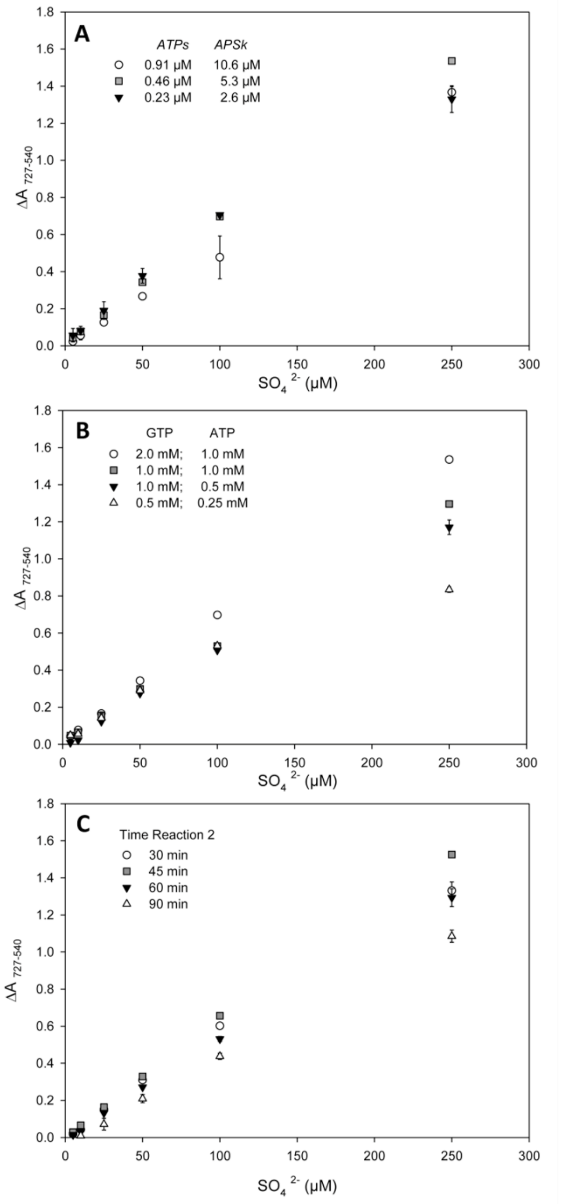

Figure S1. Optimization procedure of reaction 1 for colorimetric sulfate assay over the whole calibration range. A) ATPs and APSk concentration B) GTP and ATP concentrations C) Time for Reaction 2

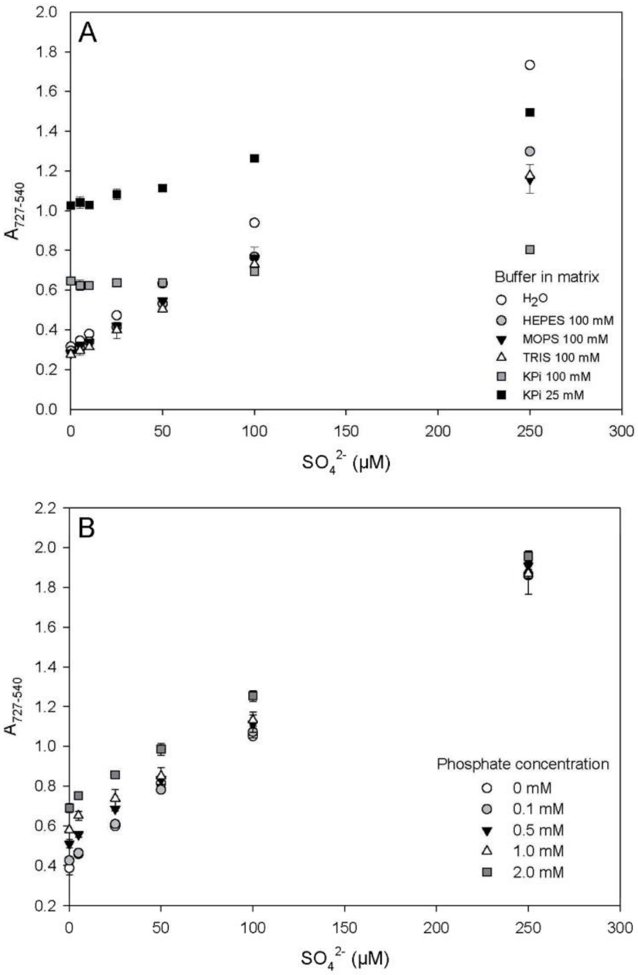

Figure S2. Analysis of the sulfate calibration curve in the presence of: A) different buffers and B) Phosphate at lower concentrations

Figure Discussion

Panel A. For better interpretation of the results, note that the sulfate blank was not subtracted, i.e. $A_{727-543}$ was plotted. For the phosphate buffer, higher blank signals than the rest of the buffers were observed. At 100 mM phosphate, the signal did not increase with increasing sulfate concentration, whereas at 25 mM, this effect was slightly lower.

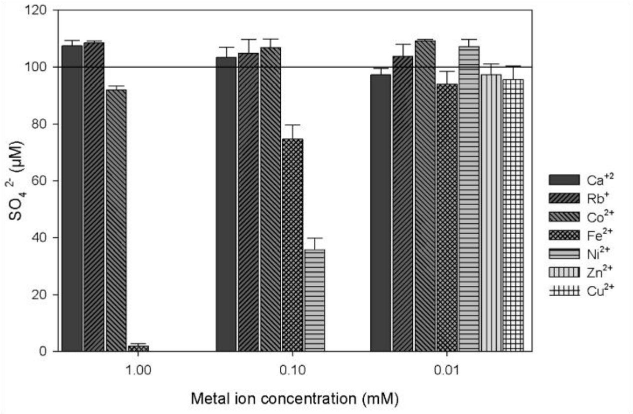

Figure S3. Analysis of sulfate in the presence of metallic ions at different concentrations; the solid line indicates the amount of spiked sulfate

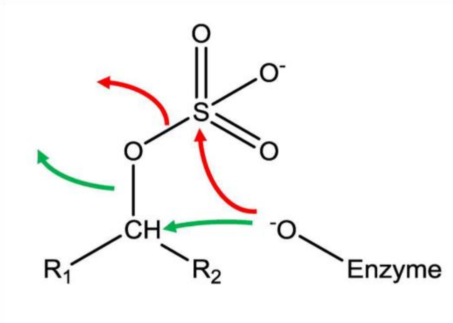

Figure S4. Simplified mechanism of the two types of sulfatases demonstrating the first nucleophilic attack and how differently the sulfate is released: red - aryl sulfatases containing a formylglycine group as reactive species and green – *sec*-alkyl sulfatases containing a Zn^{2+} activated water molecule as reactive species

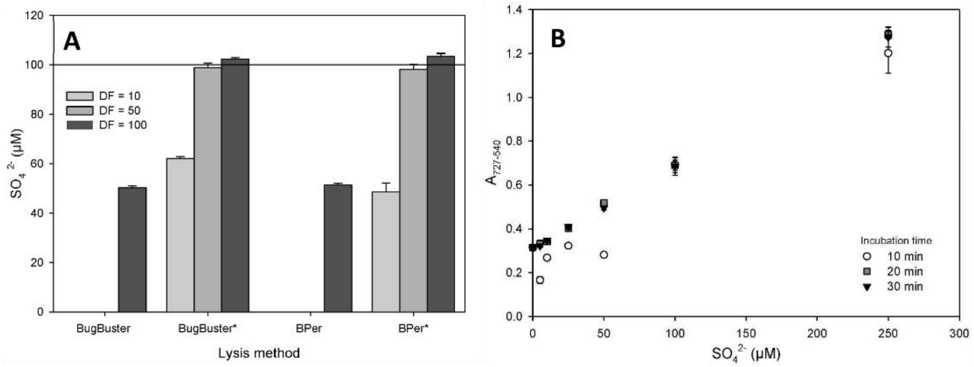

Figure S5. A. Sulfate determination in cell lysates dilutions of *E. coli* bearing pET28+ empty plasmid. The lysis solution was prepared either with BugBuster® or B-Per^{TM}, Hepes 100 mM, lysozyme (2.5 mg mL^{-1}) and DNase (10 µg mL^{-1}). The solid line indicates the amount of sulfate spiked. *Content was measured after 5 min incubation of the cell lysates at 70°C. DF; dilution factor. B. Analysis of the sulfate calibration curve containing 1:10 diluted cell lysate and incubated at 70°C for different times in 1.5 mL tubes.

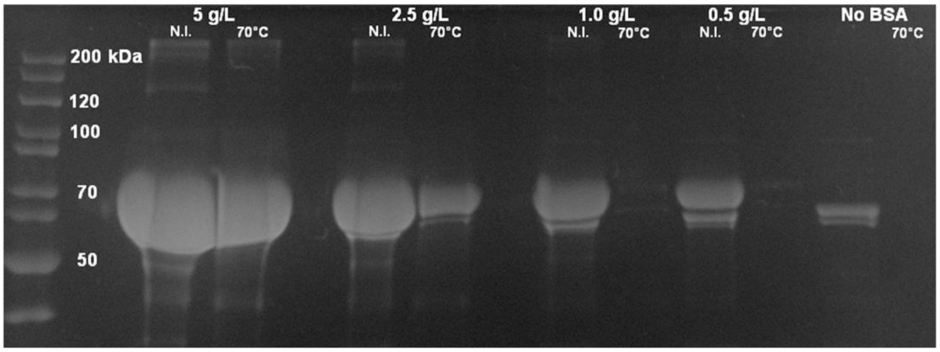

Figure S6. Polyacrylamide gel electrophoresis of cell lysates of *E. coli* bearing pASK_PAS plasmid and containing different BSA concentrations. Samples were analyzed before and after an incubation step at 70 °C for 30 min. N.I.; not incubated.

Supporting Information – Reference Section

(1) White, G. F.; Lillis, V.; Shaw, D. J., *Biochem. J.,* **1980**, *187*, 191-196.

B5. Discussion

B5.1. Enzymatic sulfatase assay: analysis of advantages, limitations and optimization potential

The main goal of the developed enzymatic assay, the detection of aryl and alkyl sulfatase activity directly from cell lysates, was successfully achieved. This was demonstrated by the experimental comparison with the most commonly applied method for HT detection of sulfatase activity based on *p*-nitrophenyl sulfate. The assay workflow, which includes bacterial growth, heterologous protein expression, sulfatase reaction, and *in situ* sulfate determination, may be well employed as part of an automated analysis platform. This aspect is very important compared to conventional methods, as it renders the assay compatible with currently employed molecular biology tools for gene mutagenesis (e.g., *error prone* PCR) or (meta) genomic mining (e.g., using fosmid libraries). Thereby, screening and engineering sulfatases in a high-throughput mode could be performed without the need of non-natural chromogenic substrates, insensitive precipitation procedures, or time-intensive chromatographic analysis of released sulfate.

On the other hand, an important limitation of the assay is its sensitivity to phosphate at > 0.1 mM. This feature may generate false positives if the sample matrixes contain this ion at higher concentrations. Therefore, this issue must be considered when devising sulfatase analysis strategies. Special attention should be paid to sulfatases acting in phosphate buffer, for example. For these enzymes, the reaction may be performed at lower buffer concentrations and the sample preparation may include a re-buffering or a dilution step after sulfatase reaction to avoid false negatives. As commonly performed in screening or improving procedures, it is advisable that any positive hits found is double-checked using an alternative sulfate analysis method or by detecting the de-sulfated product.

A very important parameter to consider when designing HT analytical procedures is the economic factor per plate (96 samples). When all purchased reagent consumables are considered, a sulfatase assay cost of 3.83€ results per analyzed plate was calculated. These numbers resulted without considering the self-produced enzymes *APSk*, *ATPs*/*GTPase,* and *PPDK*. This relatively high cost is mainly caused by only three reagents: GTP (42% total amount), the chromogenic reagent DA-64 (25%), and pyruvate oxidase (24%). Therefore, various possibilities were identified to improve the analytical and economic performance of the sulfatase assay.

For example, the relatively high absorbance signal obtained from the sulfate blank ($A_{727\text{-}540}$ ~ 0.32) not only waste the chromogenic reagent, but also impedes a better assay sensitivity. For comparison, the pyruvate assay (in which the sulfate assay is based) displays an analyte blank of $A_{727\text{-}540}$ ~ 0.02, while that of the PPi assay of $A_{727\text{-}540}$ ~ 0.11. The output signal increase ($A_{727\text{-}540}$) in the developed assay reflects that the dye DA-64 is oxidized to Bindschedler's green by the HRP. This can only occur if its substrate H_2O_2 is present in the solution. Hydrogen peroxide, in turn, can only be produced by the enzyme pyruvate oxidase, whose reaction can only be triggered either by pyrophosphate (*via PPDK* producing pyruvate), or by pyruvate itself. Consequently, the reason for the high absorbance of the sulfate blank must be the release of either pyrophosphate or pyruvate occurring independently from the initial sulfate concentration triggering the enzymatic cascade.

When $A_{727-540}$ of the master mix 2 and different blanks is tracked at 37°C over time, a clear picture of the possible explanations for this high signal can be observed (Figure 13). It is worth noting that the master mixes incubated did not interact with any other compound during this time. After 30 min incubation time, $A_{727-540}$ of the master mix containing all compounds reaches 0.1. This value is in accordance with that for the blank value of the pyrophosphate assay. Surprisingly, a similar curve is obtained when TPP (the cofactor of the pyruvate oxidase) is absent in the mixture, with a continuous increase up to 120 min. Most importantly, the increased absorbance was surpressed when one of the three components involved in the PPi catalyzing reaction is removed from the master mix. While the absence of the enzyme *PPDK* yielded a lower increment in the absorbance rate of approx. 50% compared to the master mix 2 containing all components, the observed impact of AMP resulted more significant for the $A_{727-540}$ increase. Noticeable, nearly no absorbance increase over the 120 min was observed when PEP is absent in the mixture. These results strongly suggest that phosphoenolpyruvate is mostly responsible for the signal observed in the sulfate blanks. A degradation of the phosphoenolpyruvate to phosphate and pyruvate seems feasible. As discussed above, pyruvate formation triggers the enzymatic oxidation of the DA-64 dye.

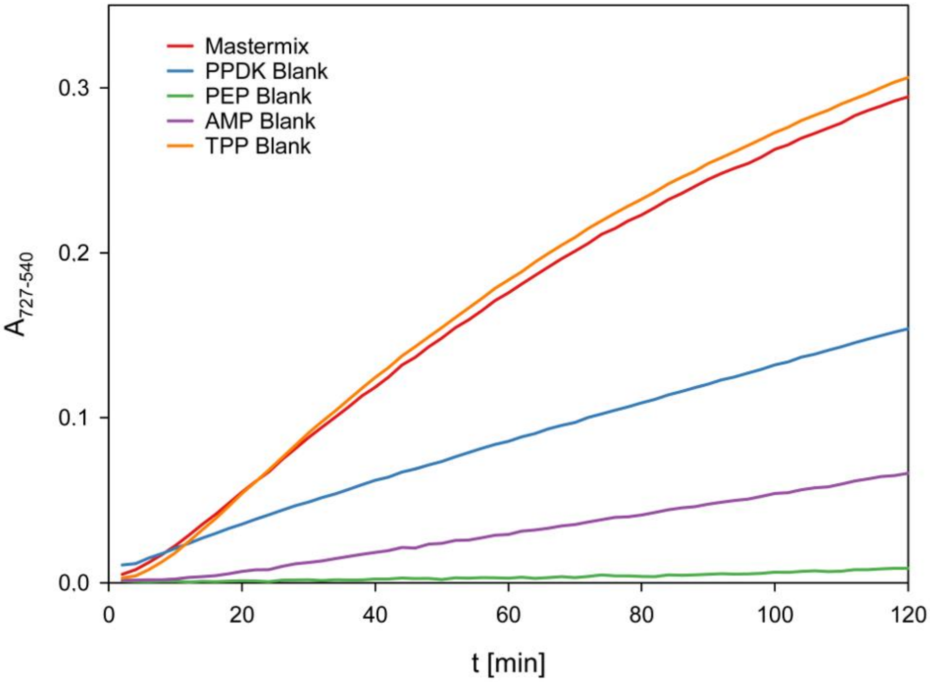

Figure 13 Absorbance increase of master mix 2 and different blank types at 37°C over time

Similarly, the nucleotides employed in the first cascade reaction (ATP and GTP) may well suffer a non-enzyme dependent hydrolysis or degradation to pyrophosphate, which would further increase the absorbance of the sulfate blank as explained above. Besides, the POX displays ATPase side-activity. If the master mix 2 of the sulfate assay is employed for generating a PPi calibration curve in water within the same range as for the sulfate assay, lower signals are observed, as shown in Figure 14. It is worth noting that this calibration curve was obtained in the same manner as in the sulfate assay, i.e., incubating master mix 1 of sulfate assay, but with PPi instead. Furthermore, when the enzymes responsible for the detection and processing of sulfate are removed from the *sulfate* assay (Figure 14), a base absorbance of ~ 0.23 is observed throughout the calibration range.

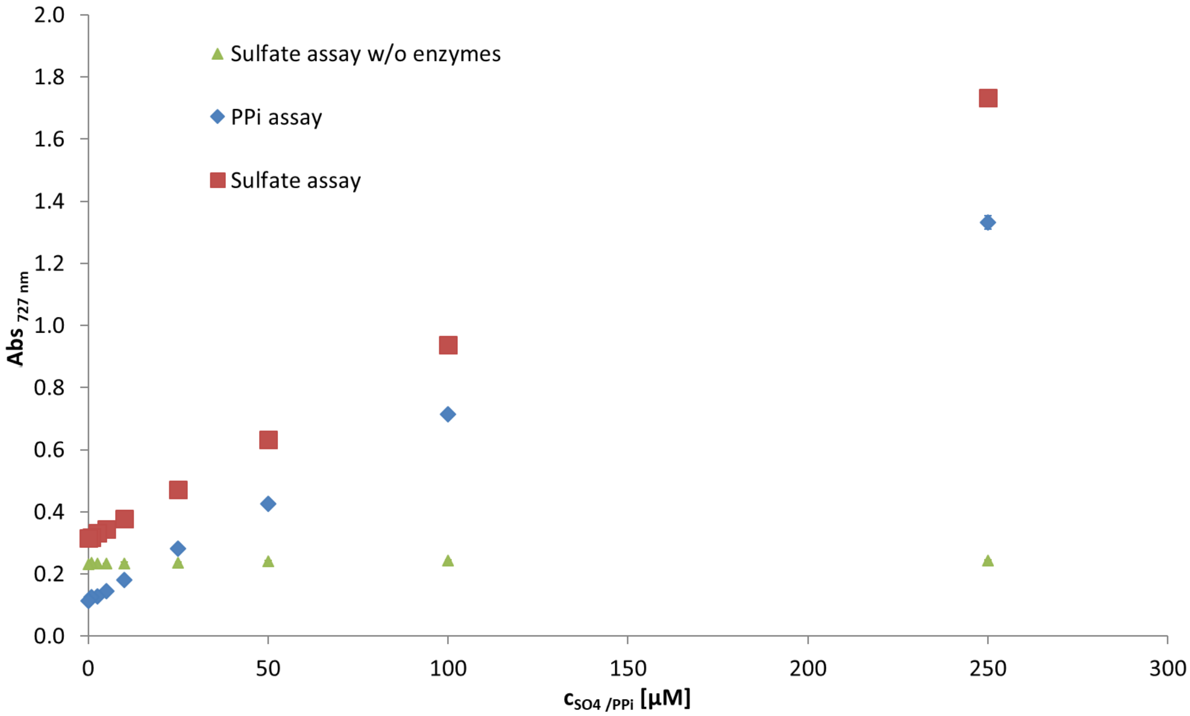

Figure 14 Comparison of pyrophosphate (PPi) and sulfate assay with and without enzymes in reaction 1

The value of the base absorbance without sulfate active enzymes (0.23) is equal to the difference between the blank value of the sulfate assay and the pyrophosphate assay. Consequently, the results point to a non-enzymatic release of PPi in the master mix 1 of the cascade. A comparison of this base absorbance with the calibration curve of PPi yields a concentration of 19 µM. This concentration would correspond to the amount of ATP or GTP which cannot be used by the *ATPs* and the *APSk* because of its degradation.

Modern enzyme engineering strategies could be applied to further improve the detection cascade. So, the sulfate assay may be significantly enhanced through targeted engineering of *ATPs*/*GTPase*. An improved enzyme variant in terms of phosphate sensitivity, for example, would allow an increased selectivity of the assay towards sulfate instead of phosphate. The costs of the assay due to the high concentration of GTP could be further reduced by a detailed examination of the native *ATPs*/*GTPase* in terms of coupling efficiency between GTP hydrolysis and APS synthesis. If necessary, a variant with decreased inhibition towards GDP could be optimized. In this way, the GTP concentration required for the assay could be decreased, thus improving the economic aspect of the assay.

B5.2. Assay application on hydrolysates from sulfated polysaccharides

The enzymatic sulfate assay was primarily designed to detect sulfatase activity on marine polysaccharides as substrates, such as carrageenan or fucoidan. In this frame, the chemical release of sulfate from such colloids (e.g., with TFA) is as suitable benchmark to evaluate the performance of the assay. The sulfate calibration curve, however, must be measured in a corresponding neutralized and diluted TFA solution to compensate matrix effects that may occur in the detection cascade, as shown in Figure 15.

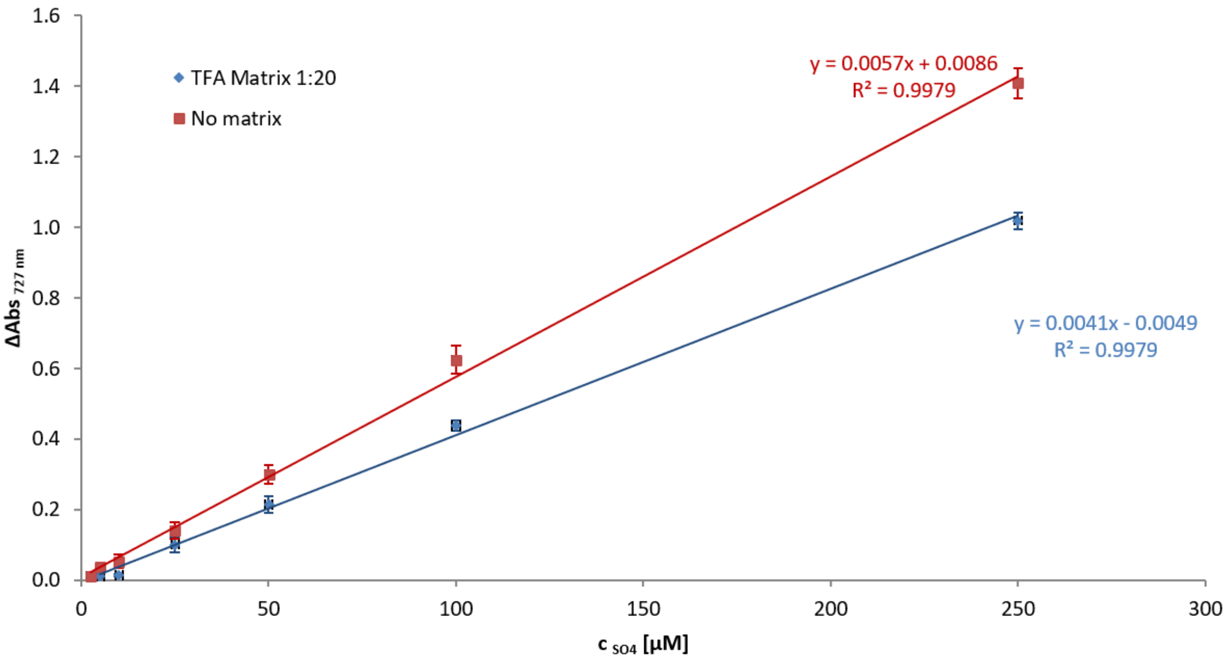

Figure 15 Sulfate calibration curve in water and in TFA matrix

Because of the impact of the TFA matrix, the calibration curve suffered a slight loss of sensitivity in comparison to water, thus showing less absorbance as shown in Figure 15. This made the detection of sulfate possible at concentrations 10 < 250 µM (LOD 2.8 µM, LOQ 5.5 µM). Despite this fact, a good correlation coefficient of $R^2 = 0.9979$ was observed. The sulfate concentration found in TFA hydrolysates of carrageenan (1 g L^{-1}) of various types and different purity grades is shown in Table 21.

Table 21: Sulfate concentration found in different carrageenan hydrolysates; $^{+}$industrial grade; *analytical grade, n=3

Carrageenan type	Theoretical conc. (mM)	Determined conc. (mM)
κ – carrageenan^{+}	2.45	2.18 ± 0.07
κ – carrageenan*		2.45 ± 0.15
ι – carrageenan^{+}	3.92	2.64 ± 0.08
ι – carrageenan*		3.48 ± 0.07
λ – carrageenan^{+}	4.76	2.38 ± 0.05

The sulfate concentration found in industrial carrageenan was lower than the theoretical values for all three analyzed kappa, iota, and lambda types. Being an extracted product from marine seaweeds with a low refinement grade, the concentration of sulfate found in technical carrageenan is correspondingly lower those for chemically pure carrageenan. The amount of sulfate found in lambda carrageenan, however, accounts for almost 50% of the theoretical concentration, so that a more comprehensive product quality analysis would be advisable. Noticeable, the sulfate amount determined in TFA hydrolysates of analytical grade carrageenan was well in accordance with the theoretical values for pure product. These results remark the robustness of the developed assay for determining sulfate, even in complex chemical matrixes.

B6. Conclusions and Perspectives

In the second part of this work, an enzymatic sulfatase assay was devised, validated and characterized. The development of this method provides a relevant tool for promising biotechnological utilization alternatives of seaweed sulfated polysaccharides, especially carrageenan. Although a certain optimization potential was identified, very good performance in terms of repeatability and reproducibility were achieved. The precision and sensitivity of the procedure were comparable to those achieved with conventional chromatographic sulfate detection methods. This colorimetric assay may be well employed in its current form for screening sulfatases using commonly employed molecular biology tools in a HT mode. Furthermore, engineering known alkyl or aryl sulfatases seems also feasible with the enzyme cascade.

To date, the genome of various marine organisms has been sequenced in which annotated genes for sulfatases can be found. Some examples include bacteria from *Pseudoalteromonas* and *Rhodopirellula* species. Culture procedures for these type or organisms are challenging and time intensive. A search for sulfate active enzymes may either start from the amplification of identified DNA motifs for sulfatases (as reported in online databases) or from genomic or metagenomic libraries using e.g., fosmids. However, important considerations should be made before screening. For example, some types of sulfatase present a post-translational modification of the amino acids involved in the active site. In this case, cysteine or serine is oxidized to form formylglycine, a catalytically essential residue for sulfate ester hydrolysis. Thus, the possibility of performing this amino acid modification in the expressing organism must be ensured.

On the other hand, engineering sulfatases using random mutagenesis, directed evolution, or rational methods is also an anticipated application of the colorimetric assay. A pre-requisite for this is the availability of a sulfatase gene that can be modified, and the resulting variants produced in proper expression systems. Interesting catalytic features, such as activity, thermal stability, pH or solvent tolerance, as well as substrate spectrum may be improved towards new application fields. In summary, the presented assay sets the basis for an accelerated development of sulfatases that allow the production of molecularly tailored carrageenan, e.g., with improved rheological properties.

References

Abbasi, T., & Abbasi, S. A. (2010). Biomass energy and the environmental impacts associated with its production and utilization. *Renewable and Sustainable Energy Reviews, 14*(3), 919-937. doi:https://doi.org/10.1016/j.rser.2009.11.006

ABEnzymes. (2011a). Rohapect(R) B1L, product description and specification. In (Vol. Rev. No. 11): ABF Ingredients.

ABEnzymes. (2011b). Rohapect(R) UF, product description and specification. In (Vol. Rev. No. 07): ABF Ingredients.

ABEnzymes. (2013). Rohament(R) CL, product description and specification. In (Vol. Rev. No. 09): ABF Ingredients.

ABO. (2017). *Algal Biomass Organization - Industrial Algae Measurements* (Version 8.0). Retrieved from http://algaebiomass.org/wp-content/gallery/2012-algae-biomass-summit/2017/12/2017_ABO_IAM_Full_v4_LowResSP.pdf.

Atkinson Jr, A. W., Gunning, B. E. S., & John, P. C. L. (1972). Sporopollenin in the cell wall of Chlorella and other algae: Ultrastructure, chemistry, and incorporation of 14C-acetate, studied in synchronous cultures. *Planta, 107*(1), 1-32.

Azanza, R. V., & Ask, E. (2017). Reproductive Biology and Eco-physiology of Farmed Kappaphycus and Eucheuma. In A. Q. Hurtado, A. T. Critchley, & I. C. Neish (Eds.), *Tropical Seaweed Farming Trends, Problems and Opportunities: Focus on Kappaphycus and Eucheuma of Commerce* (pp. 45-53). Cham: Springer International Publishing.

Azevedo, G., Torres, M. D., Sousa-Pinto, I., & Hilliou, L. (2015). Effect of pre-extraction alkali treatment on the chemical structure and gelling properties of extracted hybrid carrageenan from Chondrus crispus and Ahnfeltiopsis devoniensis. *Food Hydrocolloids, 50*, 150-158. doi:https://doi.org/10.1016/j.foodhyd.2015.03.029

Barbeyron, T., Brillet-Guéguen, L., Carré, W., Carrière, C., Caron, C., Czjzek, M., . . . Michel, G. (2016). Matching the diversity of sulfated biomolecules: Creation of a classification database for sulfatases reflecting their substrate specificity. *PLoS ONE, 11*, 1–33. doi:10.1371/journal.pone.0164846

Barsanti, L., & Gualtieri, P. (2014). *Algae: Anatomy, Biochemistry, and Biotechnology*: CRC Press.

Becker, E. W. (2007). Micro-algae as a source of protein. *Biotechnology Advances, 25*(2), 207-210. doi:https://doi.org/10.1016/j.biotechadv.2006.11.002

Bixler, H. J., & Porse, H. (2011). A decade of change in the seaweed hydrocolloids industry. *Journal of Applied Phycology, 23*(3), 321-335. doi:10.1007/s10811-010-9529-3

Blumreisinger, M., Meindl, D., & Loos, E. (1983). Cell wall composition of chlorococcal algae. *Phytochemistry, 22*(7), 1603-1604. doi:10.1016/0031-9422(83)80096-x

Bozell, J. J., & Petersen, G. R. (2010). Technology development for the production of biobased products from biorefinery carbohydrates-the US Department of Energy's "Top 10" revisited. *Green Chemistry, 12*(4), 539-554. doi:10.1039/B922014C

Brennan, L., & Owende, P. (2010). Biofuels from microalgae—A review of technologies for production, processing, and extractions of biofuels and co-products. *Renewable and Sustainable Energy Reviews, 14*(2), 557-577. doi:https://doi.org/10.1016/j.rser.2009.10.009

Brodie, J., Chan, C. X., De Clerck, O., Cock, J. M., Coelho, S. M., Gachon, C., . . . Bhattacharya, D. (2017). The Algal Revolution. *Trends in Plant Science, 22*(8), 726-738. doi:https://doi.org/10.1016/j.tplants.2017.05.005

Cantarel, B. I., Coutinho, P. M., Rancurel, C., Bernard, T., Lombard, V., & Henrissat, B. (2009). The Carbohydrate-Active EnZymes database (CAZy): An expert resource for glycogenomics. *Nucleic Acids Research, 37*(SUPPL. 1), D233-D238. doi:10.1093/nar/gkn663

Charoensiddhi, S., Conlon, M. A., Franco, C. M. M., & Zhang, W. (2017). The development of seaweed-derived bioactive compounds for use as prebiotics and nutraceuticals using enzyme technologies. *Trends in Food Science & Technology, 70*(Supplement C), 20-33. doi:https://doi.org/10.1016/j.tifs.2017.10.002

Chauhan, P. S., & Saxena, A. (2016). Bacterial carrageenases: an overview of production and biotechnological applications. *3 Biotech, 6*(2), 146. doi:10.1007/s13205-016-0461-3

Chen, C.-Y., Zhao, X.-Q., Yen, H.-W., Ho, S.-H., Cheng, C.-L., Lee, D.-J., . . . Chang, J.-S. (2013). Microalgae-based carbohydrates for biofuel production. *Biochemical Engineering Journal, 78*(0), 1-10. doi:http://dx.doi.org/10.1016/j.bej.2013.03.006

Chisti, Y. (2007). Biodiesel from microalgae. *Biotechnology Advances, 25*(3), 294-306. doi:https://doi.org/10.1016/j.biotechadv.2007.02.001

Choi, S. P., Nguyen, M. T., & Sim, S. J. (2010). Enzymatic pretreatment of Chlamydomonas reinhardtii biomass for ethanol production. *Bioresource Technology, 101*(14), 5330-5336. doi:https://doi.org/10.1016/j.biortech.2010.02.026

Clark, J. H., Budarin, V., Deswarte, F. E. I., Hardy, J. J. E., Kerton, F. M., Hunt, A. J., . . . Wilson, A. J. (2006). Green chemistry and the biorefinery: a partnership for a sustainable future. *Green Chemistry, 8*(10), 853-860. doi:10.1039/B604483M

Correa, D. F., Beyer, H. L., Possingham, H. P., Thomas-Hall, S. R., & Schenk, P. M. (2017). Biodiversity impacts of bioenergy production: Microalgae vs. first generation biofuels. *Renewable and Sustainable Energy Reviews, 74*(Supplement C), 1131-1146. doi:https://doi.org/10.1016/j.rser.2017.02.068

Cottier-Cook, E. N. N., Yacine Badis, Marnie L. Campbell, Thierry Chopin, Weiping, Dai, J. F., Peimin He, Chad L. Hewitt, Gwang Hoon Kim, Yuanzi Huo, Zengjie Jiang, Gert, Kema, X. L., Feng Liu, Hongmei Liu, Yuanyuan Liu, Qinqin Lu, Qijun Luo, Yuze Mao, Flower, E. Msuya, C. R., Hui Shen, Grant D. Stentiford, Charles Yarish, Hailong Wu, Xinming, & Yang, J. Z., Yongdong Zhou, Claire M. M. Gachon. (2016). Safeguarding the future of the global seaweed aquaculture industry. In: United Nations University, Institute for Water, Environment and Health (UNU-INWEH).

Dai, J., Wu, Y., Chen, S. W., Zhu, S., Yin, H. P., Wang, M., & Tang, J. (2010). Sugar compositional determination of polysaccharides from Dunaliella salina by modified RP-HPLC method of precolumn derivatization with 1-phenyl-3-methyl-5-pyrazolone. *Carbohydrate Polymers, 82*(3), 629-635.

De Jesus Raposo, M. F., De Morais, R. M. S. C., & De Morais, A. M. M. B. (2013). Bioactivity and applications of sulphated polysaccharides from marine microalgae. *Marine Drugs*, *11*(1), 233-252. doi:10.3390/md11010233

Delattre, C., Pierre, G., Laroche, C., & Michaud, P. (2016). Production, extraction and characterization of microalgal and cyanobacterial exopolysaccharides. *Biotechnology Advances, 34*(7), 1159-1179. doi:10.1016/j.biotechadv.2016.08.001

Demuez, M., Mahdy, A., Tomás-Pejó, E., González-Fernández, C., & Ballesteros, M. (2015). Enzymatic cell disruption of microalgae biomass in biorefinery processes. *Biotechnology and Bioengineering, 112*(10), 1955-1966. doi:10.1002/bit.25644

EPSAG. (2018). Online repositorium for algal media and recipes. Experimentelle Phykologie und Sammlung von Algenkulturen der Georg-August-Universität Göttingen. Retrieved from www.uni-goettingen.de/de/186449.html

Faber, K. (2017). *Biotransformations in organic chemistry: a textbook*. New York: SPRINGER.

Fer, M., Préchoux, A., Leroy, A., Sassi, J.-F., Lahaye, M., Boisset, C., . . . Helbert, W. (2012). Medium-throughput profiling method for screening polysaccharide-degrading enzymes in complex bacterial extracts. *Journal of Microbiological Methods, 89*(3), 222-229. doi:http://dx.doi.org/10.1016/j.mimet.2012.03.004

Fernandes, B., Dragone, G., Abreu, A. P., Geada, P., Teixeira, J., & Vicente, A. (2012). Starch determination in Chlorella vulgaris-a comparison between acid and enzymatic methods. *Journal of Applied Phycology, 24*(5), 1203-1208.

Fernandes, P. (2010). Enzymes in food processing: A condensed overview on strategies for better biocatalysts. *Enzyme Research, 2010*. doi:10.4061/2010/862537

Foley, P. M., Beach, E. S., & Zimmerman, J. B. (2011). Algae as a source of renewable chemicals: opportunities and challenges. *Green Chemistry, 13*(6), 1399-1405. doi:10.1039/C1GC00015B

Fu, C.-C., Hung, T.-C., Chen, J.-Y., Su, C.-H., & Wu, W.-T. (2010). Hydrolysis of microalgae cell walls for production of reducing sugar and lipid extraction. *Bioresource Technology, 101*(22), 8750-8754. doi:http://dx.doi.org/10.1016/j.biortech.2010.06.100

Genicot, S. M., Groisillier, A., Rogniaux, H., Meslet-Cladière, L., Barbeyron, T., & Helbert, W. (2014). Discovery of a novel iota carrageenan sulfatase isolated from the marine bacterium Pseudoalteromonas carrageenovora. *Frontiers in Chemistry, 2*. doi:10.3389/fchem.2014.00067

Geresh, S., Arad, S., Levy-Ontman, O., Zhang, W., Tekoah, Y., & Glaser, R. (2009). Isolation and characterization of poly- and oligosaccharides from the red microalga Porphyridium sp. *Carbohydrate Research, 344*(3), 343-349. doi:http://dx.doi.org/10.1016/j.carres.2008.11.012

Gerken, H. G., Donohoe, B., & Knoshaug, E. P. (2013). Enzymatic cell wall degradation of Chlorella vulgaris and other microalgae for biofuels production. *Planta, 237*(1), 239-253. doi:10.1007/s00425-012-1765-0

Ghasemi Naghdi, F., González González, L. M., Chan, W., & Schenk, P. M. (2016). Progress on lipid extraction from wet algal biomass for biodiesel production. *Microbial Biotechnology, 9*(6), 718-726. doi:10.1111/1751-7915.12360

Greenwell, H. C., Laurens, L. M. L., Shields, R. J., Lovitt, R. W., & Flynn, K. J. (2009). Placing microalgae on the biofuels priority list: a review of the technological challenges. *Journal of The Royal Society Interface*.

Griffiths, M., Harrison, S. T. L., Smit, M., & Maharajh, D. (2016). Major Commercial Products from Micro- and Macroalgae. In F. Bux & Y. Chisti (Eds.), *Algae Biotechnology: Products and Processes* (pp. 269-300). Cham: Springer International Publishing.

Gurpilhares, D. d. B., Moreira, T. R., Bueno, J. d. L., Cinelli, L. P., Mazzola, P. G., Pessoa, A., & Sette, L. D. (2016). "Algae's sulfated polysaccharides modifications: Potential use of microbial enzymes". *Process Biochemistry, 51*(8), 989-998. doi:https://doi.org/10.1016/j.procbio.2016.04.020

Hafting, J. T., Craigie, J. S., Stengel, D. B., Loureiro, R. R., Buschmann, A. H., Yarish, C., . . . Critchley, A. T. (2015). Prospects and challenges for industrial production of seaweed bioactives. *Journal of Phycology, 51*(5), 821-837. doi:10.1111/jpy.12326

Hanson, S. R., Best, M. D., & Wong, C. H. (2004). Sulfatases: Structure, mechanism, biological activity, inhibition, and synthetic utility. *Angewandte Chemie-International Edition*(43), 5736–5763. doi:10.1002/anie.200300632

Harun, R., & Danquah, M. K. (2011). Enzymatic hydrolysis of microalgal biomass for bioethanol production. *Chemical Engineering Journal, 168*(3), 1079-1084. doi:http://dx.doi.org/10.1016/j.cej.2011.01.088

Harun, R., Yip, J. W. S., Thiruvenkadam, S., Ghani, W. A. W. A. K., Cherrington, T., & Danquah, M. K. (2014). Algal biomass conversion to bioethanol-a step-by-step assessment. *Biotechnology Journal, 9*(1), 73-86.

Helbert, W. (2017). Marine Polysaccharide Sulfatases. *Frontiers in Marine Science, 4*(6). doi:10.3389/fmars.2017.00006

Hendriks, A. T. W. M., & Zeeman, G. (2009). Pretreatments to enhance the digestibility of lignocellulosic biomass. *Bioresource Technology, 100*(1), 10-18. doi:https://doi.org/10.1016/j.biortech.2008.05.027

Holdt, S. L., & Kraan, S. (2011). Bioactive compounds in seaweed: functional food applications and legislation. *Journal of Applied Phycology, 23*(3), 543-597. doi:10.1007/s10811-010-9632-5

Hu, L., Zhao, G., Hao, W., Tang, X., Sun, Y., Lin, L., & Liu, S. (2012). Catalytic conversion of biomass-derived carbohydrates into fuels and chemicals via furanic aldehydes. *RSC Advances, 2*(30), 11184-11206. doi:10.1039/c2ra21811a

Huber, G. W., Iborra, S., & Corma, A. (2006). Synthesis of Transportation Fuels from Biomass: Chemistry, Catalysts, and Engineering. *Chemical Reviews, 106*(9), 4044-4098. doi:10.1021/cr068360d

Hurd, C. L., Harrison, P. J., Bischof, K., & Lobban, C. S. (2014). *Seaweed ecology and physiology, second edition*.

Kameya, M., Himi, M., & Asano, Y. (2014). Rapid and selective enzymatic assay for l-methionine based on a pyrophosphate detection system. *Anal. Biochem., 447*(0), 33-38. doi:http://dx.doi.org/10.1016/j.ab.2013.11.002

Kapaun, E., & Reisser, W. (1995). A Chitin-like glycan in the cell-wall of a Chlorella sp (Chlorococcales, Chlorophyceae). *Planta, 197*(4), 577-582.

Kerton, F. M., Liu, Y., Omari, K. W., & Hawboldt, K. (2013). Green chemistry and the ocean-based biorefinery. *Green Chemistry, 15*(4), 860-871. doi:10.1039/C3GC36994C

Kim, K. H., Choi, I. S., Kim, H. M., Wi, S. G., & Bae, H.-J. (2014). Bioethanol production from the nutrient stress-induced microalga Chlorella vulgaris by enzymatic hydrolysis and immobilized yeast fermentation. *Bioresource Technology, 153*(0), 47-54. doi:http://dx.doi.org/10.1016/j.biortech.2013.11.059

Kirkman, H., & Kendrick, G. A. (1997). Ecological significance and commercial harvesting of drifting and beach-cast macro-algae and seagrasses in Australia: a review. *Journal of Applied Phycology, 9*(4), 311-326. doi:10.1023/a:1007965506873

Kostas, E. T., White, D. A., & Cook, D. J. (2017). Development of a bio-refinery process for the production of speciality chemical, biofuel and bioactive compounds from Laminaria digitata. *Algal Research, 28*(Supplement C), 211-219. doi:https://doi.org/10.1016/j.algal.2017.10.022

Kroth, P. G., Chiovitti, A., Gruber, A., Martin-Jezeque, V., Mock, T., Parker, M. S., . . . Bowler, C. (2008). A model for carbohydrate metabolism in the diatom Phaeodactylum tricornutum deduced from comparative whole genome analysis. *PLoS ONE, 3*(1). doi:10.1371/journal.pone.0001426

Lam, K. N., Cheng, J., Engel, K., Neufeld, J. D., & Charles, T. C. (2015). Current and future resources for functional metagenomics. *Frontiers in Microbiology, 6*(OCT). doi:10.3389/fmicb.2015.01196

Laurens, L. M. L., Markham, J., Templeton, D. W., Christensen, E. D., Van Wychen, S., Vadelius, E. W., . . . Pienkos, P. T. (2017). Development of algae biorefinery concepts for biofuels and bioproducts; a perspective on process-compatible products and their impact on cost-reduction. *Energy & Environmental Science, 10*(8), 1716-1738. doi:10.1039/C7EE01306J

Laurens, L. M. L., Nagle, N., Davis, R., Sweeney, N., Van Wychen, S., Lowell, A., & Pienkos, P. T. (2015). Acid-catalyzed algal biomass pretreatment for integrated lipid and carbohydrate-based biofuels production. *Green Chemistry, 17*(2), 1145-1158. doi:10.1039/C4GC01612B

Lee, J. W., Na, D., Park, J. M., Lee, J., Choi, S., & Lee, S. Y. (2012). Systems metabolic engineering of microorganisms for natural and non-natural chemicals. *Nature Chemical Biology, 8*(6), 536-546. doi:10.1038/nchembio.970

Lee, Y. K. (2016). Microalgae Cultivation Fundamentals. In F. Bux & Y. Chisti (Eds.), *Algae Biotechnology: Products and Processes* (pp. 1-19). Cham: Springer International Publishing.

Leis, B., Heinze, S., Angelov, A., Pham, V. T. T., Thürmer, A., Jebbar, M., . . . Liebl, W. (2015). Functional Screening of Hydrolytic Activities Reveals an Extremely Thermostable Cellulase from a Deep-Sea Archaeon. *Frontiers in Bioengineering and Biotechnology, 3*(95). doi:10.3389/fbioe.2015.00095

Lestari , S., Mäki-Arvela, P., Beltramini, J., Lu, G. Q. M., & Murzin, D. Y. (2009). Transforming Triglycerides and Fatty Acids into Biofuels. *ChemSusChem, 2*(12), 1109-1119. doi:10.1002/cssc.200900107

Loft, K. J., Bojarová, P., Slámová, K., Křen, V., & Williams, S. J. (2009). Synthesis of Sulfated Glucosaminides for Profiling Substrate Specificities of Sulfatases and Fungal β-N-Acetylhexosaminidases. *ChemBioChem, 10*(3), 565-576. doi:10.1002/cbic.200800656

Long, Z. T., Bruno, J. F., & Duffy, J. E. (2011). Food chain length and omnivory determine the stability of a marine subtidal food web. *Journal of Animal Ecology, 80*(3), 586-594. doi:10.1111/j.1365-2656.2010.01800.x

Loos, E., & Meindl, D. (1985). Cell-wall-bound lytic activity in Chlorella fusca: function and characterization of an endo-mannanase. *Planta, 166*(4), 557-562.

Lupatini, A. L., Colla, L. M., Canan, C., & Colla, E. (2017). Potential application of microalga Spirulina platensis as a protein source. *Journal of the Science of Food and Agriculture, 97*(3), 724-732. doi:10.1002/jsfa.7987

Lyon, B., & Mock, T. (2014). Polar Microalgae: New Approaches towards Understanding Adaptations to an Extreme and Changing Environment. *Biology, 3*(1), 56.

Mahdy, A., Mendez, L., Tomás-Pejó, E., del Mar Morales, M., Ballesteros, M., & González-Fernández, C. (2015). Influence of enzymatic hydrolysis on the biochemical methane potential of Chlorella vulgaris and Scenedesmus sp. *Journal of Chemical Technology & Biotechnology*, n/a-n/a. doi:10.1002/jctb.4722

Manochio, C., Andrade, B. R., Rodriguez, R. P., & Moraes, B. S. (2017). Ethanol from biomass: A comparative overview. *Renewable and Sustainable Energy Reviews, 80*(Supplement C), 743-755. doi:https://doi.org/10.1016/j.rser.2017.05.063

Markou, G., Angelidaki, I., & Georgakakis, D. (2012). Microalgal carbohydrates: an overview of the factors influencing carbohydrates production, and of main bioconversion technologies for production of biofuels. *Applied Microbiology and Biotechnology, 96*(3), 631-645. doi:10.1007/s00253-012-4398-0

Mayers, J. J., Flynn, K. J., & Shields, R. J. (2013). Rapid determination of bulk microalgal biochemical composition by Fourier-Transform Infrared spectroscopy. *Bioresource Technology, 148*, 215-220. doi:10.1016/j.biortech.2013.08.133

McConnell, B. O., & Antoniewicz, M. R. (2016). Measuring the Composition and Stable-Isotope Labeling of Algal Biomass Carbohydrates via Gas Chromatography/Mass Spectrometry. *Analytical Chemistry, 88*(9), 4624-4628. doi:10.1021/acs.analchem.6b00779

Milledge, J. J. (2011). Commercial application of microalgae other than as biofuels: a brief review. *Reviews in Environmental Science and Bio/Technology, 10*(1), 31-41. doi:10.1007/s11157-010-9214-7

Mirsiaghi, M., & Reardon, K. F. (2015). Conversion of lipid-extracted Nannochloropsis salina biomass into fermentable sugars. *Algal Research, 8*, 145-152. doi:http://dx.doi.org/10.1016/j.algal.2015.01.013

Neish, I. C., Sepulveda, M., Hurtado, A. Q., & Critchley, A. T. (2017). Reflections on the Commercial Development of Eucheumatoid Seaweed Farming. In A. Q. Hurtado, A. T. Critchley, & I. C. Neish (Eds.), *Tropical Seaweed Farming Trends, Problems and Opportunities: Focus on Kappaphycus and Eucheuma of Commerce* (pp. 1-27). Cham: Springer International Publishing.

Nielsen, S. S. (2010). Phenol-Sulfuric Acid Method for Total Carbohydrates. In S. S. Nielsen (Ed.), *Food Analysis Laboratory Manual* (pp. 47-53). Boston, MA: Springer US.

Northcote, D. H., Goulding, K. J., & Horne, R. W. (1958). Chemical composition and structure of the cell wall of Chlorella pyrenoidosa. *Biochemical Journal, 70*, 391-&.

Ogawa, K., Ikeda, Y., & Kondo, S. (1999). A new trisaccharide, α-D-glucopyranuronosyl-(1→3)-α-L-rhamnopyranosyl-(1→2)-α-L-rhamnopyranose from Chlorella vulgaris. *Carbohydrate Research, 321*(1-2), 128-131.

Ogawa, K., Yamaura, M., Ikeda, Y., & Kondo, S. (1998). New aldobiuronic acid, 3-O-alpha-D-glucopyranuronosyl-L-rhamnopyranose from an acidic polysaccharide of Chlorella vulgaris. *Bioscience Biotechnology and Biochemistry, 62*(10), 2030-2031. doi:10.1271/bbb.62.2030

Ogawa, K., Yamaura, M., & Maruyama, I. (1994). Isolation and identification of 3-o-methyl-d-galactose as a constituent of neutral polysaccharide of Chlorella vulgaris. *Bioscience Biotechnology and Biochemistry, 58*(5), 942-944.

Ogawa, K., Yamaura, M., & Maruyama, I. (1997). Isolation and identification of 2-O-methyl-L-rhamnose and 3-O-methyl-L-rhamnose as constituents of an acidic polysaccharide of Chlorella vulgaris. *Bioscience, Biotechnology and Biochemistry, 61*(3), 539-540.

Olaitan, S. A., & Northcote, D. H. (1962). Polysaccharides of Chlorella pyrenoidosa. *Biochemical Journal, 82*(3), 509-&.

Ortiz-Tena, J. G., Rühmann, B., Schieder, D., & Sieber, V. (2016). Revealing the diversity of algal monosaccharides: Fast carbohydrate fingerprinting of microalgae using crude biomass and showcasing sugar distribution in Chlorella vulgaris by biomass fractionation. *Algal Research, 17*, 227-235. doi:http://dx.doi.org/10.1016/j.algal.2016.05.008

Pauly, M., & Keegstra, K. (2008). Cell-wall carbohydrates and their modification as a resource for biofuels. *The Plant Journal, 54*(4), 559-568. doi:10.1111/j.1365-313X.2008.03463.x

Pettolino, F. A., Walsh, C., Fincher, G. B., & Bacic, A. (2012). Determining the polysaccharide composition of plant cell walls. *Nature Protocols, 7*(9), 1590-1607. doi:10.1038/nprot.2012.081

Pieper, S., Unterieser, I., Mann, F., & Mischnick, P. (2012). A new arabinomannan from the cell wall of the chlorococcal algae Chlorella vulgaris. *Carbohydrate Research, 352*, 166-176. doi:10.1016/j.carres.2012.02.007

Porse, H., & Rudolph, B. (2017). The seaweed hydrocolloid industry: 2016 updates, requirements, and outlook. *Journal of Applied Phycology, 29*(5), 2187-2200. doi:10.1007/s10811-017-1144-0

Porter, J. L., Rusli, R. A., & Ollis, D. L. (2016). Directed Evolution of Enzymes for Industrial Biocatalysis. *ChemBioChem, 17*(3), 197-203. doi:10.1002/cbic.201500280

Prechoux, A., Genicot, S., Rogniaux, H., & Helbert, W. (2016). Enzyme-Assisted Preparation of Furcellaran-Like kappa-/beta-Carrageenan. *Marine biotechnology (New York, N.Y.), 18*(1), 133-143. doi:10.1007/s10126-015-9675-3

Pulz, O. (2001). Photobioreactors: production systems for phototrophic microorganisms. *Applied Microbiology and Biotechnology, 57*(3), 287-293. doi:10.1007/s002530100702

Qian, X., Nimlos, M. R., Johnson, D. K., & Himmel, M. E. (2005). Acidic Sugar Degradation Pathways. In B. H. Davison, B. R. Evans, M. Finkelstein, & J. D. McMillan (Eds.), *Twenty-Sixth Symposium on Biotechnology for Fuels and Chemicals* (pp. 989-997). Totowa, NJ: Humana Press.

Ragauskas, A. J., Williams, C. K., Davison, B. H., Britovsek, G., Cairney, J., Eckert, C. A., . . . Tschaplinski, T. (2006). The Path Forward for Biofuels and Biomaterials. *Science, 311*(5760), 484-489. doi:10.1126/science.1114736

Reddy, C. R. K., Yokoya, N. S., Yong, W. T. L., Luhan, M. R. J., & Hurtado, A. Q. (2017). Micro-propagation of Kappaphycus and Eucheuma: Trends and Prospects. In A. Q. Hurtado, A. T. Critchley, & I. C. Neish (Eds.), *Tropical Seaweed Farming Trends, Problems and Opportunities: Focus on Kappaphycus and Eucheuma of Commerce* (pp. 91-110). Cham: Springer International Publishing.

Rhein-Knudsen, N., Ale, M. T., & Meyer, A. S. (2015). Seaweed hydrocolloid production: An update on enzyme assisted extraction and modification technologies. *Marine Drugs, 13*(6), 3340-3359. doi:10.3390/md13063340

Rodrigues, M. A., & Da Silva Bon, E. P. (2011). Evaluation of chlorella (Chlorophyta) as source of fermentable sugars via cell wall enzymatic hydrolysis. *Enzyme Research, 2011*(1).

Rühmann, B. (2016). *Development of a modular high throughput screening platform for microbial exopolysaccharide producers.* (Doctoral Thesis), Technische Universität München, Straubing, Germany. (22)

Rühmann, B., Schmid, J., & Sieber, V. (2014). Fast carbohydrate analysis via liquid chromatography coupled with ultra violet and electrospray ionization ion trap detection in 96-well format. *Journal of Chromatography A, 1350*(0), 44-50. doi:http://dx.doi.org/10.1016/j.chroma.2014.05.014

Rühmann, B., Schmid, J., & Sieber, V. (2015). High throughput exopolysaccharide screening platform: From strain cultivation to monosaccharide composition and carbohydrate fingerprinting in one day. *Carbohydrate Polymers, 122*(0), 212-220. doi:http://dx.doi.org/10.1016/j.carbpol.2014.12.021

Schenk, P. M., Thomas-Hall, S. R., Stephens, E., Marx, U. C., Mussgnug, J. H., Posten, C., . . . Hankamer, B. (2008). Second Generation Biofuels: High-Efficiency Microalgae for Biodiesel Production. *BioEnergy Research, 1*(1), 20-43. doi:10.1007/s12155-008-9008-8

Schober, M., Gadler, P., Knaus, T., Kayer, H., Birner-Grünberger, R., Gülly, C., . . . Faber, K. (2011). A stereoselective inverting sec -alkylsulfatase for the deracemization of sec -alcohols. *Org. Lett., 13*(16), 4296–4299. doi:10.1021/ol201635y

Schober, M., Toesch, M., Knaus, T., Strohmeier, G. A., Van Loo, B., Fuchs, M., . . . Faber, K. (2013). One-pot deracemization of sec-alcohols: Enantioconvergent enzymatic hydrolysis of alkyl sulfates using stereocomplementary sulfatases. *Angewandte Chemie-International Edition, 52*, 3277–3279.

Scholz, M. J., Weiss, T. L., Jinkerson, R. E., Jing, J., Roth, R., Goodenough, U., . . . Gerken, H. G. (2014). Ultrastructure and composition of the Nannochloropsis gaditana cell wall. *Eukaryotic Cell, 13*(11), 1450-1464. doi:10.1128/EC.00183-14.

Schulze, C., Reinhardt, J., Wurster, M., Ortiz-Tena, J. G., Sieber, V., & Mundt, S. (2016). A one-stage cultivation process for lipid- and carbohydrate-rich biomass of Scenedesmus obtusiusculus based on artificial and natural water sources. *Bioresource Technology, 218*, 498-504. doi:10.1016/j.biortech.2016.06.109

Schulze, C., Strehle, A., Merdivan, S., & Mundt, S. (2017). Carbohydrates in microalgae: Comparative determination by TLC, LC-MS without derivatization, and the photometric thymol-sulfuric acid method. *Algal Research, 25*, 372-380. doi:10.1016/j.algal.2017.05.001

Schulze, C., Wetzel, M., Reinhardt, J., Schmidt, M., Felten, L., & Mundt, S. (2016). Screening of microalgae for primary metabolites including β-glucans and the influence of nitrate starvation and irradiance on β-glucan production. *Journal of Applied Phycology*, 1-7. doi:10.1007/s10811-016-0812-9

Scott, S. A., Davey, M. P., Dennis, J. S., Horst, I., Howe, C. J., Lea-Smith, D. J., & Smith, A. G. (2010). Biodiesel from algae: challenges and prospects. *Current Opinion in Biotechnology, 21*(3), 277-286. doi:10.1016/j.copbio.2010.03.005

Sekar, S., & Chandramohan, M. (2008). Phycobiliproteins as a commodity: trends in applied research, patents and commercialization. *Journal of Applied Phycology, 20*(2), 113-136. doi:10.1007/s10811-007-9188-1

Singh, R. N., & Sharma, S. (2012). Development of suitable photobioreactor for algae production – A review. *Renewable and Sustainable Energy Reviews, 16*(4), 2347-2353. doi:https://doi.org/10.1016/j.rser.2012.01.026

Sinzinger, K. (2016). *Analytical Methods for Polysaccharide-Containing Biomass*. Retrieved from Straubing, Germany:

Sinzinger, K. (2017). *Enzymatic Saccharification of Scenedesmus obtusiusculus Biomass using HT-PMP-UHPLCUV-ESI-MS.* (M.Sc.), TUM, NUS, Straubing, Germany.

Smit, A. J. (2004). Medicinal and pharmaceutical uses of seaweed natural products: A review. *Journal of Applied Phycology, 16*(4), 245-262. doi:10.1023/B:JAPH.0000047783.36600.ef

Straathof, A. J. J. (2014). Transformation of Biomass into Commodity Chemicals Using Enzymes or Cells. *Chemical Reviews, 114*(3), 1871-1908. doi:10.1021/cr400309c

Suárez, E. R., Kralovec, J. A., & Bruce Grindley, T. (2010). Isolation of phosphorylated polysaccharides from algae: the immunostimulatory principle of Chlorella pyrenoidosa. *Carbohydrate Research, 345*(9), 1190-1204. doi:http://dx.doi.org/10.1016/j.carres.2010.04.004

Suárez, E. R., Kralovec, J. A., Noseda, M. D., Ewart, H. S., Barrow, C. J., Lumsden, M. D., & Grindley, T. B. (2005). Isolation, characterization and structural determination of a unique type of arabinogalactan from an immunostimulatory extract of Chlorella pyrenoidosa. *Carbohydrate Research, 340*(8), 1489-1498. doi:http://dx.doi.org/10.1016/j.carres.2005.04.003

Sui, Z. Q., Gizaw, Y., & BeMiller, J. N. (2012). Extraction of polysaccharides from a species of Chlorella. *Carbohydrate Polymers, 90*(1), 1-7. doi:10.1016/j.carbpol.2012.03.062

Sun, M., & Leyh, T. S. (2005). Anatomy of an Energy-Coupling MechanismThe Interlocking Catalytic Cycles of the ATP Sulfurylase−GTPase System. *Biochemistry, 44*, 13941–13948. doi:10.1021/bi051303e

Sweeney, M. D., & Xu, F. (2012). Biomass Converting Enzymes as Industrial Biocatalysts for Fuels and Chemicals: Recent Developments. *Catalysts, 2*(2), 244.

Takeda, H. (1988a). Classification of chlorella strains by cell-wall sugar composition. *Phytochemistry, 27*(12), 3823-3826. doi:10.1016/0031-9422(88)83025-5

Takeda, H. (1988b). Classification of Chlorella strains by means of the sugar components of the cell wall. *Biochemical Systematics and Ecology, 16*(4), 367-371. doi:http://dx.doi.org/10.1016/0305-1978(88)90027-0

Takeda, H. (1993). Taxonomical assignment of chlorococal algae from their cell-wall composition. *Phytochemistry, 34*(4), 1053-1055. doi:10.1016/s0031-9422(00)90712-x

Takeda, H. (1996). Cell wall sugars of some Scenedesmus species. *Phytochemistry, 42*(3), 673-675. doi:10.1016/0031-9422(95)00952-3

Takeda, H., & Hirokawa, T. (1978). Studies on the cell wall of Chlorella I. Quantitative changes in cell wall polysaccharides during the cell cycle of Chlorella ellipsoidea. *Plant and Cell Physiology, 19*(4), 591-598.

Templeton, D. W., & Laurens, L. M. L. (2015). Nitrogen-to-protein conversion factors revisited for applications of microalgal biomass conversion to food, feed and fuel. *Algal Research, 11*, 359-367. doi:https://doi.org/10.1016/j.algal.2015.07.013

Templeton, D. W., Quinn, M., Van Wychen, S., Hyman, D., & Laurens, L. M. L. (2012). Separation and quantification of microalgal carbohydrates. *Journal of Chromatography A, 1270*, 225-234. doi:10.1016/j.chroma.2012.10.034

Templeton, D. W., Wolfrum, E. J., Yen, J. H., & Sharpless, K. E. (2016). Compositional Analysis of Biomass Reference Materials: Results from an Interlaboratory Study. *BioEnergy Research, 9*(1), 303-314. doi:10.1007/s12155-015-9675-1

Toor, S. S., Rosendahl, L., & Rudolf, A. (2011). Hydrothermal liquefaction of biomass: A review of subcritical water technologies. *Energy, 36*(5), 2328-2342. doi:https://doi.org/10.1016/j.energy.2011.03.013

Trivedi, N., Baghel, R. S., Bothwell, J., Gupta, V., Reddy, C. R. K., Lali, A. M., & Jha, B. (2016). An integrated process for the extraction of fuel and chemicals from marine macroalgal biomass. *Scientific Reports, 6*, 30728. doi:10.1038/srep30728

Tuck, C. O., Pérez, E., Horváth, I. T., Sheldon, R. A., & Poliakoff, M. (2012). Valorization of Biomass: Deriving More Value from Waste. *Science, 337*(6095), 695-699. doi:10.1126/science.1218930

Van Wychen, S., Long, W., Black, S. K., & Laurens, L. M. L. (2017). MBTH: A novel approach to rapid, spectrophotometric quantitation of total algal carbohydrates. *Analytical Biochemistry, 518*, 90-93. doi:10.1016/j.ab.2016.11.014

Wegner, C. E., Richter-Heitmann, T., Klindworth, A., Klockow, C., Richter, M., Achstetter, T., . . . Harder, J. (2013). Expression of sulfatases in Rhodopirellula baltica and the diversity of sulfatases in the genus Rhodopirellula. *Marine Genomics, 9*, 51-61. doi:10.1016/j.margen.2012.12.001

Wei, J., Tang, Q.-X., Varlamova, O., Roche, C., Lee, R., & Leyh, T. S. (2002). Cysteine Biosynthetic Enzymes Are the Pieces of a Metabolic Energy Pump. *Biochemistry, 41*, 8493–8498. doi:10.1021/bi025953j

White, G. F., Lillis, V., & Shaw, D. J. (1980). An improved procedure for the preparation of alkyl sulphate esters suitable for the study of secondary alkylsulphohydrolase enzymes. *Biochemical Journal, 187*(1), 191-196.

White, J. S. (2014). Sucrose, HFCS, and fructose: History, manufacture, composition, applications, and production. In *Fructose, High Fructose Corn Syrup, Sucrose and Health* (pp. 13-33).

White, R. C., & Barber, G. A. (1972). An acidic polysaccharide from the cell wall of Chlorella pyrenoidosa. *BBA - General Subjects, 264*(1), 117-128.

Whitehead, C., Gomez, L. D., & McQueen-Mason, S. J. (2012) The analysis of saccharification in biomass using an automated high-throughput method. In*: Vol. 510. Methods in Enzymology* (pp. 37-50).

Wijffels, R. H., & Barbosa, M. J. (2010). An Outlook on Microalgal Biofuels. *Science, 329*(5993), 796-799. doi:10.1126/science.1189003

Yoon, H. S., Hackett, J. D., Ciniglia, C., Pinto, G., & Bhattacharya, D. (2004). A Molecular Timeline for the Origin of Photosynthetic Eukaryotes. *Molecular Biology and Evolution, 21*(5), 809-818. doi:10.1093/molbev/msh075

Zhu, Y., Romain, C., & Williams, C. K. (2016). Sustainable polymers from renewable resources. *Nature, 540*(7633), 354-362. doi:10.1038/nature21001

Ziolkowska, J. R., & Simon, L. (2014). Recent developments and prospects for algae-based fuels in the US. *Renewable & Sustainable Energy Reviews, 29*, 847-853. doi:10.1016/j.rser.2013.09.021

Zuorro, A., Miglietta, S., Familiari, G., & Lavecchia, R. (2016). Enhanced lipid recovery from Nannochloropsis microalgae by treatment with optimized cell wall degrading enzyme mixtures. *Bioresource Technology, 212*, 35-41. doi:http://dx.doi.org/10.1016/j.biortech.2016.04.025

Appendix

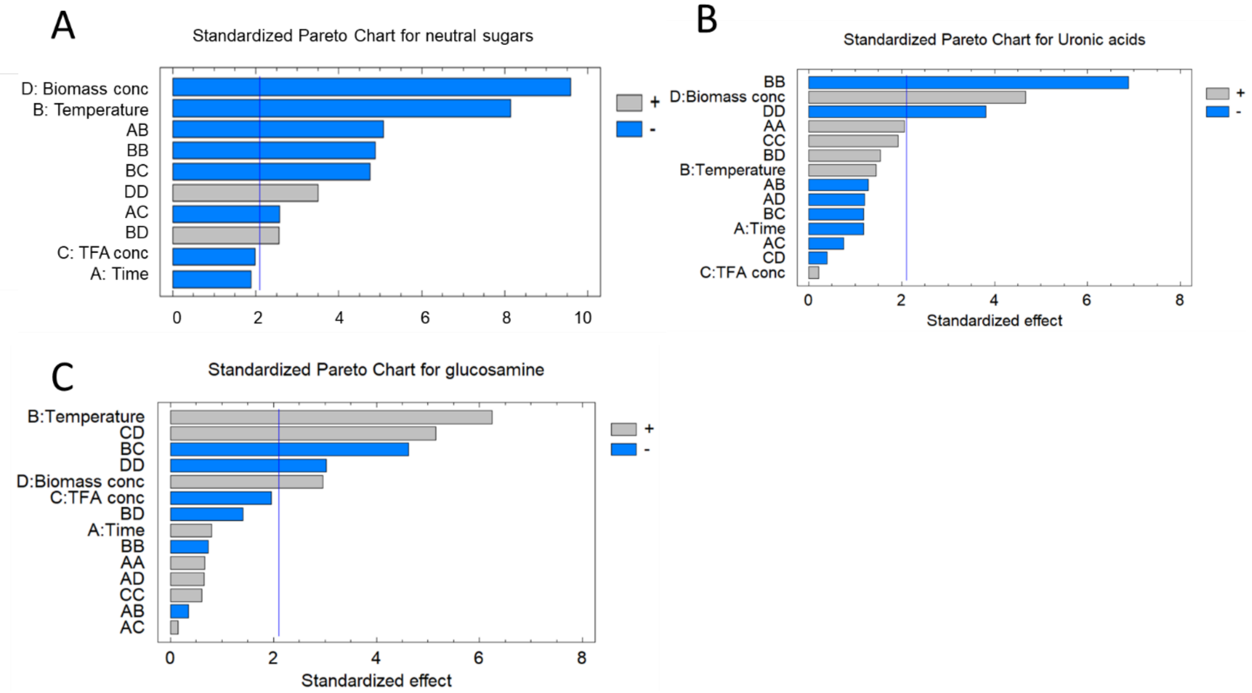

Figure A1: Pareto charts of DoE for TFA hydrolysis of *C. vulgaris* microalgal biomass for A. neutral sugars, B. uronic acids, and C. glucosamine.

Note: The span yields for uronic acids (0 – 12 mg g_B^{-1}) and glucosamine (0 – 9 mg g_B^{-1}) were rather short, so significant and non-significant factors were considered in the multiple linear regression equations. By this, a more accurate regression model can be achieved. This was not the case for neutral sugars.

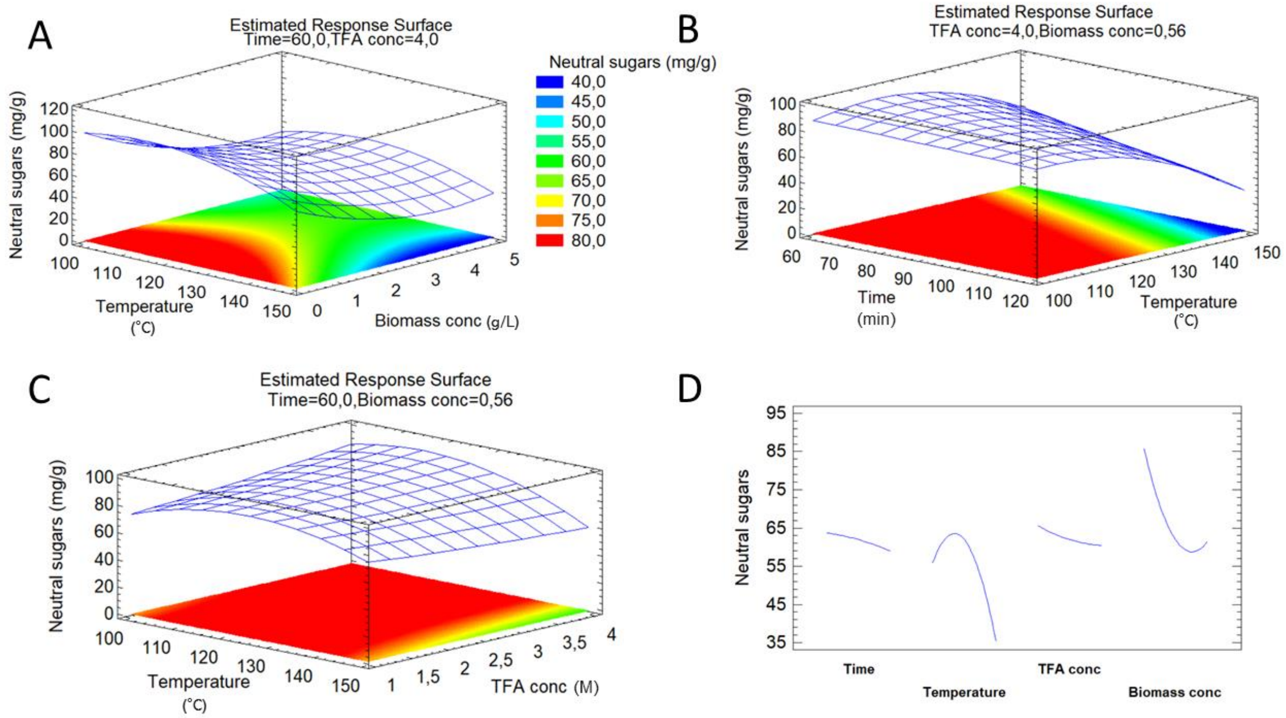

Figure A2: DoE data analysis for TFA hydrolysis of *C. vulgaris* microalgal biomass, A-C. Surface response plots for neutral sugars, D. Main effects plot

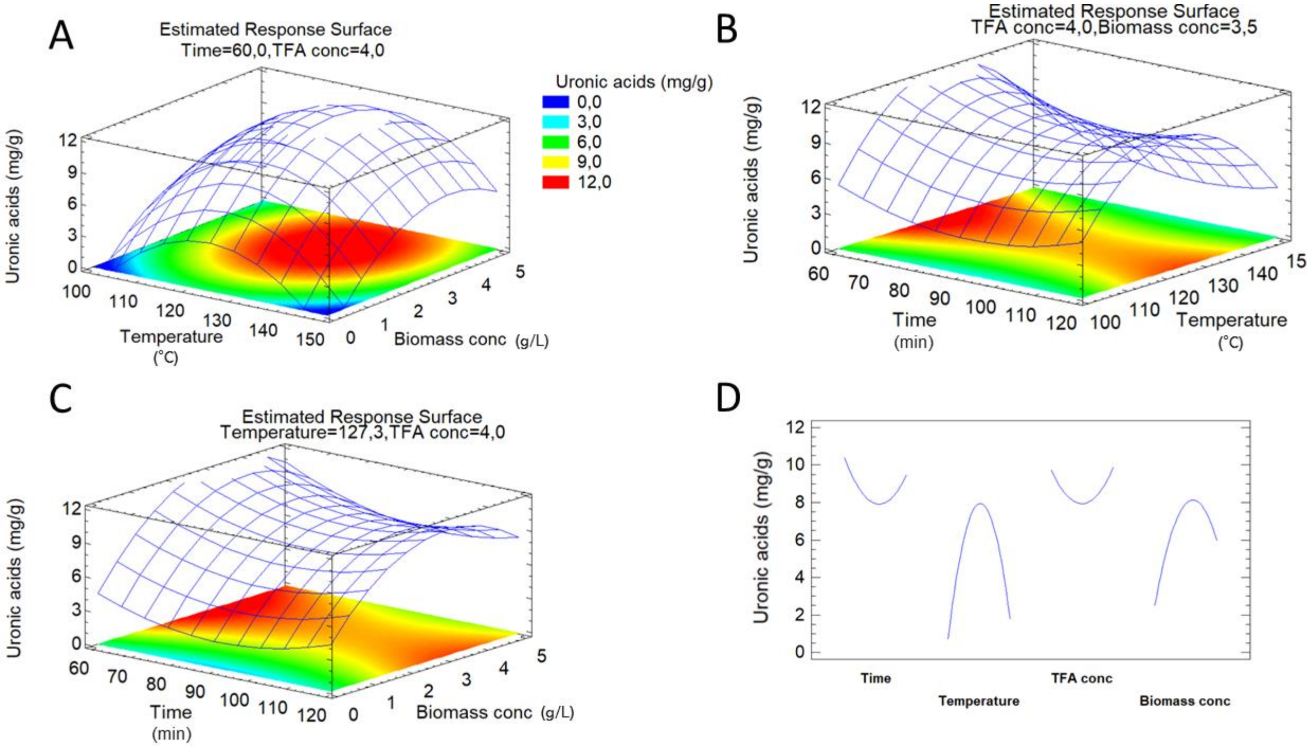

Figure A3: DoE data analysis for TFA hydrolysis of *C. vulgaris* microalgal biomass, A-C. Surface response plots for uronic acids, D. Main effects plot

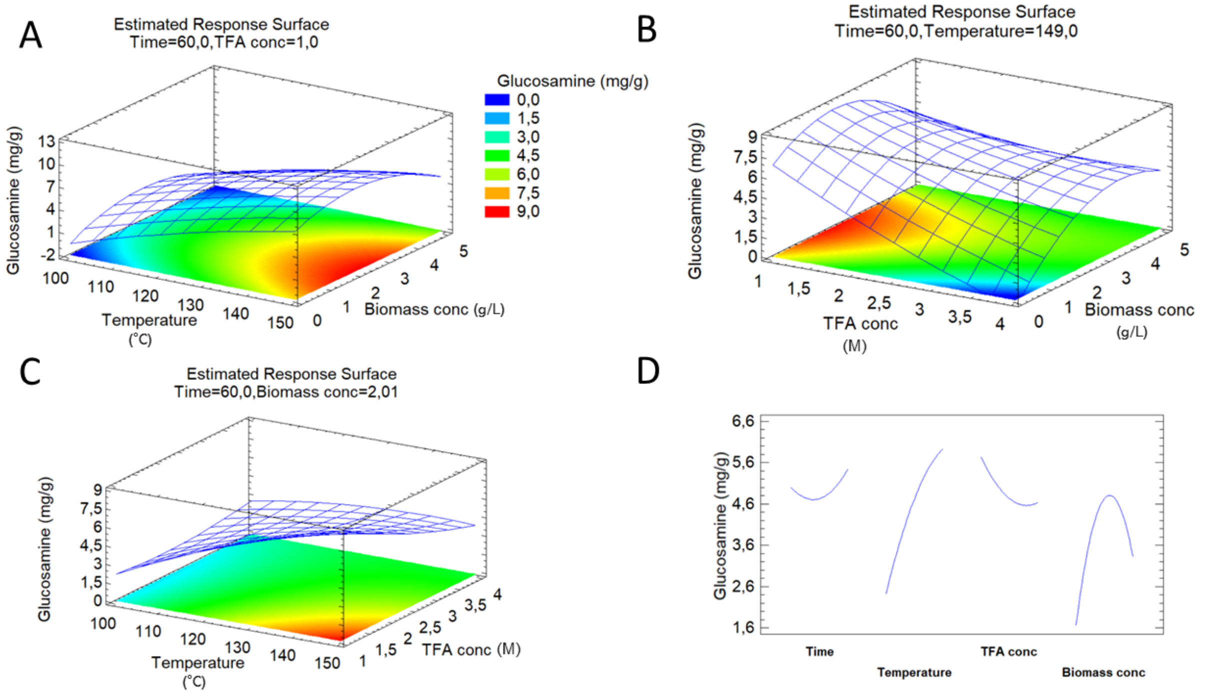

Figure A4: DoE data analysis for TFA hydrolysis of *C. vulgaris* microalgal biomass, A-C. Surface response plots for glucosamine, D. Main effects plot

Table A 1: Fitted equations for the multiple linear regression model for neutral sugars, uronic acids and glucosamine released from C. vulgaris by TFA hydrolysis. Parameters considered: A; time in min, B; temperature in °C, C; TFA concentration in M, D; biomass concentration in g L^{-1}

Output	**Equation**
Neutral sugars	$Y_{NS} = -394.4 + 1.3*A + 7.2*B + 24.0*C - 29.4*D - 9.1*10^{-3}*A*B - 7.7*10^{-2}*A*C - 2.6*10^{-2}*B^2 - 0.17*B*C + 0.06*B*D + 2.3*D^2$
Uronic acids	$Y_{UA} = -156.5 - 0.29*A + 2.76*B - 1.83*C + 4.20*D + 2.2*10^{-3}*A^2 - 6.69921*10^{-4}*A*B - 6.5*10^{-3}*A*C - 7.0*10^{-3}*A*D - 1.07*10^{-2}*B^2 - 1.24*10^{-2}*B*C + 1.07*10^{-2}*B*D + 0.83*C^2 - 4.66*10^{-3}*C*D - 0.73*D^2$
Glucosamine	$Y_{GlcN} = -27.6 - 8.4*10^{-2}*A + 0.41*B + 1.87*C + 2.33*D + 5.5*10^{-4}*A^2 - 1.4*10^{-4}*A*B + 1.0*10^{-3}*A*C + 2.9*10^{-3}*A*D - 8.7*10^{-4}*B^2 - 3.6*10^{-2}*B*C - 7.5*10^{-3}*B*D + 0.20*C^2 + 0.45*C*D - 0.44*D^2$

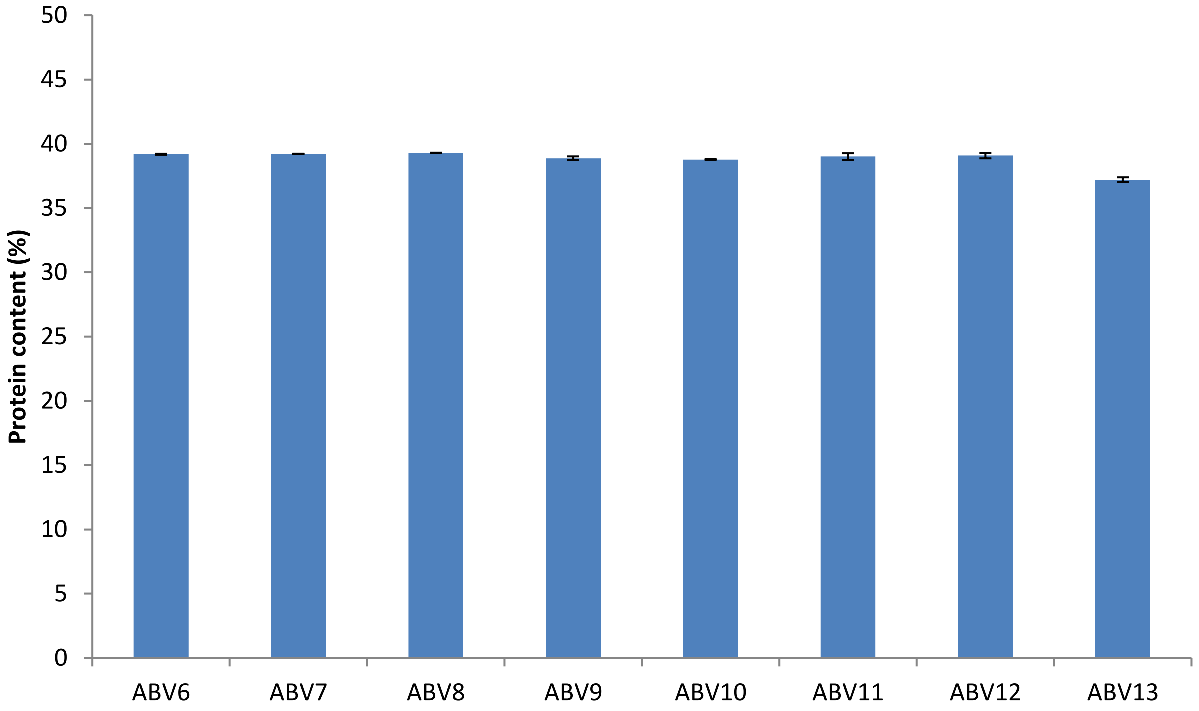

Figure A5: Protein content of the analyzed extracted biomasses from *S. obtusiusculus*.

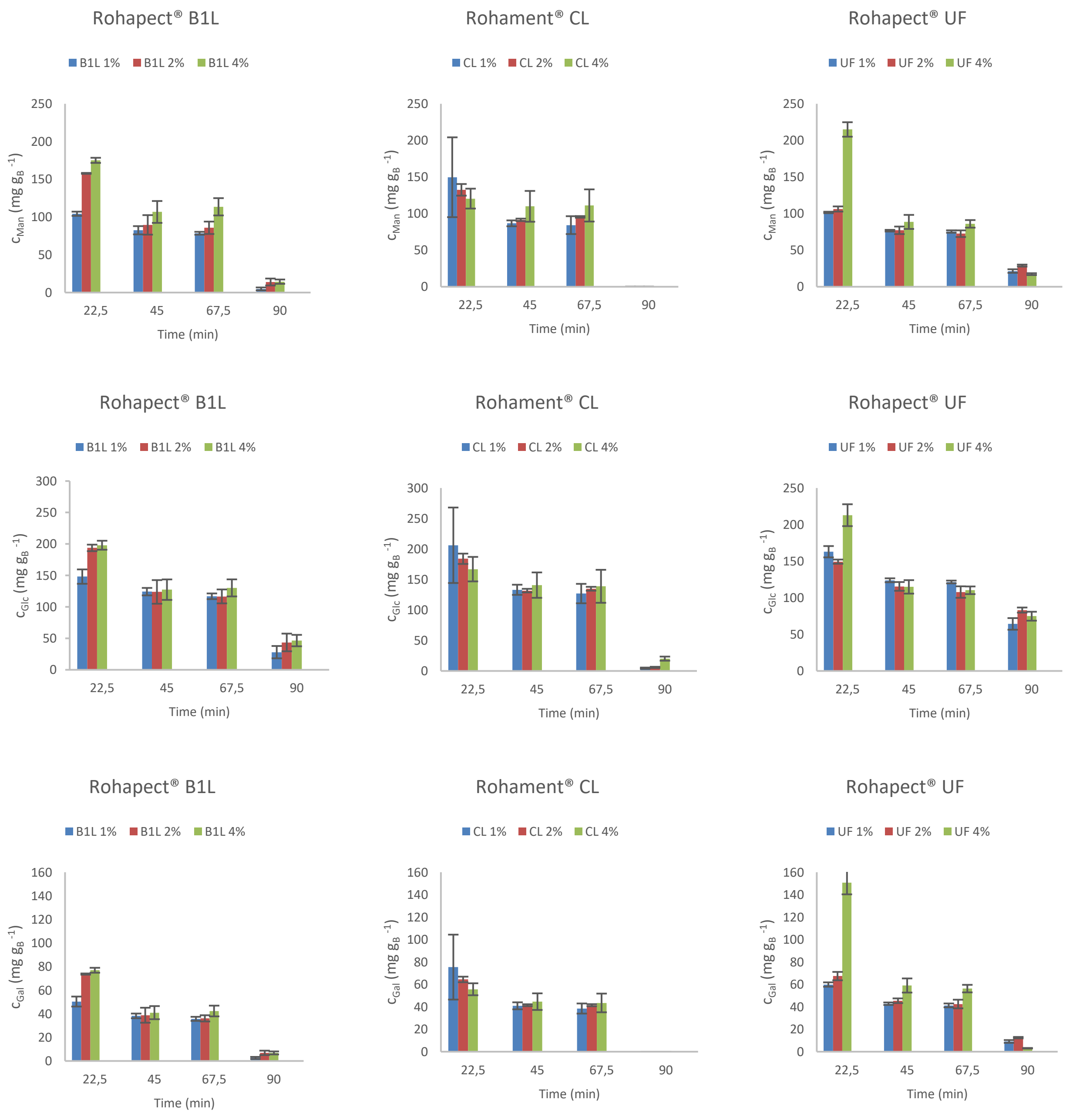

Rohapect® B1L

Rohament® CL

Rohapect® UF

Rohapect® B1L

Rohament® CL

Rohapect® UF

Rohapect® B1L

Rohament® CL

Rohapect® UF

Figure A6: Monosaccharide release from enzyme hydrolysates (liquid phase, *S. obtusiusculus*) using TFA hydrolysis (2M – 121°C) over time: From 0 to 67 min in 3 regular time intervals; Experiments with shorter time than 22 min using Rohapect® B1L 4% did not display higher sugar yields.

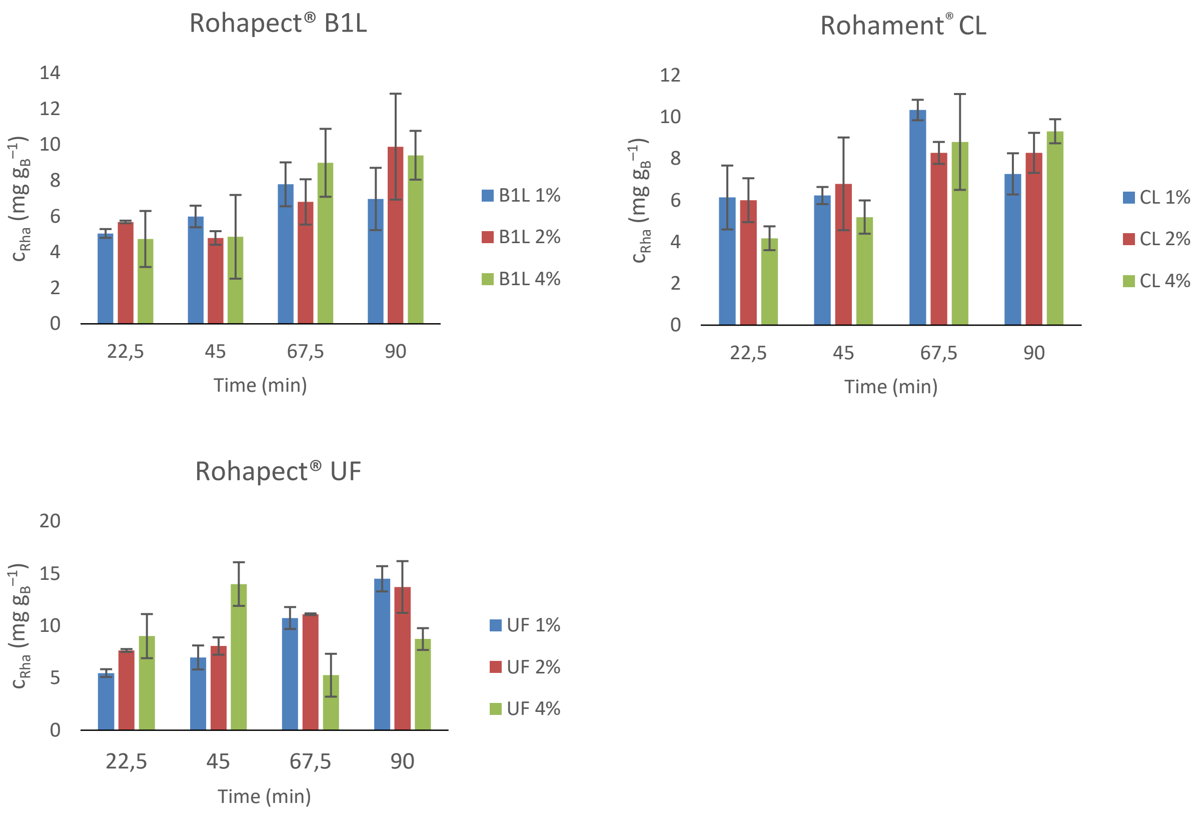

Figure A7: Rhamnose yields in mg per g biomass after different TFA hydrolysis time (2 M, 121°C) of enzymatic hydrolysates from *S. obtusiusculus* biomass ABV10 (Rohapect® B1L and UF) and ABV11 (Rohament® CL), n=3.

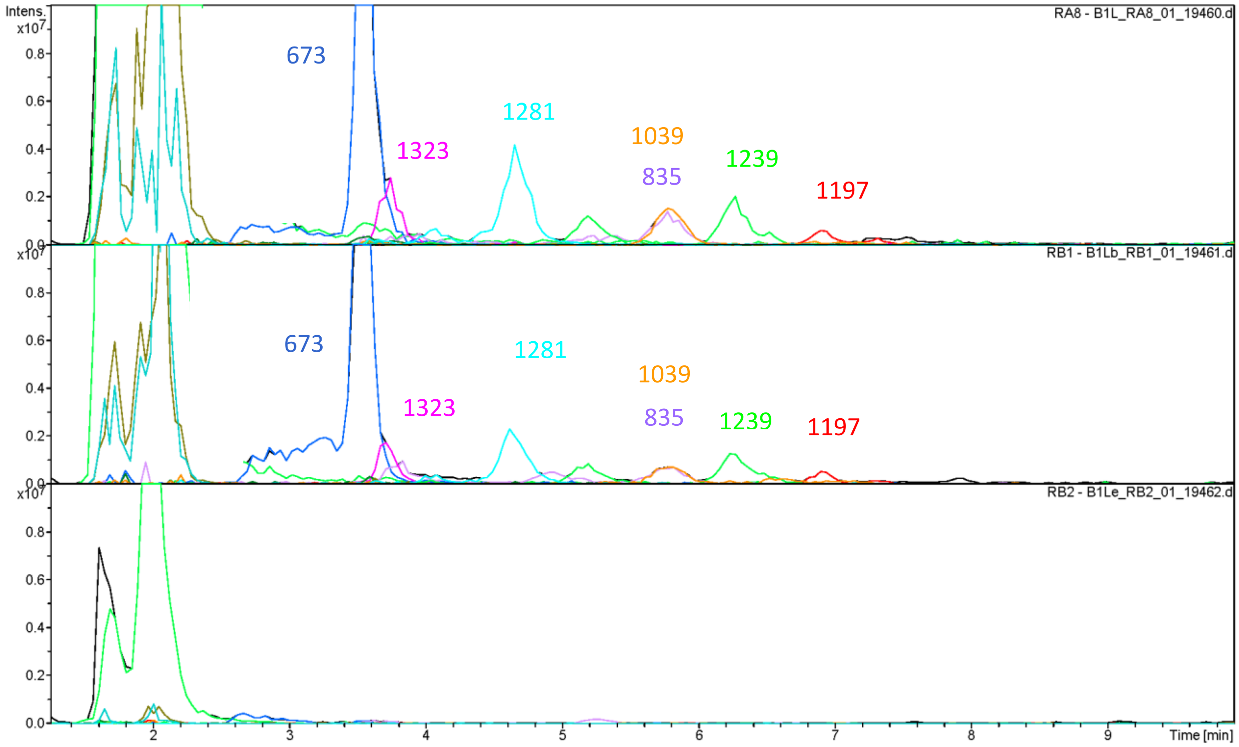

Figure A8: LC-MS analysis by EIC (color) of A. Enzyme hydrolysate (Rohapect® B1L 4% w/w); B. Biomass control; C. Enzyme control**.** Hydrolyzed biomass *S. obtusiusculus* ABV10. In black BPC (*m/z* 500 – 3,000)

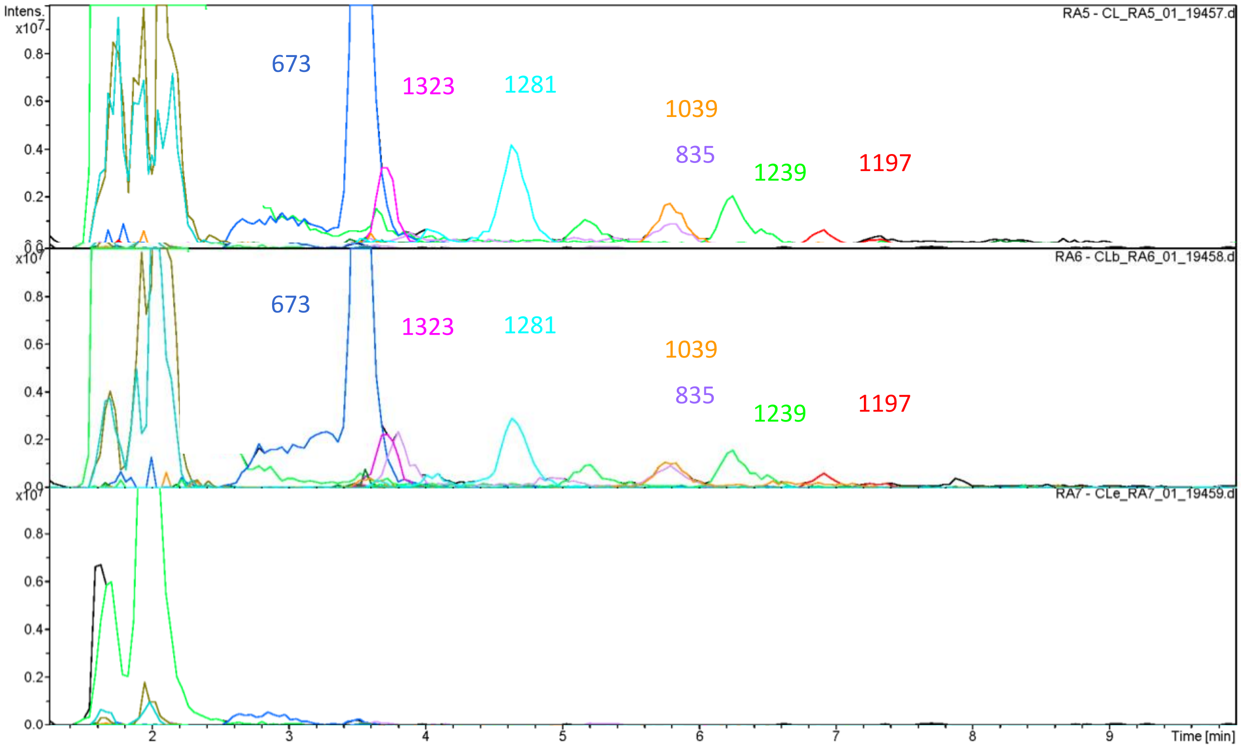

Figure A9: LC-MS analysis by EIC (color) of A. Enzyme hydrolysate (Rohament® CL 4% w/w); B. Biomass control; C. Enzyme control**.** Hydrolyzed biomass *S. obtusiusculus* ABV10. In black BPC (*m/z* 500 – 3,000)

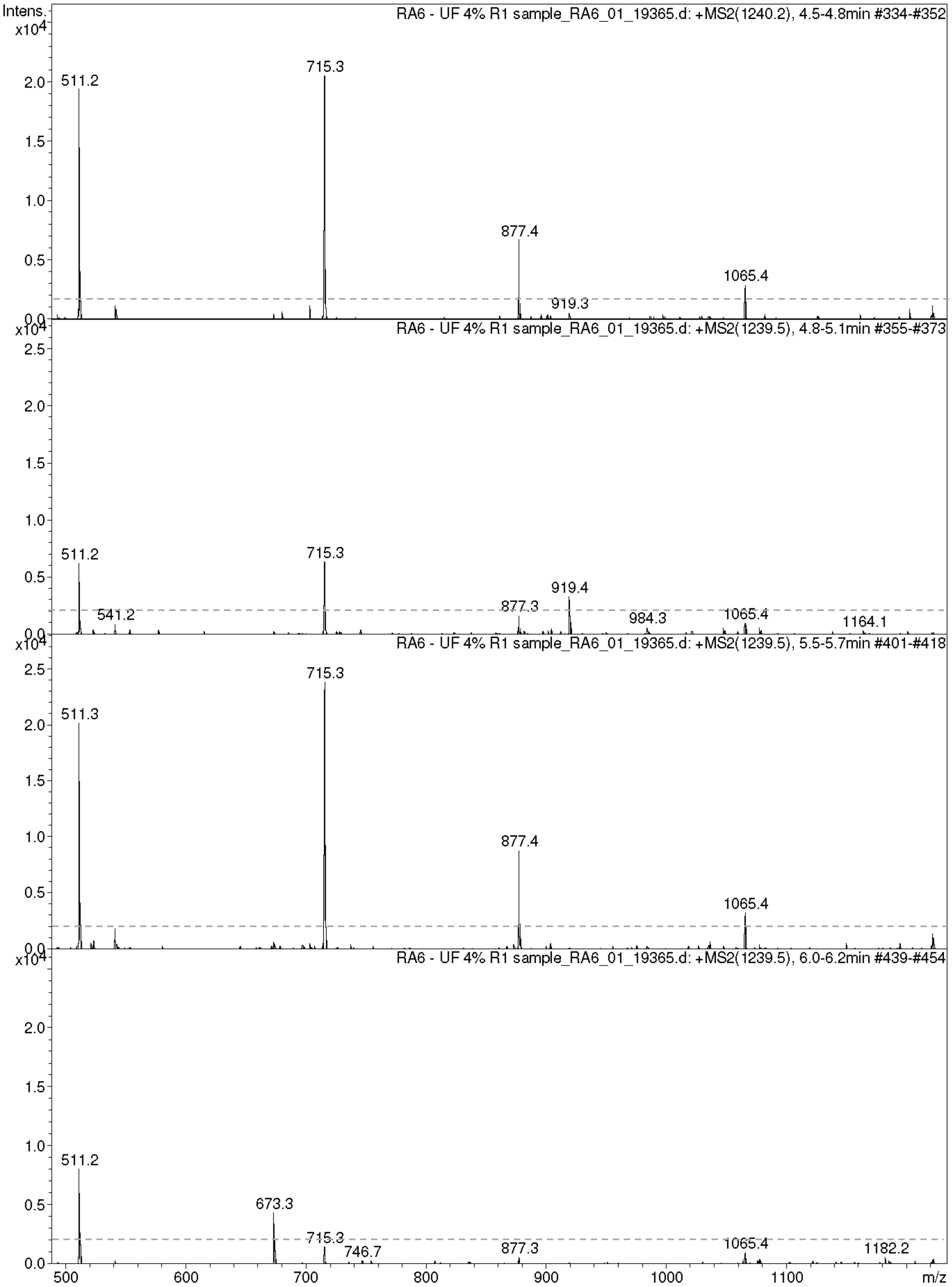

Figure A10: Averaged MS^2 spectra of peaks *m/z* 1239 from Rohapect® UF hydrolysate (4% w/w) at four different R$_t$. The dotted line indicates the designated threshold value for analysis of 2,000 (one tenth of maximal intensity found).

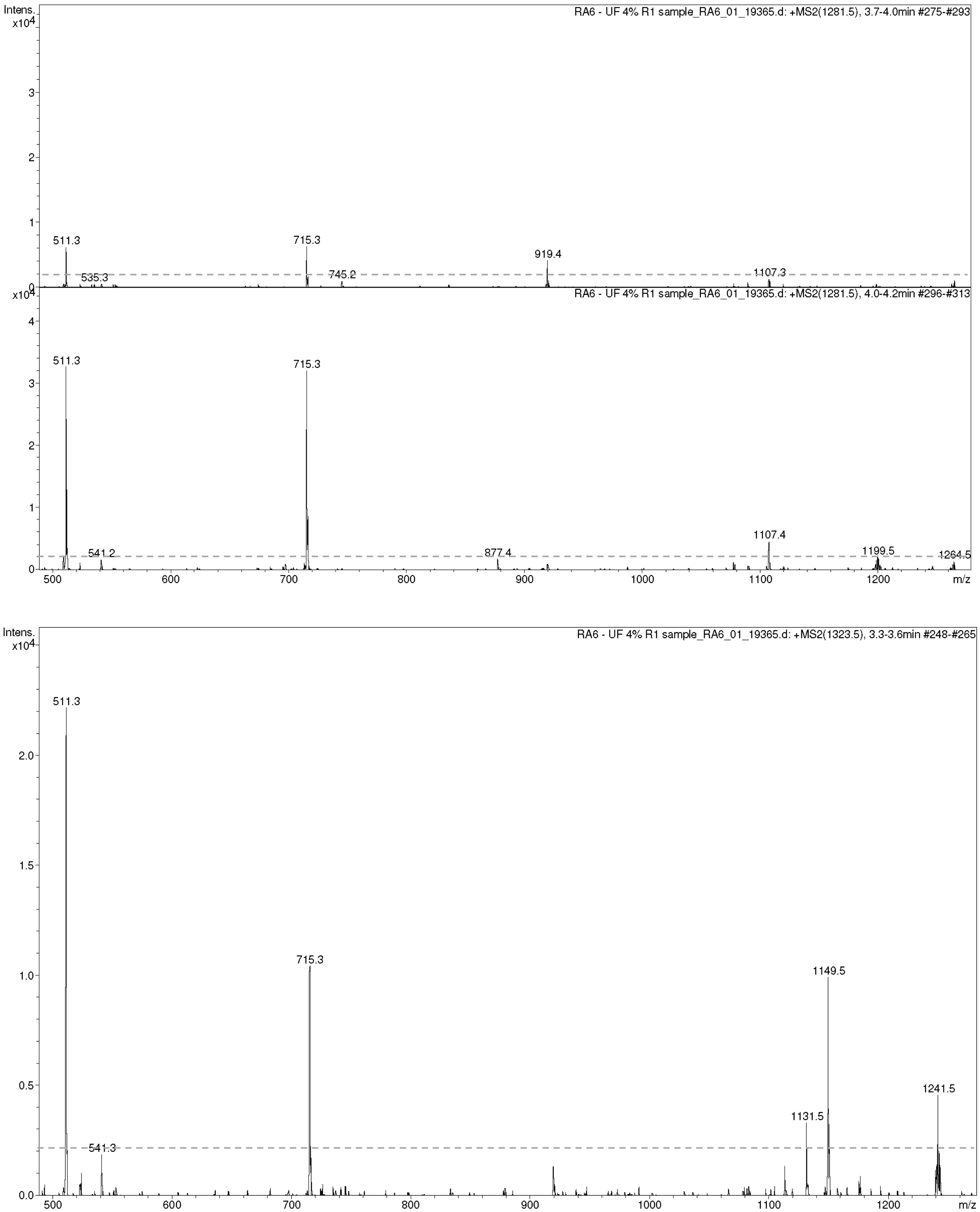

Figure A11: Averaged MS^2 spectra of peaks *m/z* 1281 (upper panel) and 1323 (lower panel) from Rohapect® UF (4% w/w) hydrolysate**.** The dotted line indicates the designated threshold value for analysis of 2,000 (one tenth of maximal intensity found).

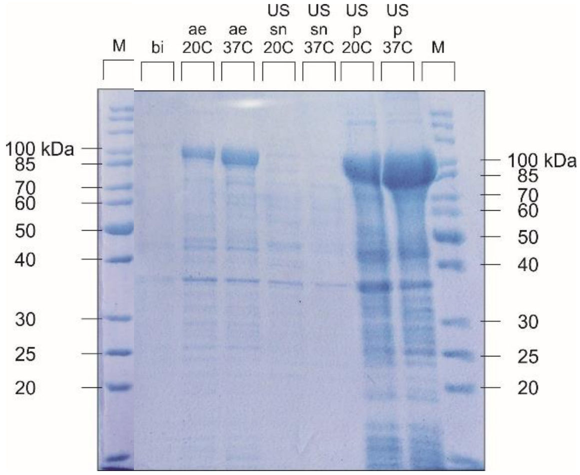
M
bi
ae 20C
ae 37C
US sn 20C
US sn 37C
US p 20C
US p 37C
M
100 kDa
85
70
60
50
40
30
25
20
100 kDa
85
70
60
50
40
30
25
20

Figure A12: SDS-PAGE of *PPDK* purification procedure

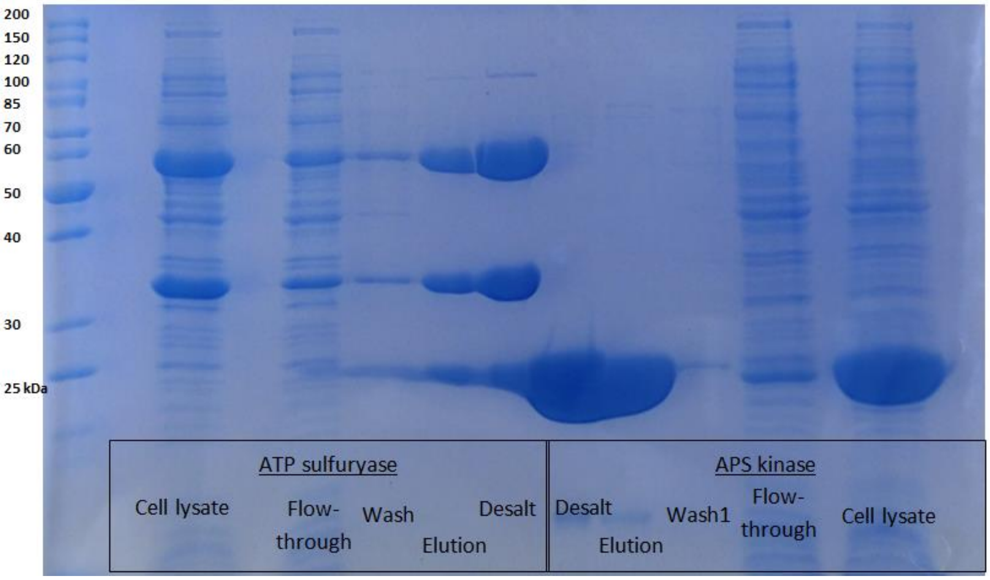
200
150
120
100
85
70
60
50
40
30
25 kDa
ATP sulfuryase
Cell lysate
Flow-through
Wash
Elution
Desalt
APS kinase
Desalt
Elution
Wash1
Flow-through
Cell lysate

Figure A13: SDS-PAGE of *ATPs* and *APSk* purification procedure

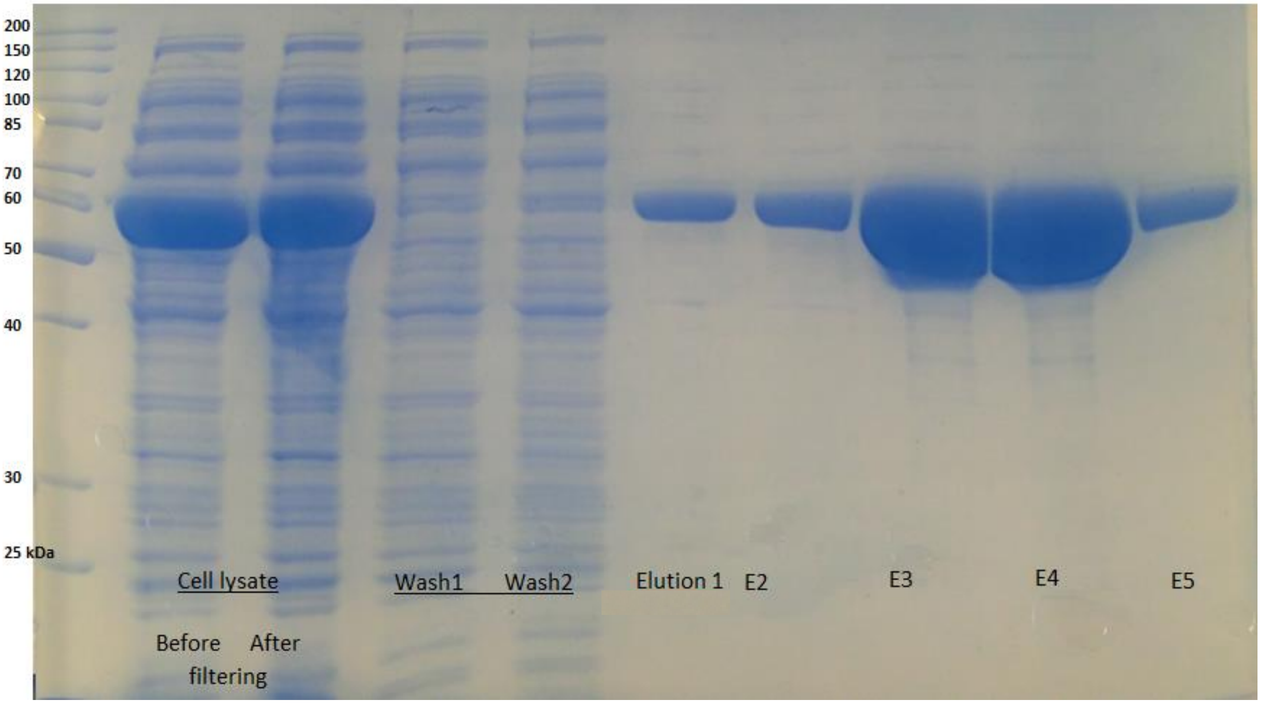
200
150
120
100
85
70
60
50
40
30
25 kDa
Cell lysate
Before After
filtering
Wash1 Wash2
Elution 1 E2
E3
E4
E5

Figure A14: SDS-PAGE of *PAS* purification procedure

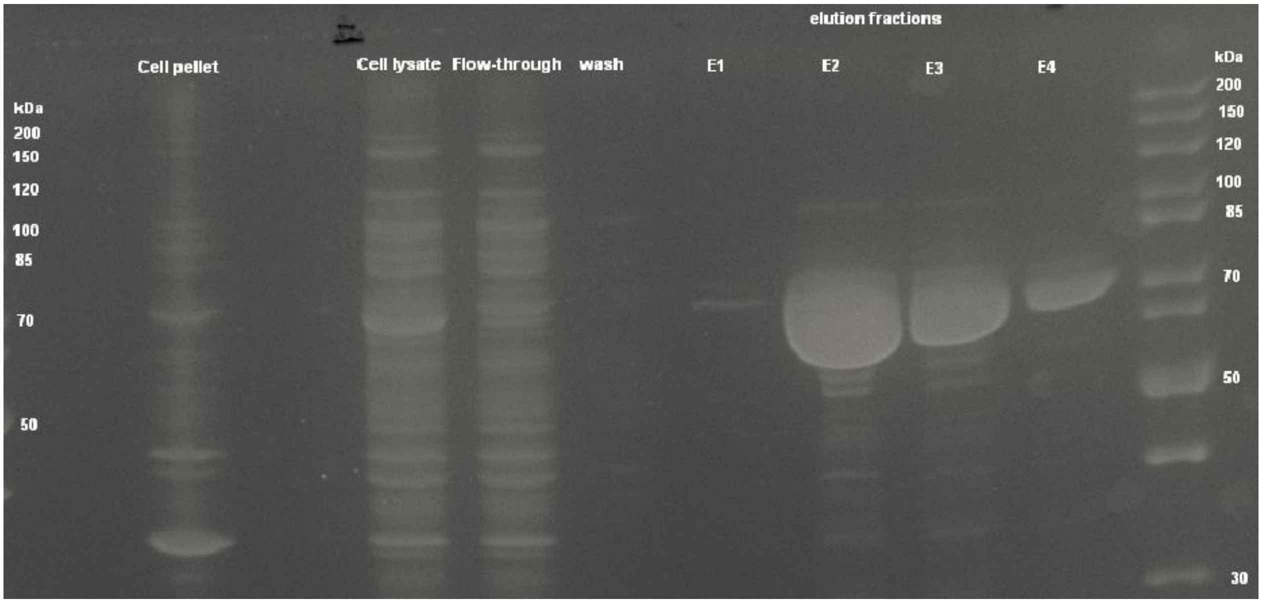
elution fractions
Cell pellet
Cell lysate
Flow-through
wash
E1
E2
E3
E4
kDa
200
150
120
100
85
70
50
kDa
200
150
120
100
85
70
50
30

Figure A15: SDS-PAGE of *PISA1* purification procedure

Abbreviations

%	Percentage
°C	Degree Celsius
µL	Microliter
ABO	Algal Biomass Organization
APS	Adenosine 5’-phosphosulfate
APSk	APS kinase
ATP	Adenosine triphosphate
ATPs	ATP sulfurylase
BG-11	Blue green medium for cyanobacteria
bp	Base pairs
BPC	Base peak chromatogram
BSA	Bovine serum albumin
CO_2	Carbon dioxide
CV	Coefficient of variation
DA-64	N-(carboxymethylamino-carbonyl)-4.4’-bis-(dimethylamino)-dephenylamine sodium salt
dd H_2O	Ultrapure water
DMF	Dimethylformamide
DMSO	Dimethyl sulfoxide
DNA	Deoxyribonucleic acid
DW	Dry weight
DWP	Deep well plate
EIC	Extracted ion chromatogram
EPS	Exopolysaccharide
EPSAG	German for *Experimentelle Phykologie und Sammlung von Algenkulturen*
FPLC	Fast protein liquid chromatography
Fuc	Fucose
g	Gram
Gal	Galactose
GC	Gas chromatography
Glc	Glucose
GlcNAc	N-Acetyl glucosamine
GTP	Guanosine triphosphate
h	Hours
HEPES	4-2-Hydroxyethyl-1-piperazineethanesulfonic acid
HILIC	Hydrophilic interaction liquid chromatography
HPAEC	High performance anion exchange chromatography
HPLC	High performance liquid chromatography
HRP	Horseradish peroxidase
HT	High-throughput

ICC	Ion charge control
IPTG	Isopropyl β-D-1-thiogalactopyranoside
IR	Infrared spectroscopy
kg	Kilogram
L	Liter
LOD	Limit of detection
m	Meter
M	Molar
m/z	Mass to charge ratio
Man	Mannose
MBTH	3-Methyl-2-benzothiazolinone hydrazone
mM	Millimolar
MOPS	3-Morpholinopropane-1-sulfonic acid
ms	Milliseconds
MS	Mass spectrometry
MS^2	Tandem mass spectrometry
MTP	Microtiter plate
M_W	Molecular weight
N.A.	Not available / not applicable
ng	Nanogram
NIST	US National Institute of Standards and Technology
NMR	Nuclear magnetic resonance
NREL	National Renewable Energy Laboratory
OD	Optical density
p.a.	*Per annum*
PAS	Arylsulfatase from *Pseudomonas aeruginosa*
PCR	Polymerase chain reaction
Pi	Inorganic phosphate
PMP	1-Phenyl-3-methyl-5-pyrazolone
POX	Pyruvate oxidase
PPDK	Pyruvate phosphate dikinase
PPi	Inorganic pyrophosphate
PTFE	Polytetrafluoroethylene
PUFA	Polyunsaturated fatty acids
Rha	Rhamnose
RP	Reverse phase
R_t	Retention time
SD	Standard deviation
SDS-PAGE	Sodium dodecyl sulfate poly acrylamide gel electrophoresis
SHF	Separate hydrolysis and fermentation
SOC	Super optimal broth with catabolize repression
sp.	Species

SWES	Seawater medium
TFA	Trifluoroacetic acid
TLC	Thin layer chromatography
TMS	Trimethyl silane
TPP	Thiamine pyrophosphate
TRIS	2-Amino-2-(hydroxymethyl) propane-1,3-diol
UPLC	Ultrahigh performance liquid chromatography
US	United states
UV	Ultraviolet
v/v	Volume per volume
w/v	Weight per volume
w/w	Weight per weight
Xyl	Xylose

List of Figures

Figure 1 Schematic representation of a microalga as renewable feedstock 11
Figure 2 Summary of classification criteria for the microalga *Chlorella* proposed by Takeda (Takeda, 1988a, 1988b, 1993) 14
Figure 3 Chemical structure of the carbohydrates found in *Chlorella* by Ogawa, (Ogawa et al., 1994, 1997) 14
Figure 4 Analytical methods for studying microalgal carbohydrates: simplicity and resolution 17
Figure 5: Multiple linear regression model for output glucose concentration in mg g_B^{-1} A. Standardized pareto diagram after excluding non-significant effects (confidence interval 95%,), B. main effects plot, C. Surface response plot for temperature (°C) and c_{TFA} (M), D. Surface response plot for time (min) and temperature (°C) 50
Figure 6 Enzymatic treatment of carbohydrate-rich biomass and its carbohydrate analysis by LC-MS 62
Figure 7 Carbohydrate composition of differently lipid-extracted biomass from *S. obtusiusculus* after TFA standard hydrolysis (see section A3.8). Glc: glucose; Man: mannose; Gal: galactose; Rha: rhamnose; Fuc: fucose; Xyl: xylose. n=3 64
Figure 8 Carbohydrate composition of differently lipid-extracted biomass from *S. obtusiusculus* after TFA standard hydrolysis (see section A3.9). Glc: glucose; Man: mannose; Gal: galactose; Rha: rhamnose; Fuc: fucose; Xyl: xylose. n=3 66
Figure 9 LC-MS analysis of pullulan 1300 as certified reference material. A. EIC of the relevant species; B. MS^2 Fragmentation analysis of *m/z* 835; C. Fragmentation analysis of *m/z* 997; D. Fragmentation analysis of *m/z* 1159 69
Figure 10 LC-MS analysis by EIC (color) of A. Enzyme hydrolysate (Rohapect® UF 4% w/w); B. Biomass control; C. Enzyme control. Hydrolyzed biomass *S. obtusiusculus* ABV10. In color are the represented specific masses, in black BPC (*m/z* 500 – 3,000) 70
Figure 11 Averaged MS fragmentation spectra of peaks found in the enzyme hydrolysate (Rohapect® UF 4% w/w). A. *m/z* 1039 (R_t 5.2 min); B. *m/z* 1197 (R_t 6.5 min). The dotted line indicates the threshold value set for analysis (2000) 71
Figure 12: Possible oligomeric sugar structure of the peaks found (*m/z* 1039, 1197 and 1239) in the enzymatic supernatant (Rohapect® UF 4% w/w) of the algal biomass of *S. obtusiusculus* ABV 10. Hex: hexose, Pen: pentose, Ac: acetylated, dHex: deoxy-hexose 79
Figure 13 Absorbance increase of master mix 2 and different blank types at 37°C over time 122
Figure 14 Comparison of pyrophosphate (PPi) and sulfate assay with and without enzymes in reaction 1123
Figure 15 Sulfate calibration curve in water and in TFA matrix 124

Figure A1: Pareto charts of DoE for TFA hydrolysis of *C. vulgaris* microalgal biomass for A. neutral sugars, B. uronic acids, and C. glucosamine. Note: The span yields for uronic acids (0 – 12 mg g_B^{-1}) and glucosamine (0 – 9 mg g_B^{-1}) were rather short, so significant and non-significant factors were considered in the multiple linear regression equations. By this, a more accurate regression model can be achieved. This was not the case for neutral sugars. 135
Figure A2: DoE data analysis for TFA hydrolysis of *C. vulgaris* microalgal biomass, A-C. Surface response plots for neutral sugars, D. Main effects plot 136
Figure A3: DoE data analysis for TFA hydrolysis of *C. vulgaris* microalgal biomass, A-C. Surface response plots for uronic acids, D. Main effects plot 136
Figure A4: DoE data analysis for TFA hydrolysis of *C. vulgaris* microalgal biomass, A-C. Surface response plots for glucosamine, D. Main effects plot 137
Figure A5: Protein content of the analyzed extracted biomasses from *S. obtusiusculus* 138
Figure A6: Monosaccharide release from enzyme hydrolysates (liquid phase, *S. obtusiusculus*) using TFA hydrolysis (2M – 121°C) over time: From 0 to 67 min in 3 regular time intervals; Experiments with shorter time than 22 min using Rohapect® B1L 4% did not display higher sugar yields. 139
Figure A7: Rhamnose yields in mg per g biomass after different TFA hydrolysis time (2 M, 121°C) of enzymatic hydrolysates from *S. obtusiusculus* biomass ABV10 (Rohapect® B1L and UF) and ABV11 (Rohament® CL), n=3. 140
Figure A8: LC-MS analysis by EIC (color) of A. Enzyme hydrolysate (Rohapect® B1L 4% w/w); B. Biomass control; C. Enzyme control. Hydrolyzed biomass *S. obtusiusculus* ABV10. In black BPC (*m/z* 500 – 3,000) 140
Figure A9: LC-MS analysis by EIC (color) of A. Enzyme hydrolysate (Rohament® CL 4% w/w); B. Biomass control; C. Enzyme control. Hydrolyzed biomass *S. obtusiusculus* ABV10. In black BPC (*m/z* 500 – 3,000) 141
Figure A10: Averaged MS^2 spectra of peaks *m/z* 1239 from Rohapect® UF hydrolysate (4% w/w) at four different R_t. The dotted line indicates the designated threshold value for analysis of 2,000 (one tenth of maximal intensity found). 142
Figure A11: Averaged MS^2 spectra of peaks *m/z* 1281 (upper panel) and 1323 (lower panel) from Rohapect® UF (4% w/w) hydrolysate. The dotted line indicates the designated threshold value for analysis of 2,000 (one tenth of maximal intensity found). 143
Figure A12: SDS-PAGE of *PPDK* purification procedure 144
Figure A13: SDS-PAGE of *ATPs* and *APSk* purification procedure 144
Figure A14: SDS-PAGE of *PAS* purification procedure 145
Figure A15: SDS-PAGE of *PISA1* purification procedure 145

List of Tables

Table 1: Overview of lab equipment used 22
Table 2: Overview of electronic media employed 23
Table 3: Overview of the enzymes and reagents used 24
Table 4: Overview of the special consumables employed 26
Table 5: Overview of the microalgal strains for PMP UHPLC-MS method transfer, evaluation, and validation. N.A. not available. 27
Table 6: Overview of the biomasses from *S. obtusiusculus* A189 addressed throughout this work 28
Table 7: Overview of microalgal strains cultured at The University of Queensland for method characterization 28
Table 8. Overview of the commercially available hydrolases for the saccharification of algal biomass. c_p: protein concentration, T_{opt}: optimal temperature 30
Table 9 Monosaccharide yield (in mg per g dry biomass) of *C. vulgaris* after TFA hydrolysis under different conditions. Block 1-4: 2^4- Central Composite Design. The CP are marked in light red. Block 5: additional samples, marked light blue (see Text). *t*: time, *T*: temperature, *c*: concentration, B: biomass, Glc: glucose, NS: neutral sugars, GlcN: glucosamine, UA: uronic acids. Dimers are expressed as the sum of the peak area. Darker green indicates higher monosaccharide concentration. 48
Table 10 Comparative results of average (µ), standard deviation (SD) and coefficient of variation (CV) of the measured central point (CP, n=9) with the minimal and maximal values found. [a] excluding glucose 49
Table 11 Hydrolysis parameters found to maximize sugar yields of *C. vulgaris* biomass within the DoE range. Values obtained by multiple linear regression analysis of the data generated. Underlined bold entries indicate statistically significant parameters according to the corresponding pareto analysis. TFA: Trifluoroacetic acid 51
Table 12 Monosaccharides found in enzyme hydrolysates of standard polymers. Initial concentration of pectin and xylan: 50 g L^{-1}. Galactomannan: 5 g L^{-1}. For the recovery calculations, the addition of water due to hydrolysis was considered. [a] As a sucrose content of 36.7% (w/w) was measured in pectin, 34.9 g L^{-1} were accounted for a 100% recovery (including mass increase by water addition due to hydrolysis). 63
Table 13 Average total carbohydrate content of *S. obtusiusculus* defatted biomass after enzymatic and TFA hydrolysis. µ = mean value of all enzymatic treatments; SD: standard deviation; CV: coefficient of variation 67
Table 14 MS^2 fragments of the peaks found in the liquid supernatant of the biomass treatment with Rohapect® UF 4% w/w. Hex: hexose, Pen: pentose, Ac: acetylated, d-Hex: deoxy-hexose. [a]Threshold intensity of significant fragments: 2000. [b]Identity of monosaccharides was assumed based on fragments with lower intensity than threshold. [d]Fragment resulted from loss of water of fragment 1149. [u]Unidentified fragment with Δ*m/z* 82 77
Table 15 Main products obtained from seaweeds. Condensed from (Holdt & Kraan, 2011) 84
Table 16: Carbohydrate-active enzymes of industrial relevance 97
Table 17 Molecular biology tools for cloning the enzymes' genes involved in the sulfatase assay 100
Table 18: Materials employed for over-expressing the enzymes employed for the sulfatase assay 101
Table 19: Materials employed for purifying the enzymes employed for the sulfatase assay. N.A. not applied 101

Table 20: Parameters for determining the concentration of purified enzymes prior to addition of glycerol to 20% (v/v) final concentration 102
Table 21: Sulfate concentration found in different carrageenan hydrolysates; $^+$industrial grade; *analytical grade, n=3 124

Curriculum Vitae

Geburtsdatum und -ort: 27.01.1987 in Morelia, Mexiko

	Südzucker AG
Seit 02/2020	Gruppenleiter Biokonversion/Downstream Processing Zentralabteilung Forschung, Entwicklung und Services
01/2019-01/2020	Betriebsingenieur Werk Offstein
10/2017-12/2018	Trainee Technik Zentralabteilung Ingenieurwesen
02/2014-09/2017	Technische Universität München Wissenschaftlicher Mitarbeiter / Doktorand Lehrstuhl für Chemie Biogener Rohstoffe
04/2013-11/2013	Masterarbeit: *Enzymatic Lipase-catalyzed Synthesis of novel Bio Surfactants Based on Renewable Feedstocks* Fraunhofer Institut für Grenzflächen und Bioverfahrenstechnik
10/2011-11/2013	Master of Science M.Sc. Industrielle Biotechnologie Technische Universität München
02/2011-08/2011	Project Manager R&D GS Foods Mexico
08/2006-12/2010	Diplom Ing. (FH) Biochemical Engineering Instituto Tecnológico de Morelia (MX)

List of Publications

Ortiz-Tena, José G.; Rühmann, Broder, and Sieber, Volker (2018): Colorimetric determination of sulfate *via* an enzyme cascade for high-throughput detection of sulfatase activity. Analytical Chemistry, Vol. 90 (4), pp. 2526-2533. DOI: 10.1021/acs.analchem.7b03719

Ortiz-Tena, José G.; Schieder, Doris, and Sieber, Volker (2017): Carrageenan and More: Biorefinery Approaches with Special Reference to the Processing of *Kappaphycus*. In: Tropical Seaweed Farming Trends, Problems and Opportunities: Developments in Applied Phycology Book Series. Vol. 9. Springer, 2017.

Schulze, Christian; Reinhardt, Jakob; Wurster, Martina; **Ortiz-Tena, José G.;** Sieber, Volker, and Mundt, Sabine (2016): A one-stage cultivation process for lipid- and carbohydrate-rich biomass of *Scenedesmus obtusiusculus* based on artificial and natural water sources. Bioresource Technology. Vol. 218, pp. 498-504. DOI: 10.1016/j.biortech.2016.06.109

Ortiz-Tena, José G.; Rühmann, Broder, Schieder, Doris; and Sieber, Volker (2016): Revealing the diversity of algal monosaccharides: Fast carbohydrate fingerprinting of microalgae using crude biomass and showcasing sugar distribution in *Chlorella vulgaris* by biomass fractionation. Algal Research. Vol. 17, pp. 227-235. DOI: 10.1016/j.algal.2016.05.008